AMINO ACIDS UNDER HYDROTHERMAL CONDITIONS: APPARENT MOLAR VOLUMES, APPARENT MOLAR HEAT CAPACITIES, AND ACID/BASE DISSOCIATION CONSTANTS FOR AQUEOUS α-ALANINE, β-ALANINE, GLYCINE, AND PROLINE AT TEMPERATURES FROM 25 TO 250°C AND PRESSURES UP TO 30.0 MPa

RODNEY GEORGE FRANCIS CLARKE


CENTRE FOR NFLD. STUDIES
MEMORIAL UNIVERSITY
OF NEWFOUNDLAND

AMINO ACIDS UNDER HYDROTHERMAL CONDITIONS: APPARENT MOLAR VOLUMES, APPARENT MOLAR HEAT CAPACITIES, AND ACID/BASE DISSOCIATION CONSTANTS FOR AQUEOUS α-ALANINE, β-ALANINE, GLYCINE, AND PROLINE AT TEMPERATURES FROM 25 TO 250°C AND PRESSURES UP TO 30.0 MPa.

by

Rodney George Francis Clarke

A thesis submitted to the
School of Graduate Studies
in partial fulfilment of the
requirements for the degree of
Doctor of Philosophy.

Department of Chemistry
Memorial University of Newfoundland

August, 2000

St. John's Newfoundland

ABSTRACT

Amino acids are members of a unique group of compounds that exist in solution as zwitterions. Yet the thermodynamic properties of aqueous amino acids have not been measured at temperatures above 343 K. The amino acids studied in this work have been chosen based on their hydrothermal stability and their solubility in water. A series of batch experiments confirmed that aqueous α-alanine, glycine, and proline were stable on the time scale required for our measurements at the temperatures, pressures, and molalities required for this work.

The apparent molar volumes V_ϕ of aqueous α-alanine, β-alanine, and proline have been determined using platinum vibrating tube densitometers at temperatures from 298 K to 523 K and at pressures from steam saturation to 30 MPa. Values of the standard partial molar volumes V° for the aqueous amino acids increase with temperature, then deviate toward negative values at temperatures above 398 K, consistent with an increase in the critical temperature in the solutions relative to water. The apparent molar heat capacities $C_{p,\phi}$ of aqueous α-alanine, β-alanine, glycine, and proline have been determined using a differential flow calorimeter and a Picker flow microcalorimeter at temperatures from 298 K to 498 K and at pressures from steam saturation to 30 MPa. Values of the standard partial molar heat capacities C_p° for the aqueous amino acids increase with temperature, then deviate toward negative values at temperatures above 373 K to 423 K, also consistent with an

increase in the critical temperature in the solutions relative to water. The values of both V° and C_p° increase with increasing pressure. Comprehensive equations to describe the standard-state properties over the experimental temperature range are reported.

The deviation toward negative values by V° and C_p° is opposite to the behaviour predicted by the correlations developed by Shock and Helgeson (*Geochim. Cosmochim. Acta.* **54**, 915-945, 1990) and Amend and Helgeson (*J. Chem. Soc., Faraday Trans.* **93**, 1927-1941, 1997). The temperature dependence of V° and C_p° predicted using the very recent functional-group additivity model of Yezdimer *et al.* (*Chem. Geol.* **164**, 259-280, 2000) is only in qualitative agreement with the experimental results. The contribution to V° and C_p° from the solvent polarization by the large dipole moment of the zwitterions deviates toward negative infinity as T_c is approached, in a manner similar to the experimental values of V° and C_p° for each of the aqueous amino acids. While this agreement is qualitatively consistent, it is not quantitatively consistent, which suggests that the non-electrostatic hydration effects are of similar magnitude to the solvent polarization effects.

The acid/base dissociation constants for aqueous α-alanine have been determined from 423 K to 523 K using a UV-visible spectrophotometer and the colorimetric indicators developed by Xiang and Johnston (*J. Sol. Chem.* **26**, 13-30, 1997) and Ryan *et al.* (*J. Phys. Chem.* **101**, 1827-1835, 1997). The dissociation constants that were estimated with the functional-group additivity model of Yezdimer *et al.* (*Chem. Geol.* **164**, 259-280, 2000) and those obtained from the isocoulombic extrapolation of room temperature data were found to

be an upper limit for the measured values. The contribution of non-zwitterionic forms of the aqueous amino acids to the experimentally determined values of V° and C_p° were negligible at all but the highest temperatures.

In this work, the first experimentally determined apparent molar volumes V_ϕ for aqueous α-alanine, β-alanine, and proline were obtained at $T \geq 343$ K. The first experimentally determined apparent molar heat capacities $C_{p,\phi}$ for aqueous amino acids at $T \geq 328$ K were obtained in this work. The first experimentally determined acid/base dissociation constants for aqueous α-alanine obtained at $T \geq 423$ K were also obtained in this work.

ACKNOWLEDGEMENTS

There are many people that deserve credit for helping me to accomplish this educational landmark:

My parents, George and Christine, who have given me confidence and faith in myself through their constant love, support, and encouragement. My brother, Adam, who is just beginning his journey and helps me to see each day as a new adventure. My sister, Nancy, who helps me to realise that many new challenges are waiting for me to explore. My grandmother, Blanche Francis, who taught me through her wisdom and vitality that every second of this life should be celebrated. My grandmother and aunt, Blanche and Joan Clarke, for their kindness and many carpentry projects that provided some weekend relief from my research.

My supervisor, Dr. Peter Tremaine, and the hydrothermal chemistry group (past and present) for their help and support in the realm of chemistry. The staff of the machine shop (especially Randy Thorn) and the electronics shop (especially Carl Mulcahy) at Memorial University of Newfoundland for helping to keep my equipment running and my project on schedule. The amino acid analysis facility, also at Memorial University of Newfoundland, for their analysis of my solutions. Dr.Vladimír Majer for the use of his high temperature and pressure differential flow calorimeter at Université Blaise Pascal in Clermont-Ferrand, France. This work was supported financially by the Natural Sciences and Engineering

Council of Canada, the International Association for the Properties of Water and Steam, and Memorial University of Newfoundland.

Finally, my fiancé and best friend, Karen Leonard, for her patience and support over the past four years. You have helped me through many difficult times and shared in all of my accomplishments both large and small. Without you, my life and this degree would not have been as good. And this is just the beginning of a wonderful life together.

TABLE OF CONTENTS

LIST OF FIGURES

LIST OF TABLES

LIST OF ABBREVIATIONS AND SYMBOLS

a_i	functional group specific adjustable parameter
a_j	temperature and pressure independent parameter characteristic of an aqueous ion or electrolyte, j = 1 to 5
A	Arrhenius frequency factor, fitting parameter
$A(\lambda)$	absorbance at a given wavelength
A^-	deprotonated form of an aqueous amino acid
Ac	acridine
AcH^+	protonated acridine
A_j	fitting parameter, j = 0 to 14
b	temperature and/or pressure dependent function; adjustable parameter
b_i	functional group specific adjustable parameter
b_j	temperature and pressure independent parameter characteristic of an aqueous ion or electrolyte, j = 1 to 3
c	temperature and/or pressure dependent function
c_i	functional group specific adjustable parameter
c_j	temperature and pressure independent parameter characteristic of an aqueous ion or electrolyte, j = 1 to 3
c_p	specific heat capacity of a solution
$c_{p,\,1}$	specific heat capacity of a solvent
$c_{p,\,w}$	specific heat capacity of water
C	concentration of a dissolved species in $mol \cdot L^{-1}$
$C_{H,\,i}$	integration constant for ionic groups obtained from experimentally determined values of the standard partial molar enthalpy of hydration of functional group i
C_k	concentration of species k in $mol \cdot mL^{-1}$
$C^*_{p,\,1}$	molar heat capacity of a solvent
C°_p	standard partial molar heat capacity
$C^\circ_{p,\,Amino}$	contribution to the standard partial molar heat capacity due to the amino acid functional group
$C^\circ_{p,\,Anionic}$	standard partial molar heat capacity of A^-
$C^\circ_{p,\,Cationic}$	standard partial molar heat capacity of H_2A^+
$C^\circ_{p,\,Neutral}$	standard partial molar heat capacity of HA°
$C^\circ_{p,Zwitterionic}$	standard partial molar heat capacity of $HA^\pm$
$C^{corr}_{p,\,i}$	correction to the standard partial molar heat capacity of functional group i
$C^{ig}_{p,\,i}$	molar heat capacity of functional group i in the ideal gas state
$C^\circ_{p,\,i}$	standard partial molar heat capacity of functional group i

$C^{o}_{p,\,intr}$	intrinsic gas phase standard partial molar heat capacity of a species (0.10 MPa, ideal gas)
$C_{p,\,w}$	molar heat capacity of water
$C^{ig}_{p,\,w}$	molar heat capacity of water in the ideal gas state at 0.1 MPa
$C_{p,\,sol}$	heat capacity of a solution
$C_{p,\,\phi}$	apparent molar heat capacity of a solute
$C_{S,\,i}$	integration constant for ionic groups obtained from experimentally determined values of the standard partial molar entropy of hydration of functional group i
ΔC^{o}_{p}	standard partial molar heat capacity of reaction at a given temperature T
$\Delta C^{o}_{p,n}$	non-solvation contribution to the standard partial molar heat capacity
$\Delta C^{o}_{p,s}$	solvation contribution to the standard partial molar heat capacity
$\Delta_{hyd} C^{o}_{p,ss}$	change in the standard partial molar heat capacity arising from the difference in standard states between the gas phase (0.1 MPa, ideal gas) and solution (hypothetical 1 molal solution)
$\Delta_{hyd} C^{o}_{p,\,i}$	standard partial molar heat capacity of hydration of functional group i
$\Delta_{r} C^{o}_{p}$	standard partial molar heat capacity of reaction at a pressure p
$\Delta_{solv} C^{o}_{p,\,Born}$	standard partial molar heat capacity of polarization for a dissolved ionic species
$\Delta_{solv}\, C^{o}_{p,\,dipole}$	standard partial molar heat capacity of polarization for a dissolved neutral dipolar species
$\Delta_{solv} C^{o}_{p,\,hydr}$	standard partial molar heat capacity due to the short-range hydration effects arising from the hydrogen-bonded "structure" of water in the immediate vicinity of the solute
$\Delta_{solv} C^{o}_{p,\,non\text{-}dipole}$	$(C^{o}_{p,\,intr} + \Delta_{solv} C^{o}_{p,\,hydr})$
$\Delta_{solv} C^{o}_{p,\,pol}$	standard partial molar heat capacity due to the long-range polarization of water caused by the localized charge distribution within the solute
$\Delta_{solv} C^{o}_{p,\,ss}$	change in the standard partial molar heat capacity arising from the difference in standard states between the gas phase (0.10 MPa, ideal gas) and solution (hypothetical 1 molal solution)
d	distance between charges in a zwitterion
d_i	functional group specific adjustable parameter
d_j	temperature and pressure independent fitting parameter, $j = 0$ to 7
e	charge on an electron
e_i	functional group specific adjustable parameter
E	standard partial molar expansibility of a solution
E_A	activation energy
f	heat-loss correction factor
F_m	mass flow rate
F_{m1}	mass flow rate of a reference fluid

F_{m2}	mass flow rate of a sample solution
F_{V1}	volumetric flow rate of a reference fluid
F_{V2}	volumetric flow rate of a sample solution
ΔF_m	change in the mass flow rate from F_{m1}
g_i	functional group specific adjustable parameter
G°_{aq}	Gibbs free energy of an aqueous species (hypothetical 1 molal standard state)
G°_{intr}	intrinsic gas phase Gibbs free energy of a species (0.10 MPa, ideal gas)
G_w	molar Gibbs free energy of water
G^{ig}_w	molar Gibbs free energy of water in the ideal gas state at 0.1 MPa
ΔG°	the Gibbs free energy of ionization for an aqueous species
$\Delta G^{\circ}_{T,p}$	the Gibbs free energy of reaction at a given temperature T and pressure p
$\Delta G^{\circ}_{Tr,pr}$	the Gibbs free energy of reaction at the reference temperature T_r and pressure p_r
$\Delta_f G^{\circ}$	standard partial molar Gibbs free energy of formation as a function of temperature
$\Delta_f G^{\circ}_i$	standard partial molar Gibbs free energy of formation of functional group i
$\Delta_f G^{\circ}_i [T_r, p_r]$	standard partial molar Gibbs free energy of formation of functional group i at T_r and p_r
$\Delta_{hyd} G^{\circ}_i$	standard partial molar Gibbs free energy of hydration of functional group i
$\Delta_{hyd} G^{\circ}_{ss}$	change in the standard partial molar Gibbs free energy arising from the difference in standard states between the gas phase (0.1 MPa, ideal gas) and solution (hypothetical 1 molal solution)
$\Delta_r G^{\circ}$	standard partial molar Gibbs free energy of reaction
$\Delta_{solv} G^{o}_{Born}$	ionic contribution to the Gibbs free energy of polarization
$\Delta_{solv} G^{o}_{dipole}$	dipole contribution to the Gibbs free energy of polarization
$\Delta_{solv} G^{o}_{hydr}$	Gibbs free energy due to the short-range hydration effects arising from the hydrogen-bonded "structure" of water in the immediate vicinity of the solute
$\Delta_{solv} G^{o}_{octopole}$	octopole contribution to the Gibbs free energy of polarization
$\Delta_{solv} G^{o}_{pol}$	Gibbs free energy due to the long-range polarization of water caused by the localized charge distribution within the solute
$\Delta_{solv} G^{o}_{quadrupole}$	quadrupole contribution to the Gibbs free energy of polarization
$\Delta_{solv} G^{o}_{ss}$	Gibbs free energy arising from the difference in standard states between the gas phase (1 bar, ideal gas) and solution (hypothetical 1 molal solution)
H^{corr}_i	correction to the standard partial molar enthalpy of functional group i
H_w	molar enthalpy of water
H^{ig}_w	molar enthalpy of water in the ideal gas state at 0.1 MPa

$HA^{\pm}$	zwitterionic form of an aqueous amino acid
HA^{o}	neutral form of an aqueous amino acid
H_2A^{+}	protonated form of an aqueous amino acid
HX	protonated form of an aqueous colorimetric indicator
ΔH°	enthalpy of ionization for an aqueous species
$\Delta_f H^{\circ}$	standard partial molar enthalpy of formation as a function of temperature
$\Delta_f H^{\circ}_i$	standard partial molar enthalpy of formation of functional group i
$\Delta_f H^{\circ}_i [T_r, p_r]$	standard partial molar enthalpy of formation of functional group i at T_r and p_r
$\Delta_{hyd} H^{\circ}_i$	standard partial molar enthalpy of hydration of functional group i
$\Delta_{hyd} H^{\circ}_i [T_r, p_r]$	standard partial molar enthalpy of hydration of functional group i at T_r and p_r
$\Delta_{hyd} H^{o}_{ss}$	change in the standard partial molar enthalpy arising from the difference in standard states between the gas phase (0.1 MPa, ideal gas) and solution (hypothetical 1 molal solution)
$\Delta_r H^{\circ}_{T, p}$	standard partial molar enthalpy of reaction at a temperature T and a pressure p
$\Delta_r H^{\circ}_{Tr, pr}$	standard partial molar enthalpy of reaction at T_r and p_r
$\Delta_{solv} H^{o}_{Born}$	enthalpy of polarization for a dissolved ionic species
$\Delta_{solv} H^{o}_{dipole}$	enthalpy of polarization for a dissolved neutral dipolar species
j	fitting parameter
k	rate constant
K	ionization constant for an aqueous species; equilibrium constant associated with a reaction
K_4	(K_2 / K_w)
K_a	acid dissociation constant for acetic acid
K_{a1}	first acid dissociation constant for phosphoric acid
K_d	characteristic constant of a vibrating tube densitometer
$K_{Indicator}$	equilibrium constant for the deprotonation of a colorimetric indicator
K_j	equilibrium constant, j = 1 to 3
$K_{T, p}$	equilibrium constant associated with a reaction at a given temperature T and pressure p
$K_{Tr, pr}$	equilibrium constant associated with a reaction at T_r and p_r
K_w	dissociation constant of water
$K_{\beta\text{-}naphthoic}$	equilibrium constant for the deprotonation of β-naphthoic acid
$K^{-1}_{Acridine}$	equilibrium constant for the protonation of acridine
m	molality of a solution
m°	1 mol·kg^{-1}
M	molar mass

M_1	molar mass of a solvent
M_2	molar mass of a solute
M_w	molar mass of water
n_1	moles of pure solvent
n_2	moles of solute
n_i	number of occurrences of functional group i in a solute
n_k	number of molecules of species k per unit volume
N	total number of distinct functional groups in a solute
N_A	Avogadro's number
Nap^-	deprotonated β-naphthoic acid
NapH	β-naphthoic acid
p	pressure
p°	0.1 MPa
p_r	reference pressure (usually taken to be 0.1 MPa)
P	molar polarizability
q	magnitude of an electrical charge
Q	Born function
r	radius of a gaseous species
R	universal gas constant
r_e	effective radius
S_i^{corr}	correction to the standard partial molar entropy of functional group i
S_w	molar entropy of water
S_w^{ig}	molar entropy of water in the ideal gas state at 0.1 MPa
ΔS°	entropy of ionization for an aqueous species
$\Delta S_{T,p}^{\circ}$	entropy of reaction at a given temperature T and pressure p
$\Delta S_{Tr,pr}^{\circ}$	entropy of reaction at a reference temperature T_r and pressure p_r
$\Delta_f S^\circ$	standard partial molar entropy of formation as a function of temperature
$\Delta_f S_i^\circ$	standard partial molar entropy of formation of functional group i
$\Delta_f S_i^\circ [T_r, p_r]$	standard partial molar entropy of formation of functional group i at T_r and p_r
$\Delta_{hyd} S_i^\circ$	standard partial molar entropy of hydration of functional group i
$\Delta_{hyd} S_i^\circ [T_r, p_r]$	standard partial molar entropy of hydration of functional group i at T_r and p_r
$\Delta_{hyd} S_{ss}^{o}$	change in the standard partial molar entropy arising from the difference in standard states between the gas phase (0.1 MPa, ideal gas) and solution (hypothetical 1 molal solution)
$\Delta_{solv} S_{Born}^{o}$	entropy of polarization for a dissolved ionic species
$\Delta_{solv} S_{dipole}^{o}$	entropy of polarization for a dissolved neutral dipolar species
$t_{1/2}$	half life

T	temperature
T_c	critical temperature of water equal to 647.126 K
T_d	temperature of the delay line in the differential flow calorimeter
T_r	reference temperature (usually taken to be 298.15 K)
T_R	(T/373.15 K)
V	volume
V_1^*	molar volume of a pure solvent
V^o	standard partial molar volume
V°_{Amino}	contribution to the standard partial molar volume due to the amino acid functional group
$V^\circ_{Anionic}$	standard partial molar volume of A^-
$V^\circ_{Cationic}$	standard partial molar volume of H_2A^+
V°_i	standard partial molar volume of functional group i
V^o_{intr}	intrinsic gas phase standard partial molar volume
$V^\circ_{Neutral}$	standard partial molar volume of HA^o
$V^\circ_{Zwitterionic}$	standard partial molar volume of $HA^\pm$
V_{sol}	volume of a solution
V^o_{ss}	standard partial molar volume arising from the difference in standard states between the gas phase (0.1 MPa, ideal gas) and solution (hypothetical 1 molal solution)
V_w	molar volume of water
V_ϕ	apparent molar volume of a solute
ΔV°	standard partial molar volume of ionization for an aqueous species
ΔV^o_n	non-solvation contribution to the standard partial molar volume
ΔV^o_s	solvation contribution to the standard partial molar volume
$\Delta V^o_{T,p}$	standard partial molar volume of reaction at a given temperature T and pressure p
$\Delta_{solv}V^o_{Born}$	standard partial molar volume of polarization for a dissolved ionic species
$\Delta_{solv}V^o_{dipole}$	standard partial molar volume of polarization for a dissolved neutral dipolar species
$\Delta_{solv}V^o_{hydr}$	standard partial molar volume due to the short-range hydration effects arising from the hydrogen-bonded "structure" of water in the immediate vicinity of the solute
$\Delta_{solv}V^o_{pol}$	standard partial molar volume due to the long-range polarization of water caused by the localized charge distribution within the solute
$\Delta_{solv}V^o_{ss}$	standard partial molar volume arising from the difference in standard states between the gas phase (0.10 MPa, ideal gas) and solution (hypothetical 1 molal solution)

W	power required to increase the temperature of a fluid in the differential flow calorimeter by ΔT
W_1	power required to increase the temperature of the reference fluid in the differential flow calorimeter by ΔT
W_2	power required to increase the temperature of the sample solution in the differential flow calorimeter by ΔT
ΔW	$W_1 - W_2$
X^-	deprotonated form of an aqueous colorimetric indicator
Z	ionic charge
Z_e	effective charge on a neutral aqueous organic species
α_{0k}	constant that depends only on k
α_1	solvent expansitivity coefficient
α_w	expansitivity coefficient of water
β_w	compressibility coefficient of water
δ	molar dielectric increment
δ_i	functional group specific parameter determined by the charge on the functional group
$\Delta_{a,i}$	functional group specific parameter
$\Delta_{b,i}$	functional group specific parameter
$\Delta_{c,i}$	functional group specific parameter
$\Delta_{d,i}$	functional group specific parameter
ε	dielectric constant associated with a dissolved species
ε_r	solvent dielectric constant
ε_o	permittivity of free space
$\varepsilon_{Ac}(\lambda)$	effective molal extinction coefficient for Ac at a given value of λ
$\varepsilon_{AcH^+}(\lambda)$	effective molal extinction coefficient for AcH^+ at a given value of λ
$\varepsilon_{HX}(\lambda)$	effective molal extinction coefficient for HX at a given value of λ
$\varepsilon_{Nap^-}(\lambda)$	effective molal extinction coefficient for Nap^- at a given value of λ
$\varepsilon_{NapH}(\lambda)$	effective molal extinction coefficient for NapH at a given value of λ
$\varepsilon_{X^-}(\lambda)$	effective molal extinction coefficient for X^- at a given value of λ
ϑ	5000 $cm^3 \cdot kg^{-1}$
θ	1500 K
Θ	solvent parameter equal to 228 K
κ_S°	standard partial molar adiabatic compressibility
κ_T°	standard partial molar isothermal compressibility
$\Delta\kappa_T^\circ$	standard partial molar isothermal compressibility of ionization for an aqueous species
$\Delta_{solv}\kappa_{T,Born}^o$	standard partial molar isothermal compressibility of polarization for a dissolved ionic species

$\Delta_{solv}\kappa_{T,dipole}^{o}$	standard partial molar isothermal compressibility of polarization for a dissolved neutral dipolar species
λ	-10000 $cm^3 \cdot kg^{-1}$; wavelength
Λ	conversion factor between different possible aqueous standard states
Λ_G	correction factor for the standard partial molar Gibbs free energy
Λ_S	correction factor for the standard partial molar entropy
μ	dipole moment
μ_o	gas phase dipole moment
$\boldsymbol{\mu}_k$	permanent dipole moment of aqueous molecule k
$\bar{\boldsymbol{\mu}}_k$	vector sum of the dipole moment of aqueous molecule k and the dipole moments due to all of the neighbouring molecules
ξ	temperature independent coefficient characteristic of an aqueous ion or electrolyte at a given pressure
Ξ_i°	contribution to Ξ° due to functional group i
Ξ_{ss}	standard state term
ρ	solution density
ρ_1	solvent density
ρ_{Td}	density of a sample solution at the temperature of the delay line in the differential flow calorimeter
$\rho_{w,Td}$	density of a reference fluid at the temperature of the delay line in the differential flow calorimeter
ρ_w	density of water
σ	temperature independent coefficient characteristic of an aqueous ion or electrolyte at a given pressure; overall weighted standard deviation obtained from a least squares fit
σ_δ	standard deviation associated with a molar dielectric increment
σ_μ	standard deviation associated with a dipole moment
$\sigma_{V_{298}^o}$	uncertainty associated with V^o at 298.15 K
$\sigma_{V_T^o}$	uncertainty associated with V^o at temperatures other than 298.15 K
τ	resonance period of a solution in the densitometer U-tube
τ_w	resonance period of water in the densitometer U-tube
$\Phi_k(\boldsymbol{r}_k)$	reaction potential
Ψ	solvent parameter equal to 260.0 MPa
ω	temperature and pressure dependent Born coefficient
ω_e	temperature and pressure independent effective Born coefficient

CHAPTER 1.0 INTRODUCTION

1.1 The Importance of Amino Acids.

The properties of amino acids in hydrothermal solutions are of intense interest to biochemists and geochemists interested in understanding the metabolic processes in thermophilic bacteria and the possible mechanisms for the origin of life at deep ocean vents.

Spies *et al.* (1980) divide deep ocean vents into two broad classes: Galápagos-type vents and sulfide-mound hot-water vents. The most common type of hydrothermal vent is the Galápagos-type vent. These vents are characterised by ~ 290 K vent water in ~ 275 K surroundings. The fauna associated with the Galápagos-type vents include crabs, white clams, and giant tube worms and is their most visible feature. Sulfide-mound hot-water vents are characterised by ~ 650 ± 30 K vent water in ~ 275 K surroundings. The vent water is ejected through a limited number of chimneys or stacks with a relatively high velocity either as a clear fluid, or as a plume of white or black suspended particles. The discovery of these high temperature vents marked the first time that liquid water at temperatures well in excess of 373 K had been found in open contact with the biosphere. Since the high pressures, which permit these superheated conditions, counteract some of the destructive effects of high temperature on biochemical systems, it is reasonable to wonder whether thermophilic organisms exist in these high temperature vents. The extreme environment created by the high temperature vents resembles the conditions thought to have existed on primitive Earth, and it has been postulated that these vents were the source of life on Earth. Bada *et al.*

(1995), Baross and Deming (1983), Crabtree (1997), Miller and Bada (1988), Ranganayaki *et al.* (1977), Shock (1990), Shock (1992), Trent *et al.* (1984), and Yanagawa and Kojima (1985) have considered various aspects of this hypothesis. However, all of these studies lack reliable, experimentally determined, thermodynamic data for biomolecules, including amino acids, under hydrothermal conditions.

Amino acids exist in solution primarily as zwitterions as demonstrated by the calculations given in Section 4.5. As such, their properties are intermediate between ions, which carry an overall non-zero charge, and neutral organic species, which have little or no localization of charge. Tanger and Helgeson (1988) and Shock and Helgeson (1988) have developed a revised version of the Helgeson-Kirkham-Flowers (HKF) model capable of predicting the thermodynamic properties of aqueous ions and electrolytes at elevated temperatures and pressures. Shock (1990, 1992, 1995), Shock and Helgeson (1990), and Amend and Helgeson (1997) have extended the revised HKF model to predict the thermodynamic properties of aqueous organic species. Although this model includes predictions for amino acids, the predictive correlations are based on the limited amount of high temperature data available in 1988. Moreover, the failure of Shock, Helgeson, and Amend to consider the zwitterionic nature of the aqueous amino acids suggests that the extrapolated results are very uncertain at high temperatures. Except for the very recent measurements of the standard partial molar volumes for glycine, by Hakin *et al.* (1998), there are no experimental values for the thermodynamic properties of aqueous amino acids above

348 K in the literature. The lack of reliable, experimentally determined, thermodynamic data for amino acids under hydrothermal conditions has allowed these questionable predictions to remain untested.

The goal of this research is to determine the thermodynamic properties of aqueous amino acids at high temperatures and pressures and to use these data to identify the contribution of major solvation effects.

1.2 Thermodynamics of Aqueous Solutions.

1.2.1 Thermodynamic Relationships.

The Gibbs free energy of reaction $\Delta G^{\circ}_{T,p}$ at a given temperature T and pressure p can be used to calculate the equilibrium constant $K_{T,p}$ associated with the reaction at the specified conditions.

$$lnK_{T,p} = \frac{-\Delta G^{o}_{T,p}}{RT} \qquad (1.2.1.1)$$

Here R is the gas constant. Expressions for the change in $\Delta G^{\circ}_{T,p}$ with respect to temperature and pressure are given in equations (1.2.1.2) and (1.2.1.3), respectively.

$$\left(\frac{\partial \Delta G^{o}_{T,p}}{\partial T}\right)_{p} = -\Delta S^{o}_{T,p} \qquad (1.2.1.2)$$

$$\left(\frac{\partial \Delta G^{o}_{T,p}}{\partial p}\right)_{T} = \Delta V^{o}_{T,p} \qquad (1.2.1.3)$$

Here $\Delta S_{T,p}^{\circ}$ is the entropy of reaction and $\Delta V_{T,p}^{\circ}$ is the standard partial molar volume of reaction at the temperature and pressure of interest. Integration of equations (1.2.1.2) and (1.2.1.3) yields the following expression for $\Delta G_{T,p}^{\circ}$:

$$\Delta G_{T,p}^{o} = \Delta G_{Tr,pr}^{o} - \int_{T_r}^{T} \Delta S_{T,p}^{o} dT + \int_{p_r}^{p} \Delta V_{Tr,p}^{o} dp \qquad (1.2.1.4)$$

T_r is the reference temperature (usually taken to be 298.15 K) and p_r is the reference pressure (usually taken to be 0.1 MPa). $\Delta G_{Tr,pr}^{\circ}$ is the Gibbs free energy of reaction at the temperature and pressure of reference. If the system under consideration remains at constant pressure then the temperature dependence of $\Delta S_{T,p}^{\circ}$ can be expressed as:

$$\left(\frac{\partial \Delta S_{T,p}^{o}}{\partial T} \right)_{p} = \frac{\Delta C_{p}^{o}}{T} \qquad (1.2.1.5)$$

Here ΔC_p° is the standard partial molar heat capacity of reaction at the temperature and pressure of interest. Integration of equation (1.2.1.5) gives:

$$\Delta S_{T,p}^{o} = \Delta S_{Tr,pr}^{o} + \int_{T_r}^{T} \frac{\Delta C_{p}^{o}}{T} dT \qquad (1.2.1.6)$$

1.2.2 Apparent Molar Volumes.

The molar volume of a pure solvent is denoted as V_1^* and has units of $cm^3 \cdot mol^{-1}$. Add n_2 moles of a solute to n_1 moles of the pure solvent and the volume of the resulting solution

is denoted as V_{sol} which has units of cm^3. The apparent molar volume V_ϕ of the solute is defined as the change in the volume of the solution when n_2 moles of a solute are added to n_1 moles of pure solvent, per mole of the solute. This concept is expressed mathematically as follows:

$$V_\phi = \frac{V_{sol} - n_1 V_1^*}{n_2} \tag{1.2.2.1}$$

If 1000 g of solvent is considered, then equation (1.2.2.1) becomes:

$$V_\phi = \left(\frac{V_{sol}}{m}\right) - \left(\frac{1000\, V_1^*}{m\, M_1}\right) \tag{1.2.2.2}$$

Here M_1 is the molar mass of the solvent and m is the molality of the solution. Expressing V_ϕ in terms of density ρ rather than volume using:

$$V = \frac{M}{\rho} \tag{1.2.2.3}$$

yields:

$$V_\phi = \left(\frac{1000(\rho_1 - \rho)}{(m\rho\rho_1)}\right) + \left(\frac{M_2}{\rho}\right) \tag{1.2.2.4}$$

Here ρ and ρ_1 are the densities of the solution and solvent, respectively and M_2 is the molar mass of the solute.

1.2.3 Apparent Molar Heat Capacities.

Likewise, the apparent molar heat capacity $C_{p,\phi}$ of the solute is defined as:

$$C_{p,\phi} = \frac{C_{p,sol} - n_1 C_{p,1}^*}{n_2} \qquad (1.2.3.1)$$

Here $C_{p,sol}$ is the heat capacity of the solution with units $J \cdot K^{-1}$ and $C_{p,1}^*$ is the molar heat capacity of the pure solvent with units $J \cdot mol^{-1} \cdot K^{-1}$. If 1000 g of solvent is considered, then equation (1.2.3.1) becomes:

$$C_{p,\phi} = \left(\frac{C_{p,sol}}{m} \right) - \left(\frac{1000 C_{p,1}^*}{m M_1} \right) \qquad (1.2.3.2)$$

Expressing $C_{p,sol}$ and $C_{p,1}^*$ as specific heat capacities gives:

$$C_{p,\phi} = M_2 c_p + \left[\frac{1000 (c_p - c_{p,1})}{m} \right] \qquad (1.2.3.3)$$

where c_p and $c_{p,1}$ are the specific heat capacities of the solution and solvent, respectively.

1.2.4 The Density Model.

It was observed by Franck (1956, 1961) that the ionization constant K of many aqueous species exhibits approximately linear behaviour at elevated temperatures and pressures when log K is plotted against log ρ_w for a very wide range of ρ_w. This observation led Marshall and Franck (1981) to develop the following expression to represent the ionization constant of water at temperatures up to 1273 K and at pressures up to 1000 MPa.

$$\log K = \left(d_1 + \frac{d_2}{T} + \frac{d_3}{T^2} + \frac{d_4}{T^3} \right) + \left(d_5 + \frac{d_6}{T} + \frac{d_7}{T^2} \right) \log \rho_w \qquad (1.2.4.1)$$

Here d_1, d_2, d_3, d_4, d_5, d_6, and d_7 are fitting parameters, and ρ_w is the density of water. Mesmer *et al.* (1988) later demonstrated that equation (1.2.4.1) can be used as a general expression to represent most ionization and ion-pairing reactions.

Equation (1.2.4.1) can be used to obtain expressions for other thermodynamic quantities. An expression for $\Delta G°$, the Gibbs free energy of ionization for an aqueous species was obtained through the following elementary relationship:

$$\Delta G^{\,o} = -RT \ln K \qquad (1.2.4.2)$$

Hence:

$$\Delta G^{\,o} = -2.303RT \left[\left(d_1 + \frac{d_2}{T} + \frac{d_3}{T^2} + \frac{d_4}{T^3} \right) + \left(d_5 + \frac{d_6}{T} + \frac{d_7}{T^2} \right) \log \rho_w \right] \qquad (1.2.4.3)$$

Similarly, an expression for the enthalpy of ionization for an aqueous species $\Delta H°$ was obtained from the relation:

$$\Delta H^{\,o} = \left(\frac{\partial \left(\frac{\Delta G^{\,o}}{T} \right)}{\partial \left(\frac{1}{T} \right)} \right)_p = -T^2 \left[\frac{\partial}{\partial T} \left(\frac{\Delta G^{\,o}}{T} \right) \right]_p \qquad (1.2.4.4)$$

Hence:

$$\Delta H^{o} = -2.303R\left[d_2 + \frac{2d_3}{T} + \frac{3d_4}{T^2} + \left(d_6 + \frac{2d_7}{T}\right)\log\rho_w\right] - RT^2\alpha_w\left(d_5 + \frac{d_6}{T} + \frac{d_7}{T^2}\right) \quad (1.2.4.5)$$

Here $\alpha_w = -(1/\rho_w)(\partial\rho_w/\partial T)_p$ is the expansitivity coefficient of water. Expressions for the standard partial molar heat capacity of ionization ΔC_p^o, the entropy of ionization $\Delta S°$, the standard partial molar volume of ionization $\Delta V°$, and the standard partial molar isothermal compressibility of ionization $\Delta\kappa_T{}^o$ were obtained for an aqueous species from the relationships:

$$\Delta C_p{}^o = \left(\frac{\partial \Delta H^o}{\partial T}\right)_p \quad (1.2.4.6)$$

$$\Delta S^o = -\left(\frac{\partial \Delta G^o}{\partial T}\right)_p \quad (1.2.4.7)$$

$$\Delta V^o = \left(\frac{\partial \Delta G^o}{\partial p}\right)_T \quad (1.2.4.8)$$

$$\Delta\kappa_T{}^o = -\left(\frac{\partial \Delta V^o}{\partial p}\right)_T \quad (1.2.4.9)$$

Hence:

$$\Delta C_p{}^o = 2.303R\left[\frac{2d_3}{T^2} + \frac{6d_4}{T^3} + \left(\frac{2d_7}{T^2}\right)\log\rho_w\right] - R\alpha_w\left(2d_5T - \frac{2d_7}{T}\right) - RT^2\left(d_5 + \frac{d_6}{T} + \frac{d_7}{T^2}\right)\left(\frac{\partial\alpha_w}{\partial T}\right)_p \quad (1.2.4.10)$$

$$\Delta S^o = 2.303R\left[d_1 - \frac{d_3}{T^2} - \frac{2d_4}{T^3} + \left(d_5 - \frac{d_7}{T^2}\right)\log\rho_w\right] - RT\alpha_w\left(d_5 + \frac{d_6}{T} + \frac{d_7}{T^2}\right) \quad (1.2.4.11)$$

$$\Delta V^{o} = -RT\beta_{w}\left(d_5 + \frac{d_6}{T} + \frac{d_7}{T^2}\right) \tag{1.2.4.12}$$

$$\Delta\kappa_T{}^{o} = RT\left(d_5 + \frac{d_6}{T} + \frac{d_7}{T^2}\right)\left(\frac{\partial\beta_w}{\partial p}\right)_T \tag{1.2.4.13}$$

Here $\beta_w = (1/\rho_w)(\partial\rho_w/\partial p)_T$ is the compressibility coefficient of water. In practice the d_3, d_4, d_5, and d_7 fitting parameters are often set equal to zero when modelling systems at temperatures less than 573 K. Therefore, a simplified form of the density model used by authors such as Anderson *et al.* (1991) can be summarized as follows:

$$\log K = \left(d_1 + \frac{d_2}{T}\right) + \left(\frac{d_6}{T}\right)\log\rho_w \tag{1.2.4.14}$$

$$\Delta G^{o} = -2.303RT\left[\left(d_1 + \frac{d_2}{T}\right) + \left(\frac{d_6}{T}\right)\log\rho_w\right] \tag{1.2.4.15}$$

$$\Delta H^{o} = -2.303R\left(d_2 + d_6\log\rho_w\right) - d_6 RT\alpha_w \tag{1.2.4.16}$$

$$\Delta C_p{}^{o} = -RTd_6\left(\frac{\partial\alpha_w}{\partial T}\right)_p \tag{1.2.4.17}$$

$$\Delta S^{o} = R\,(2.303d_1 - d_6\alpha_w) \tag{1.2.4.18}$$

$$\Delta V^{o} = -d_6 R\beta_w \tag{1.2.4.19}$$

$$\Delta\kappa_T{}^{o} = d_6 R\left(\frac{\partial\beta_w}{\partial p}\right)_T \tag{1.2.4.20}$$

1.3 Solvation Models.

1.3.1 Solute Hydration.

The Gibbs free energy $\Delta_{solv}G^o$ associated with transferring a species from an ideal gas into solution at infinite dilution can be expressed as:

$$\Delta_{solv}G^{\circ} = G^{\circ}_{aq} - G^{\circ}_{intr} - \Delta_{solv}G^{\circ}_{ss} \qquad (1.3.1.1)$$

Here G°_{aq} is the Gibbs free energy of the aqueous species (hypothetical 1 molal standard state), and G°_{intr} is the intrinsic gas phase Gibbs free energy of the species (0.10 MPa, ideal gas). The term $\Delta_{solv}G^{\circ}_{ss}$ is the change in the Gibbs free energy arising from the difference in standard states between the gas phase and solution (Ben-Naim, 1987),

$$\Delta_{solv}G^{\circ}_{ss} = RT\ln\left(\frac{RTm^{\circ}\rho_w}{p^{\circ}}\right) \qquad (1.3.1.2)$$

where $m^\circ = 1$ mol·kg^{-1} and $p^\circ = 0.1$ MPa.

The Gibbs free energy of solvation $\Delta_{solv}G^\circ$ arises in part as a result of configurational changes in the water caused by the presence of the solute. These are commonly identified with two major effects, the long-range polarization of water caused by the localized charge distribution within the solute $\Delta_{solv}G^{\circ}_{pol}$, and short-range hydration effects arising from the hydrogen-bonded "structure" of water in the immediate vicinity of the solute $\Delta_{solv}G^{\circ}_{hydr}$.

$$\Delta_{solv}G^{\circ} = \Delta_{solv}G^{\circ}_{pol} + \Delta_{solv}G^{\circ}_{hydr} \qquad (1.3.1.3)$$

When a dissolved species has a significant charge distribution, as in the case of ions and zwitterions, there is a polarization of the bulk solvent due to long-range interactions

between the dissolved species and the solvent molecules. The electric field produced by the charge distribution within the solute polarizes surrounding solvent molecules. If the solvent molecules have a permanent dipole moment, they will orient themselves around the dissolved species. These long-range interactions can be modelled by using an extension of the Born continuum model as discussed by Böttcher (1973). In this model a dissolved species is represented by a collection of discrete charges q_k contained in a cavity embedded in a structureless polarizable dielectric continuum that represents the solvent. The collection of charges induces a reaction potential in the dielectric continuum that in turn acts back on the dissolved charges. The energy of interaction of the solute with its environment is simply the difference in the reversible work required to form the charge distribution in the presence of the dielectric continuum, relative to that in a vacuum. Thus, the Gibbs free energy of polarization $\Delta_{solv}G^{o}_{pol}$ may be expressed as:

$$\Delta_{solv}G^{o}_{pol} = 0.5\sum_{k} q_k \Phi_R(\boldsymbol{r}_k) \qquad (1.3.1.4)$$

where $\Phi_k(\boldsymbol{r}_k)$ is the reaction potential. Expansion of this summation gives the following:

$$\Delta_{solv}G^{o}_{pol} = \Delta_{solv}G^{o}_{Born} + \Delta_{solv}G^{o}_{dipole} + \Delta_{solv}G^{o}_{quadrupole} + \Delta_{solv}G^{o}_{octopole} + \ldots \qquad (1.3.1.5)$$

Here $\Delta_{solv}G^{o}_{Born}$ is the ionic contribution to the Gibbs free energy of polarization, $\Delta_{solv}G^{o}_{dipole}$ is the dipole contribution to the Gibbs free energy of polarization, $\Delta_{solv}G^{o}_{quadrupole}$ is the quadrupole contribution, $\Delta_{solv}G^{o}_{octopole}$ is the octopole contribution, and so on. $\Delta_{solv}G^{o}_{Born}$ is discussed further in Section 1.3.2.1 and $\Delta_{solv}G^{o}_{dipole}$ is discussed further in Section 1.3.2.2.

The hydration term $\Delta_{solv}G^{o}_{hydr}$ represents the effect of perturbations in the solvent near the solute where both the finite size of the solvent and the short range interactions between the solvated species and the surrounding solvent molecules are important. These short range interactions may include hydrogen bonding between the solute and the nearest solvent molecules and perturbations of the bulk solvent structure in the immediate vicinity of the solute. $\Delta_{solv}G^{o}_{hydr}$ is difficult to model and is often represented by an empirical function. The solvation process is illustrated in Figure 1.3.1.1.

The standard partial molar volume V^{o} of an aqueous species is related to the Gibbs free energy of the aqueous species G^{o}_{aq} through the following expression:

$$V^{o} = \left(\frac{\partial G^{o}_{aq}}{\partial p} \right)_{T} \tag{1.3.1.6}$$

Combining equation (1.3.1.6) with equations (1.3.1.1) and (1.3.1.3) yields the expression:

$$V^{o} = V^{o}_{intr} + \Delta_{solv}V^{o}_{ss} + \Delta_{solv}V^{o}_{pol} + \Delta_{solv}V^{o}_{hydr} \tag{1.3.1.7}$$

The corresponding expression for the standard partial molar heat capacity C^{o}_{p} of an aqueous species can be obtained from the expression:

$$C^{o}_{p} = -2T\left[\frac{\partial}{\partial T}\left(\frac{G^{o}_{aq}}{T} \right) \right]_{p} - T^{2}\left[\frac{\partial^{2}}{\partial T^{2}}\left(\frac{G^{o}_{aq}}{T} \right) \right]_{p} \tag{1.3.1.8}$$

Combining equation (1.3.1.8) with equations (1.3.1.1) and (1.3.1.3) yields the expression:

$$C^{o}_{p} = C^{o}_{p,intr} + \Delta_{solv}C^{o}_{p,ss} + \Delta_{solv}C^{o}_{p,pol} + \Delta_{solv}C^{o}_{p,hydr} \tag{1.3.1.9}$$

a) Ionic Species

b) Dipolar Species

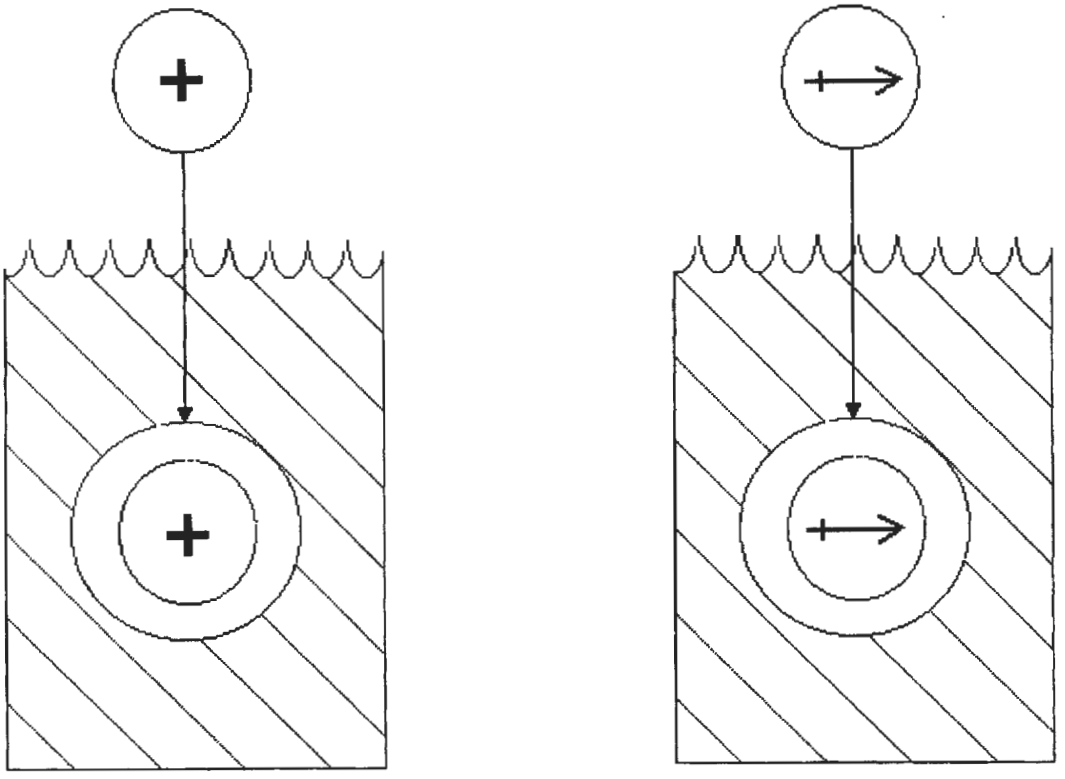

Figure 1.3.1.1 Schematic diagram of the solvation process.

1.3.2 Long Range Polarization.

1.3.2.1 Born Equation.

Often, when the dissolved species is ionic, only the first term in the $\Delta_{solv}G^{o}_{pol}$ summation is significant and therefore all other terms can be neglected. This leads to the well known Born equation for the Gibbs free energy of polarization for a dissolved ionic species $\Delta_{solv}G^{o}_{Born}$ (Born, 1920):

$$\Delta_{solv}G^{o}_{Born} = \frac{-(Ze)^2 N_A}{8\pi\varepsilon_o r_e}\left(\frac{(\varepsilon_r - 1)}{\varepsilon_r}\right) \qquad (1.3.2.1)$$

Here Z is the ionic charge, e is the charge on an electron, N_A is Avogadro's number, ε_r is the solvent dielectric constant, ε_0 is the permittivity of free space, and r_e is the *effective* radius of the dissolved species, *i.e.* the radius of the cavity in the bulk solvent. All quantities are in SI units.

Equation (1.3.2.1) can be used to obtain expressions for a number of other thermodynamic quantities. An expression for the enthalpy of polarization for a dissolved ionic species $\Delta_{solv}H^{o}_{Born}$ was obtained through the elementary relationship:

$$\Delta_{solv}H^{o}_{Born} = \left(\frac{\partial\left(\frac{\Delta_{solv}G^{o}_{Born}}{T}\right)}{\partial\left(\frac{1}{T}\right)}\right)_p = -T^2\left[\frac{\partial}{\partial T}\left(\frac{\Delta_{solv}G^{o}_{Born}}{T}\right)\right]_p \qquad (1.3.2.2)$$

Hence:

$$\Delta_{solv}H^{o}_{Born} = \frac{-(Ze)^2 N_A}{8\pi\varepsilon_o r_e}\left[1 - \left(\frac{1}{\varepsilon_r}\right) - \frac{T}{\varepsilon_r^{\,2}}\left(\frac{\partial\varepsilon_r}{\partial T}\right)_p\right] \tag{1.3.2.3}$$

Expressions for the standard partial molar heat capacity of polarization $\Delta_{solv}C^{o}_{p,Born}$, the entropy of polarization $\Delta_{solv}S^{o}_{Born}$, the standard partial molar volume of polarization $\Delta_{solv}V^{o}_{Born}$, and the standard partial molar compressibility of polarization $\Delta_{solv}\kappa^{o}_{T,Born}$ are obtained from the relationships:

$$\Delta_{solv}C^{o}_{p,\,Born} = \left(\frac{\partial\Delta_{solv}H^{o}_{Born}}{\partial T}\right)_p \tag{1.3.2.4}$$

$$\Delta_{solv}S^{o}_{Born} = -\left(\frac{\Delta_{solv}G^{o}_{Born}}{\partial T}\right)_p \tag{1.3.2.5}$$

$$\Delta_{solv}V^{o}_{Born} = \left(\frac{\partial\Delta_{solv}G^{o}_{Born}}{\partial p}\right)_T \tag{1.3.2.6}$$

$$\Delta_{solv}\kappa^{o}_{T,\,Born} = -\left(\frac{\Delta_{solv}V^{o}_{Born}}{\partial p}\right)_T \tag{1.3.2.7}$$

Hence:

$$\Delta_{solv}C^{o}_{p,Born} = \frac{-(Ze)^2 N_A}{8\pi\varepsilon_o r_e}\left[\frac{2T}{\varepsilon_r^{\,3}}\left(\frac{\partial\varepsilon_r}{\partial T}\right)_p^2 - \frac{T}{\varepsilon_r^{\,2}}\left(\frac{\partial^2\varepsilon_r}{\partial T^2}\right)_p\right] \tag{1.3.2.8}$$

$$\Delta_{solv}S^{o}_{Born} = \frac{(Ze)^2 N_A}{8\pi\varepsilon_o r_e}\left(\frac{1}{\varepsilon_r^2}\right)\left(\frac{\partial\varepsilon_r}{\partial T}\right)_p \tag{1.3.2.9}$$

$$\Delta_{solv}V^{o}_{Born} = \frac{-(Ze)^2 N_A}{8\pi\varepsilon_o r_e}\left(\frac{1}{\varepsilon_r^2}\right)\left(\frac{\partial\varepsilon_r}{\partial p}\right)_T \qquad (1.3.2.10)$$

$$\Delta_{solv}\kappa^{o}_{T,\,Born} = \frac{-(Ze)^2 N_A}{8\pi\varepsilon_o r_e}\left[\left(\frac{2}{\varepsilon_r^3}\right)\left(\frac{\partial\varepsilon_r}{\partial p}\right)_T^2 - \left(\frac{1}{\varepsilon_r^2}\right)\left(\frac{\partial^2\varepsilon_r}{\partial p^2}\right)_T\right] \qquad (1.3.2.11)$$

1.3.2.2 Dipole Solvation.

The Gibbs free energy of polarization for a dissolved neutral species reflects only the multipole moment terms in equation (1.3.1.5) since the first term is equal to zero. Often, when the neutral species is dipolar, only the second term in the $\Delta_{solv}G^{o}_{pol}$ summation is significant and therefore all other terms can be neglected. Beveridge and Schnuelle (1975) gave the following expression for the Gibbs free energy of polarization for a dissolved neutral dipolar species $\Delta_{solv}G^{o}_{dipole}$:

$$\Delta_{solv}G^{o}_{dipole} = \frac{\mu^2 N_A}{4\pi\varepsilon_o r_e^3}\left(\frac{(1-\varepsilon_r)}{(2\varepsilon_r+1)}\right) \qquad (1.3.2.12)$$

Here μ is the dipole moment of the charge distribution.

Although expressions for $\Delta_{solv}H^{o}_{Born}$, $\Delta_{solv}C^{o}_{p,\,Born}$, $\Delta_{solv}S^{o}_{Born}$, $\Delta_{solv}V^{o}_{Born}$, and $\Delta_{solv}\kappa^{o}_{T,\,Born}$ have been derived from equation (1.3.2.1) by Shock *et al.* (1992), Cobble and Murray (1977), and Wood *et al.* (1981), to our knowledge similar expressions for $\Delta_{solv}H^{o}_{dipole}$, $\Delta_{solv}C^{o}_{p,\,dipole}$, $\Delta_{solv}S^{o}_{dipole}$, $\Delta_{solv}V^{o}_{dipole}$, and $\Delta_{solv}\kappa^{o}_{T,\,dipole}$ have not been reported. Therefore, this author used the expression for $\Delta_{solv}G^{o}_{dipole}$ found in equation (1.3.2.12) with the standard thermodynamic

identities to obtain expressions for each of the thermodynamic quantities listed above. Expressions for the standard partial molar properties of solvent polarization for neutral dipolar species were derived from the relationships:

$$\Delta_{solv}H^{o}_{dipole} = \left(\frac{\partial\left(\frac{\Delta_{solv}G^{o}_{dipole}}{T} \right)}{\partial\left(\frac{1}{T} \right)} \right)_{p} = -T^{2}\left[\frac{\partial}{\partial T}\left(\frac{\Delta_{solv}G^{o}_{dipole}}{T} \right) \right]_{p} \qquad (1.3.2.13)$$

$$\Delta_{solv}C^{o}_{p,dipole} = \left(\frac{\partial \Delta_{solv}H^{o}_{dipole}}{\partial T} \right)_{p} \qquad (1.3.2.14)$$

$$\Delta_{solv}S^{o}_{dipole} = -\left(\frac{\Delta_{solv}G^{o}_{dipole}}{\partial T} \right)_{p} \qquad (1.3.2.15)$$

$$\Delta_{solv}V^{o}_{dipole} = \left(\frac{\partial \Delta_{solv}G^{o}_{dipole}}{\partial p} \right)_{T} \qquad (1.3.2.16)$$

$$\Delta_{solv}\kappa^{o}_{T,dipole} = -\left(\frac{\Delta_{solv}V^{o}_{dipole}}{\partial p} \right)_{T} \qquad (1.3.2.17)$$

to yield:

$$\Delta_{solv}H^{o}_{dipole} = \frac{N_A}{4\pi\varepsilon_o r_e^{3}}\left[\mu^{2}\left(\frac{(1-\varepsilon_r)}{(2\varepsilon_r+1)} \right) + \left(\frac{3T\mu^{2}}{(2\varepsilon_r+1)^{2}} \right)\left(\frac{\partial \varepsilon_r}{\partial T} \right)_{p} \right]$$

$$- \frac{N_A T\mu}{2\pi\varepsilon_o r_e^{3}}\left(\frac{1-\varepsilon_r}{2\varepsilon_r+1} \right)\left(\frac{\partial \mu}{\partial T} \right)_{p} \qquad (1.3.2.18)$$

$$\Delta_{solv}C^{o}_{p,dipole} = \frac{N_A}{4\pi\varepsilon_o r_e^3}\left[\left(\frac{\partial\varepsilon_r}{\partial T}\right)_p\left(\frac{\partial\mu}{\partial T}\right)_p\left(\frac{12T\mu}{(2\varepsilon_r+1)^2}\right)\right]$$

$$+\frac{N_A}{4\pi\varepsilon_o r_e^3}\left[\left(\frac{3T\mu^2}{(2\varepsilon_r+1)^2}\right)\left(\frac{\partial^2\varepsilon_r}{\partial T^2}\right)_p-\left(\frac{12T\mu^2}{(2\varepsilon_r+1)^3}\right)\left(\frac{\partial\varepsilon_r}{\partial T}\right)_p^2\right]$$

$$-\frac{N_A}{4\pi\varepsilon_o r_e^3}\left[\left(\frac{2T\mu(1-\varepsilon_r)}{(2\varepsilon_r+1)}\right)\left(\frac{\partial^2\mu}{\partial T^2}\right)_p+\left(\frac{2T(1-\varepsilon_r)}{(2\varepsilon_r+1)}\right)\left(\frac{\partial\mu}{\partial T}\right)_p^2\right] \quad (1.3.2.19)$$

$$\Delta_{solv}S^{o}_{dipole} = \frac{N_A}{4\pi\varepsilon_o r_e^3}\left[\left(\frac{3\mu^2}{(2\varepsilon_r+1)^2}\right)\left(\frac{\partial\varepsilon_r}{\partial T}\right)_p-2\mu\left(\frac{1-\varepsilon_r}{2\varepsilon_r+1}\right)\left(\frac{\partial\mu}{\partial T}\right)_p\right] \quad (1.3.2.20)$$

$$\Delta_{solv}V^{o}_{dipole} = \frac{\mu^2 N_A}{4\pi\varepsilon_o r_e^3}\left(\frac{-3}{(2\varepsilon_r+1)^2}\right)\left(\frac{\partial\varepsilon_r}{\partial p}\right)_T \quad (1.3.2.21)$$

$$\Delta_{solv}\kappa^{o}_{T,dipole} = \left(\frac{-N_A\mu^2}{4\pi\varepsilon_o r_e^3}\right)\left[\left(\frac{12}{(2\varepsilon_r+1)^3}\right)\left(\frac{\partial\varepsilon_r}{\partial p}\right)_T^2-\left(\frac{3}{(2\varepsilon_r+1)^2}\right)\left(\frac{\partial^2\varepsilon_r}{\partial p^2}\right)_T\right] \quad (1.3.2.22)$$

1.3.3 The Revised Helgeson-Kirkham-Flowers Model for Ionic and Organic Species.

Figures 1.3.3.1 and 1.3.3.2 illustrate the standard partial molar volumes measured by Shvedov and Tremaine (1997) for aqueous dimethylamine and dimethylammonium chloride, respectively. The behaviour of the V° data obtained for dimethylamine is typical of that observed for many aqueous non-electrolytes. Similarly, the behaviour of the V° data obtained for dimethylammonium chloride is typical of that observed for aqueous ions. The values of

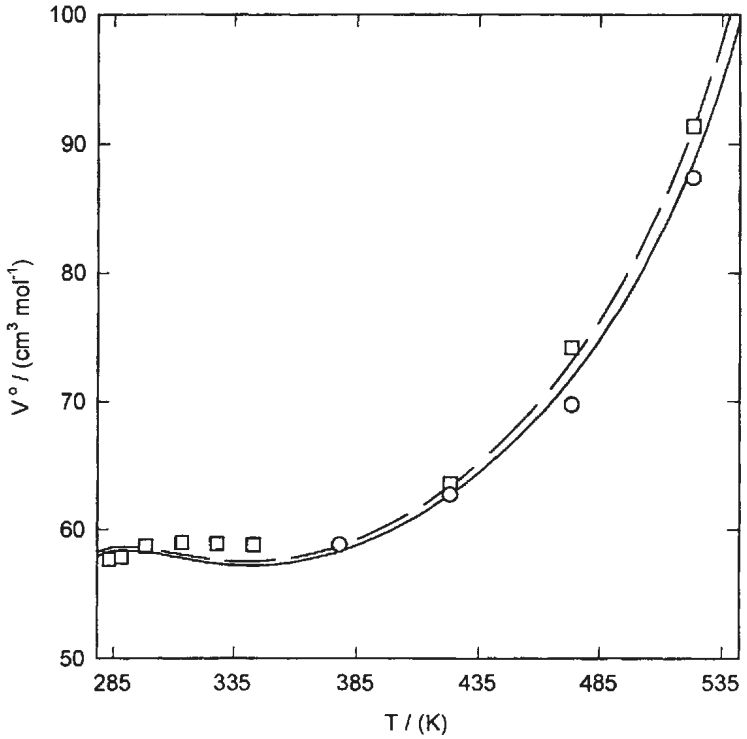

Figure 1.3.3.1 The standard partial molar volumes of V° of dimethylamine determined by Shvedov and Tremaine (1997). Symbols are the fitted isotherms:○, 10 MPa; □, steam saturation pressure. Lines are fitted values.

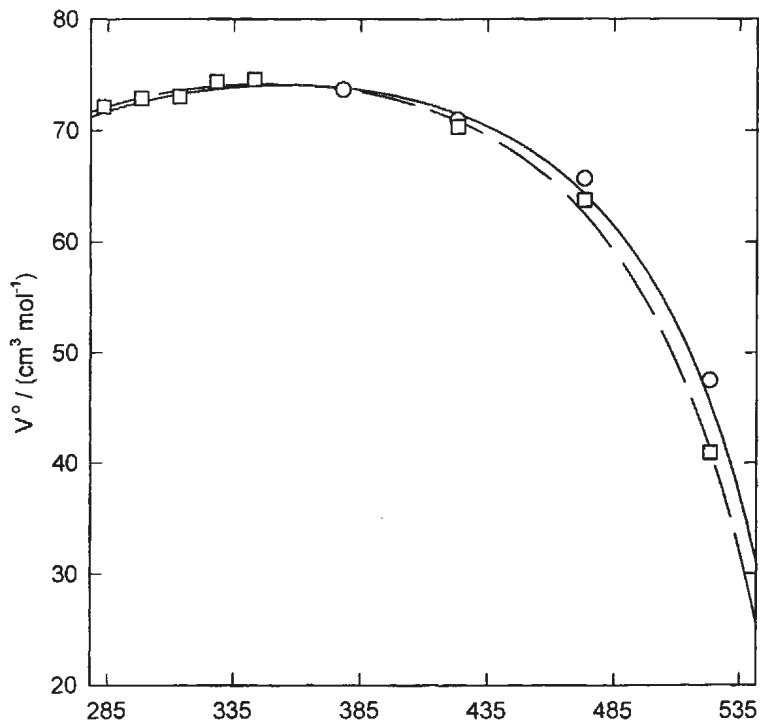

Figure 1.3.3.2 The standard partial molar volumes of V° of dimethylammonium chloride determined by Shvedov and Tremaine (1997). Symbols are the fitted isotherms:○, 10 MPa; □, steam saturation pressure. Lines are fitted values.

V° for aqueous ions pass through a shallow maximum and then decrease sharply at temperatures above 573 K. The values of V° for aqueous non-electrolytes show the opposite behaviour. In the limit as the temperature increases toward the critical temperature of water, the values of V° for aqueous ions increase toward $+\infty$ and the values of V° for aqueous non-electrolytes decrease toward $-\infty$. Although the direction of change in the values of V° are opposite for aqueous ions and non-electrolytes, the manner in which they change is very similar. As the pressure increases the values of V° for aqueous non-electrolytes decrease and the values of V° for aqueous ions increase. For both ions and non-electrolytes the magnitude of the pressure dependence increases with increasing temperature due to the increase in the compressibility of water. Similar behaviour is observed for the standard partial molar heat capacities of aqueous ions and non-electrolytes (Biggerstaff, 1988; White *et al.*, 1987).

Helgeson and Kirkham (1976) and Helgeson *et al.* (1981) realised that the high temperature behaviour of V° and C_p° for aqueous ions and electrolytes could be described with the Born equation discussed in Section 1.3.2.1. Therefore, they developed a pragmatic "equation-of-state" based on the Born equation. The revised Helgeson-Kirkham-Flowers (HKF) model has been used successfully to predict the standard partial molar thermodynamic properties of aqueous ions and electrolytes up to $T = 723$ K and $p = 500$ MPa.

Helgeson *et al.* (1981), Tanger and Helgeson (1988) and Shock and Helgeson (1988) considered each standard partial molar property of an aqueous ion or electrolyte to be a combination of a non-electrostatic term and an electrostatic term. Therefore, the standard

partial molar volume V° was defined as:

$$V^{o} = \Delta V^{o}_{non-electrostatic} + \Delta V^{o}_{electrostatic} \tag{1.3.3.1}$$

where:

$$\Delta V^{o}_{non-electrostatic} = V^{o}_{intr} + \Delta_{solv} V^{o}_{hydr} + \Delta_{solv} V^{o}_{ss} \tag{1.3.3.2}$$

$$\Delta V^{o}_{electrostatic} = \Delta_{solv} V^{o}_{pol} \tag{1.3.3.3}$$

The terms V°_{intr}, $\Delta_{solv} V^{o}_{hydr}$, $\Delta_{solv} V^{o}_{ss}$, and $\Delta_{solv} V^{o}_{pol}$ were defined in Section 1.3.1. Tanger and Helgeson (1988) demonstrated that $\Delta V^{\circ}_{non\text{-}electrostatic}$ could be represented empirically as:

$$\Delta V^{o}_{non-electrostatic} = \sigma + \xi\left(\frac{1}{T-\Theta}\right) \tag{1.3.3.4}$$

To ensure that the revised HKF model is consistent with the pseudo-critical point of supercooled water, the solvent parameter Θ was set equal to 228 K. The terms σ and ξ correspond to temperature independent coefficients characteristic of an aqueous ion or electrolyte at a given pressure.

$$\sigma = a_1 + a_2\left(\frac{1}{\Psi+p}\right) \tag{1.3.3.5}$$

$$\xi = a_3 + a_4\left(\frac{1}{\Psi+p}\right) \tag{1.3.3.6}$$

where Ψ is a solvent parameter equal to 260.0 MPa. a_1, a_2, a_3, and a_4 are temperature and pressure independent parameters characteristic of an aqueous ion or electrolyte. For aqueous

ions and electrolytes $\Delta V^{\circ}_{electrostatic}$ was represented by a modified Born transfer model:

$$\Delta V^{o}_{electrostatic} = -\omega Q + \left(\frac{1-\varepsilon_r}{\varepsilon_r}\right)\left(\frac{\partial \omega}{\partial p}\right)_T \tag{1.3.3.7}$$

where ω is the temperature and pressure dependent Born coefficient, ε_r is the dielectric constant of the solvent, and Q is the Born function.

$$\omega = \frac{(Ze)^2 N_A}{8\pi\varepsilon_o r_e} \tag{1.3.3.8}$$

$$Q = \frac{1}{\varepsilon_r}\left(\frac{\partial \ln \varepsilon_r}{\partial p}\right)_T \tag{1.3.3.9}$$

The term $-\omega Q$ is equivalent to the term $\Delta_{solv}V^{o}_{Born}$ discussed in Section 1.3.2.1. In the revised HKF model $r_e = r + (0.94\text{Å})Z$ where r is the crystallographic radius. Therefore, equation (1.3.3.1) can be rewritten as:

$$V^{o} = a_1 + a_2\left(\frac{1}{\Psi + p}\right) + \left[a_3 + a_4\left(\frac{1}{\Psi + p}\right)\right]\left(\frac{1}{T-\Theta}\right) - \omega Q + \left(\frac{1-\varepsilon_r}{\varepsilon_r}\right)\left(\frac{\partial \omega}{\partial p}\right)_T \tag{1.3.3.10}$$

Similarly, the standard partial molar heat capacity C_p^{o} was defined as:

$$C_p^{o} = \Delta C^{o}_{p,\,non\text{-}electrostatic} + \Delta C^{o}_{p,\,electrostatic} \tag{1.3.3.11}$$

where:

$$\Delta C^{o}_{p,\,non\text{-}electrostatic} = C^{o}_{p,\,intr} + \Delta_{solv} C^{o}_{p,\,hydr} + \Delta_{solv} C^{o}_{p,\,ss} \tag{1.3.3.12}$$

$$\Delta C^{o}_{p,\,electrostatic} = \Delta_{solv} C^{o}_{p,\,pol} \tag{1.3.3.13}$$

The terms $C^{o}_{p,\,intr}$, $\Delta_{solv}C^{o}_{p,\,hydr}$, $\Delta_{solv}C^{o}_{p,\,ss}$, and $\Delta_{solv}C^{o}_{p,\,pol}$ were defined in Section 1.3.1. Tanger and Helgeson (1988) demonstrated that $\Delta C^{o}_{p,non\text{-}electrostatic}$ could be represented empirically as:

$$\Delta C^{o}_{p,\,non-electrostatic} = c_1 + c_2\left(\frac{1}{T-\Theta}\right)^2 - 2T\left(\frac{1}{T-\Theta}\right)^3\left[a_3(p-p_r) + a_4\ln\left(\frac{\Psi+p}{\Psi+p_r}\right)\right] \tag{1.3.3.14}$$

where c_1 and c_2 are temperature and pressure independent parameters characteristic of an aqueous ion or electrolyte and p_r is the reference pressure which is usually 0.1 MPa. For aqueous ions and electrolytes $\Delta C^{o}_{p,electrostatic}$ is represented by a modified Born transfer model:

$$\Delta C^{o}_{p,\,electrostatic} = \omega TX + 2TY\left(\frac{\partial\omega}{\partial T}\right)_p - T\left(\frac{1-\varepsilon_r}{\varepsilon_r}\right)\left(\frac{\partial^2\omega}{\partial T^2}\right)_p \tag{1.3.3.15}$$

$$X = \frac{1}{\varepsilon_r}\left|\left(\frac{\partial^2 \ln\varepsilon_r}{\partial T^2}\right)_p - \left(\frac{\partial \ln\varepsilon_r}{\partial T}\right)_p^2\right| \tag{1.3.3.16}$$

$$Y = \frac{1}{\varepsilon_r}\left(\frac{\partial \ln\varepsilon_r}{\partial T}\right)_p \tag{1.3.3.17}$$

The term ωTX is equivalent to the term $\Delta_{solv}C^{o}_{p,Born}$ discussed in Section 1.3.2.1. Therefore, equation (1.3.3.11) can be rewritten as:

$$C_p^{o} = c_1 + c_2\left(\frac{1}{T-\Theta}\right)^2 - 2T\left(\frac{1}{T-\Theta}\right)^3\left|a_3(p-p_r) + a_4\ln\left(\frac{\Psi+p}{\Psi+p_r}\right)\right|$$

$$+\omega TX+2TY\left(\frac{\partial\omega}{\partial T}\right)_p-T\left(\frac{1-\varepsilon_r}{\varepsilon_r}\right)\left(\frac{\partial^2\omega}{\partial T^2}\right)_p \qquad (1.3.3.18)$$

As illustrated by Figures 1.3.3.1 and 1.3.3.2 the temperature and pressure dependent standard partial molar properties for aqueous non-electrolytes are virtually a mirror image of the standard partial molar properties for aqueous ions and electrolytes. This symmetrical behaviour exhibited by the aqueous non-electrolytes and electrolytes suggests that the equations of state used for aqueous ions and electrolytes could be conveniently used as fitting functions to represent the temperature and pressure dependence of the standard partial molar properties of neutral aqueous organic species. Shock and Helgeson (1990) recognized these similarities and extended the use of the revised HKF model to neutral aqueous organic species. This use of the Born equation for neutral aqueous organic species was not based on any physical model. The following expressions were given by Shock and Helgeson (1990) to predict the standard partial molar volume V° and heat capacity C_p° of a neutral aqueous organic species.

$$V^\circ=a_1+a_2\left(\frac{1}{\Psi+p}\right)+\left[a_3+a_4\left(\frac{1}{\Psi+p}\right)\right]\left(\frac{1}{T-\Theta}\right)-\omega_e Q \qquad (1.3.3.19)$$

$$C_p^\circ=c_1+c_2\left(\frac{1}{T-\Theta}\right)^2-2T\left(\frac{1}{T-\Theta}\right)^3\left[a_3(p-p_r)+a_4\ln\left(\frac{\Psi+p}{\Psi+p_r}\right)\right]$$

$$+\frac{\omega_e T}{\varepsilon_r}\left[\left(\frac{\partial^2\ln\varepsilon_r}{\partial T^2}\right)_p-\left(\frac{\partial\ln\varepsilon_r}{\partial T}\right)_p^2\right] \qquad (1.3.3.20)$$

The temperature and pressure *dependent* Born coefficient ω in equations (1.3.3.10) and (1.3.3.18) was replaced with a temperature and pressure *independent* effective Born coefficient ω_e in equations (1.3.3.19) and (1.3.3.20).

$$\omega_e = \frac{(Z_e e)^2 N_A}{8\pi\varepsilon_o r_e} \qquad (1.3.3.21)$$

Here Z_e is the "effective charge" on the neutral aqueous organic species. For neutral aqueous organic species ω_e is a fitting parameter that can be either positive or negative. According to equation (1.3.3.21), a negative value for ω_e will result in an effective charge on the dissolved species that is an imaginary number, reinforcing the point that equations (1.3.3.19) and (1.3.3.20) have no physical reality.

The revised HKF model as modified by Shock and Helgeson (1990) allows for the prediction of standard partial molar thermodynamic properties of neutral aqueous organic species up to T = 1273 K and p = 500 MPa. To give the revised HKF model predictive capabilities, it was fitted to all available temperature and pressure dependent experimental data for neutral aqueous organic species. The values of the fitting parameters were then correlated with the room temperature thermodynamic data that were available for each of the fitted species.

The applicability of the model is severely restricted since its predictive capabilities are based on the limited number of neutral aqueous organic species for which there were temperature and pressure dependent thermodynamic data available in 1988. Table 1.3.3.1

summarizes these species and the temperature and pressure range of their thermodynamic data. The danger in using such a limited number of species to determine predictive correlations for any model arises from the non-uniformity of the species themselves. The model is being applied to neutral organic species as different as hydrocarbons which remain non-polar in aqueous solution (Shock, 1995), carboxylic acids which are polar (Shock and Helgeson, 1990), and the amino acids which exist as *highly* polar zwitterions in aqueous solution (Amend and Helgeson, 1997). The temperature and pressure dependence of the thermodynamic properties of these compounds can be very different.

Table 1.3.3.1 The experimental data used by Shock and Helgeson (1990) to develop the predictive correlations for the revised HKF model as modified for neutral aqueous organic species.

Species	Thermodynamic Property	Temperature Range K	Pressure Range MPa
Methanol	V°	274.15 - 323.15	0.1
Ethanol	V°	274.15 - 323.15	0.1
1-Propanol	V°	274.15 - 323.15	0.1
2-Propanol	V°	274.15 - 323.15	0.1
1-Butanol	V°	273.65 - 323.15	0.1
2-Butanol	V°	273.65 - 323.15	0.1
1-Pentanol	V°	274.15 - 323.15	0.1
CH_3COOH	V°	283.15 - 313.15	0.1
C_2H_4	V°	298.22 - 716.52	20.0 - 34.6
HCOOH	C_p°	293.15 - 393.15	0.1
CH_3COOH	C_p°	283.15 - 393.15	0.1
CH_3CH_2COOH	C_p°	293.15 - 403.15	0.1
C_2H_4	C_p°	302.10 - 722.21	18.1 - 32.5

1.4 Yezdimer-Sedlbauer-Wood Functional Group Additivity Model.

Several authors have shown that the standard partial molar thermodynamic properties of aqueous solutes can be predicted with reasonable accuracy near ambient conditions using functional group additivity (Cabani *et al.*, 1981; Hoiland, 1986; Gianni and Lepori, 1996). Criss and Wood (1996) and Inglese *et al.* (1997) have demonstrated that functional group additivity maintains its accuracy at temperatures up to 523 K and pressures up to 28 MPa. Recent work by Yezdimer *et al.* (2000) has led to the development of a new functional group additivity model capable of predicting standard partial molar thermodynamic properties of many aqueous organic species at temperatures up to 623 K and at pressures up to 100 MPa.

Any standard partial molar thermodynamic property of a solute Ξ° can be written as:

$$\Xi^{o} = (1 - Z)\left(\Xi_{ss} + \Lambda\right) + \sum_{i=1}^{N} n_i \Xi_i^{o} \qquad (1.4.1)$$

Here Z is the charge on the solute, Ξ_{ss} is the standard state term, N is the total number of distinct functional groups in the solute, n_i is the number of occurrences of functional group i in the solute, and Ξ_i° is the contribution to Ξ° due to functional group i. The factor $(1 - Z)$ ensures that there is a standard-state term for each particle (ionic or neutral) in solution. This factor also ensures that equation (1.4.1) is consistent with the hydrogen convention scale for aqueous ions; $\Xi^\circ(H^+) = 0$. Λ is a conversion factor between different possible aqueous standard states. For the hypothetical 1 molal standard state:

$$\Lambda_G = RT \ln(M_w m^{o}) \qquad (1.4.2)$$

$$\Lambda_S = -R\ln(M_w m^{\circ}) \qquad (1.4.3)$$

Here Λ_G is the correction factor for the standard partial molar Gibbs free energy, Λ_S is the correction factor for the standard partial molar entropy, M_w is the molar mass of water, and m° is equal to 1 mol·kg^{-1}. Λ is equal to zero for all of the other standard partial molar thermodynamic properties.

The Yezdimer-Sedlbauer-Wood functional group additivity model for aqueous organic species uses the equations of state developed by Sedlbauer *et al.* (2000) to model the behaviour of Ξ_i°. Sedlbauer *et al.* based their equations of state on the following expression for the standard partial molar volume of functional group *i*:

$$V_i^o = d_i(V_w - V_{ss}^o) + \rho_w \beta_w RT\left[(a_i + b_i(e^{\hat{\upsilon}\rho_w} - 1) + c_i e^{\theta/T} + \delta_i(e^{\lambda\rho_w} - 1)\right] \qquad (1.4.4)$$

where V_w is the molar volume of water; V_{ss}^o is the standard partial molar volume arising from the difference in standard states between the gas phase (0.1 MPa, ideal gas) and solution (hypothetical 1 molal solution); while ρ_w and β_w are the density and compressibility coefficient of water. The terms θ = 1500 K, λ = -10000 cm^3·kg^{-1}, $\hat{\upsilon}$ = 5000 cm^3·kg^{-1} are coefficients that do not depend on the solute. The terms a_i, b_i, c_i, and d_i are functional-group-specific adjustable parameters. The charge on functional group *i* determines the value of δ_i.

$$\delta_i = \begin{cases} 0.35\,a_i & Z = 0 \\ 0 & Z = 1 \\ -0.645 & Z = -1 \end{cases} \qquad (1.4.5)$$

The standard partial molar Gibbs free energy of formation of functional group i is given as:

$$\Delta_f G_i^{\,o} = \Delta_f G_i^{\,o}[T_r, p_r] - \Delta_f S_i^{\,o}[T_r, p_r](T - T_r) + \Delta_{solv} G_i^{\,o} - \Delta_{solv} H_i^{\,o}[T_r, p_r]$$

$$+ T\Delta_{solv} S_i^{\,o}[T_r, p_r] + \int_{T_r}^{T} C_{p,i}^{ig}\, dT - T\int_{T_r}^{T} \frac{C_{p,i}^{ig}}{T}\, dT \qquad (1.4.6)$$

where T_r is the reference temperature (usually taken to be 298.15 K) and p_r is the reference pressure (usually taken to be 0.1 MPa). $\Delta_f G_i^{\circ}[T_r, p_r]$ and $\Delta_f S_i^{\circ}[T_r, p_r]$ are the standard partial molar Gibbs free energy and entropy of formation for functional group i at T_r and p_r. $\Delta_{solv} S_i^{\circ}[T_r, p_r]$ and $\Delta_{solv} H_i^{\circ}[T_r, p_r]$ are the standard partial molar entropy and enthalpy of solvation. $\Delta_{solv} G_i^{\circ}$ is the standard partial molar Gibbs free energy of solvation of functional group i and $C_{p,i}^{ig}$ is the molar heat capacity of functional group i in the ideal gas state.

The standard partial molar enthalpy and entropy of formation of functional group i were expressed as:

$$\Delta_f H_i^{\,o} = \Delta_f H_i^{\,o}[T_r, p_r] + \Delta_{solv} H_i^{\,o} - \Delta_{solv} H_i^{\,o}[T_r, p_r] + \int_{T_r}^{T} C_{p,i}^{ig}\, dT \qquad (1.4.7)$$

$$\Delta_f S_i^{\,o} = \Delta_f S_i^{\,o}[T_r, p_r] + \Delta_{solv} S_i^{\,o} - \Delta_{solv} S_i^{\,o}[T_r, p_r] + T\int_{T_r}^{T} \frac{C_{p,i}^{ig}}{T}\, dT \qquad (1.4.8)$$

Here $\Delta_f H_i^{\circ}[T_r, p_r]$ is the standard partial molar enthalpy of formation of functional group i at T_r and p_r. $\Delta_{solv} H_i^{\circ}$ and $\Delta_{solv} S_i^{\circ}$ are the standard partial molar enthalpy and entropy of solvation of functional group i. The standard partial molar heat capacity of functional group

i was given as:

$$C_{p,i}^{\ o} = \Delta_{solv} C_{p,\,i}^{\ o} + C_{p,\,i}^{\ ig} \tag{1.4.9}$$

where $\Delta_{solv} C^{\circ}_{p,\,i}$ is the standard partial molar heat capacity of solvation of functional group *i*. The standard partial molar Gibbs free energy, enthalpy, entropy, and heat capacity of solvation of functional group *i* were expressed as:

$$\Delta_{solv} G_i^{\ o} = RT\left[(a_i + c_i e^{\,\theta/T} - b_i - \delta_i)\,\rho_w + \left(\frac{b_i}{\vartheta}\right)(e^{\,\vartheta\rho_w} - 1) + \left(\frac{\delta_i}{\lambda}\right)(e^{\,\lambda\rho_w} - 1)\right]$$

$$+ d_i\left(G_w - G_w^{\ ig} - \Delta_{solv} G_{ss}^{\ o}\right) + H_i^{\ corr} - TS_i^{\ corr} \tag{1.4.10}$$

$$\Delta_{solv} H_i^{\ o} = -RT^2\left[a_i + b_i(e^{\,\vartheta\rho_w} - 1) + c_i e^{\,\theta/T} + \delta_i(e^{\,\lambda\rho_w} - 1)\right]\left(\frac{\partial\rho_w}{\partial T}\right)_p + H_i^{\ corr}$$

$$+ d_i\left(H_w - H_w^{\ ig} - \Delta_{solv} H_{ss}^{\ o}\right) + RT\theta c_i e^{\,\theta/T}\left(\frac{\rho_w}{T}\right) \tag{1.4.11}$$

$$\Delta_{solv} S_i^{\ o} = -R\left[(a_i + c_i e^{\,\theta/T} - b_i - \delta_i)\,\rho_w + \left(\frac{b_i}{\vartheta}\right)(e^{\,\vartheta\rho_w} - 1) + \left(\frac{\delta_i}{\lambda}\right)(e^{\,\lambda\rho_w} - 1)\right]$$

$$- RT\left[a_i + b_i(e^{\,\vartheta\rho_w} - 1) + c_i e^{\,\theta/T} + \delta_i(e^{\,\lambda\rho_w} - 1)\right]\left(\frac{\partial\rho_w}{\partial T}\right)_p + S_i^{\ corr}$$

$$+ d_i\left(S_w - S_w^{\ ig} - \Delta_{solv} S_{ss}^{\ o}\right) + R\theta c_i e^{\,\theta/T}\left(\frac{\rho_w}{T}\right) \tag{1.4.12}$$

$$\Delta_{solv}C^{o}_{p,i} = -RT\theta^2 c_i e^{\theta/T}\left(\frac{\rho_w}{T^3}\right) - RT^2(\vartheta b_i e^{\vartheta\rho_w} + \lambda\delta_i e^{\lambda\rho_w})\left(\frac{\partial\rho_w}{\partial T}\right)^2_p$$

$$-2RT\left(\frac{\partial\rho_w}{\partial T}\right)_p\left[a_i + b_i(e^{\vartheta\rho_w} - 1) + c_i e^{\theta/T} + \delta_i(e^{\lambda\rho_w} - 1) - c_i e^{\theta/T}\left(\frac{\theta}{T}\right)\right]$$

$$-RT^2\left[a_i + b_i(e^{\vartheta\rho_w} - 1) + c_i e^{\theta/T} + \delta_i(e^{\lambda\rho_w} - 1)\right]\left(\frac{\partial^2\rho_w}{\partial T^2}\right)_p$$

$$+d_i\left(C_{p,w} - C^{ig}_{p,w} - \Delta_{solv}C^{o}_{p,ss}\right) + C^{corr}_{p,i} \qquad (1.4.13)$$

Here G_w, H_w, S_w, and $C_{p,w}$ are the molar Gibbs free energy, enthalpy, entropy, and heat capacity of water. G^{ig}_w, H^{ig}_w, S^{ig}_w, and $C^{ig}_{p,w}$ are the molar Gibbs free energy, enthalpy, entropy, and heat capacity of water in the ideal gas state at 0.1 MPa. $\Delta_{solv}G^{o}_{ss}$, $\Delta_{solv}H^{o}_{ss}$, $\Delta_{solv}S^{o}_{ss}$, and $\Delta_{solv}C^{o}_{p,ss}$ represent the change in the standard partial molar Gibbs free energy, enthalpy, entropy, and heat capacity arising from the difference in standard states between the gas phase (0.1 MPa, ideal gas) and solution (hypothetical 1 molal solution). H^{corr}_i and S^{corr}_i are the corrections to the standard partial molar enthalpy and entropy of functional group i.

The change in the standard partial molar Gibbs free energy arising from the difference in standard states between the gas phase and solution was given as:

$$\Delta_{solv}G^{o}_{ss} = RT\ln\left(\frac{\rho_w RT}{M_w P^{o}}\right) \qquad (1.4.14)$$

where $p^{\circ} = 0.1$ MPa. The standard state corrections for all other thermodynamic properties can be obtained in the usual manner from equation (1.4.14).

The correction to the standard partial molar enthalpy, heat capacity, and entropy of functional group *i* were expressed as:

$$H_i^{corr} = \begin{cases} e_i\left[(2T_c - \Theta)(T_c - T) + \left(\frac{T^2 - T_c^2}{2}\right) + (T_c - \Theta)^2 \ln\left(\frac{T - \Theta}{T_c - \Theta}\right)\right] & Z = 0;\ T < T_c \\ C_{H,i} + \left(\frac{g_i(T^2 - T_c^2)}{2}\right) + (T - T_c)(e_i - g_i T_c) & \\ \qquad + e_i(\Theta - T_c)\ln\left(\frac{T - \Theta}{T_c - \Theta}\right) & Z \neq 0;\ T < T_c \\ 0 & Z = 0;\ T \geq T_c \\ C_{H,i} & Z \neq 0;\ T \geq T_c \end{cases} \quad (1.4.15)$$

$$C_{p,i}^{corr} = \begin{cases} \frac{e_i(T - T_c)^2}{T - \Theta} & Z = 0;\ T < \mathrm{T_c} \\ (T - T_c)\left| g_i + \frac{e_i}{T - \Theta} \right| & Z \neq 0;\ T < T_c \\ 0 & T \geq T_c \end{cases} \quad (1.4.16)$$

$$S_i^{corr} = \begin{cases} e_i\left[T - T_c - \left(\frac{T_c^2}{\Theta}\right)\ln\left(\frac{T}{T_c}\right) + \left(\frac{(T_c-\Theta)^2}{\Theta}\right)\ln\left(\frac{T-\Theta}{T_c-\Theta}\right)\right] & Z=0;\ T<T_c \\ C_{S,i} + g_i(T-T_c) + \left(\frac{T_c(e_i - g_i\Theta)}{\Theta}\right)\ln\left(\frac{T}{T_c}\right) + \left(\frac{e_i(\Theta - T_c)}{\Theta}\right)\ln\left(\frac{T-\Theta}{T_c-\Theta}\right) & Z\neq 0;\ T<T_c \\ 0 & Z=0;\ T\geq T_c \\ C_{S,i} & Z\neq 0;\ T\geq T_c \end{cases} \quad (1.4.17)$$

Here T_c = 647.126 K is the critical temperature of water, Θ is a solvent parameter equal to 228 K, e_i and g_i are functional group specific adjustable parameters. $C_{H,\,i}$ and $C_{S,\,i}$ are integration constants for the ionic groups that can be obtained from experimentally determined values of the standard partial molar enthalpy and entropy of solvation of functional group *i*. Yezdimer *et al.* (2000) obtained the following expression for the ideal gas heat capacity of functional group *i* using the method outlined by Reid *et al.* (1987).

$$C_{p,\,i}^{ig} = (-37.93 + \Delta_{a,\,i}) + T(0.210 + \Delta_{b,\,i}) + T^2(3.91\cdot 10^{-4} + \Delta_{c,\,i}) + T^3(2.06\cdot 10^{-7} + \Delta_{d,\,i}) \quad (1.4.18)$$

The terms $\Delta_{a,i}$, $\Delta_{b,i}$, $\Delta_{c,i}$, and $\Delta_{d,i}$ are functional group specific parameters. These parameters are summarized in Table 1.4.1.

Table 1.4.1 Parameters used in the calculation of the ideal gas heat capacity of functional group *i*.

Functional Group	$\Delta_{a,i} \cdot 10^{-1}$ ($J \cdot K^{-1} \cdot mol^{-1}$)	$\Delta_{b,i} \cdot 10$ ($J \cdot K^{-2} \cdot mol^{-1}$)	$\Delta_{c,i} \cdot 10^{4}$ ($J \cdot K^{-3} \cdot mol^{-1}$)	$\Delta_{d,i} \cdot 10^{7}$ ($J \cdot K^{-4} \cdot mol^{-1}$)
C (hydrocarbon)	-4.425	3.1004	-4.74	2.2835
H (hydrocarbon)	2.125	-1.0604	2.09	-1.0835
$CONH_2$	3.35	0.258	1.283	-0.9474
COO^-	2.41	0.427	0.804	-0.687
COOH	2.41	0.427	0.804	-0.687
NH_2	2.69	-0.412	1.64	-0.976
NH_3^+	2.69	-0.412	1.64	-0.976
OH	2.57	-0.691	1.77	-0.988
Amino	5.1	0.015	2.444	-1.663

1.5 Experimental Apparatus for Measurements Under Hydrothermal Conditions.

1.5.1 Vibrating-Tube Densitometer.

It was first demonstrated by Kratky *et al.* (1969) that the density of a fluid can be obtained by measuring the natural vibrational frequency of a tube containing that fluid. By flowing the fluid through the vibrating tube Picker *et al.* (1974) demonstrated that density measurements could be made quickly with ppm precision. Commercial versions of the vibrating tube densitometer were developed for use at temperatures up to 423 K. Recently, Wood and coworkers (Albert and Wood, 1984; Wood *et al.*, 1989; Majer *et al.*, 1991) constructed a high temperature and pressure version of the vibrating tube densitometer capable of operation up to 673 K and 40 MPa. The use of a flow system reduces the residence time of the sample solutions in the vibrating tube densitometer. Thus increasing the temperature range for compounds with limited hydrothermal stability. The high temperature and pressure densitometer is not commercially produced and there are fewer than a dozen working instruments worldwide. The densitometers used in this work are described in Sections 2.3 and 2.4, respectively.

The density of the fluid in all vibrating-tube densitometers is determined from the usual expression:

$$\rho = \rho_w + K_d (\tau^2 - \tau_w^2) \qquad (1.5.1.1)$$

where ρ and ρ_w are the densities of the fluid and the reference fluid, respectively; τ and τ_w are the resonance periods for the fluid and water, respectively; and K_d is a characteristic

constant which is determined by calibration with two reference fluids, usually dry nitrogen gas, water, or aqueous NaCl. The densities of water and the standard solutions of NaCl were obtained for our work from the equations of state reported by Hill (1990) and Archer (1992), respectively. Apparent molar volumes, V_ϕ, were calculated from these densities according to the definition:

$$V_\phi = \left(\frac{1000(\rho_w - \rho)}{(m\rho\rho_w)} \right) + \left(\frac{M_2}{\rho} \right) \qquad (1.5.1.2)$$

where m is the molality and M_2 is the molar mass of the solute.

1.5.2 Differential Flow Calorimeter.

It is difficult to measure apparent molar heat capacities using batch calorimeters because large corrections are required for the heat capacity of the calorimeter cell and for vapor pressure effects. Picker *et al.* (1971) developed the first differential flow calorimeter based on a design that incorporates twin flow cells that are connected in series. The differential flow calorimeter is shown schematically in Figure 1.5.2.1. To measure heat capacities at high temperatures and pressures, Wood and coworkers (Smith-Magowan and Wood, 1981; White and Wood, 1982) constructed a high temperature and pressure version of the Picker flow microcalorimeter. The differential flow calorimeters used in this work are described in Sections 2.5 and 2.6, respectively.

The mass flow rate of a fluid in a flow calorimeter cell is denoted F_m. If the power

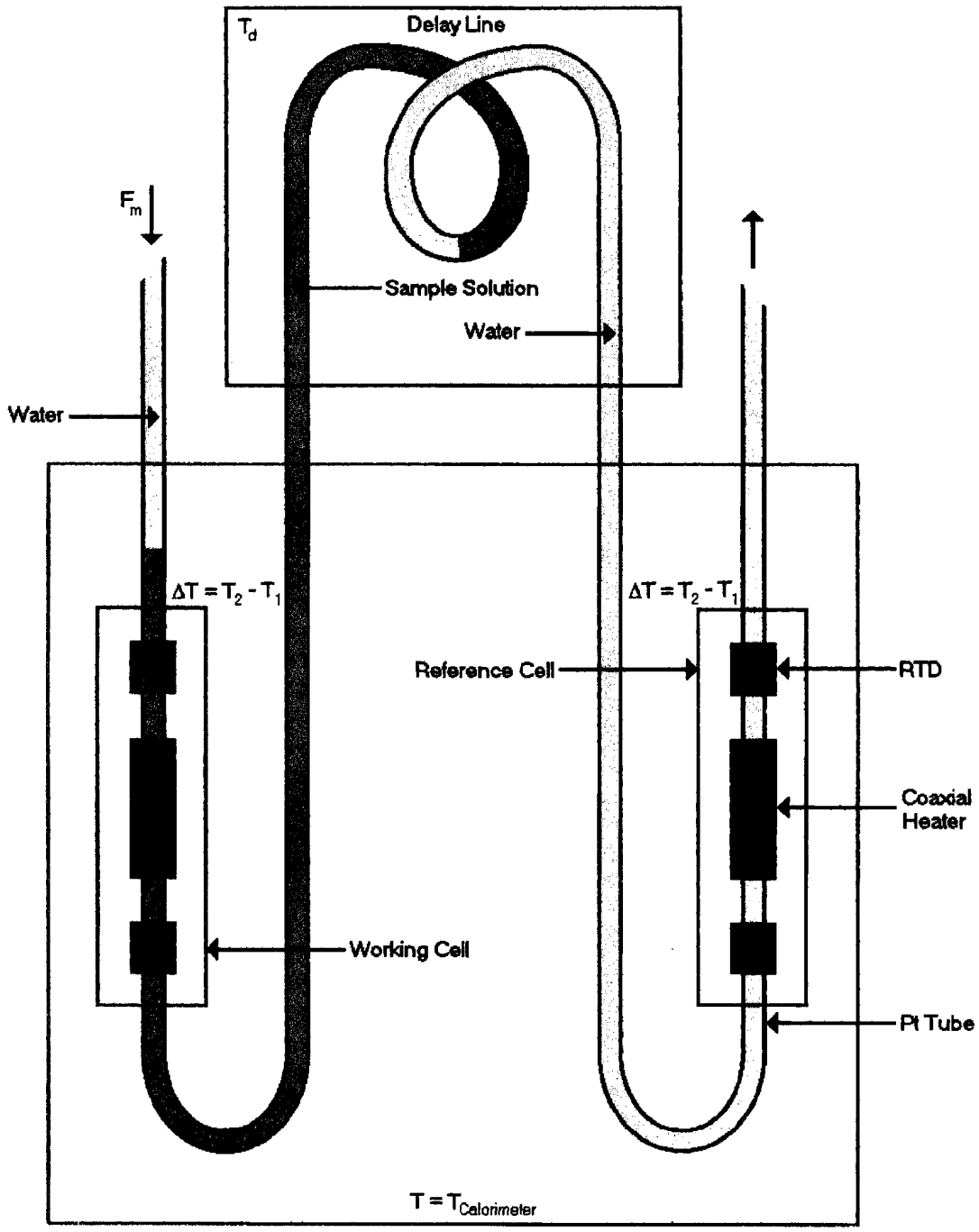

Figure 1.5.2.1 Schematic diagram of the differential flow calorimeter.

required to increase the temperature of the fluid in the cell by ΔT is W, then the specific heat capacity of the fluid can be expressed as:

$$c_p = \frac{W}{F_m \Delta T} \tag{1.5.2.1}$$

where c_p is the specific heat capacity of the fluid, which has units of $J \cdot K^{-1} g^{-1}$. The differential flow calorimeter is based on a twin cell design in which the reference cell in the calorimeter contains the solvent (water) and the working cell contains the sample solution. The temperature change in the reference cell is set equal to the temperature change in the working cell so that:

$$\frac{c_{p,w}}{c_p} = \frac{W_1 F_{m2}}{W_2 F_{m1}} \tag{1.5.2.2}$$

where $c_{p,w}$ and c_p are the specific heat capacities of the reference fluid and sample solution. Here W_1 is the power required to increase the temperature of the reference fluid by ΔT; W_2 is the power required to increase the temperature of the sample solution by the same ΔT; and F_{m1} and F_{m2} are the mass flow rates of the reference fluid and sample solution, respectively. The use of a tubular delay line to connect the two cells in series causes the volumetric flow rates at the interface between the two fluids to be equal.

$$F_{V1} = F_{V2} \tag{1.5.2.3}$$

where F_{V1} and F_{V2} are the volumetric flow rates of the reference fluid and sample solution in the delay line, respectively. The corresponding mass flow rates, F_{m1} and F_{m2}, can be

calculated from the relationship:

$$\frac{F_{m1}}{\rho_{w,T_d}} = \frac{F_{m2}}{\rho_{T_d}} \tag{1.5.2.4}$$

where T_d is the temperature of the delay line, $\rho_{w,Td}$ and ρ_{Td} are the densities of the reference fluid and sample solution at $T = T_d$. Combining equation (1.5.2.2) with equation (1.5.2.4) and setting $W_2 = W_1 + \Delta W$ gives the expression:

$$c_p = c_{p,w}\left(1 + \frac{\Delta W}{W_1}\right)\left(\frac{\rho_{w,T_d}}{\rho_{T_d}}\right) \tag{1.5.2.5}$$

Small fluctuations in the flow rate have little effect on ΔW since the reference and working cells are connected in series. Any change in W_1 caused by a fluctuation in the flow rate will be mirrored by a change in W_2. Equation (1.5.2.5) is valid only if all of the applied power was used to increase the temperature of the fluids in the cells. In practice, some of the applied power was used to heat the material surrounding the cell through convection, radiation, and conduction. Therefore, a heat-loss correction factor f (White *et al.*, 1982) was introduced into equation (1.5.2.5).

$$c_p = c_{p,w}\left(1 + f\frac{\Delta W}{W_1}\right)\left(\frac{\rho_{w,T_d}}{\rho_{T_d}}\right) \tag{1.5.2.6}$$

Apparent molar heat capacities $C_{p,\phi}$ can then be calculated according to the equation:

$$C_{p,\phi} = M_2 c_p + \left(\frac{1000(c_p - c_{p,w})}{m}\right) \tag{1.5.2.7}$$

An absolute calibration similar to that described by White and Wood (1982) was used

to determine the heat-loss correction factor f at each temperature and pressure. In this calibration both the working cell and reference cell contained water driven by a single pump. Changes in the heat capacity of the water in the working cell were simulated by injecting additional water into the working cell using a second pump. This resulted in an increase in the mass flow rate of the water in the working cell. Since $c_p = c_{p,w}$ and $\rho_{Td} = \rho_{w,Td}$, then equation (1.5.2.6) can be rewritten as:

$$f = \frac{W_1 \Delta F_m}{F_{m1} \Delta W} \tag{1.5.2.8}$$

where ΔF_m is the change in the mass flow rate from F_{m1}.

1.5.3 UV-Visible Spectrophotometer

The temperature dependent acid/base dissociation constants for an aqueous amino acid are most easily determined by measuring the pH of an amino acid buffer solution. Electrodes have been developed to measure the pH of aqueous solutions at high temperatures and pressures (MacDonald *et al.*, 1992). However, it is often difficult to use these electrodes in conjunction with a flow system. The use of a flow system for compounds with limited hydrothermal stability is desirable since it extends the range of temperatures over which measurements can be made.

Recently, Bennett and Johnston (1994) developed a high temperature and pressure flow system for use with any commercially available UV-visible spectrophotometer at temperatures up to 713 K and pressures up to 35 MPa. Acid/base dissociation constants have

been measured for several colorimetric indicators that are stable in subcritical and supercritical water (Ryan *et al.*, 1997; Xiang and Johnston, 1997; Xiang and Johnston, 1994). The UV-visible absorption spectrum of a solution containing one of these colorimetric indicators can be used to determine the pH of the solution as a function of temperature. The amino acid solutions are particularly well suited for pH determination with colorimetric indicators since the amino acid solutions do not absorb at the wavelengths that characterize the colorimetric indicators.

An aqueous colorimetric indicator can exist in either the protonated form HX or the deprotonated form X^-. The equilibrium can be summarized as:

$$HX \underset{\rightleftharpoons}{K_{Indicator}} X + H^- \qquad (1.5.3.1)$$

where $K_{Indicator}$ is the molar equilibrium constant. From equation (1.5.3.1) the following expression is obtained for the molarity of H^+:

$$[H^+] = \frac{K_{Indicator}[HX]}{[X^-]} = \frac{K_{Indicator} m_{HX}}{m_{X^-}} \qquad (1.5.3.2)$$

The concentration of a solute can be converted from molarity to molality by dividing the molarity of the solute by the density of the solution. At a constant temperature and pressure the UV-visible absorption spectrum for a solution containing only HX will obey the expression:

$$A(\lambda) = m_{HX}\, \varepsilon_{HX}(\lambda) \qquad (1.5.3.3)$$

where λ is the wavelength, $A(\lambda)$ is the absorbance at a given λ, and $\varepsilon_{HX}(\lambda)$ is the effective molal extinction coefficient for HX at a given value of λ. The effective molal extinction coefficient is equal to the product of the molar extinction coefficient, the path length of the cell, and the density of the solution. For a solution containing only X^-:

$$A(\lambda) = m_{X^-} \cdot \varepsilon_{X^-}(\lambda) \qquad (1.5.3.4)$$

where $\varepsilon_{X^-}(\lambda)$ is the effective molal extinction coefficient for X^- at a given value of λ. At a constant temperature and pressure the UV-visible absorption spectrum for a solution containing both HX and X^- will obey the expression:

$$A(\lambda) = m_{HX} \cdot \varepsilon_{HX}(\lambda) + m_{X^-} \cdot \varepsilon_{X^-}(\lambda) \qquad (1.5.3.5)$$

The value of $\varepsilon_{HX}(\lambda)$ can be determined at a given temperature and pressure by measuring the UV-visible absorption spectrum for a solution containing only HX at a known molality. Similarly, the value of $\varepsilon_{X^-}(\lambda)$ can be determined at a given temperature and pressure by measuring the UV-visible absorption spectrum for a solution containing only X^- at a known molality. The molality of HX and X^- present in a solution containing both forms of the indicator can then be determined from the UV-visible absorption spectrum of that solution.

The temperature dependent values of $K_{Indicator}$ have been determined for a number of hydrothermally stable colorimetric indicators. Acridine, β-naphthoic acid, and β-naphthol have been studied by Ryan *et al.* (1997), Xiang and Johnston (1997), and Xiang and Johnston (1994), respectively. Of these colorimetric indicators only acridine and β-naphthoic acid

have suitable values of $pK_{Indicator}$ for use in this work. The acidic and basic structures of acridine and β-naphthoic acid are illustrated in Figure 1.5.3.1.

The equilibrium constant for the protonation of acridine $K^{-1}_{Acridine}$ was measured at 24.13 MPa and 298.15 K ≤ T ≤ 653.15 K (Xiang, 1996; Ryan *et al.*, 1997). The value of $K_{Acridine}$ can be represented by the expression:

$$\ln K_{Acridine} = -12.43 - 3663.04\left(\frac{1}{T} - \frac{1}{T_r}\right) - \left(\frac{15874.31}{T}\right)\left(\frac{1}{\varepsilon_r} - \frac{1}{78.38011}\right) \qquad (1.5.3.6)$$

Here T_r = 298.15 K is the reference temperature and ε_r is the solvent dielectric constant. The equilibrium constant for the deprotonation of β-naphthoic acid $K_{\beta\text{-}naphthoic}$ was measured at 34.47 MPa and 298.15 K ≤ T ≤ 673.15 K (Xiang and Johnston, 1997) and can be represented by the expression:

$$\log K_{\beta\text{-}naphthoic} = -13.553 + \left(\frac{7.824\cdot 10^3}{T}\right) - \left(\frac{1.704\cdot 10^6}{T^2}\right) + \left(\frac{6.318\cdot 10^7}{T^3}\right) +$$

$$\left[-19.193 + \left(\frac{1.974\cdot 10^4}{T}\right) - \left(\frac{13.336\cdot 10^4}{T}\right)\right] \log \rho_w \qquad (1.5.3.7)$$

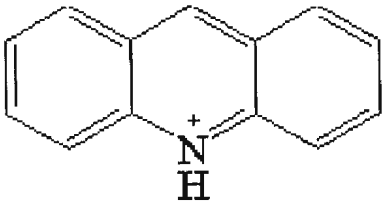

Protonated Acridine

AcH^+

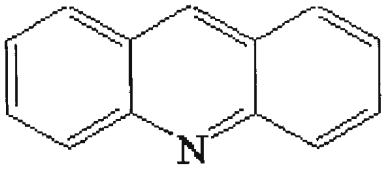

Acridine

Ac

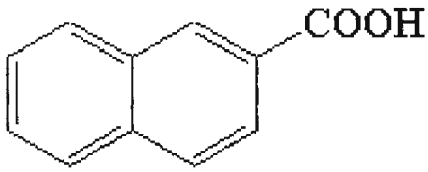

β-Naphthoic Acid

NapH

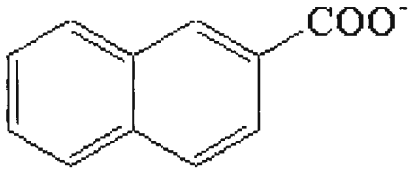

Deprotonated β-Naphthoic Acid

Nap^-

Figure 1.5.3.1 The structure of acridine and β-naphthoic acid in the acidic and basic forms.

1.6 Amino Acids Under Hydrothermal Conditions.

1.6.1 Experimental Requirements.

When determining the suitability of an amino acid for use in high temperature and pressure densitometry and calorimetry, a number of points must be considered.

First, the aqueous amino acid must be thermally stable up to a temperature of at least 573 K. Any hydrothermal reactions that occur will alter the concentration of the aqueous amino acid and will introduce new species into the solution. The measured apparent molar properties will then contain contributions from both the unreacted amino acid and the thermal reaction products. Therefore, knowledge of the identity, molality, and apparent molar properties of the thermal products would be required to obtain the apparent molar properties of the amino acid. Often the molalities of thermal products cannot be determined exactly and their apparent molar properties are unknown. Sometimes the thermal reaction product itself cannot be conclusively identified.

Second, the amino acid must have a solubility that does not decrease as the temperature increases from 298 K to 573 K. A decrease in the solubility of the aqueous amino acid with increasing temperature could allow the most concentrated solutions at room temperature to become supersaturated at the higher operating temperatures of the densitometer and calorimeter. The resulting precipitate could block the platinum U-tube in the densitometer or the platinum cells in the calorimeter.

Finally, the amino acid must have a solubility of at least 0.3 $mol \cdot kg^{-1}$ at 298 K to

allow accurate extrapolation to infinite dilution. To determine the standard partial molar properties of the aqueous amino acids, the apparent molar properties must be known as a function of molality. If the concentration range is very narrow, then obtaining a reliable extrapolation to infinite dilution will be difficult. In addition, the uncertainty associated with the measured apparent molar properties increases as the molality decreases. For a sparingly soluble amino acid, the large uncertainties associated with the measured apparent molar properties and the narrow concentration range will translate into an unacceptably large uncertainty in the measured standard partial molar properties.

1.6.2 Choice of Amino Acids for Hydrothermal Measurements.

A search of the relevant literature revealed only a few studies that have been conducted to investigate the hydrothermal stability of amino acids. Abelson (1957), Bada and Miller (1970), Povoledo and Vallentyne (1964), Vallentyne (1964), Vallentyne (1968), and White (1984) have measured approximate first-order rate constants for the decomposition of several dilute aqueous amino acids at the temperatures and pressures used in this work. The rate constant k for the decomposition can be described by the Arrhenius equation.

$$k = Ae^{-E_A/RT} \qquad (1.6.2.1)$$

Here A is the Arrhenius frequency factor, E_A is the activation energy in cal·mol^{-1}, R is the gas constant equal to 1.9872 cal·K^{-1}·mol^{-1}, and T is the absolute temperature. Table 1.6.2.1 summarizes the values of A and E_A reported in the studies listed above. For comparison

purposes Table 1.6.2.1 includes an estimated half-life $t_{1/2}$ for each of the aqueous amino acids at 573 K. Of the amino acids listed in Table 1.6.2.1, only glutamic acid, proline, glycine, phenylalanine, α-alanine, and leucine have enough hydrothermal stability to be useful at the experimental residence times, temperatures, and pressures used in this work.

The temperature-dependent solubility data for these thermally stable amino acids were found in a compilation by Greenstein and Winitz (1961) and are displayed in Figure 1.6.2.1. Although the solubility of each candidate amino acid increases with temperature, it is clear that glutamic acid, phenylalanine, and leucine are insufficiently soluble in water to be of use. Therefore α-alanine, proline, and glycine are the "best" model systems for studying the properties of amino acids under hydrothermal conditions.

A series of batch experiments, described in Section 2.2, confirmed that α-alanine and proline are suitable for study at the temperatures, pressures, and molalities used in this work. Glycine was found to be significantly less stable. The structures of α-alanine, glycine, and proline are illustrated in Figure 1.6.2.2. Figure 1.6.2.2 also includes the structure of β-alanine which was included in this study for comparative purposes.

Table 1.6.2.1 The Arrhenius frequency factor A and activation energy E_A for the thermal decomposition of selected amino acids as a function of temperature and the calculated half-lives $t_{1/2}$ at 573 K.

Amino Acid	Source	A	E_A / (cal·mol^{-1})	$t_{1/2}$ / (hour)†
Glutamic Acid	Povoledo and Vallentyne (1964)	1.2×10^{9}	35700	6.74
Proline	Vallentyne (1968)	1.5×10^{12}	42400	1.91
Glycine	Vallentyne (1964)	------	------	1.4 - 2.1
Phenylalanine	Vallentyne (1964)	1.7×10^{8}	30750	0.592
α-Alanine	Vallentyne (1964)	3.0×10^{13}	44020	0.401
Leucine	Vallentyne (1968)	1.7×10^{14}	45200	0.197
Arginine·HCl	Vallentyne (1968)	1.2×10^{5}	19800	5.72×10^{-2}
Serine	Vallentyne (1964)	4.0×10^{9}	29330	7.40×10^{-3}
Threonine	Vallentyne (1964)	1.9×10^{12}	33800	7.84×10^{-4}
Aspartic Acid	Bada and Miller (1970)	2.2×10^{14}	36820	9.67×10^{-5}

†The half life refers to the time required for the concentration of an aqueous amino acid to decrease by one half.

Note: 1 cal = 4.184 J.

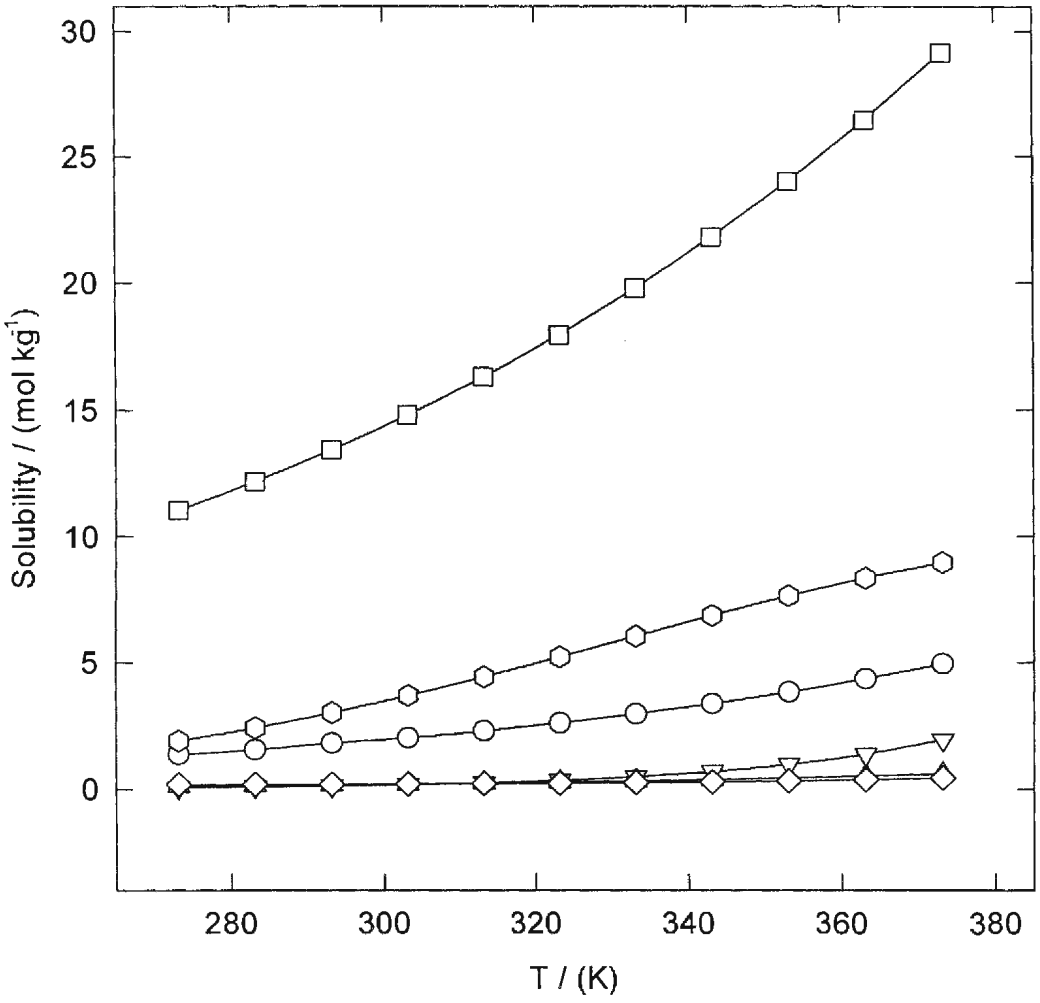

Figure 1.6.2.1 The solubility of L-proline, glycine, DL-α-alanine, DL-glutamic acid, L-phenylalanine, and L-leucine plotted against temperature. □, L-proline; [ ], glycine;○, DL-α-alanine; ▽, DL-glutamic acid; Δ, L-phenylalanine; ◇, L-leucine

α-Alanine

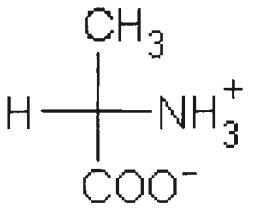

β-Alanine

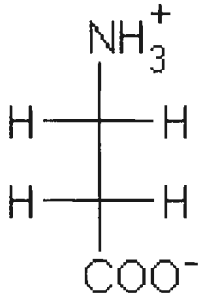

Glycine

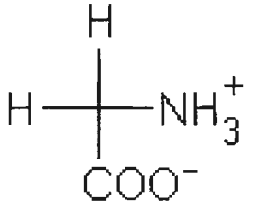

Proline

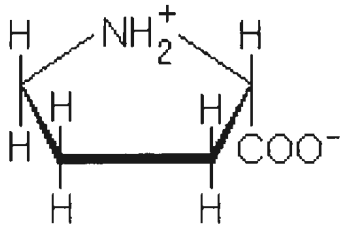

Figure 1.6.2.2 The structure of α-alanine, β-alanine, glycine, and proline.

1.6.3 Thermodynamic Data in the Literature.

A search of the relevant literature identified a number of studies that have been conducted to measure thermodynamic quantities for aqueous α-alanine, β-alanine, glycine, and proline. Although the majority of these studies were limited to 298.15 K, several were conducted as a function of temperature between 278.15 K and 343.15 K. The results of these studies are summarized in Tables 1.6.3.1 and 1.6.3.2. Our literature review also identified temperature dependent values of the molar dielectric increment δ and the dipole moment μ for α-alanine, β-alanine, glycine, and proline. These are summarized in Table 1.6.3.3.

Table 1.6.3.1 Standard partial molar volumes V° and standard partial molar heat capacities C_p° of aqueous α-alanine, β-alanine, glycine, and proline at 0.1 MPa as found in the relevant literature.

	α-Alanine	β-Alanine	Glycine	Proline
T / (K)	V° / ($cm^3 \cdot mol^{-1}$)			
278.15	58.64 ± 0.02 [c]		41.07 ± 0.01 [c] 41.2 [bb]	80.43 ± 0.02 [c]
283.15			41.9 [bb]	
288.15	59.73 ± 0.01 [c] 59.67 ± 0.18 [e] 59.9 ± 0.1 [j]	57.48 ± 0.01 [g] 57.0 ± 0.2 [aa]	42.29 ± 0.02 [c] 42.48 [e] 42.4 ± 0.1 [j] 42.5 ± 0.2 [aa] 42.4 [bb]	81.71 ± 0.02 [b] 81.57 ± 0.01 [c] 81.93 ± 0.01 [g]
291.15	60.2 ± 0.1 [d]	57.6 ± 0.3 [f]	42.9 ± 0.1 [d]	
293.15			42.8 [bb]	
297.15	60.65 ± 0.1 [p]		43.39 ± 0.1 [p]	
298.15	60.52 ± 0.01 [c] 60.5 ± 0.1 [d] 60.47 ± 0.03 [e] 60.4 ± 0.1 [j] 60.42 ± 0.02 [l] 60.50 ± 0.02 [m] 60.54 ± 0.09 [o] 60.45 ± 0.01 [q] 60.50 ± 0.07 [r] 60.47 ± 0.1 [s] 60.3 ± 0.2 [t] 60.6 [u] 60.61 [dd]	58.3 ± 0.2 [f] 58.71 ± 0.01 [g] 58.25 ± 0.02 [m] 58.63 ± 0.48 [o] 58.28 ± 0.1 [s] 58.5 ± 0.3 [t] 58.7 [u] 59.65 [z] 57.9 ± 0.2 [aa] 58.72 [dd]	43.19 ± 0.01 [c] 43.4 ± 0.1 [d] 43.26 [e] 43.09 ± 0.05 [h] 43.3 ± 0.1 [j] 43.19 ± 0.02 [l] 43.23 ± 0.01 [m] 43.17 ± 0.02 [n] 43.33 ± 0.12 [o] 43.25 ± 0.01 [q] 43.19 ± 0.02 [r] 43.5 ± 0.2 [t] 43.3 [u] 42.9 ± 0.2 [aa] 43.22 [cc]	82.61 ± 0.02 [b] 82.50 ± 0.01 [c] 83.13 ± 0.02 [g] 82.46 ± 0.05 [h] 82.5 ± 0.2 [j] 82.65 ± 0.03 [k] 82.63 ± 0.05 [l] 82.68 ± 0.02 [n] 82.83 ± 0.08 [r] 81.0 [u]

	α-Alanine	β-Alanine	Glycine	Proline
308.15	60.96 ± 0.02 [c]	59.06 ± 0.01 [g]	43.81 ± 0.02 [c]	83.22 ± 0.02 [c]
	61.2 ± 0.1 [d]	59.25 [y]	44.0 ± 0.1 [d]	83.62 ± 0.02 [g]
	60.9 ± 0.1 [j]		43.8 ± 0.1 [j]	
	61.16 [y]		43.87 [y]	
313.15	61.14 ± 0.13 [e]	59.1 ± 0.3 [f]	44.01 [e]	83.64 ± 0.01 [b]
	61.2 ± 0.15 [j]	59.54 [y]	43.9 ± 0.1 [j]	83.6 ± 0.2 [j]
	61.35 [y]		44.00 [y]	
318.15	61.46 ± 0.02 [c]	59.75 [y]	44.00 ± 0.03 [c]	83.86 ± 0.04 [c]
	61.5 ± 0.1 [d]		44.3 ± 0.1 [d]	
	61.46 [y]		44.15 [y]	
323.15	61.61 [y]	59.84 [y]	44.25 [y]	
328.15	61.53 ± 0.11 [e]	59.2 ± 0.3 [f]	44.51 [e]	84.46 ± 0.03 [b]
	61.6 ± 0.2 [j]		44.3 ± 0.1 [j]	84.5 ± 0.3 [j]
333.15	61.85 [y]	60.03 [y]	44.38 [y]	
343.15	62.24 [y]	60.18 [y]	44.47 [y]	
T / (K)	C_p^o / (J·mol^{-1}·K^{-1})			
278.15	99.37 [dd]	16.90 [dd]		
288.15	126.3 [e]		15.2 [e]	161.4 ± 0.3 [b]
298.15	141.2 [e]	73.2 ± 1 [s]	37.6 [e]	177.9 ± 0.4 [b]
	145.2 ± 1 [p]	81.2 ± 8.4 [w]	36.7 ± 1 [p]	172.3 ± 0.9 [k]
	141.4 ± 0.2 [q]	76.44 [dd]	39.2 ± 0.4 [q]	170 ± 3 [x]
	142.5 ± 1 [s]		61.1 ± 8.4 [w]	
	147.7 ± 2.1 [w]		47 ± 5 [x]	
	141 ± 4 [x]		44 ± 3 [x]	
	146 ± 5 [x]		31.4 [ee]	
	140.96 [dd]			
	167.4 [ee]			
303.15	150 ± 25 [v]	91 ± 7 [v]	43 ± 20 [v]	225 ± 13 [v]
305.15	153.6 ± 2.1 [w]	91.2 ± 8.4 [w]	65.3 ± 4.2 [w]	
	146.8 [dd]	86.2 [dd]		

	α-Alanine	β-Alanine	Glycine	Proline
313.15	153.7 [e] 153.39 [dd]	97.65 [dd]	57.8 [e]	197.6 ± 0.4 [b]
328.15	166.5 [e]		76.4 [e]	226.5 ± 6.7 [b]

[b] Hakin *et al.* (1997); [c] Kikuchi *et al.* (1995); [d] Chalikian *et al.* (1994); [e] Hakin *et al.* (1994); [f] Chalikian *et al.* (1993); [g] Wadi and Goyal (1992); [h] Belibagli and Ayranci (1990); [j] Kharakoz (1989); [k] Jolicoeur *et al.* (1986); [l] Mishra and Ahluwalia (1984); [m] Ogawa *et al.* (1984); [n] Vliegen *et al.* (1984); [o] Cabani *et al.* (1981); [p] DiPaola and Belleau (1978); [q] Jolicoeur and Boileau (1978); [r] Millero *et al.* (1978); [s] Ahluwalia *et al.* (1977); [t] Shahidi and Farrell (1978); [u] Kirchnerova *et al.* (1976); [v] Prasad and Ahluwalia (1976); [w] Cabani *et al.* (1977); [x] Spink and Wadsö (1975); [y] Gopal *et al.* (1973); [z] Pepela and Dunlop (1972); [aa] Devine and Lowe (1971); [bb] Tyrrell and Kennerley (1968); [cc] Ellerton *et al.* (1964); [dd] Gucker and Allen (1942); [ee] Zittle and Schmidt (1935).

Table 1.6.3.2 Standard partial molar isothermal compressibilities κ_T° and standard partial molar adiabatic compressibilities κ_S° of aqueous α-alanine, β-alanine, glycine, and proline at 0.1 MPa as found in the relevant literature.

	κ_S° $cm^3 \cdot mol^{-1} \cdot GPa^{-1}$	κ_T° $cm^3 \cdot mol^{-1} \cdot GPa^{-1}$	κ_S° $cm^3 \cdot mol^{-1} \cdot GPa^{-1}$	κ_T° $cm^3 \cdot mol^{-1} \cdot GPa^{-1}$
T / (K)	α-Alanine		β-Alanine	
278.15	-39.78 ± 0.07 [a]	-39.48 ± 0.07 *		
288.15	-31.01 ± 0.07 [a]	-29.11 ± 0.07 *		
	-30.4 ± 0.2 [e]	-28.5 ± 0.2 *		
291.15	-27.7 ± 0.2 [b]	-25.6 ± 0.2 *	-30.0 ± 0.4 [d]	-26.9 ± 0.4 *
298.15	-25.16 ± 0.07 [a]	-23.00 ± 0.07 *	-26.3 ± 0.4 [d]	-23.3 ± 0.4 *
	-24.2 ± 0.2 [b]	-22.0 ± 0.2 *	-26.36 ± 0.11 [f]	-23.39 ± 0.11 *
		-20.2 ± 0.8 [c]	-21.5 ± 0.7 [g]	-18.5 ± 0.7 *
	-25.1 ± 0.2 [e]	-22.9 ± 0.2 *	-27.69 [j]	-24.72 *
	-24.74 ± 0.18 [f]	-22.58 ± 0.18 *		
	-21.6 ± 0.5 [g]	-19.4 ± 0.5 *		
	-25.03 ± 0.13 [h]	-22.87 ± 0.13 *		
	-26.80 [j]	-24.64 *		
308.15	-20.87 ± 0.11 [a]	-19.02 ± 0.11 *		
	-20.2 ± 0.2 [b]	-18.3 ± 0.2 *		
313.15	-19.8 ± 0.2 [e]	-18.2 ± 0.2 *	-21.0 ± 0.5 [d]	-19.7 ± 0.5 *
318.15	-17.85 ± 0.18 [a]	-16.61 ± 0.18 *		
	-17.5 ± 0.2 [b]	-16.3 ± 0.2 *		
328.15	-16.8 ± 0.4 [e]	-16.2 ± 0.4 *	-18.7 ± 0.5 [d]	-19.5 ± 0.5 *

	κ_S° $cm^3 \cdot mol^{-1} \cdot GPa^{-1}$	κ_T° $cm^3 \cdot mol^{-1} \cdot GPa^{-1}$	κ_S° $cm^3 \cdot mol^{-1} \cdot GPa^{-1}$	κ_T° $cm^3 \cdot mol^{-1} \cdot GPa^{-1}$
T / (K)	Glycine		Proline	
278.15	-35.28 ± 0.05 [a]	-35.00 ± 0.05 *	-44.14 ± 0.04 [a]	-43.84 ± 0.04 *
288.15	-31.66 ± 0.04 [a]	-29.78 ± 0.04 *	-32.96 ± 0.05 [a]	-30.89 ± 0.05 *
	-31.3 ± 0.4 [e]	-29.4 ± 0.4 *		
291.15	-28.4 ± 0.2 [b]	-26.3 ± 0.2 *		
298.15	-26.50 ± 0.10 [a]	-24.17 ± 0.10 *	-24.11 ± 0.04 [a]	-21.38 ± 0.04 *
	-25.4 ± 0.2 [b]	-23.1 ± 0.2 *	-23.4 ± 0.4 [e]	-20.7 ± 0.4 *
		-20.8 ± 0.8 [c]	-23.25 ± 0.11 [h]	-20.52 ± 0.11 *
	-26.6 ± 0.2 [e]	-24.3 ± 0.2 *		
	-27.16 ± 0.36 [f]	-24.83 ± 0.36 *		
	-25.0 ± 0.6 [g]	-22.7 ± 0.6 *		
	-27.00 ± 0.44 [h]	-24.67 ± 0.44 *		
	-27.19 [j]	-24.86 *		
308.15	-23.59 ± 0.05 [a]	-21.29 ± 0.05 *	-18.14 ± 0.03 [a]	-15.20 ± 0.03 *
	-22.5 ± 0.2 [b]	-20.2 ± 0.2 [b]		
313.15	-22.4 ± 0.2 [e]	-20.2 ± 0.2 *	-12.7 ± 0.4 [e]	-9.7 ± 0.4 *
318.15	-21.56 ± 0.12 [a]	-19.52 ± 0.12 *	-15.19 ± 0.04 [a]	-12.24 ± 0.04 *
	-20.5 ± 0.2 [b]	-18.5 ± 0.2 *		
328.15	-20.3 ± 0.2 [e]	-18.6 ± 0.2 *	-9.4 ± 0.3 [e]	-6.7 ± 0.3 *

[a] Kikuchi *et al.* (1995); [b] Chalikian *et al.* (1994); [c] Yayanos (1993); [d] Chalikian *et al.* (1993); [e] Kharakoz (1991); [f] Ogawa *et al.* (1984); [g] Cabani *et al.* (1981); [h] Millero *et al.* (1978); [j] Gucker *et al.* (1950); * values of κ_T° calculated from the corresponding standard partial molar adiabatic compressibilities as described in Section 7.1.

Table 1.6.3.3 Molar dielectric increments δ and dipole moments μ of aqueous solutions of α-alanine, β-alanine, glycine, and proline at 0.1 MPa.

	δ / ($m^3 \cdot mol^{-1}$)	$\mu^\dagger$ / (Debye)	δ / ($m^3 \cdot mol^{-1}$)	$\mu^\dagger$ / (Debye)
T / (K)	α-Alanine		β-Alanine	
273.15	30.4 ± 1.5 [d]	17.4 ± 0.4	37.9 ± 1.9 [d]	19.4 ± 0.5
283.15	27.9 ± 1.4 [d]	17.0 ± 0.4	36.5 ± 1.8 [d]	19.4 ± 0.5
291.15	23.57 [j]	15.82	42.25 [j]	21.19
293.15	25.5 ± 1.3 [d]	16.5 ± 0.4	34.6 ± 1.7 [d]	19.2 ± 0.5
298.15	23.5 [b]	16.0	27.9 ± 0.2 [a]	17.4 ± 0.1
298.15	23.2 [e]	15.9	35.0 [g]	19.5
298.15	23.16 [f]	15.87	34.56 [f]	19.39
298.15	27.7 [i]	17.4		
303.15			32.4 ± 1.6 [d]	18.9 ± 0.5
313.15	22.0 ± 1.1 [d]	15.9 ± 0.4	31.0 ± 1.6 [d]	18.8 ± 0.5
323.15	21.3 ± 1.1 [d]	15.8 ± 0.4	30.0 ± 1.5 [d]	18.8 ± 0.5
T / (K)	Glycine		Proline	
291.15	23.0 [j]	15.6		
293.15			—	20.0 ± 1.0 [c]
298.15	24.0 ± 0.6 [a]	16.2 ± 0.2	21 [h]	15
298.15	24 [b]	16		
298.15	22.58 [f]	15.67		
298.15	26.4 [i]	16.9		
313.15			—	17.7 ± 0.9 [c]

[a] Edward *et al.* (1974); [b] Kirchnerova *et al.* (1976); [c] Shepherd and Grant (1968); [d] Aaron and Grant (1967); [e] Osborn (1945); [f] Wyman and McMeekin (1933); [g] Devoto (1933); [h] Devoto (1931); [i] Devoto (1930); [j] Hederstrand (1928); [†] values of the dipole moment μ calculated from the corresponding molar dielectric increment δ according to equation (7.2.14) as described in Section 7.2.

1.7 Experimental Objectives.

The goal of this research is to determine the thermodynamic properties of aqueous amino acids at high temperatures and pressures and to use these data to identify the contribution of major solvation effects. To accomplish this goal a number of more specific objectives were defined.

- determine the most suitable amino acids for use under hydrothermal conditions.
- measure V_ϕ of aqueous α-alanine, β-alanine, and proline and calculate $V°$.
- measure $C_{p,\phi}$ of aqueous α-alanine, β-alanine, glycine, and proline and calculate C_p^o.
- fit an appropriate equation of state to the experimental results.
- compare experimental values of $V°$ and C_p^o with predicted by both the revised HKF model and the Yezdimer-Sedlbauer-Wood functional group additivity model.
- measure the temperature dependent speciation of the aqueous amino acids studied in this work and compare with predicted values.
- determine the contribution to the experimental values of V^o and C_p^o by the non-zwitterionic forms of the aqueous amino acids.
- estimate the contribution of solvation effects to V^o and C_p^o.

Based on the literature search described in Sections 1.6.1 and 1.6.2 aqueous α-alanine, proline, and glycine were selected to be the "best" model systems for studying the properties of amino acids under hydrothermal conditions. A set of batch experiments,

described in Sections 2.2 and 3.1 confirmed their thermal stability at our experimental temperatures and pressures. Although less stable under hydrothermal conditions, β-alanine was also included in this study for comparative purposes.

The apparent molar volumes V_ϕ of aqueous α-alanine, β-alanine, and proline were determined with platinum vibrating tube densitometers in our laboratory at temperatures from 298 K to 523 K and at pressures in excess of steam saturation (Sections 2.3, 2.4, and 3.2). The standard partial molar volumes V° were determined isothermally from the apparent molar volumes (Section 3.2). It was found that the values of V° increased with increasing temperature and then deviated toward negative values at temperatures above 398 K in a manner similar to aqueous ions and electrolytes.

The apparent molar heat capacities $C_{p,\phi}$ of aqueous α-alanine, β-alanine, glycine, and proline were determined with the differential flow calorimeter at Université Blaise Pascal at temperatures from 323 K to 498 K and at pressures in excess of steam saturation (Sections 2.5, 2.6, and 3.3). These results were then used to determine standard partial molar heat capacities C_p° (Section 3.3). The values of C_p° increased with increasing temperature and then deviated toward negative values at temperatures above 373 to 423 K, in a manner similar to that observed for V°.

The molality, temperature, and pressure dependence of the apparent molar properties are most conveniently represented by an equation of state. In the first attempt to model the experimentally determined data, both the density model and the revised HKF model were

fitted to the $V_\phi(m, T, p)$ results (Section 3.4.2). Although the density model reproduced the V_ϕ results better than the revised HKF model (Section 4.2), it could not simultaneously represent $V_\phi(m, T, p)$ and $C_{p,\phi}(m, T, p)$ with sufficient accuracy. Therefore, the density model was extended to include a number of additional temperature and/or pressure dependent terms and was fitted to the isothermally determined values of V° and C_p° rather than to the entire data set of V_ϕ and $C_{p,\phi}$. The results are given in Section 3.4.3.

The experimentally determined values of V° and C_p° were compared to the values predicted by both the revised HKF model (Section 4.3) and the Yezdimer-Sedlbauer-Wood functional group additivity model (Section 4.4.1). The deviation toward negative values by V° and C_p° is opposite to the behaviour predicted by the revised HKF model. Although the Yezdimer-Sedlbauer-Wood functional group additivity model predicts the deviation toward negative values, it is only in qualitative agreement with the experimental results. The experimentally determined values of V° and C_p° were used to recalculate the parameters for the amino acid functional group used in the Yezdimer-Sedlbauer-Wood functional group additivity model (Section 4.4.2). However, insufficient flexibility in the equation of state used in this model prevented any significant improvement in its prediction of V° and C_p°.

Three methods were used to determine the temperature dependent speciation of the aqueous amino acids (Section 4.5.1). The speciation of aqueous α-alanine was determined from measurements made using high temperature and pressure UV-visible spectroscopy and colorimetric indicators (Sections 2.7, 3.5, and 4.5.5). This is one of the first studies to use the

colorimetric indicators developed by Johnston and coworkers (Ryan *et al.*, 1997; Xiang and Johnston 1997; Xiang and Johnston, 1994). The speciation was also estimated from room temperature data assuming constant heat capacities for the isocoulombic equilibria among the various forms of the aqueous amino acid (Section 4.5.2). A second estimate was obtained using the Yezdimer-Sedlbauer-Wood functional group additivity model (Section 4.5.3). When the measured and estimated values were compared, it was found that the estimated values represented an upper limit for the degree of dissociation of an aqueous amino acid (Section 4.5.6).

The contribution to the experimentally determined values of V^o and C_p^o by the non-zwitterionic forms of the aqueous amino acids were estimated using the degree of dissociation and the standard partial molar properties for the ionic and neutral forms of each amino acid estimated using the Yezdimer-Sedlbauer-Wood functional group additivity model (Section 4.5.4). It was found that the contribution of neutral and ionic species to the experimental values of C_p^o and V° became significant only at temperatures above 373 K. Even at these temperatures the contributions were estimated to be no greater than ± 0.2 $cm^3 \cdot mol^{-1}$ and -2 $J \cdot K^{-1} \cdot mol^{-1}$.

The contributions to the experimentally determined values of V° by the intrinsic molar gas phase volume, the partial molar volume of polarization, the molar volume due to standard state correction, and the molar volume of hydration were calculated and it was found that there is qualitative agreement between the partial molar volume of polarization

and the V° values (Sections 4.6.1 to 4.6.4). By increasing the effective radius used in the estimation of the partial molar volume of polarization the temperature dependence of the molar volume of hydration can be greatly decreased (Section 4.6.5). It was also found that there is qualitative agreement between the partial molar heat capacity of polarization and the C_p° values (Section 4.7).

CHAPTER 2.0 EXPERIMENTAL

2.1 Materials.

DL-α-Alanine was obtained from BDH (Assay 98.5% to 100.5%) and from Aldrich (Assay 99%), β-Alanine was obtained from Aldrich (Assay 99+%), and Glycine was obtained from Aldrich (Assay 99+%). Before use, the α-alanine, β-alanine, and glycine were recrystallized according to the method of Perrin and Armarego (1988). Each compound was dissolved in a minimum amount of hot water (T = 343 K). The resulting solutions were filtered while hot to remove any insoluble material. Hot ethanol (T = 333 K) was then added slowly to the hot filtrates until a 60/40 ethanol to water ratio was obtained. The resulting precipitates were allowed to digest for five hours at which time the white solids were collected and washed with cold water followed by cold ethanol. The purified α-alanine, β-alanine, and glycine were dried under vacuum, over Drierite, for 120 hours at room temperature.

L-Proline was obtained from Aldrich (Assay 99+ %). Before use, an attempt was made to recrystallize the proline according to the method of Perrin and Armarego (1988). This method failed to precipitate any purified proline and therefore the following modified method was employed. The proline was dissolved in a minimum amount of hot anhydrous ethanol (T = 333 K). The resulting solution was filtered while hot to remove any insoluble material. Warm, anhydrous diethyl ether was then added slowly to the hot filtrate until the

first permanent cloudiness was obtained. The resulting precipitate was allowed to digest for five hours at which time the white solid was collected and washed with cold ethanol followed by cold diethyl ether. The purified proline was dried under vacuum, over Drierite, for 120 hours at room temperature.

Sodium hydroxide solution 50% w/w (Certified) was obtained from Fisher Scientific and used to prepare a 0.099165 ± 0.000006 mol·kg^{-1} stock solution. The concentration of the stock solution was determined in triplicate by pH titration against potassium hydrogen phthalate (Analar, Analytical Reagent). Trifluoromethanesulfonic (triflic) acid was obtained from Alfa Aesar (Assay 99%) and used to prepare a 0.097918 ± 0.000007 mol·kg^{-1} stock solution. Glacial acetic acid (Certified A.C.S.) was obtained from BDH and used to prepare a 0.20034 ± 0.00018 mol·kg^{-1} stock solution. Phosphoric acid (Certified A.C.S.) was obtained from Caledon and used to prepare a 0.19983 ± 0.00001 mol·kg^{-1} stock solution. The concentration of each stock solution (triflic acid, acetic acid, and phosphoric acid) was determined in triplicate by pH titration against tris(hydroxymethyl)aminomethane (Aldrich, Assay 99.9+%). A buffer solution of α-alanine $m(H_2A^+)$ = 0.048974 mol·kg^{-1} and $m(HA^{\pm})$ = 0.050483 mol·kg^{-1} was prepared by adding triflic acid to a stock solution of α-alanine (m = 0.19898 mol·kg^{-1}). A second buffer solution of α-alanine $m(A^-)$ = 0.049658 mol·kg^{-1} and $m(HA^{\pm})$ = 0.049680 mol·kg^{-1} was prepared by adding aqueous sodium hydroxide to a stock solution of α-alanine (m = 0.19898 mol·kg^{-1}). A buffer solution of phosphoric acid $m(H_2PO_4^-)$ = 0.049293 mol·kg^{-1} and $m(H_3PO_4)$ = 0.049279 mol·kg^{-1} was prepared by adding aqueous

sodium hydroxide to a stock solution of phosphoric acid. A buffer solution of acetic acid $m(CH_3COO^-) = 0.049838$ mol·kg^{-1} and $m(CH_3COOH) = 0.049776$ mol·kg^{-1} was prepared by adding aqueous sodium hydroxide to a stock solution of acetic acid.

NaCl (Fisher Scientific, Certified A.C.S., Crystal) was dried at 473 K for 20 hours prior to use. DL-α-alanyl-DL-α-alanine (Aldrich, Assay 98 %), L-prolyl-glycine (Sigma), L-prolyl-hydroxy-L-proline (Sigma), butylamine (Aldrich, Assay 99+ %), ethylamine hydrochloride (Aldrich, Assay 98 %), 2-naphthoic acid (Aldrich, Assay 98 %), and acridine (Aldrich, Assay 97 %) were used without further purification. Degassed, nanopure water (resistivity > 8 MΩ·cm) was used in all of the experiments.

2.2 Hydrothermal Stability Tests.

2.2.1 Apparatus

Batch experiments to determine the hydrothermal stability of the aqueous amino acids were conducted in sealed Pyrex tubes (~17 cm long, 6 mm outside diameter, 1 mm wall thickness) contained in an oven designed for this purpose.

The oven used in the batch experiments is shown in Figure 2.2.1. The oven consisted of a cylindrical brass block into which thirteen holes had been drilled. The radius of each hole was slightly larger than the radius of the Pyrex tubes and each hole was approximately 15 cm deep. The brass block was capped by a removable cylindrical aluminum block containing an identical set of holes with an approximate depth of 2.5 cm. The core was

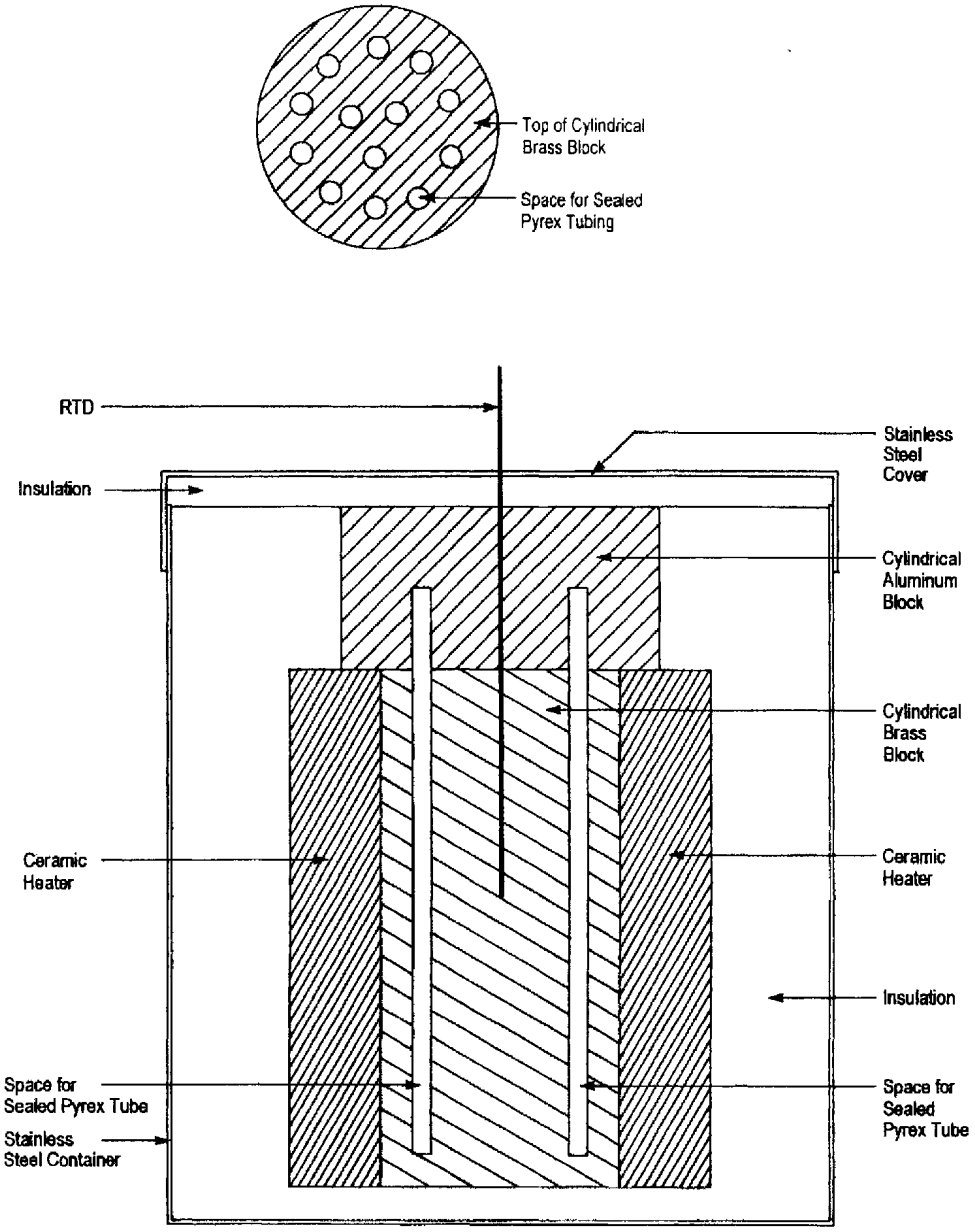

Figure 2.2.1 Schematic diagram of the oven used in the batch experiments.

surrounded by a cylindrical ceramic heater that was controlled by an OMEGA CN76030 Temperature Controller. An insulated stainless steel container surrounded both the heater and the core to prevent heat loss and to contain explosion debris. This oven configuration required approximately twenty minutes to warm from room temperature to 523 K.

The tubes were prepared from 40 cm lengths of Pyrex tubing that were subsequently cut in half using a fine-tipped oxygen torch. The use of the torch also served to seal one end of each 20 cm tube produced. The batch experiments were conducted using one molal amino acid solutions. Each aliquot of amino acid solution was sealed in a Pyrex tube such that the ratio of solution to air in the tube was approximately 1 : 2. This allowed more than sufficient space for thermal expansion and it reduced the frequency of explosion.

2.2.2 Methods.

To obtain meaningful results from the batch experiments it was necessary to keep the time taken to heat the amino acid samples, from room temperature to 523 K, as brief as possible. In order to place the sealed tubes in the oven, the aluminum cap had to be removed. If the oven was preheated to 523 K before the tubes were added, a dangerously large thermal gradient was produced in the tubes. The bottom portion of each tube quickly came to thermal equilibrium with the brass block. The top portion of each tube remained in thermal equilibrium with the atmosphere until the aluminum cap was replaced. Although the interval between loading the tubes into the brass block and replacing the aluminum cap was kept

small, the large thermal gradient resulted in a one hundred percent explosion rate. Therefore, the following procedure was developed for the loading, heating, and sampling of the tubes. At the start of each run ten tubes containing the same amino acid solution were loaded into the oven, which was at room temperature. Once the tubes were secured, the oven was heated from room temperature to 523 K over a period of approximately 20 minutes. Several tubes were removed from the oven after 90 minutes and the remaining tubes were removed after 72 hours. Visual observations were made when the solutions were hot (523 K) and when the solutions had cooled to room temperature. The concentrations of the amino acids and their decomposition products were measured at room temperature using a Beckman 121MB Amino Acid Analyser as described in Section 2.8.

2.3 Density Measurements at High Temperatures and Pressures.

2.3.1 Apparatus.

Density measurements were made at high temperatures and pressures using the platinum vibrating-tube densitometer constructed by Xiao (1997). During the course of this project the core of the densitometer was completely rebuilt by the author. The design of the densitometer is essentially that given by Albert and Wood (1984) as modified by Corti *et al.* (1990) and described in detail by Xiao *et al.* (1997). The densitometer is shown schematically in Figure 2.3.1 and discussed briefly below.

The U-shaped vibrating tube in this densitometer (2 mm outside diameter, 0.2 mm

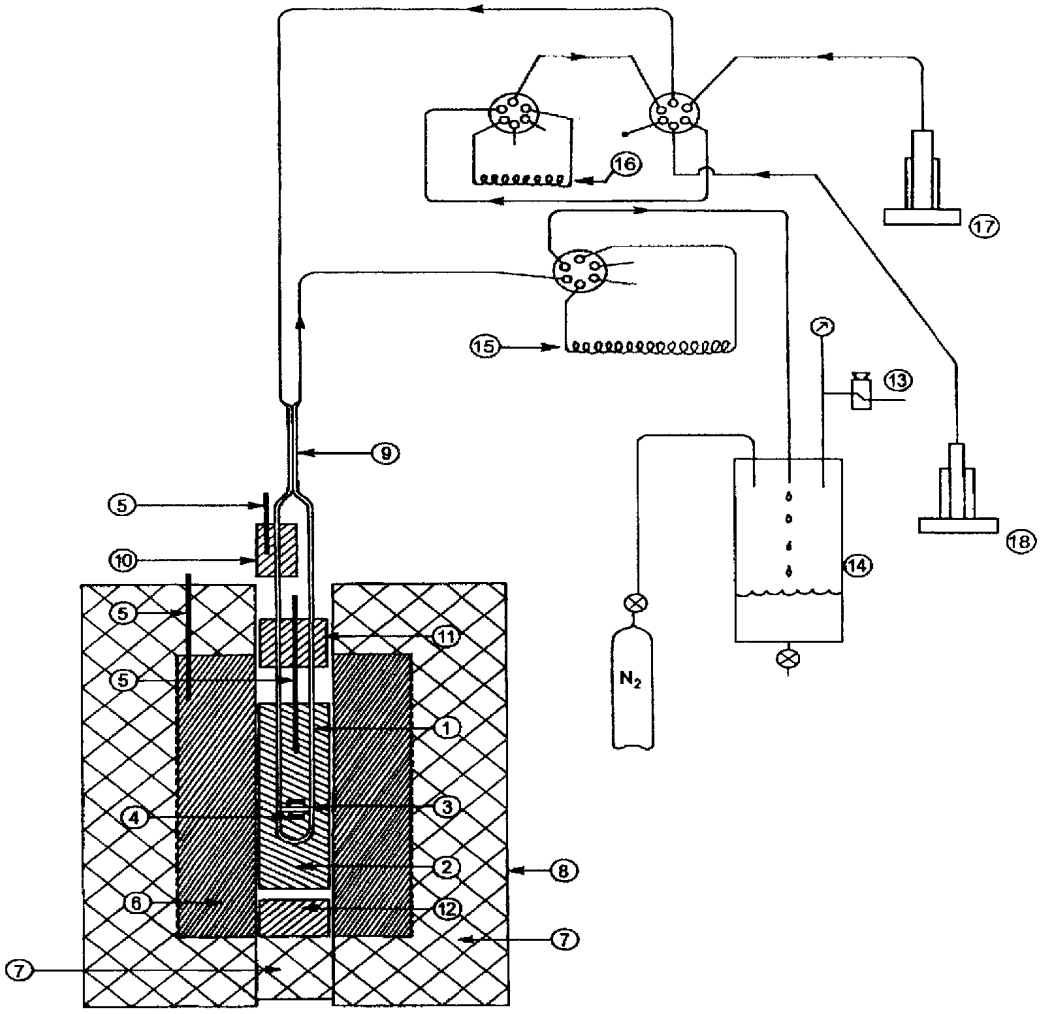

Figure 2.3.1 Schematic diagram of the densitometer. 1, platinum U-shaped vibrating tube; 2, densitometer cell body; 3, Inconel rods for sensing and driver current; 4, permanent magnet; 5, RTD; 6, brass oven; 7, thermal insulation; 8, stainless steel container; 9, heat exchanger; 10, aluminum preheater; 11, aluminum heat shield; 12, brass heat shield; 13, back-pressure regulator; 14, stainless steel reservoir; 15, sampling loop; 16, injection loop; 17, pump; 18, pre-pressurizing pump.

wall thickness) was fabricated from an alloy (90% platinum + 10% iridium). To house the U-tube, a slot (10 cm long, 3 cm wide, and 2.75 cm deep) was machined into a cylindrical brass block (20 cm long, 5.5 cm diameter). The ends of the U-tube exited through two holes machined into the brass cylinder and were secured in these holes with silver solder. Two Inconel rods (0.3 mm diameter) were mounted on the U-tube with ceramic adhesive and were connected to a feedback amplifier using fine silver wires. A permanent, horseshoe magnet was attached to the brass cylinder such that the Inconel rods rested between its poles. The temperature of the brass cylinder was measured by a 100 Ω platinum RTD located in a hole machined along the axis of the brass cylinder. The temperature was monitored by a Hewlett-Packard 3478A multimeter. The RTD was calibrated to an estimated accuracy of 0.02 K by measuring the ice point of water and the freezing points of tin and lead (supplied by NIST as standard reference materials). This assembly constituted the core of the densitometer.

Two strands of insulated heating wire (nickel + chromium) were wound around a cylindrical brass block (30 cm long, 20 cm o.d., 5.5 cm i.d.) in a symmetrical counter-current configuration to minimize electromagnetic inductance. This large brass cylinder and its insulated heating wires were placed in an insulated stainless steel container. This assembly constituted the oven of the densitometer into which the core was placed. The oven temperature was controlled by an Omega CN2011P2-D3 temperature controller and was measured by a 100 Ω platinum RTD located near the outer circumference of the large brass cylinder. Stable temperature control was provided by both the large thermal mass of the large

brass cylinder and the insulation surrounding it. The fluctuation in temperature measured by the RTD in the core remained less than 0.03 K at $T = 523$ K.

Exterior to the core, the inlet and outlet ends of the densitometer U-tube came together to form a heat exchanger as shown in Figure 2.3.1. Between the heat exchanger and the entrance to the core the inlet tube passed through a small aluminum cylinder that served as a preheater. The aluminum cylinder is surrounded by a Chromalox heater that was controlled to 0.2 K by an Omega CN76122 temperature controller. The temperature of the preheater was measured by a 100 Ω platinum RTD located near the outer circumference of the aluminum cylinder. The heat exchanger, preheater and associated tubing were wrapped in insulation to prevent heat loss.

An Isco 260D high pressure pump delivered water to the system at a constant volumetric flow rate (0.0117 $mL \cdot s^{-1}$ for aqueous proline and aqueous β-alanine, 0.00833 $mL \cdot s^{-1}$ for aqueous α-alanine). A two-position six-port valve was used to direct the flow of water either directly into the densitometer, to act as a reference fluid or into a 15 cm^3 injection loop to force the sample solution into the densitometer. The injection loop was constructed from 3.2 mm o.d. PEEK tubing (Upchurch Scientific). The sample solution was loaded into the injection loop using a second two-position six-port valve and a filling syringe and was pre-pressurized to the system pressure by an HPLC pump. The pressure of the flow system was maintained by a nitrogen filled cylinder and a back-pressure regulator (Tescom model 26-1722-24). The system pressure was measured by an Omega PX623 pressure

transducer and an Omega DP41-E process indicator.

The design for the electronic circuit was based on the phase-locked loop described by Wood *et al.* (1989). The period of vibration was measured with a Hewlett-Packard 5316A universal counter.

2.3.2 Methods.

Aqueous NaCl and water were used to calibrate the densitometer at each temperature and pressure using the literature values of Archer (1992) and Hill (1990), respectively.

Seven to thirteen 15 mL sample solutions of α-alanine and proline were injected into the densitometer along with approximately 300 mL of water from the Isco pump at each temperature and pressure at which measurements were made. The effluent from the densitometer was collected in a stainless steel reservoir under an atmosphere of nitrogen at the operating pressure of the densitometer. At the conclusion of a set of measurements the reservoir was emptied into a sample vial that was under an atmosphere of nitrogen at ambient pressure so that the solutions could be analysed for thermal decomposition products. The procedure for β-alanine was similar, except that the effluent samples were collected in a sampling loop that was added to the densitometer on the output side of the core. A two-position six-port valve was used to direct the flow of the effluent either directly into the stainless steel reservoir or into the reservoir through the 3 cm^3 sampling loop. The sampling loop was constructed from 3.2 mm o.d. PEEK tubing (Upchurch Scientific). As the sample

solution passed through the sampling loop it was diverted to a nitrogen filled syringe. The effluent was analysed for the presence of thermal products using a Beckman 121MB Amino Acid Analyser.

2.4 Density Measurements at Room Temperature.

The density measurements made at 298.10 K and 0.1 MPa were obtained using a Sodev 03D vibrating-tube densitometer equipped with a platinum cell. The design of the densitometer is essentially that given by Picker *et al.* (1974). A Sodev CT-L circulating bath was used to maintain the temperature of the densitometer to within ± 0.01 K. The temperature of the densitometer was measured by an Omega 44107 thermistor that had been calibrated with a Hewlett-Packard 2804A quartz-crystal thermometer traceable to NIST standards. Aqueous NaCl and water were used to calibrate the densitometer at each temperature and pressure using the literature values of Archer (1992) and Hill (1990), respectively.

2.5 Specific Heat Capacity Measurements at High Temperatures and Pressures.

2.5.1 Apparatus.

Specific heat capacity measurements were made at high temperatures and pressures using the differential flow calorimeter at Université Blaise Pascal in Clermont-Ferrand, France. The design of the calorimeter is described by Hnědkovský *et al.* (1999). The

calorimeter is shown schematically in Figure 2.5.1 and discussed briefly below.

The two matched cells in this calorimeter (200 mm length, 2 mm outside diameter, 0.4 mm wall thickness) were fabricated from a platinum-iridium alloy tube. One cell is referred to as the reference cell and the other is referred to as the working cell. The centre section of each cell was wrapped tightly with a nichrome coaxial heater (ThermoCoax, 0.5 mm outside diameter) that was silver soldered directly to the cells. A 100 Ω RTD was attached to the inlet end of the cell with high temperature ceramic cement (OmegaBond 600). A second 100 Ω RTD was attached to the outlet end of the cell with high temperature ceramic cement (OmegaBond 600). A similar arrangement of RTDs was used in the working cell. The cells were positioned in separate cavities that had been machined into a rectangular aluminum block. A platinum-iridium alloy transport tube (1.2 mm outside diameter, 0.2 mm wall thickness) was welded into each end of each cell. To ensure that the temperature of the fluid entering each cell was equal to the temperature of the aluminum block, the inlet transport tubes were placed in grooves inside the aluminum block. The temperature of the block was controlled with a decade resistance box. This assembly constituted the core of the calorimeter.

The calorimeter core was suspended from the cover of a cylindrical stainless steel container that was referred to as the inner jacket. The inner jacket was housed in a second cylindrical stainless steel container that was referred to as the outer jacket. The outer jacket was housed in a third cylindrical stainless steel container that was referred to as the vacuum

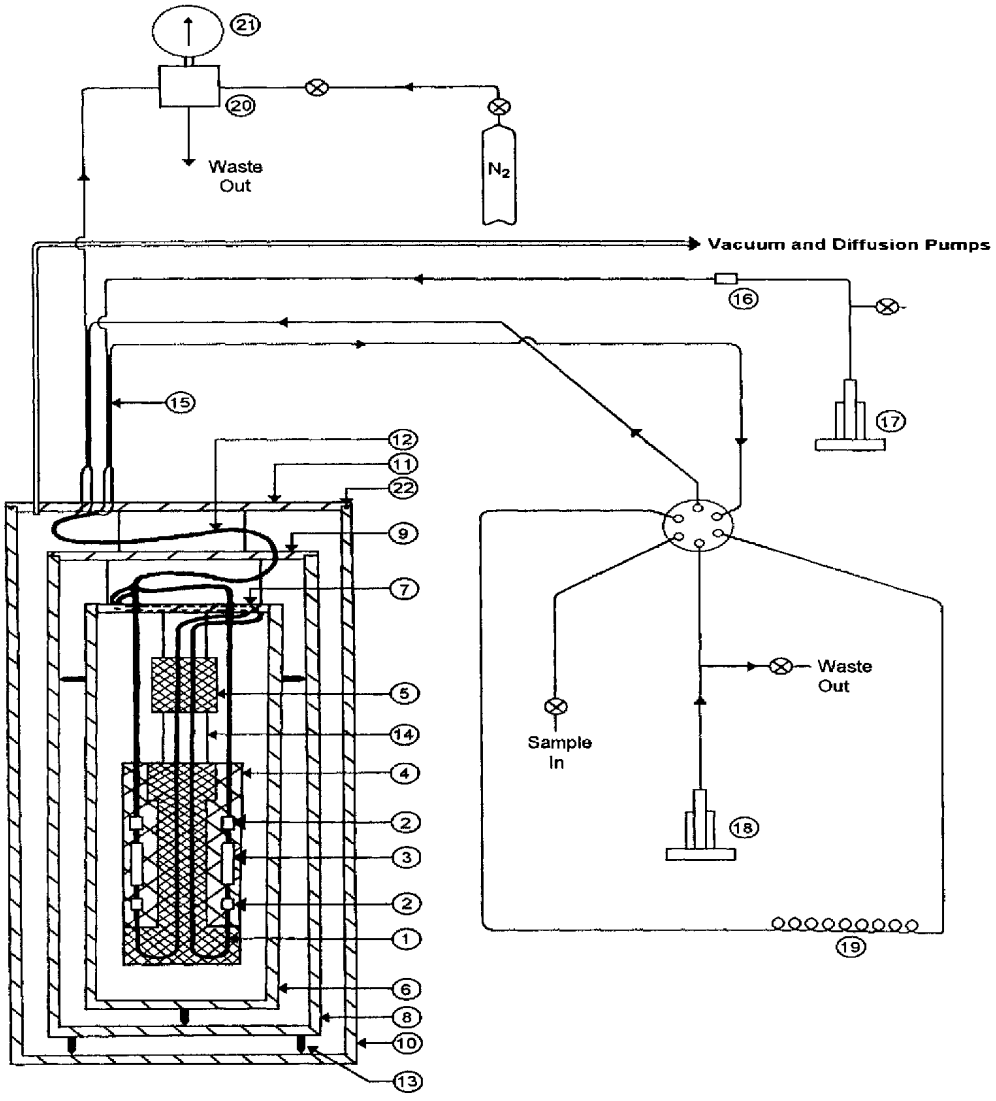

Figure 2.5.1 Schematic diagram of the calorimeter. 1, platinum-iridium tube; 2, RTD; 3, nichrome coaxial heater; 4, rectangular aluminum block; 5, small aluminum block (preheater); 6, inner jacket; 7, inner jacket cover; 8, outer jacket; 9, outer jacket cover; 10, vacuum jacket; 11, vacuum jacket cover; 12, four tube counter-current heat exchanger; 13, positioning pin; 14, support rod; 15, two tube counter-current heat exchanger; 16, check valve; 17, HPLC pump; 18, pre-pressurizing pump; 19, injection loop; 20, back-pressure regulator; 21, pressure gauge; 22, O-ring.

jacket. The temperature of the inner and outer jackets were each controlled with a decade resistance box. A vacuum of approximately 7 Pa was maintained within the vacuum jacket.

A four-stage preheating system was used to maintain the temperature of the core of the calorimeter. Exterior to the vacuum jacket, the inlet and outlet transport tubes for the working cell came together to form a counter-current heat exchanger. A similar configuration existed for the reference cell. This pair of counter-current heat exchangers constituted the first stage of the preheating system. Between the vacuum jacket and the inner jacket, all four transport tubes came together to form a 60 cm counter-current heat exchanger. These tubes were silver soldered together and were wrapped with a nichrome coaxial heater. The heater was controlled by a regulator using a thermocouple with its reference end placed in the upper part of the aluminum block. This constituted the second stage of the preheating system. Two circular grooves were machined into the cover of the inner jacket. The third stage of the preheating system was created when each inlet tube was placed into a circular groove. A regulator, using a thermocouple with its reference end placed in the upper part of the aluminum block, was used to control the temperature of the cover of the inner jacket. Between the cover of the inner jacket and the aluminum block, the inlet tubes passed through a small aluminum block that served as the final stage of the preheating system. A regulator, using a thermocouple with its reference end placed in the upper part of the aluminum block, was used to control the temperature of the small aluminum block.

An HPLC pump (SpectraSERIES P100) delivered water to the system at a constant

volumetric flow rate (2.20 $mL \cdot min^{-1}$). The reference and working cells are connected in series to compensate for fluctuations in the flow rate. A portion of this delay line was thermostated at 298.15 K (Bromma 7600 Precision Thermostat thermostatic bath and proportional controller). As can be seen in Figure 2.5.1 the water from the pump passes through the reference cell before reaching the two-position six-port valve. This valve was used to direct the flow of water either directly into the working cell or into a thermostated injection loop to force the sample solution into the working cell. The sample solution was loaded into the injection loop using a filling syringe and was pre-pressurized to the system pressure using a high pressure pump. The pressure of the flow system was maintained by a back-pressure regulator. The system pressure was measured using a Heise CM-63931 pressure gauge.

2.5.2 Methods.

The four RTDs that were attached to the reference and working cells formed the arms of a Wheatstone bridge with a Wagner earth. The output signal from the Wheatstone bridge was amplified by a lock-in amplifier (Stanford research, SR510). The nichrome coaxial heater that surrounded the reference cell heated the water by approximately 2 K as it passed through the reference cell. The nichrome coaxial heater that surrounded the working cell heated the fluid of interest by approximately 2 K as it passed through the working cell. When the fluid passing through the working cell was water, the power supplied to the nichrome coaxial heater that surrounded the working cell was recorded as the water baseline. When the

fluid passing through the working cell was the sample solution, the power supplied to the nichrome coaxial heater that surrounded the working cell was readjusted so that the bridge balance remained unchanged. The readjusted power was recorded as the sample plateau. This technique allowed the temperature rise in the working cell to remain constant (within 0.2 mK) as the identity of the fluid flowing through the cell changed. The amount of power dissipated across the nichrome coaxial heater in the working cell was calculated from the voltage across the heater and the voltage across a standard resistor that was in series with the heater. This allowed the power to be determined with a precision better than 20 μW.

The absolute calibration of White and Wood (1982) was used to calibrate the calorimeter at each temperature and pressure. The absolute calibration is discussed in Section 1.5.2.

2.6 Specific Heat Capacity Measurements at Room Temperature.

The specific heat capacity measurements made at 298.10 K and 0.1 MPa were obtained using a Picker flow microcalorimeter equipped with platinum cells. The design of the microcalorimeter and the principles of its operation are given by Picker *et al.* (1971), Desnoyer *et al.* (1976), Smith-Magowan and Wood (1981), and White and Wood (1982). A Sodev circulating bath was used to maintain the temperature of the microcalorimeter to within ± 0.01 K. The temperature of the calorimeter was measured by an Omega 44107 thermistor that had been calibrated with a Hewlett-Packard 2804A quartz-crystal

thermometer traceable to NIST standards. Aqueous NaCl and water were used to calibrate the microcalorimeter using the literature values of Archer (1992) and Hill (1990), respectively.

2.7 Spectroscopic Measurements at High Temperatures and Pressures.

2.7.1 Apparatus.

Spectroscopic measurements were made at high temperatures and pressures using a Varian Cary 50 spectrophotometer (190 - 1100 nm) and a high pressure and temperature flow system. The design and construction of the spectroscopic flow system were carried out by Trevani *et al.* (in prep.) and is similar in concept to that developed by Chlistunoff *et al.* (1999). The spectroscopic flow system is shown schematically in Figure 2.7.1 and discussed briefly below.

The cylindrical flow cell (35 mm outside diameter, 40 mm long) was fabricated from titanium. A cylindrical channel was machined along the principal axis of the titanium cylinder as illustrated in Figure 2.7.2. The central portion of this channel acted as the sample compartment in the flow cell. A sapphire window (10 mm diameter, 5 mm thick, Crystal Systems) was placed at each end of the sample compartment (producing an 18 mm optical path length). A Teflon washer (9 mm outside diameter, 5 mm inside diameter) was placed on each side of each window to provide a seal between the sapphire windows and the titanium flow cell. The Teflon washers also cushioned the sapphire windows during thermal

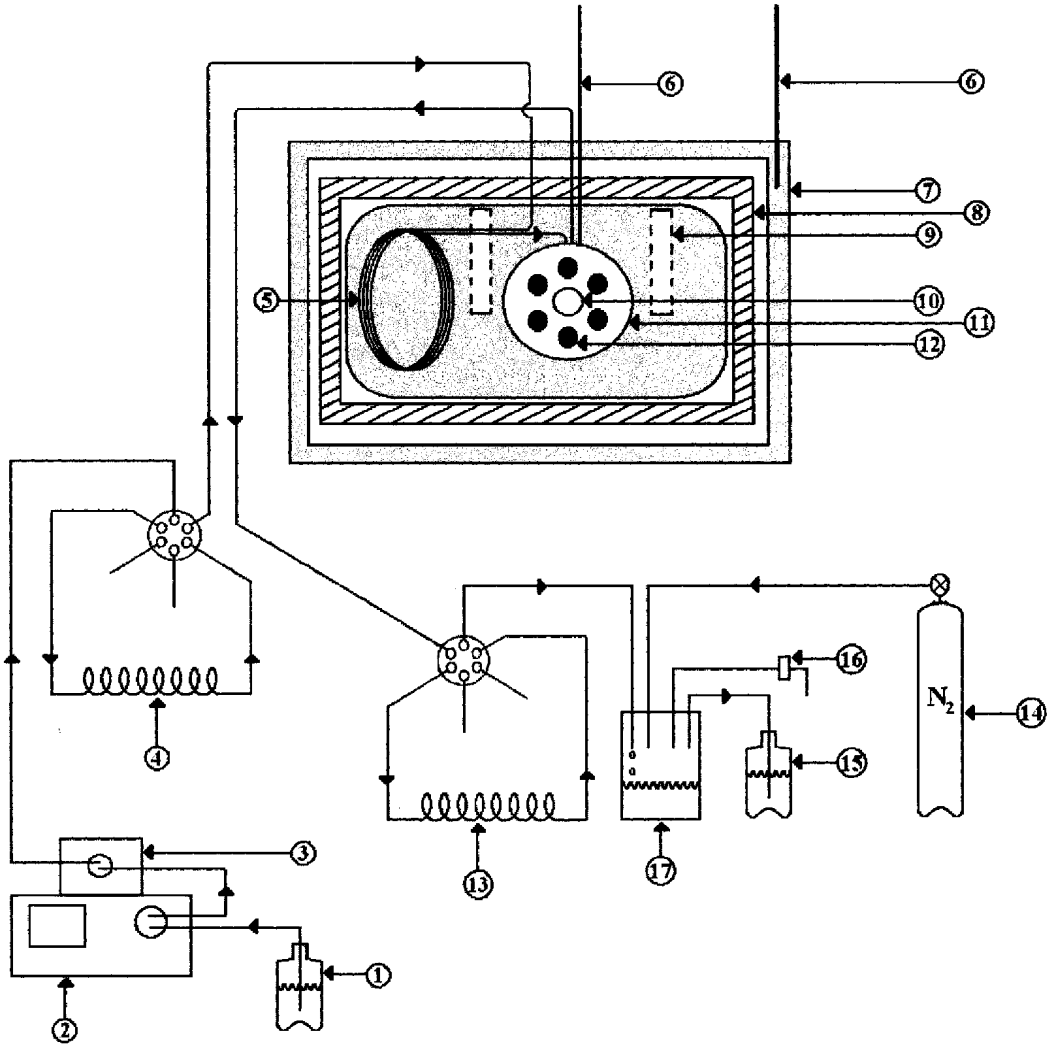

Figure 2.7.1 Schematic diagram of the spectroscopic flow system. 1, water reservoir; 2, Gilson 305 HPLC piston pump; 3, Gilson 805 manometric module; 4, injection loop; 5, preheater; 6, Chromega-Alomega thermocouple; 7, brass/aluminum housing; 8, ceramic insulation; 9, cartridge heater; 10, sapphire window; 11, titanium flow cell; 12, bolt; 13, sampling loop; 14, nitrogen cylinder; 15, reservoir for solution effluent; 16, back pressure regulator; 17, stainless steel reservoir.

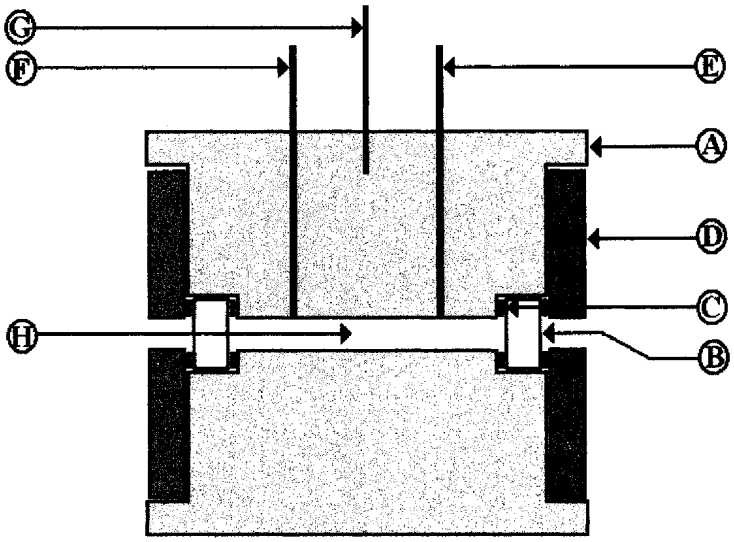

Figure 2.7.2 Schematic diagram of the spectroscopic flow cell. A, cylindrical titanium flow cell; B, sapphire window; C, Teflon washer; D, titanium disc; E, sample solution outlet; F, sample solution inlet; G, Chromega-Alomega thermocouple; H, sample compartment.

expansion of the flow cell. Each sapphire window was secured in place by a titanium disc (28 mm outside diameter, 5 mm inside diameter, 4 mm thick) that was bolted to the end of the cylindrical flow cell. As shown in Figure 2.7.2 the sample solution entered and exited the flow cell through $^{1}/_{16}$" titanium tubing.

The flow cell was mounted in a two-piece brass oven (total dimensions of the brass oven: 104 mm length, 63 mm height, 40 mm width). Two Cromalux CIR-20203 cartridge heaters (120 V, 200 W) were placed in holes machined into the brass oven. A coil of titanium tubing ($^{1}/_{16}$" outside diameter) was wound around a groove machined into the brass oven. This coil of tubing served as the preheater for the flow cell. The brass oven was surrounded by a ceramic insulation (Rescor 310-COTRONICS). The entire insulated cell/oven system was mounted in a small box constructed of brass and aluminum. This housing was cooled by internal water circulation. The temperature of the flow cell was controlled (± 1 K) by an Omega CN76000 temperature controller and was measured by a Chromega-Alomega thermocouple located in the body of the flow cell. The temperature of the housing remained near room temperature and was monitored by a Chromega-Alomega thermocouple located in the body of the housing. The entire flow cell assembly was placed in the sample compartment of a Varian 50 spectrophotometer. Cary Win UV Scan Application software was used to record the absorption spectra

A Gilson 305 HPLC piston pump delivered water to the system at a constant volumetric flow rate (0.3000 $mL \cdot s^{-1}$). A two-position six-port valve was used to direct the

flow of water either directly into the flow cell, to act as a reference fluid or into a 18 cm^3 injection loop to force the sample solution into the flow cell. The injection loop was constructed from 3.2 mm o.d. PEEK tubing (Upchurch Scientific). The sample solution was loaded into the injection loop using a filling syringe and was pre-pressurized to the system pressure. The pressure of the flow system was maintained by a nitrogen filled cylinder and a back-pressure regulator (Tescom model 26-1700). The system pressure was measured by a Gilson 805 manometric module. A two-position six-port valve was used to direct the flow of the solution effluent either directly into the stainless steel reservoir or into the reservoir through a sampling loop. The sampling loop was constructed from 3.2 mm o.d. PEEK tubing (Upchurch Scientific).

2.7.2 Methods.

The value of K_1 and K_2 for α-alanine were estimated using methods described in Section 4.5.2. As illustrated in Figures 2.7.3 and 2.7.4 the estimated values of pK_1 and pK_2 begin to lie within the indicator range of acridine and β-naphthoic acid, respectively, as the temperature approaches the critical temperature of water.

At each temperature and pressure the spectroscopic measurements were made relative to a water baseline. To obtain the effective molal extinction coefficients, $\varepsilon_{AcH^+}(\lambda)$, $\varepsilon_{Ac}(\lambda)$, $\varepsilon_{NapH}(\lambda)$, and $\varepsilon_{Nap^-}(\lambda)$, the UV-visible absorption spectrum was measured for solutions containing acridine ($m = 3.49 \cdot 10^{-5}$ mol·kg^{-1}) and triflic acid ($m = 0.0203$ mol·kg^{-1}), acridine

($m = 3.63 \cdot 10^{-5}$ mol·kg^{-1}) and sodium hydroxide ($m = 0.0981$ mol·kg^{-1}), β-naphthoic acid ($m = 1.45 \cdot 10^{-4}$ mol·kg^{-1}) and triflic acid ($m = 0.100$ mol·kg^{-1}), β-naphthoic acid ($m = 1.43 \cdot 10^{-4}$ mol·kg^{-1}) and sodium hydroxide ($m = 0.0123$ mol·kg^{-1}), respectively.

In aqueous solution an amino acid can exist in either the zwitterionic form $HA^{\pm}$, the neutral form HA^{o}, the deprotonated form A^{-}, or the protonated form H_2A^{+}. The equilibria between the zwitterionic and ionic forms of an amino acid can be summarized as:

$$H_2A^{+} \underset{\rightleftharpoons}{K_1} HA^{\pm} + H^{+} \tag{2.7.2.1}$$

$$HA^{\pm} \underset{\rightleftharpoons}{K_2} A^{-} + H^{+} \tag{2.7.2.2}$$

where K_1 and K_2 are the molar equilibrium constants. From equations (2.7.2.1) and (2.7.2.2) the following expressions are obtained for K_1 and K_2:

$$K_1 = \frac{[HA^{\pm}][H^{+}]}{[H_2A^{+}]} = \frac{m_{HA^{\pm}}[H^{+}]}{m_{H_2A^{+}}} \tag{2.7.2.3}$$

$$K_2 = \frac{[A^{-}][H^{+}]}{[HA^{\pm}]} = \frac{m_{A^{-}}[H^{+}]}{m_{HA^{\pm}}} \tag{2.7.2.4}$$

The concentration of a solute can be converted from molarity to molality by dividing the molarity of the solute by the density of the solution. Combining equations (1.5.3.2) and (2.7.2.3) gives an expression for K_1:

$$K_1 = \frac{K_{Indicator}[HA^{\pm}][HX]}{[H_2A^{+}][X^{-}]} = \frac{K_{Indicator} m_{HA^{\pm}} m_{HX}}{m_{H_2A^{+}} m_{X^{-}}} \tag{2.7.2.5}$$

Similarly, combining equations (1.5.3.2) and (2.7.2.4) gives an expression for K_2:

$$K_2 = \frac{K_{Indicator}[A^-][HX]}{[HA^{\pm}][X^-]} = \frac{K_{Indicator} m_{A^-} m_{HX}}{m_{HA^{\pm}} m_{X^-}} \qquad (2.7.2.6)$$

Solid acridine was added to the α-alanine buffer solution (H_2A^+ / $HA^{\pm}$) until the molality of the acridine was approximately $3.7 \cdot 10^{-5}$ mol·kg^{-1}. Solid β-naphthoic acid was added to the α-alanine buffer solution (A^- / $HA^{\pm}$) until the molality of the β-naphthoic acid was approximately $1.4 \cdot 10^{-4}$ mol·kg^{-1}. UV-visible absorption spectra were obtained for each buffer solution in the presence and absence of the appropriate colorimetric indicator.

To test the accuracy of the measured acid/base dissociation constants obtained using UV-visible spectroscopy and colorimetric indicators, the first acid dissociation constant of phosphoric acid and the acid dissociation constant of acetic acid were measured. The first acid dissociation of phosphoric acid is expressed as:

$$H_3PO_4 \underset{\rightleftharpoons}{K_{a1}} H_2PO_4^- + H^+ \qquad (2.7.2.7)$$

where K_{a1} is the first acid dissociation constant for phosphoric acid. As illustrated in Figure 2.7.3 the values of pK_{a1} obtained by Mesmer and Baes (1974) lie within the indicator range of acridine at temperatures above 425 K. The acid dissociation of acetic acid is expressed as:

$$CH_3COOH \underset{\rightleftharpoons}{K_a} CH_3COO^- + H^+ \qquad (2.7.2.8)$$

where K_a is the acid dissociation constant for acetic acid. As illustrated in Figure 2.7.4 the

values of pK_a obtained by Mesmer *et al.* (1989) lie within the indicator range of β-naphthoic acid over the entire temperature range under consideration. From equations (2.7.2.7) and (2.7.2.8) the following expressions are obtained for K_{a1} and K_a:

$$K_{a1} = \frac{[H_2PO_4^-][H^+]}{[H_3PO_4]} = \frac{m_{H_2PO_4^-}[H^+]}{m_{H_3PO_4}} \qquad (2.7.2.9)$$

$$K_a = \frac{[CH_3COO^-][H^+]}{[CH_3COOH]} = \frac{m_{CH_3COO^-}[H^+]}{m_{CH_3COOH}} \qquad (2.7.2.10)$$

Substitution of equation (1.5.3.2) into equations (2.7.2.9) and (2.7.2.10) gives:

$$K_{a1} = \frac{K_{Indicator}[H_2PO_4^-][HX]}{[H_3PO_4][X^-]} = \frac{K_{Indicator} m_{H_2PO_4^-} m_{HX}}{m_{H_3PO_4} m_{X^-}} \qquad (2.7.2.11)$$

$$K_a = \frac{K_{Indicator}[CH_3COO^-][HX]}{[CH_3COOH][X^-]} = \frac{K_{Indicator} m_{CH_3COO^-} m_{HX}}{m_{CH_3COOH} m_{X^-}} \qquad (2.7.2.12)$$

Solid acridine was added to the $H_2PO_4^-$ / H_3PO_4 buffer solution until the molality of the acridine was approximately $3.7 \cdot 10^{-5}$ mol·kg^{-1}. Solid β-naphthoic acid was added to the CH_3COO^- / CH_3COOH buffer solution until the molality of the β-naphthoic acid was approximately $1.4 \cdot 10^{-4}$ mol·kg^{-1}. UV-visible absorption spectra were obtained for each buffer solution in the presence and absence of the appropriate colorimetric indicator.

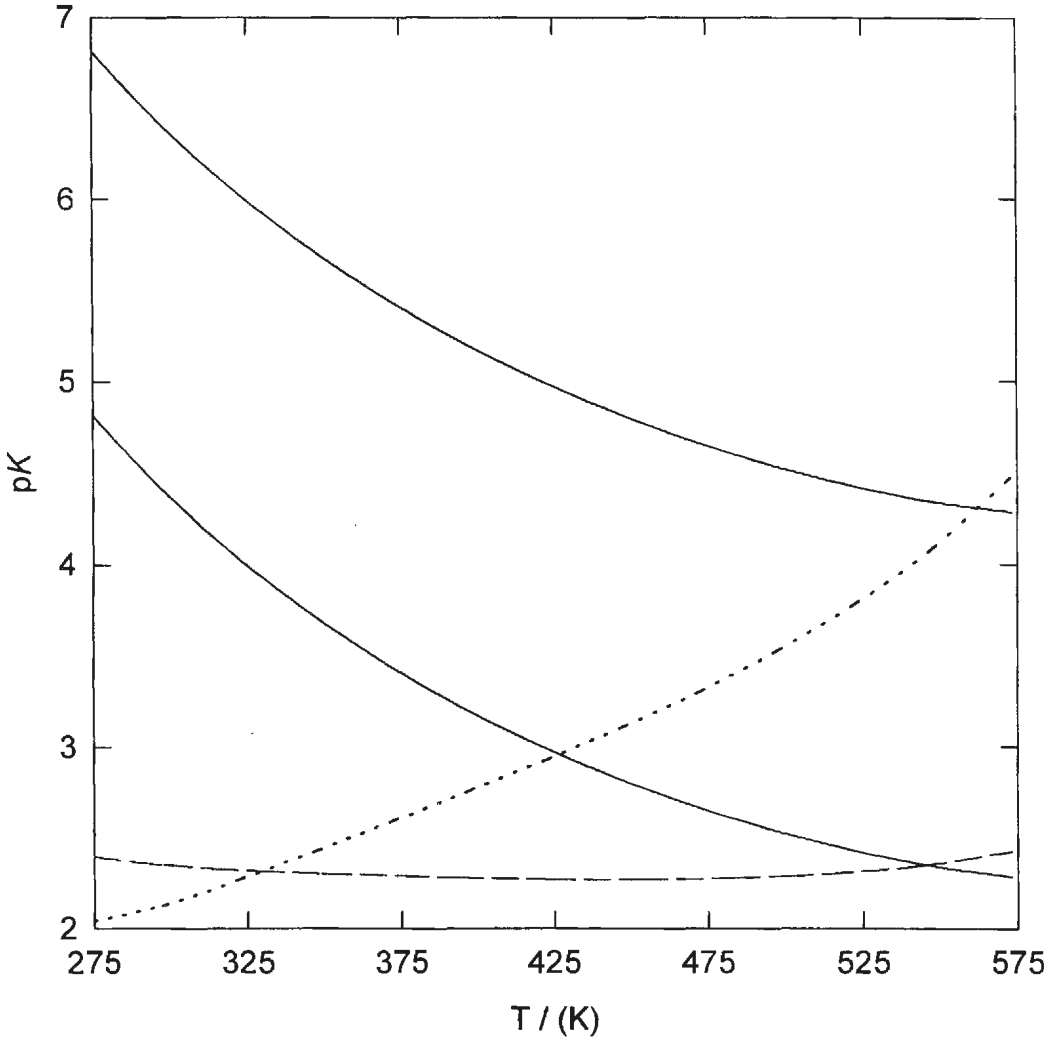

Figure 2.7.3 Comparison of the indicator range of acridine with the predicted values of pK_1 for α-alanine and the values of pK_{a1} for phosphoric acid as a function of temperature. Lines represent the following: —, $pK_{Acridine} \pm 1$ (indicator range); ---, pK_1 as estimated in Section 4.5.2; ·····, pK_{a1} obtained from Mesmer and Baes (1974)

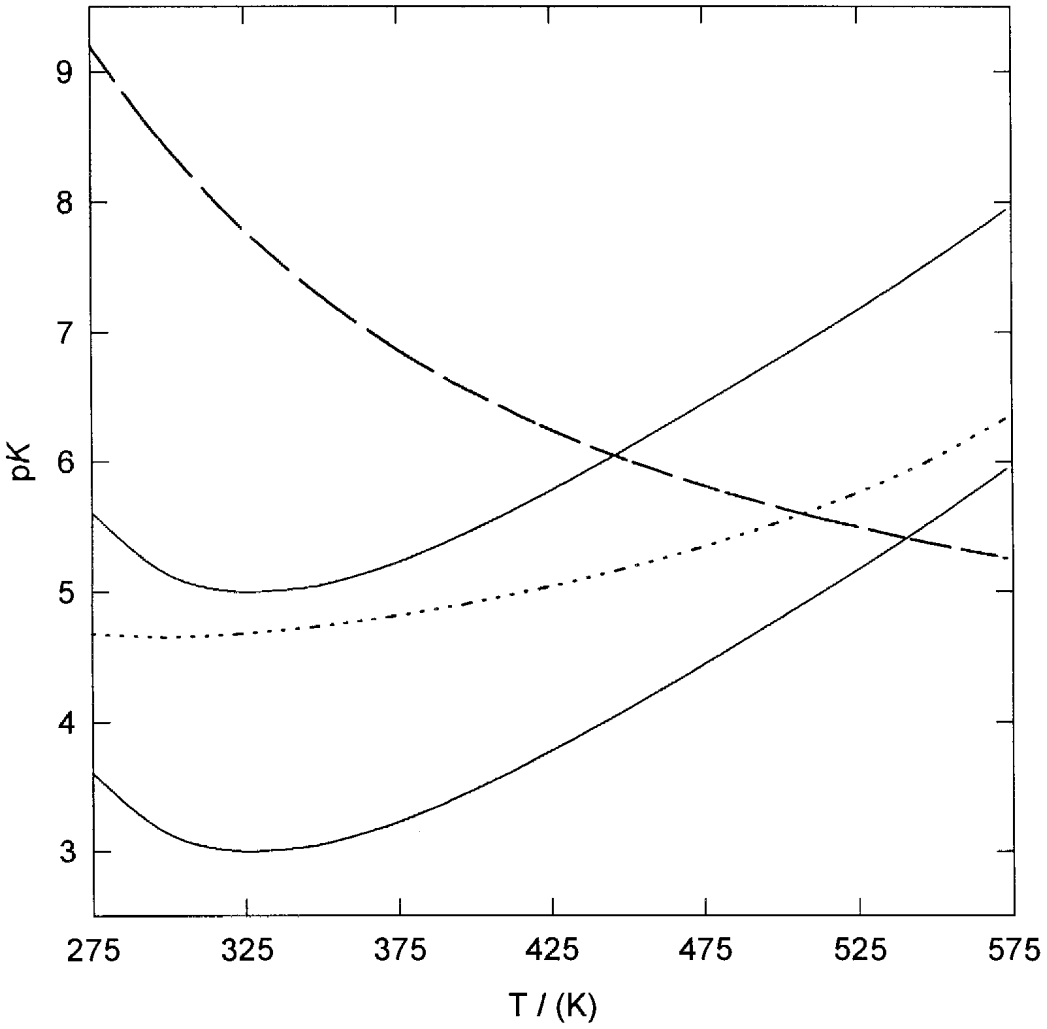

Figure 2.7.4 Comparison of the indicator range of β-naphthoic acid with the predicted values of pK_2 for α-alanine and the values of pK_a for acetic acid as a function of temperature. Lines represent the following: —, $pK_{\beta\text{-}naphthoic} \pm 1$ (indicator range); ---, pK_2 as estimated in Section 4.5.2; ·····, pK_a obtained from Mesmer *et al.* (1989).

2.8 Analytical Methods.

A Beckman 121MB Amino Acid Analyser was used to measure approximate amino acid concentrations in the batch experiments and to analyse for hydrothermal products in the effluent from the densitometer. The amino acid analyser detects ninhydrin-active species over a wide range of concentrations, with the optimal concentration being 3 $mmol \cdot kg^{-1}$. Separation is achieved by ion chromatography of the $R_3C(NH_3)^+$ species in a dilute solution of acid containing trace amounts of ninhydrin which acts as a colorimetric indicator. The separated ninhydrin-active species are detected by a UV-visible detector and recorded as an ion chromatograph (absorbance versus retention time). The amino acid analyser was calibrated with a set of standard solutions, each containing a single ninhydrin-active species at a known concentration. The set of standard solutions for each sample solution must include a standard for each ninhydrin-active species that is possibly present. Comparison of the peak locations in the sample chromatograph to those in the standard chromatograph indicates the identity of the species in the sample solution. For a given class of compounds, the peak location depends primarily on the molar mass of the species and thus two different species with the same molar mass may have overlapping peaks. This property can be exploited if a particular ninhydrin-active species cannot be obtained for use in a standard solution. The concentration of each species was determined by comparing the area under the peak in the sample chromatograph to the area under the peak in the corresponding standard chromatograph.

For α-alanine, β-alanine, glycine, and proline the primary thermal reactions are amino acid condensation (Flegmann and Tattersall, 1979; Fox and Dose, 1977; Wilson and Cannan, 1937) and decarboxylation (Vallentyne, 1964). Equations (2.8.1) and (2.8.2) represent amino acid condensation and decarboxylation, respectively.

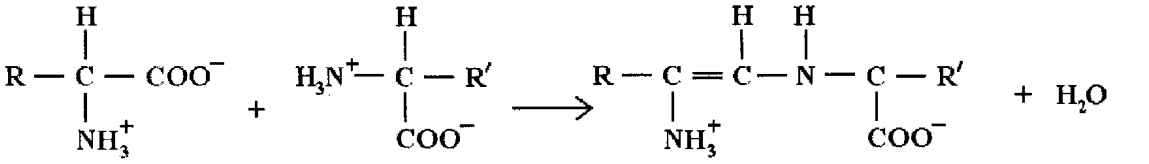

(2.8.1)

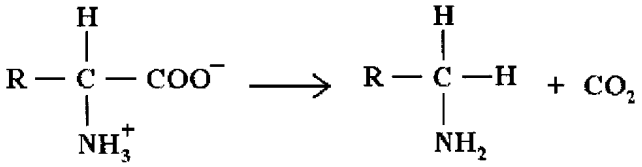

(2.8.2)

With respect to amino acid condensation, the primary product involving α-alanine would be α-alanyl-α-alanine, the primary product involving β-alanine would be β-alanyl-β-alanine, the primary product involving glycine would be glycyl-glycine, and the primary product involving proline would be prolyl-proline. With respect to decarboxylation, α-alanine and β-alanine would yield ethylamine, glycine would yield methylamine, and proline would yield butylamine. These thermal products are all ninhydrin-active and can be detected by the amino acid analyser. The set of standard solutions used to calibrate the amino acid analyser consisted of a 3 mmol·kg^{-1} solution for each of the following: L-prolyl-hydroxy-L-proline, L-prolyl-glycine (these two compounds have molar masses just above and below the molar mass of prolyl-proline, and therefore should indicate the approximate position of a prolyl-

proline peak), butylamine, proline, α-alanyl-α-alanine (which has the same molar mass as β-alanyl-β-alanine and should indicate the approximate position of the β-alanyl-β-alanine peak), ethylamine, α-alanine and β-alanine. To test the detection limit of the Beckman 121MB Amino Acid Analyser, two 3 $mmol \cdot kg^{-1}$ solutions of each amino acid (α-alanine, β-alanine and proline) were prepared. In the first set of solutions the impurities were added until their concentrations were approximately 10% of the amino acid concentration (L-prolyl-hydroxy-L-proline, L-prolyl-glycine, and butylamine to the proline solution; α-alanyl-α-alanine and ethylamine to both the α-alanine solution and the β-alanine solution). In the second set of solutions the impurities were added until their concentrations were approximately 1% of the amino acid concentration. All impurities were detected except the 1% ethylamine in the α-alanine solution. Therefore, the detection limit for all of the impurities, with the exception of the 1% ethylamine in the α-alanine solution, was less than 0.03 $mmol \cdot kg^{-1}$. The detection limit for the 1% ethylamine in the α-alanine solution was less than 0.3 $mmol \cdot kg^{-1}$.

CHAPTER 3.0 RESULTS

3.1 Amino Acid Thermal Decomposition.

The results of the batch thermal decomposition experiments described in Section 2.2 are summarized in Table 3.1.1. It was found that 51% of the α-alanine and 18% of the proline had undergone thermal reaction in the first 1.5 hours of heating at 523 K. At the end of 1.5 hours of heating neither amino acid solution contained any precipitate. After 72.0 hours of heating both amino acids had undergone complete thermal reaction and a precipitate was found in both solutions. These results confirmed that α-alanine and proline are suitable for study at the temperatures, pressures, molalities, and times used in this work ($\leq$ 10 minutes in the hot zone of the densitometer, calorimeter, or spectroscopic flow cell). After 1.5 hours of heating at 523 K, a precipitate was observed in the glycine solution, suggesting that the glycine is considerably less stable than the other two candidate amino acids.

No decomposition products were detected in the α-alanine or proline effluent that had passed through the densitometer at any of the temperatures or pressures of this study. At 523 K, both the α-alanine and proline effluents were clear and colorless while under a nitrogen atmosphere. However, upon exposure to the laboratory atmosphere both of these effluents developed a yellow coloration over a period of 30 minutes. The concentrations of the colored impurities were below the detection limit of the amino acid analyser. At temperatures below 423 K no decomposition products were detected in the β-alanine

Table 3.1.1 Thermal decomposition results for α-alanine, proline, and glycine solutions after 0, 1.5, and 72.0 h at 523 K.

Appearance	$t = 0$ h	$t = 1.5$ h	$t = 72.0$ h
		α-Alanine	
hot	clear, colorless	clear, colorless	clear, slight yellow coloration
cold	clear, colorless	clear, very slight yellow coloration	colorless liquid, white precipitate
		51 % thermally reacted †	100 % thermally reacted †
		Proline	
hot	clear, colorless	clear, slight yellow coloration	yellow liquid, white precipitate
cold	clear, colorless	clear, slight yellow coloration	yellow liquid, white and yellow precipitate
		18 % thermally reacted †	100 % thermally reacted †
		Glycine	
hot	clear, colorless	clear, yellow-brown coloration	yellow-brown liquid, white precipitate
cold	clear, colorless	yellow-brown liquid, white precipitate	yellow liquid, white precipitate

† The Beckman 121 MB Amino Acid Analyser was used to determine the percent of amino acid which had undergone thermal reaction during the batch experiments.

effluent. Ammonia was detected in the β-alanine effluent obtained at 473 K. The amino acid analysis indicated that at this temperature approximately 26 % of the β-alanine had been converted to ammonia. At 473 K, the β-alanine experiments produced effluent that remained clear and colorless upon exposure to the laboratory atmosphere.

An attempt to measure the densities of α-alanine solutions at 573 K yielded erratic results for V_ϕ that deviated to high positive values at low molalities (this type of behaviour for both V_ϕ and $C_{p,\phi}$ was used as an indicator of thermal decomposition). Analysis of the effluent solutions from the densitometer at 20 MPa and 10 MPa revealed that there had been decomposition to ammonia (10.9 and 13.4 mol percent, respectively), ethylamine (23.3 and 32.0 mol percent, respectively) and trace amounts of α-alanyl-α-alanine. These results suggest that the rate of thermal decomposition decreases with increasing pressure.

3.2 Apparent Molar Volumes.

The experimentally determined relative densities ($\rho - \rho_w$) are listed in Tables 3.2.1, 3.2.2, 3.2.3, and 3.2.4 for aqueous α-alanine, β-alanine, glycine, and proline, respectively. Apparent molar volumes V_ϕ were calculated from the densities according to the definition:

$$V_\phi = \left(\frac{1000(\rho_w - \rho)}{(m\rho\rho_w)} \right) + \left(\frac{M_2}{\rho} \right) \qquad (1.5.1.2)$$

where ρ and ρ_w are the densities of the amino acid solution and water, respectively, m is the molality, and M_2 is the molar mass of the solute (89.093 $g \cdot mol^{-1}$ for α-alanine and β-alanine,

75.067 g·mol^{-1} for glycine, 115.131 g·mol^{-1} for proline). The experimental apparent molar volumes are listed in Tables 3.2.1, 3.2.2, 3.2.3, and 3.2.4 for aqueous α-alanine, β-alanine, glycine, and proline, respectively. The values of the average temperature and pressure were calculated from the experimental values measured for a given set of amino acid solutions, as listed in Tables 3.2.1 to 3.2.4, and the associated calibration experiments.

Simple polynomial expressions were used to fit the molality dependence of the apparent molar volume data for each amino acid studied at each temperature and pressure. The polynomial function chosen for α-alanine and β-alanine was:

$$V_\phi = V^o + bm + cm^2 \qquad (3.2.1)$$

where V° is the standard partial molar volume, b and c are temperature and/or pressure dependent adjustable parameters. The polynomial function chosen for glycine and proline was:

$$V_\phi = V^o + bm \qquad (3.2.2)$$

Xiao and Tremaine (1996) observed that the uncertainty associated with experimentally determined apparent molar volumes increases as the molality of the sample solutions decreases. Therefore, the apparent molar volumes measured in this work were given a weight equal to the molality of the solution in the least squares fits. The values of V°, b, and c obtained by fitting equation (3.2.1) to each set of isothermal volumetric data for α-alanine and β-alanine are summarized in Table 3.2.5. The values of V° and b obtained by fitting equation (3.2.2) to each set of isothermal volumetric data for glycine and proline are also

summarized in Table 3.2.5. The fitted isotherms for α-alanine are plotted in Figures 3.2.1, 3.2.2, and 3.2.3; the fitted isotherms for β-alanine are plotted in Figures 3.2.4, 3.2.5, and 3.2.6; the fitted isotherms for glycine are plotted in Figure 3.2.7; and the fitted isotherms for proline are plotted in Figures 3.2.8, 3.2.9, and 3.2.10.

As illustrated in Figures 3.2.1 to 3.2.10, the simple polynomial expressions (linear or quadratic) accurately reproduce the apparent molar volumes obtained at each temperature and pressure. It is also observed that there is very little scatter in the experimental results. The standard partial molar volumes listed in Table 3.2.5 increase with temperature until $T \approx 423$ K and then deviate toward negative values.

Table 3.2.1 Densities relative to water ($\rho - \rho_w$) and apparent molar volumes V_ϕ for aqueous solutions of α-alanine as a function of molality m.

T K	p MPa	ρ_w g·cm^{-3}	m mol·kg^{-1}	$10^2 \cdot (\rho - \rho_w)$ g·cm^{-3}	V_ϕ cm^3·mol^{-1}
		$T_{average}$ = 298.10 K; $p_{average}$ = 0.100 MPa			
298.10	0.100	0.997055	0.95258	2.529	61.10
298.10	0.100	0.997055	0.83574	2.237	61.05
298.10	0.100	0.997055	0.63154	1.717	60.94
298.10	0.100	0.997055	0.52269	1.433	60.89
298.10	0.100	0.997055	0.40562	1.122	60.83
298.10	0.100	0.997055	0.31134	0.8677	60.76
298.10	0.100	0.997055	0.16204	0.4572	60.62
298.10	0.100	0.997055	0.10203	0.2889	60.58
		$T_{average}$ = 298.137 K; $p_{average}$ = 0.100 MPa			
298.137	0.100	0.997045	1.21451	3.165	61.20
298.137	0.100	0.997045	0.59160	1.623	60.77
298.137	0.100	0.997045	0.28780	0.8061	60.69
298.136	0.100	0.997045	0.14896	0.4242	60.46
298.139	0.100	0.997044	0.080101	0.2278	60.61
298.134	0.100	0.997046	0.080101	0.2280	60.58
		$T_{average}$ = 333.21 K; $p_{average}$ = 10.047 MPa			
333.20	10.033	0.987465	1.00958	2.555	62.64
333.19	10.041	0.987471	0.80030	2.059	62.54
333.20	10.041	0.987470	0.63154	1.648	62.42
333.20	10.045	0.987469	0.52269	1.378	62.31
333.21	10.045	0.987465	0.40562	1.082	62.17
333.21	10.051	0.987468	0.31134	0.8384	62.08
333.22	10.055	0.987464	0.16204	0.4431	61.90
333.22	10.055	0.987462	0.10203	0.2809	61.81

T K	p MPa	ρ_w g·cm^{-3}	m mol·kg^{-1}	$10^2 \cdot (\rho - \rho_w)$ g·cm^{-3}	V_ϕ cm^3·mol^{-1}
		$T_{average}$ = 381.70 K; $p_{average}$ = 10.057 MPa			
381.69	10.060	0.956791	1.00958	2.596	63.31
381.70	10.062	0.956783	0.80030	2.106	62.98
381.70	10.058	0.956776	0.63154	1.684	62.88
381.71	10.059	0.956773	0.52269	1.410	62.73
381.71	10.062	0.956777	0.40562	1.108	62.57
381.70	10.060	0.956784	0.31134	0.8592	62.41
381.70	10.054	0.956780	0.16204	0.4553	62.13
381.70	10.052	0.956774	0.10203	0.2892	61.96
		$T_{average}$ = 422.42 K; $p_{average}$ = 10.036 MPa			
422.15	10.064	0.923300	1.00958	2.749	62.69
422.19	10.013	0.923254	0.80030	2.224	62.39
422.28	10.079	0.923197	0.80030	2.225	62.39
422.59	10.007	0.922868	0.63154	1.782	62.21
422.27	10.016	0.923151	0.52269	1.490	62.07
422.27	10.018	0.923161	0.40562	1.170	61.87
422.28	10.014	0.623151	0.31134	0.9081	61.68
422.27	10.093	0.923227	0.16204	0.4814	61.33
422.27	10.097	0.923233	0.10203	0.3054	61.18
		$T_{average}$ = 477.24 K; $p_{average}$ = 10.058 MPa			
477.15	10.045	0.866437	1.00958	3.078	60.08
477.10	10.045	0.866482	0.80030	2.479	59.85
477.16	10.053	0.866348	0.63154	1.982	59.65
477.28	10.064	0.866288	0.52269	1.658	59.43
477.30	10.061	0.866249	0.40562	1.303	59.15
477.36	10.068	0.866188	0.31134	1.009	58.96
477.36	10.070	0.866242	0.16204	0.5358	58.42

T / K	p / MPa	ρ_w / g·cm^{-3}	m / mol·kg^{-1}	$10^2 \cdot (\rho - \rho_w)$ / g·cm^{-3}	V_ϕ / cm^3·mol^{-1}
		$T_{average}$ = 523.36 K; $p_{average}$ = 10.063 MPa			
523.33	10.071	0.805661	1.00958	3.469	55.26
523.39	10.075	0.805566	0.80030	2.800	54.79
523.40	10.073	0.805556	0.63154	2.248	54.23
523.38	10.072	0.805574	0.52269	1.882	53.86
523.39	10.060	0.805552	0.40562	1.479	53.43
523.36	10.054	0.805598	0.31134	1.147	53.08
523.33	10.049	0.805636	0.10203	0.3849	52.21
		$T_{average}$ = 334.65 K; $p_{average}$ = 19.977 MPa			
334.61	19.976	0.990941	1.00958	2.519	62.90
334.60	19.977	0.990952	0.80030	2.033	62.75
334.61	19.979	0.990944	0.63154	1.628	62.62
334.65	19.976	0.990922	0.52269	1.362	62.51
334.71	19.978	0.990894	0.40562	1.069	62.39
334.67	19.979	0.990924	0.31134	0.8322	62.17
333.65	19.977	0.990923	0.16204	0.4380	62.11
		$T_{average}$ = 383.20 K; $p_{average}$ = 19.939 MPa			
383.23	19.940	0.960211	1.00958	2.612	63.01
383.23	19.942	0.960219	0.80030	2.103	62.91
383.21	19.944	0.960230	0.63154	1.678	62.86
383.21	19.944	0.960238	0.52269	1.405	62.71
383.20	19.944	0.960240	0.40562	1.103	62.58
383.19	19.941	0.960247	0.31134	0.8553	62.43
383.15	19.927	0.960262	0.10203	0.2873	62.06
		$T_{average}$ = 423.47 K; $p_{average}$ = 19.976 MPa			
423.45	19.973	0.927458	1.00958	2.739	62.67
423.45	19.973	0.927450	0.80030	2.202	62.59
423.41	19.977	0.927471	0.63154	1.763	62.42

T K	p MPa	ρ_w g·cm^{-3}	m mol·kg^{-1}	$10^2 \cdot (\rho - \rho_w)$ g·cm^{-3}	V_ϕ cm^3·mol^{-1}
423.45	19.981	0.927444	0.52269	1.475	62.27
423.50	19.980	0.927404	0.40562	1.159	62.08
423.49	19.979	0.927399	0.31134	0.8990	61.89
423.50	19.977	0.927382	0.10203	0.3024	61.40
		$T_{average}$ = 478.67 K; $p_{average}$ = 19.967 MPa			
478.68	19.958	0.871814	1.00958	3.037	60.51
478.68	19.962	0.871824	0.80030	2.441	60.36
478.67	19.969	0.871859	0.63154	1.956	60.10
478.71	19.966	0.871806	0.52269	1.636	59.89
478.71	19.968	0.871819	0.40562	1.288	59.54
478.69	19.967	0.871823	0.31134	0.9974	59.36
478.64	19.974	0.871887	0.16204	0.5284	58.93
478.63	19.971	0.871899	0.10203	0.3355	58.70
		$T_{average}$ = 523.39 K; $p_{average}$ = 19.934 MPa			
523.43	19.933	0.815751	1.00958	3.349	57.02
523.42	19.934	0.815764	0.80030	2.713	56.39
523.41	19.932	0.815789	0.63154	2.178	55.89
523.40	19.935	0.815814	0.52269	1.827	55.46
523.39	19.936	0.815812	0.40562	1.436	55.06
523.38	19.936	0.815844	0.31134	1.119	54.46
523.36	19.936	0.815874	0.16204	0.5939	53.75
523.36	19.935	0.815856	0.10203	0.3778	53.32
		$T_{average}$ = 298.131 K; $p_{average}$ = 30.769 MPa			
298.138	30.795	1.010457	1.21451	3.013	62.03
298.137	30.789	1.010455	0.59160	1.550	61.57
298.135	30.780	1.010452	0.28780	0.7769	61.26
298.131	30.769	1.010449	0.14896	0.4055	61.27

Table 3.2.2 Densities relative to water ($\rho - \rho_w$) and apparent molar volumes V_ϕ for aqueous solutions of β-alanine as a function of molality m.

T K	p MPa	ρ_w g·cm^{-3}	m mol·kg^{-1}	$10^2 \cdot (\rho - \rho_w)$ g·cm^{-3}	V_ϕ cm^3·mol^{-1}
		$T_{average}$ = 298.141 K; $p_{average}$ = 0.100 MPa			
298.141	0.100	0.997044	1.33911	3.650	59.75
298.141	0.100	0.997044	0.64444	1.873	59.01
298.141	0.100	0.997044	0.30578	0.9170	58.65
298.141	0.100	0.997044	0.081648	0.2505	58.35
		$T_{average}$ = 334.59 K; $p_{average}$ = 10.314 MPa			
334.64	10.318	0.986850	0.099806	0.2935	59.91
334.62	10.318	0.986847	0.20334	0.5842	60.42
334.60	10.320	0.986873	0.30406	0.8726	60.28
334.63	10.318	0.986849	0.40204	1.132	60.66
334.59	10.320	0.986866	0.49491	1.387	60.64
334.57	10.315	0.986879	0.59810	1.658	60.79
334.57	10.308	0.986878	0.79238	2.158	60.98
334.58	10.309	0.986869	0.92083	2.475	61.14
334.56	10.304	0.986879	1.1858	3.114	61.38
		$T_{average}$ = 383.34 K; $p_{average}$ = 10.355 MPa			
383.41	10.343	0.955644	0.099806	0.3040	59.69
383.40	10.350	0.955638	0.20334	0.6123	59.87
383.36	10.354	0.955667	0.30406	0.9053	60.06
383.30	10.351	0.955714	0.40204	1.177	60.43
383.28	10.354	0.955742	0.49491	1.446	60.33
383.30	10.355	0.955731	0.59810	1.728	60.49
383.31	10.362	0.955723	0.79238	2.246	60.77
383.32	10.367	0.955717	0.92083	2.580	60.90
383.32	10.365	0.955708	1.1858	3.247	61.17

T K	p MPa	ρ_w g·cm^{-3}	m mol·kg^{-1}	$10^2 \cdot (\rho - \rho_w)$ g·cm^{-3}	V_ϕ cm^3·mol^{-1}
		$T_{average}$ = 423.60 K; $p_{average}$ = 10.290 MPa			
423.57	10.289	0.922157	0.20334	0.6446	58.92
423.57	10.292	0.922114	0.30406	0.9547	59.08
423.57	10.290	0.922126	0.40204	1.250	59.26
423.58	10.290	0.922132	0.49491	1.524	59.43
423.58	10.291	0.922108	0.59810	1.824	59.57
423.58	10.292	0.922135	0.79238	2.379	59.77
423.60	10.293	0.922117	0.92083	2.728	60.01
423.59	10.292	0.922101	1.1858	3.434	60.32
		$T_{average}$ = 478.78 K; $p_{average}$ = 10.326 MPa			
478.76	10.318	0.864732	0.099806	0.3461	56.43
478.78	10.323	0.864720	0.30406	1.035	56.85
478.77	10.316	0.864709	0.40204	1.356	57.02
478.77	10.324	0.864721	0.49491	1.656	57.20
478.78	10.323	0.864719	0.59810	1.974	57.57
478.78	10.331	0.864723	0.79238	2.574	57.86
478.80	10.341	0.864715	0.92083	2.969	57.92
478.81	10.343	0.864694	1.1858	3.739	58.34
		$T_{average}$ = 423.63 K; $p_{average}$ = 20.533 MPa			
423.56	20.515	0.927617	0.099806	0.3134	59.36
423.58	20.523	0.927628	0.20334	0.6311	59.57
423.58	20.530	0.927599	0.30406	0.9339	59.75
423.64	20.537	0.927539	0.40204	1.223	59.91
423.64	20.540	0.927584	0.49491	1.492	60.05
423.64	20.540	0.927566	0.59810	1.784	60.21
423.65	20.542	0.927567	0.79238	2.321	60.49
423.65	20.549	0.927545	0.92083	2.675	60.54
423.67	20.551	0.927566	1.1858	3.355	60.96

T K	p MPa	ρ_w g·cm^{-3}	m mol·kg^{-1}	$10^2 \cdot (\rho - \rho_w)$ g·cm^{-3}	V_ϕ cm^3·mol^{-1}
		$T_{average}$ = 478.61 K; $p_{average}$ = 20.577 MPa			
478.54	20.538	0.872398	0.099806	0.3362	57.64
478.61	20.551	0.872329	0.20334	0.6783	57.85
478.59	20.577	0.872365	0.30406	1.005	58.05
478.60	20.579	0.872361	0.40204	1.315	58.27
478.60	20.594	0.872368	0.49491	1.606	58.42
478.60	20.591	0.872364	0.59810	1.923	58.59
478.62	20.590	0.872355	0.79238	2.503	58.92
478.62	20.594	0.872356	0.92083	2.877	59.13
478.63	20.598	0.872345	1.1858	3.623	59.51
		$T_{average}$ = 298.140 K; $p_{average}$ = 30.898 MPa			
298.146	30.925	1.010509	1.33911	3.503	60.46
298.142	30.904	1.010500	0.64444	1.797	59.80
298.139	30.887	1.010494	0.30578	0.8827	59.38
298.137	30.863	1.010483	0.15021	0.4396	59.25

Table 3.2.3 Densities relative to water (ρ - ρ_w) and apparent molar volumes V_ϕ for aqueous solutions of glycine as a function of molality m.

T K	p MPa	ρ_w g·cm^{-3}	m mol·kg^{-1}	10^2·(ρ - ρ_w) g·cm^{-3}	V_ϕ cm^3·mol^{-1}
		$T_{average}$ = 298.152 K; $p_{average}$ = 0.100 MPa			
298.150	0.100	0.997041	2.26777	6.222	44.87
298.154	0.100	0.997039	1.07932	3.194	44.09
298.152	0.100	0.997040	0.51944	1.593	43.73
298.148	0.100	0.997042	0.25386	0.7957	43.39
298.152	0.100	0.997041	0.096647	0.3048	43.41
		$T_{average}$ = 298.149 K; $p_{average}$ = 30.828 MPa			
298.147	30.811	1.010460	2.26777	6.070	45.33
298.148	30.821	1.010464	1.07932	3.127	44.51
298.150	30.836	1.010471	0.51944	1.567	44.04
298.150	30.836	1.010471	0.25386	0.7775	43.94

Table 3.2.4 Densities relative to water ($\rho - \rho_w$) and apparent molar volumes V_ϕ for aqueous solutions of proline as a function of molality m.

T / K	p / MPa	ρ_w / g·cm^{-3}	m / mol·kg^{-1}	$10^2 \cdot (\rho - \rho_w)$ / g·cm^{-3}	V_ϕ / cm^3·mol^{-1}
		$T_{average}$ = 298.147 K; $p_{average}$ = 0.100 MPa			
298.151	0.100	0.997039	1.78958	4.980	83.32
298.151	0.100	0.997039	1.19889	3.508	83.11
298.140	0.100	0.997044	0.52161	1.624	82.80
298.146	0.100	0.997043	0.25336	0.8128	82.53
298.147	0.100	0.997042	0.097388	0.3150	82.68
		$T_{average}$ = 334.56 K; $p_{average}$ = 10.157 MPa			
334.58	10.142	0.986798	0.14512	0.4435	84.91
334.61	10.160	0.986796	0.20055	0.6099	84.92
334.60	10.164	0.986800	0.24921	0.7543	84.94
334.59	10.163	0.986807	0.29640	0.8931	84.96
334.59	10.078	0.986770	0.30165	0.9086	84.96
334.53	10.165	0.986831	0.34868	1.045	84.99
334.51	10.166	0.986849	0.39582	1.182	85.00
334.51	10.167	0.986847	0.44101	1.311	85.02
334.53	10.165	0.986840	0.49425	1.462	85.03
334.55	10.164	0.986825	0.59753	1.751	85.08
334.60	10.098	0.986773	0.71024	2.058	85.13
334.57	10.160	0.986815	0.78254	2.254	85.15
334.60	10.108	0.986770	0.79617	2.290	85.16
		$T_{average}$ = 383.39 K; $p_{average}$ = 10.168 MPa			
383.36	10.125	0.955576	0.20055	0.6093	86.66
383.39	10.148	0.955564	0.24921	0.7536	86.69
383.14	10.108	0.955736	0.30165	0.9076	86.70
383.41	10.185	0.955562	0.39582	1.180	86.78
383.42	10.187	0.955556	0.44101	1.309	86.79

T K	p MPa	ρ_w g·cm^{-3}	m mol·kg^{-1}	$10^2 \cdot (\rho - \rho_w)$ g·cm^{-3}	V_ϕ cm^3·mol^{-1}
383.16	10.101	0.955714	0.71024	2.054	86.94
383.36	10.197	0955608	0.78254	2.246	87.00
383.12	10.095	0.955730	0.79617	2.283	86.99
		$T_{average}$ = 423.71 K; $p_{average}$ = 10.173 MPa			
423.68	10.168	0.928291	0.20055	0.6331	87.14
423.70	10.169	0.931214	0.29640	0.9270	87.21
423.56	10.130	0.931475	0.30165	0.9426	87.22
423.72	10.174	0.932776	0.34868	1.085	87.25
423.73	10.179	0.934184	0.39582	1.226	87.28
423.73	10.182	0.938827	0.44101	1.360	87.31
423.55	10.142	0.943402	0.71024	2.134	87.49
423.56	10.140	0.945751	0.79617	2.371	87.58
		$T_{average}$ = 479.04 K; $p_{average}$ = 10.115 MPa			
479.01	10.134	0.864309	0.20055	0.6878	86.60
479.03	10.126	0.864262	0.24921	0.8499	86.70
479.03	10.118	0.864274	0.34868	1.177	86.82
479.05	10.110	0.864240	0.39582	1.331	86.87
479.06	10.098	0.864224	0.44101	1.476	86.93
479.07	10.088	0.864199	0.49425	1.645	87.00
479.05	10.094	0.864226	0.59753	1.966	87.18
479.06	10.092	0.864210	0.78254	2.533	87.33
		$T_{average}$ = 524.07 K; $p_{average}$ = 10.094 MPa			
524.05	10.056	0.804564	0.14512	0.5565	83.28
524.06	10.059	0.804558	0.20055	0.7659	83.31
524.06	10.070	0.804563	0.24921	0.9476	83.38
524.08	10.085	0.804547	0.29640	1.123	83.40
524.05	10.103	0.804618	0.34868	1.315	83.46
523.98	10.118	0.804738	0.39582	1.487	83.50
524.06	10.123	0.804683	0.44101	1.651	83.55
524.16	10.122	0.804477	0.49425	1.842	83.62

T K	p MPa	ρ_w g·cm^{-3}	m mol·kg^{-1}	$10^2 \cdot (\rho - \rho_w)$ g·cm^{-3}	V_ϕ cm^3·mol^{-1}
524.08	10.116	0.804589	0.59753	2.208	83.71
524.09	10.112	0.804565	0.78254	2.848	83.90
		$T_{average}$ = 334.93 K; $p_{average}$ = 20.199 MPa			
334.92	20.200	0.990873	0.20055	0.6041	85.00
334.89	20.202	0.990893	0.29640	0.8845	85.04
334.97	20.192	0.990855	0.44101	1.298	85.10
335.00	20.188	0.990833	0.49425	1.448	85.11
334.97	20.195	0.990851	0.59753	1.734	85.15
334.90	20.221	0.991058	0.71024	2.038	85.20
334.92	20.199	0.990878	0.78254	2.231	85.23
		$T_{average}$ = 383.66 K; $p_{average}$ = 20.157 MPa			
383.67	20.184	0.959997	0.14512	0.4400	86.63
383.63	20.163	0.960018	0.24921	0.7485	86.66
383.64	20.153	0.960012	0.29640	0.8860	86.69
383.68	20.141	0.959986	0.34868	1.037	86.71
383.71	20.135	0.959949	0.39582	1.173	86.71
383.63	20.159	0.960018	0.44101	1.302	86.73
383.65	20.165	0.960007	0.49425	1.451	86.76
383.63	20.152	0.960010	0.59753	1.739	86.79
383.21	20.212	0.960351	0.71024	2.044	86.84
383.68	20.144	0.959990	0.78254	2.239	86.86
383.22	20.207	0.960342	0.79617	2.274	86.86
		$T_{average}$ = 423.90 K; $p_{average}$ = 20.205 MPa			
424.00	20.197	0.927062	0.14512	0.4570	87.12
423.89	20.194	0.927167	0.24921	0.7768	87.18
423.86	20.200	0.927199	0.29640	0.9196	87.22
423.82	20.204	0.927503	0.30165	0.9350	87.22
423.90	20.207	0.927140	0.39582	1.217	87.27
423.80	20.209	0.927279	0.59753	1.801	87.41
423.53	20.204	0.927487	0.71024	2.117	87.48

T K	p MPa	ρ_w g·cm^{-3}	m mol·kg^{-1}	$10^2 \cdot (\rho - \rho_w)$ g·cm^{-3}	V_ϕ cm^3·mol^{-1}
423.94	20.215	0.927136	0.78254	2.318	87.53
423.40	20.207	0.927623	0.79617	2.354	87.54
		$T_{average}$ = 479.15 K; $p_{average}$ = 20.194 MPa			
479.15	20.195	0.871466	0.14512	0.4939	86.80
479.18	20.200	0.871475	0.20055	0.6793	86.83
479.12	20.200	0.871520	0.24921	0.8397	86.91
479.13	20.190	0.871494	0.29640	0.9938	86.97
478.59	20.136	0.872067	0.30165	1.010	86.99
479.15	20.179	0.871460	0.34868	1.163	87.02
479.14	20.184	0.871477	0.39582	1.314	87.08
479.14	20.190	0.871469	0.44101	1.458	87.13
479.15	20.195	0.871469	0.49425	1.625	87.19
479.19	20.197	0.871456	0.59753	1.945	87.30
478.60	20.136	0.872051	0.71024	2.285	87.44
479.13	20.198	0.871488	0.78254	2.501	87.52
478.61	20.135	0.872039	0.79617	2.539	87.53
		$T_{average}$ = 523.98 K; $p_{average}$ = 20.240 MPa			
523.96	20.223	0.815290	0.14512	0.5422	84.44
523.94	20.239	0.815333	0.20055	0.7457	84.50
523.98	20.248	0.815325	0.24921	0.9222	84.58
523.90	20.250	0.815443	0.29640	1.092	84.64
523.37	20.177	0.816092	0.30165	1.110	84.66
523.94	20.248	0.815314	0.34868	1.279	84.69
523.93	20.247	0.815372	0.39582	1.445	84.79
523.99	20.249	0.815289	0.44101	1.603	84.85
524.02	20.245	0.815249	0.49425	1.788	84.93
524.02	20.235	0.815228	0.59753	2.141	85.07
523.41	20.183	0.816026	0.71024	2.518	85.22
524.06	20.245	0.815194	0.78254	2.757	85.32
523.41	20.184	0.816030	0.79617	2.799	85.36

T / K	p / MPa	ρ_w / g·cm^{-3}	m / mol·kg^{-1}	$10^2 \cdot (\rho - \rho_w)$ / g·cm^{-3}	V_ϕ / cm^3·mol^{-1}
$T_{average}$ = 298.142 K; $p_{average}$ = 30.798 MPa					
298.143	30.803	1.010456	1.78958	4.760	83.94
298.141	30.795	1.010453	1.19889	3.364	83.67
298.142	30.795	1.010454	0.52161	1.561	83.34
298.142	30.798	1.010457	0.25336	0.7816	83.08
298.143	30.797	1.010457	0.097388	0.3023	83.29

Table 3.2.5 Values of $V°$, b, and c obtained by fitting either equation (3.2.1) or equation (3.2.2) to each set of isothermal volumetric data for each amino acid.

T / (K)	p / (MPa)	V^o / ($cm^3 \cdot mol^{-1}$)	b / ($cm^3 \cdot kg \cdot mol^{-2}$)	c / ($cm^3 \cdot kg^2 \cdot mol^{-3}$)
		α-Alanine		
298.131	30.769	61.11 ± 0.05	0.75 ± 0.07	—
334.65	19.977	61.89 ± 0.02	1.41 ± 0.06	-0.41 ± 0.04
383.20	19.939	61.86 ± 0.07	2.18 ± 0.23	-1.03 ± 0.18
423.47	19.976	61.11 ± 0.01	2.95 ± 0.02	-1.39 ± 0.01
478.67	19.967	58.30 ± 0.06	3.89 ± 0.22	-1.68 ± 0.17
523.39	19.934	52.81 ± 0.11	6.05 ± 0.39	-1.88 ± 0.30
333.21	10.047	61.65 ± 0.01	1.55 ± 0.05	-0.56 ± 0.04
381.70	10.057	61.72 ± 0.03	2.65 ± 0.12	-1.32 ± 0.12
422.42	10.036	60.89 ± 0.01	2.95 ± 0.01	-1.35 ± 0.01
477.24	10.058	57.91 ± 0.07	3.72 ± 0.25	-1.57 ± 0.18
523.36	10.063	51.68 ± 0.07	4.89 ± 0.22	-1.31 ± 0.17
298.10	0.100	60.50 ± 0.02	0.90 ± 0.07	-0.28 ± 0.06
298.137	0.100	60.49 ± 0.05	0.56 ± 0.08	—
		β-Alanine		
298.140	30.898	59.09 ± 0.03	1.03 ± 0.04	—
423.63	20.533	59.26 ± 0.09	1.68 ± 0.28	-0.22 ± 0.19
334.59	10.315	59.72 ± 0.06	2.09 ± 0.17	-0.59 ± 0.11
383.34	10.355	59.57 ± 0.12	1.86 ± 0.37	-0.43 ± 0.25
423.60	10.290	58.60 ± 0.07	1.72 ± 0.21	-0.23 ± 0.14
298.141	0.100	58.29 ± 0.02	1.10 ± 0.03	—
		Glycine		
298.149	30.828	43.68 ± 0.08	0.73 ± 0.04	—
298.152	0.100	43.31 ± 0.05	0.69 ± 0.04	—
		Proline		
298.142	30.798	83.20 ± 0.05	0.40 ± 0.05	—
334.93	20.199	84.92 ± 0.01	0.39 ± 0.01	—
383.66	20.157	86.58 ± 0.01	0.36 ± 0.01	—

T / (K)	p / (MPa)	V^o / ($cm^3 \cdot mol^{-1}$)	b / ($cm^3 \cdot kg \cdot mol^{-2}$)	c / ($cm^3 \cdot kg^2 \cdot mol^{-3}$)
423.90	20.205	87.02 ± 0.01	0.65 ± 0.01	—
479.15	20.194	86.63 ± 0.01	1.14 ± 0.01	—
523.98	20.240	84.22 ± 0.01	1.42 ± 0.01	—
334.56	10.157	84.84 ± 0.01	0.40 ± 0.01	—
383.39	10.168	86.54 ± 0.01	0.57 ± 0.02	—
423.71	10.173	87.00 ± 0.01	0.72 ± 0.02	—
479.04	10.115	86.40 ± 0.03	1.22 ± 0.07	—
524.07	10.094	83.12 ± 0.01	1.00 ± 0.01	—
298.147	0.100	82.63 ± 0.02	0.39 ± 0.02	—

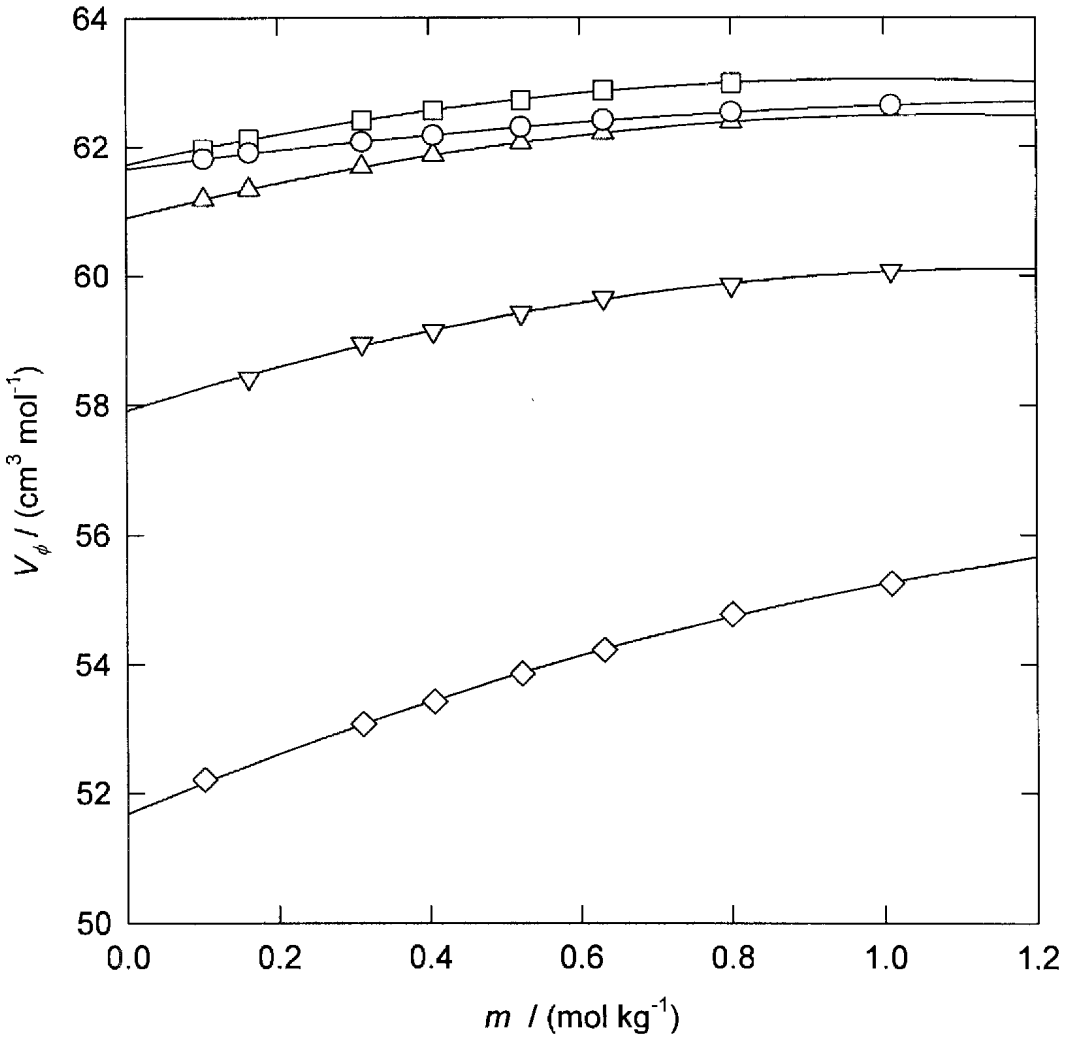

Figure 3.2.1 The apparent molar volumes V_ϕ of α-alanine from 333.2 K to 523.4 K at 10.05 MPa plotted against molality. Symbols are experimental results: □, 381.7 K; ○, 333.2 K; Δ, 422.4 K; ▽, 477.2 K; ◇, 523.4 K. Lines are the isothermal fits to the experimental data.

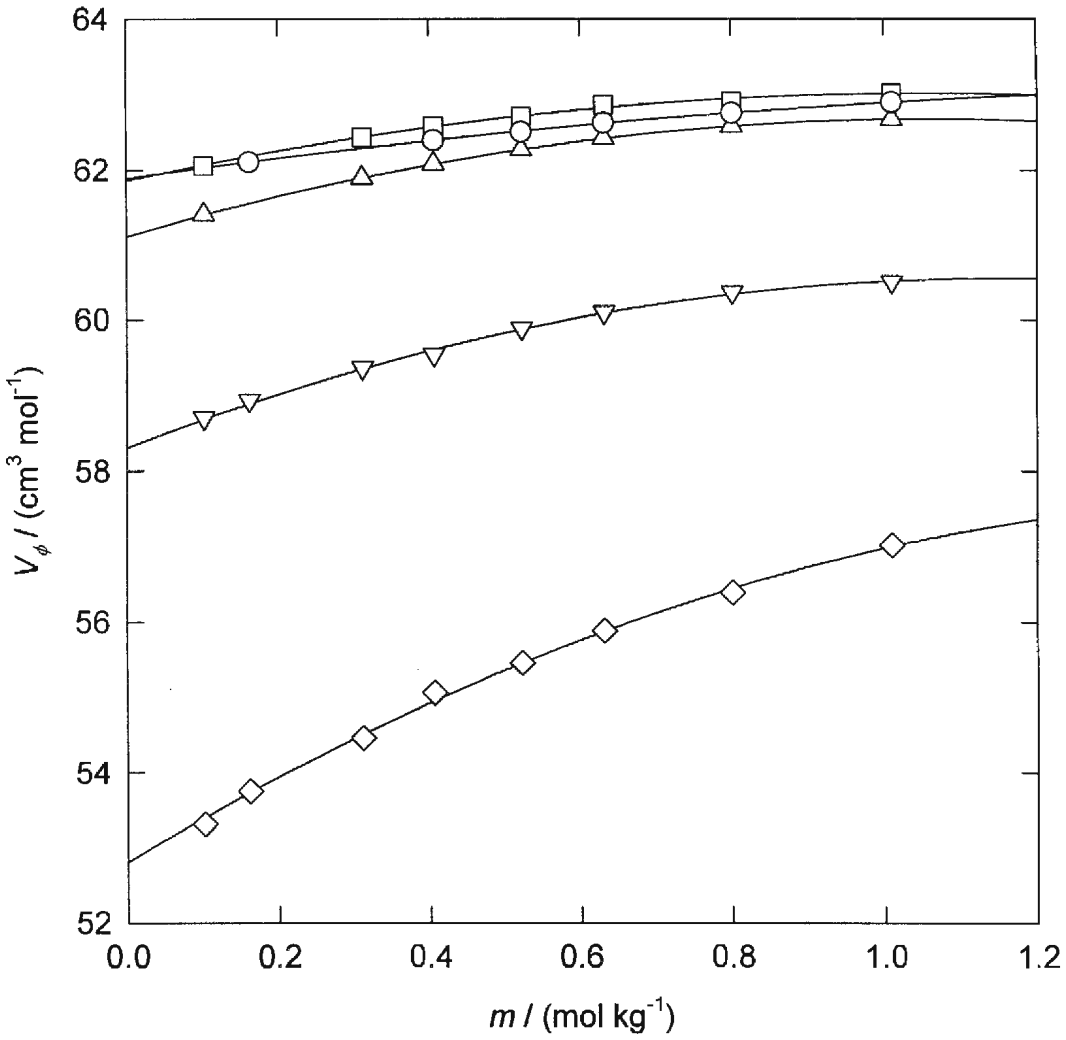

Figure 3.2.2 The apparent molar volumes V_ϕ of α-alanine from 334.6 K to 523.4 K at 19.96 MPa plotted against molality. Symbols are experimental results: □, 383.2 K; ○, 334.6 K; Δ, 423.5 K; ∇, 478.7 K; ◇, 523.4 K. Lines are the isothermal fits to the experimental data.

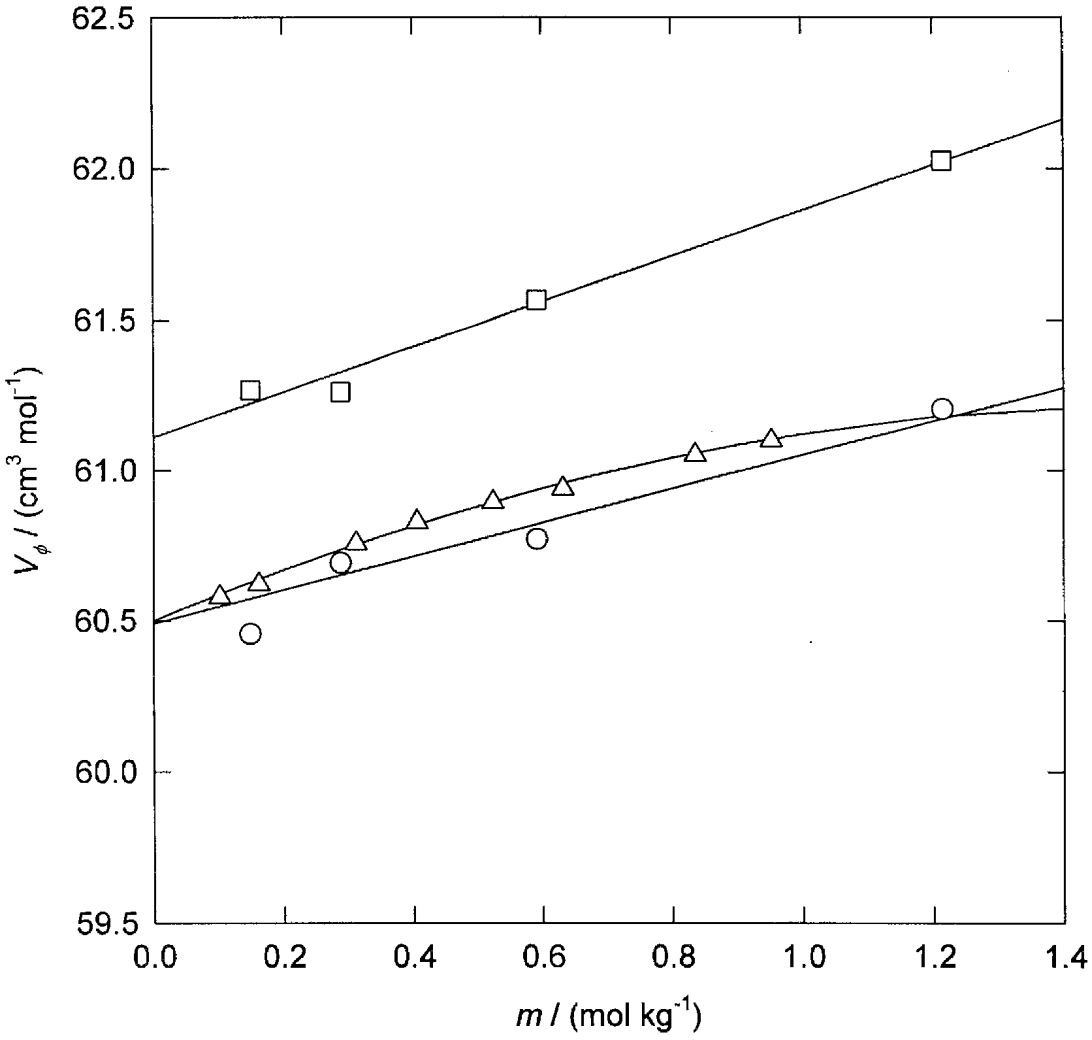

Figure 3.2.3 The apparent molar volumes V_ϕ of α-alanine from 0.10 MPa to 30.77 MPa at 298.1 K plotted against molality. Symbols are experimental results: Δ, 0.10 MPa; ○, 0.10 MPa; □, 30.77 MPa. Lines are the isothermal fits to the experimental data.

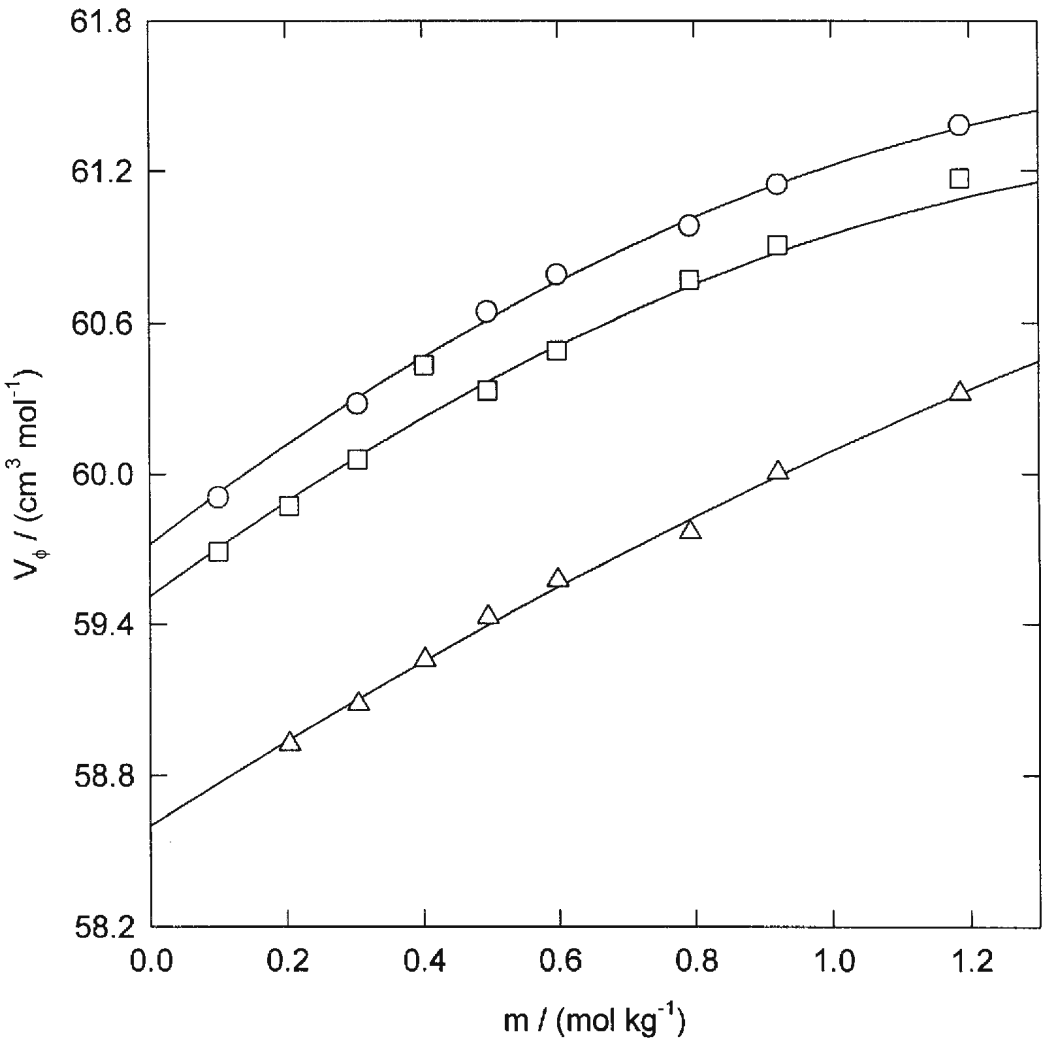

Figure 3.2.4 The apparent molar volumes V_ϕ of β-alanine from 334.6 K to 423.6 K at 10.32 MPa plotted against molality. Symbols are experimental results: ○, 334.6 K; □, 383.3 K; Δ, 423.6 K. Lines are the isothermal fits to the experimental data.

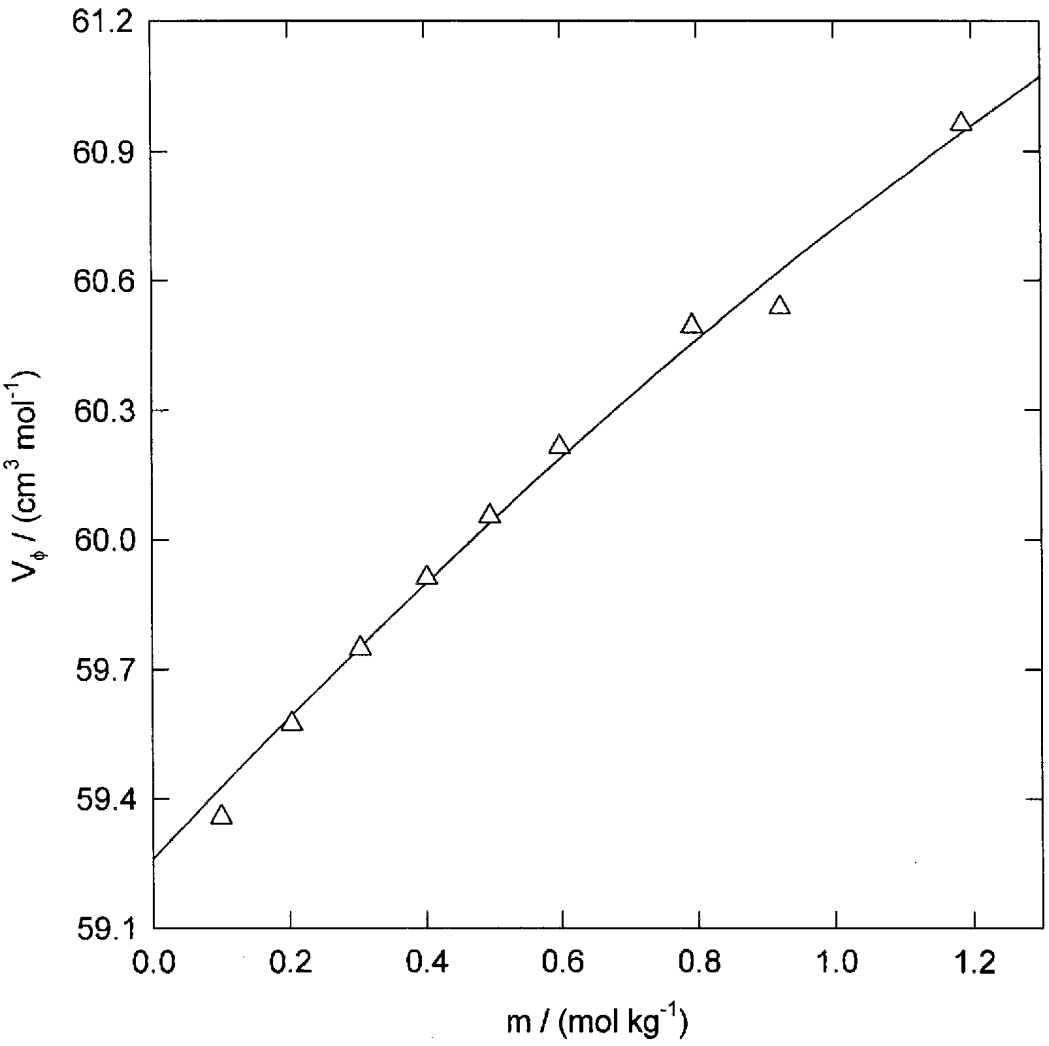

Figure 3.2.5 The apparent molar volumes V_ϕ of β-alanine at 423.6 K and 20.53 MPa plotted against molality. Symbols are experimental results: Δ, 423.6 K. The line is the isothermal fit to the experimental data.

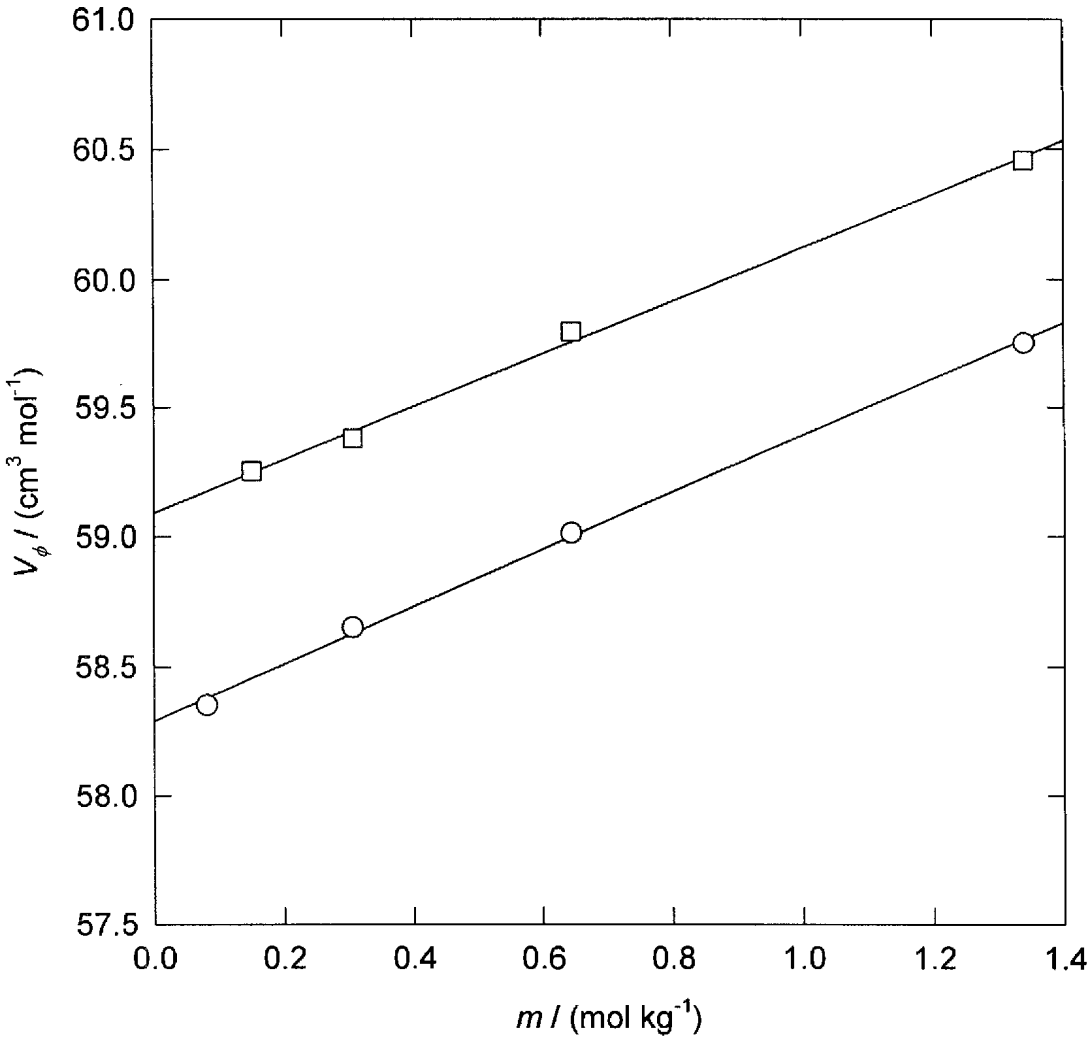

Figure 3.2.6 The apparent molar volumes V_ϕ of β-alanine from 0.10 MPa to 30.90 MPa at 298.1 K plotted against molality. Symbols are experimental results: ○, 0.10 MPa; □, 30.90 MPa. Lines are the isothermal fits to the experimental data.

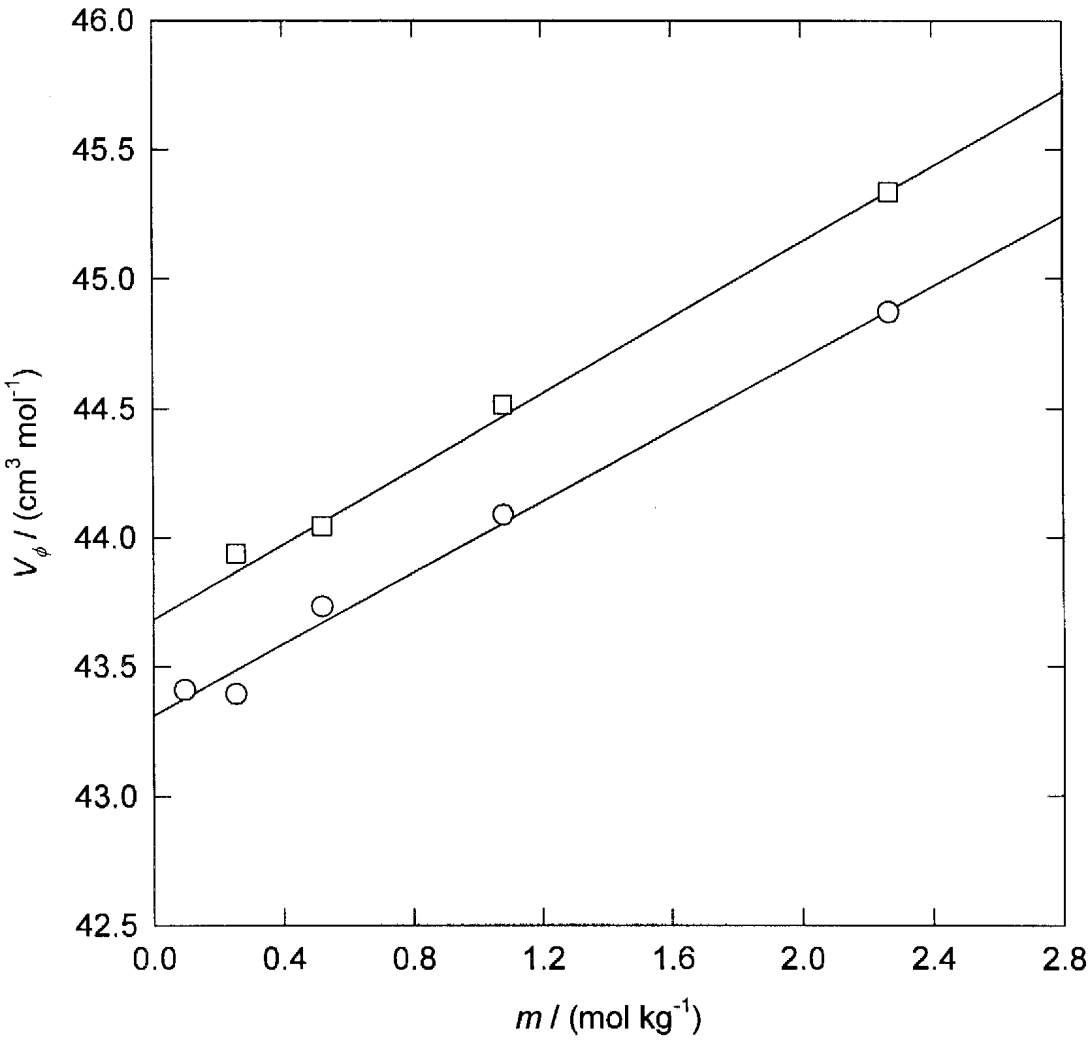

Figure 3.2.7 The apparent molar volumes V_ϕ of glycine from 0.10 MPa to 30.83 MPa at 298.1 K plotted against molality. Symbols are experimental results: ○, 0.10 MPa; □, 30.83 MPa. Lines are the isothermal fits to the experimental data..

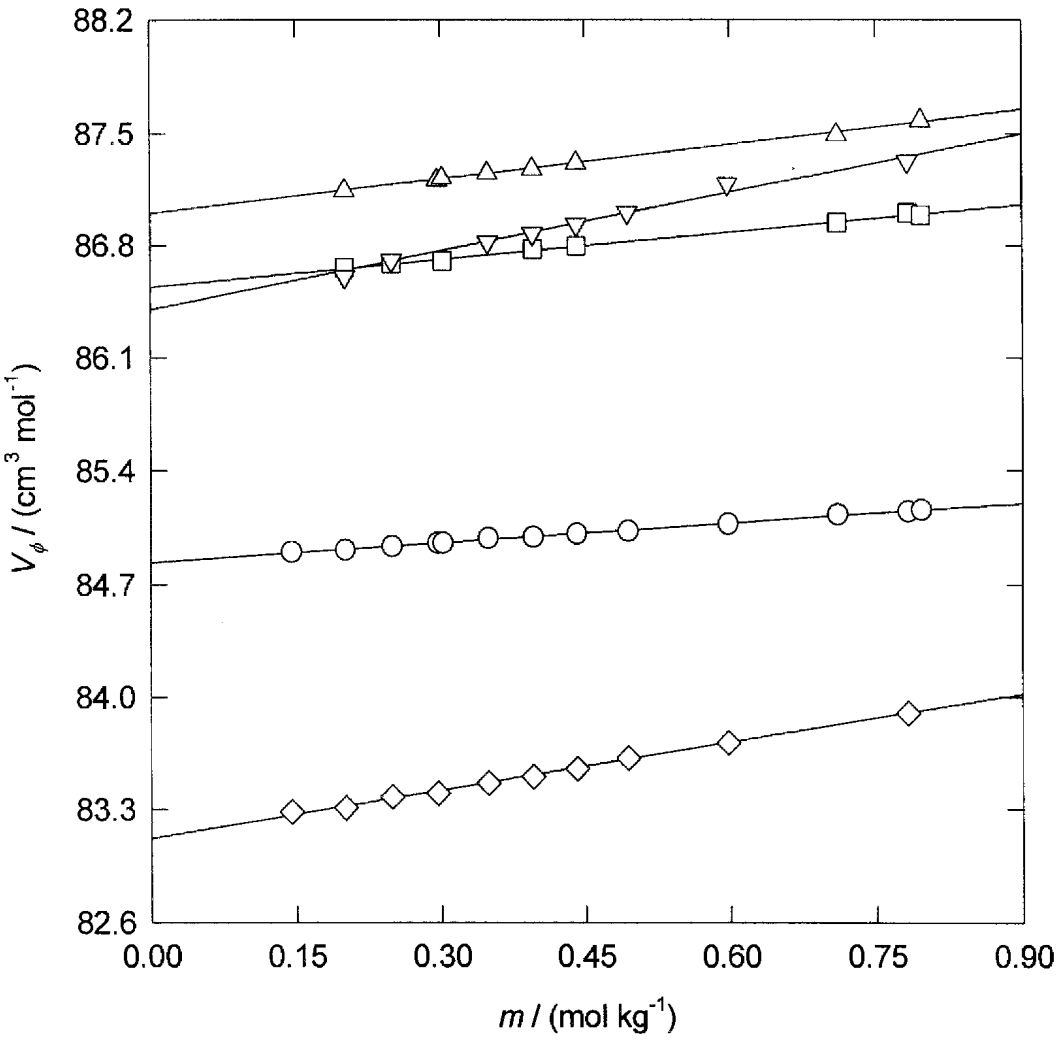

Figure 3.2.8 The apparent molar volumes V_ϕ of proline from 334.6 K to 524.1 K at 10.14 MPa plotted against molality. Symbols are experimental results: Δ, 423.7 K; ∇, 479.0 K; □, 383.4 K; ○, 334.6 K; ◇, 524.1 K. Lines are the isothermal fits to the experimental data.

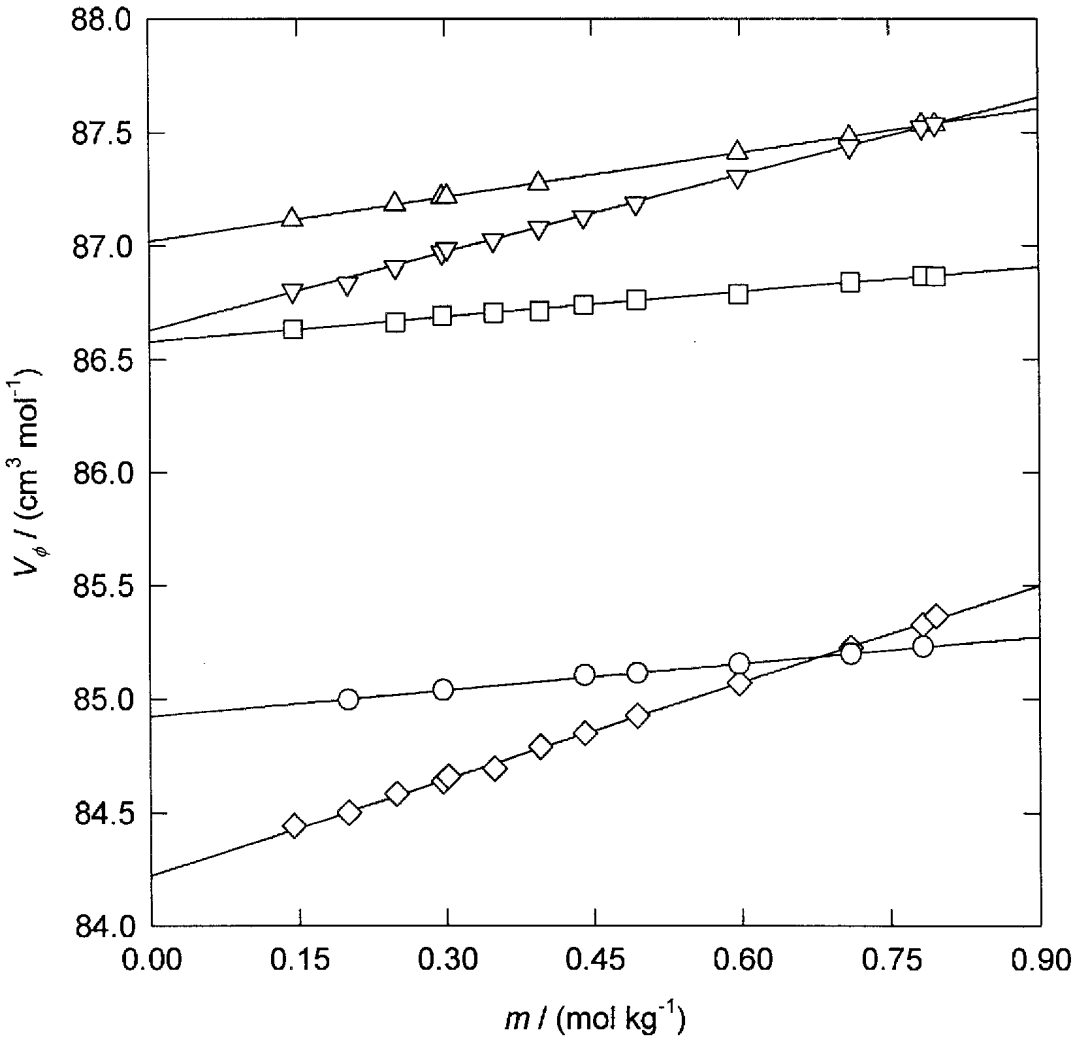

Figure 3.2.9 The apparent Molar Volumes V_ϕ of proline from 334.9 K to 524.0 K at 20.20 MPa plotted against molality. Symbols are experimental results: Δ, 423.9 K; ∇, 479.1 K; □, 383.7 K; ○, 334.9 K; ◇, 524.0 K. Lines are the isothermal fits to the experimental data.

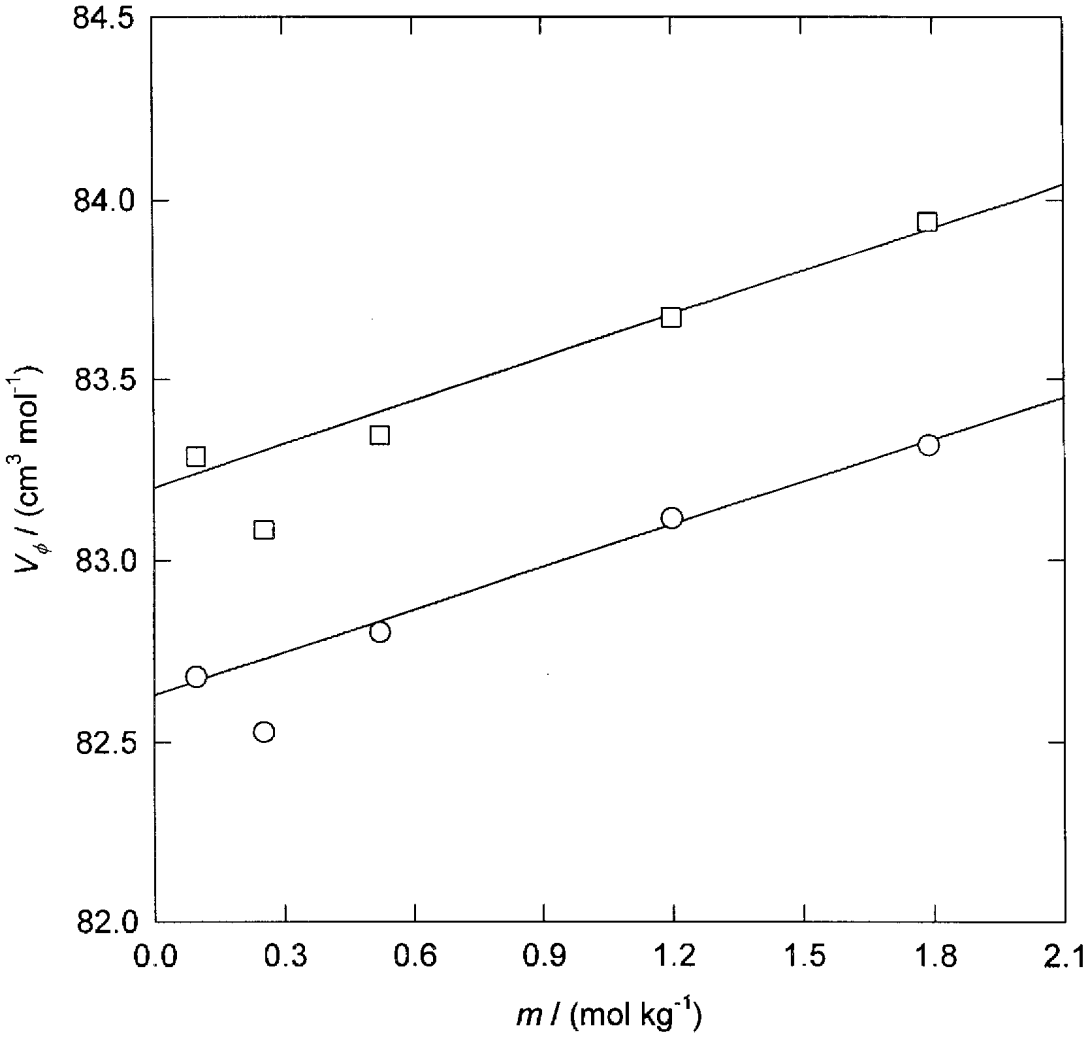

Figure 3.2.10 The apparent molar volumes V_ϕ of proline from 0.10 MPa to 30.80 MPa at 298.1 K plotted against molality. Symbols are experimental results: ○, 0.10 MPa; □, 30.80 MPa. Lines are the isothermal fits to the experimental data.

3.3 Apparent Molar Heat Capacities.

The experimentally determined values of $(f \cdot \Delta W / W)$ are listed in Tables 3.3.1, 3.3.2, 3.3.3, and 3.3.4 for aqueous α-alanine, β-alanine, glycine, and proline, respectively. Specific heat capacities c_p calculated from the values of $(f \cdot \Delta W / W)$ according to equation (1.5.2.6).

$$c_p = c_{p,w}\left(1 + f\frac{\Delta W}{W_1}\right)\left(\frac{\rho_{w,T_d}}{\rho_{T_d}}\right) \qquad (1.5.2.6)$$

were used to calculate apparent molar heat capacities $C_{p,\phi}$:

$$C_{p,\phi} = M_2 c_p + \left(\frac{1000\,(c_p - c_{p,w})}{m}\right) \qquad (1.5.2.7)$$

Here $c_{p,w}$ is the specific heat capacity of the reference fluid; $\rho_{w,Td}$ and ρ_{Td} are the densities of the reference fluid and sample solution at the temperature of the delay line; M_2 is the molar mass of the solute and m is the molality of the sample solution. The experimental apparent molar heat capacities are listed in Tables 3.3.1, 3.3.2, 3.3.3, and 3.3.4.

Simple polynomial expressions were used to fit the molality dependence of the apparent molar heat capacity data for each amino acid studied at each temperature and pressure. The polynomial function chosen for glycine and proline was:

$$C_{p,\phi} = C_p^{\,o} + bm + cm^2 \qquad (3.3.1)$$

where C_p° is the standard partial molar heat capacity, b and c are temperature and/or pressure dependent adjustable parameters. The polynomial function chosen for α-alanine and β-alanine was:

$$C_{p,\phi} = C_p{}^o + bm \qquad (3.3.2)$$

The apparent molar heat capacities measured in this work were given a weight equal to the molality of the solution in the least squares fit. The values of C_p°, b, and c obtained by fitting equation (3.3.1) to each set of isothermal calorimetric data for glycine and proline are summarized in Table 3.3.5. The values of C_p° and b obtained by fitting equation (3.3.2) to each set of isothermal calorimetric data for α-alanine and β-alanine are also summarized in Table 3.3.5. The fitted isotherms for α-alanine are plotted in Figures 3.3.1, 3.3.2, and 3.3.3; the fitted isotherms for β-alanine are plotted in Figures 3.3.4 and 3.3.5; the fitted isotherms for glycine are plotted in Figures 3.3.6 and 3.3.7; and the fitted isotherms for proline are plotted in Figures 3.3.8 and 3.3.9.

As illustrated in Figures 3.3.1 to 3.2.9, the simple polynomial expressions (linear or quadratic) accurately reproduce the apparent molar heat capacities obtained at each temperature and pressure. The scatter observed in the experimental results is relatively small and tends to decrease with increasing molality. The standard partial molar heat capacities listed in Table 3.3.5 increase with temperature until $T \approx 373$ K to 423 K and then deviate toward negative values.

Table 3.3.1 Apparent molar heat capacities $C_{p,\phi}$ of aqueous α-alanine as a function of molality m.

T / K	p / MPa	m / mol·kg^{-1}	$(f \cdot \Delta W / W) \cdot 10^3$	$C_{p,\phi}$ / J·mol^{-1}·K^{-1}
$T_{average}$ = 298.10 K; $p_{average}$ = 0.10 MPa; $c_{p,w\ average}$ = 4.1814 J·g^{-1}·K^{-1}				
298.10	0.10	0.10203	-2.75	142.38
298.10	0.10	0.31134	-8.08	142.63
298.10	0.10	0.40562	-10.37	144.28
298.10	0.10	0.52269	-13.11	146.31
298.10	0.10	0.63154	-15.68	146.43
298.10	0.10	0.83574	-20.28	148.01
298.10	0.10	0.95258	-22.87	148.48
$T_{average}$ = 323.173 K; $p_{average}$ = 0.10 MPa; $c_{p,w\ average}$ = 4.1814 J·g^{-1}·K^{-1}				
323.173	0.10	0.080118	-1.58	169.06 (3.60)
323.173	0.10	0.080118	-1.60	168.41 (3.67)
323.173	0.10	0.14899	-2.97	168.22 (1.93)
323.173	0.10	0.14899	-2.96	168.52 (2.33)
323.173	0.10	0.28786	-5.59	169.97 (0.95)
323.173	0.10	0.28786	-5.64	169.14 (1.09)
323.173	0.10	0.59173	-11.34	170.29 (0.57)
323.173	0.10	0.59173	-11.35	170.24 (0.58)
323.173	0.10	1.21477	-22.02	173.79 (0.41)
323.173	0.10	1.21477	-22.05	173.67 (0.42)
$T_{average}$ = 373.563 K; $p_{average}$ = 2.08 MPa; $c_{p,w\ average}$ = 4.2116 J·g^{-1}·K^{-1}				
373.562	2.05	0.080118	-1.32	184.34 (7.36)
373.562	2.05	0.080118	-1.41	179.70 (6.30)
373.562	2.09	0.14899	-2.60	180.24 (3.71)
373.562	2.09	0.14899	-2.53	182.43 (3.31)
373.563	2.09	0.28786	-4.82	183.03 (2.20)
373.563	2.09	0.28786	-4.71	184.70 (2.65)
373.563	2.10	0.59173	-9.66	184.39 (1.11)
373.563	2.10	0.59173	-9.73	183.83 (0.92)

T / K	p / MPa	m / mol·kg^{-1}	$(f \cdot \Delta W / W) \cdot 10^3$	$C_{p,\phi}$ / J·mol^{-1}·K^{-1}
373.564	2.10	0.59173	-9.61	184.72 (1.18)
373.564	2.07	1.21477	-18.69	187.86 (0.52)
373.564	2.07	1.21477	-18.97	186.80 (0.47)
$T_{average}$ = 423.772 K; $p_{average}$ = 2.01 MPa; $c_{p,w\ average}$ = 4.3038 J·g^{-1}·K^{-1}				
423.769	2.00	0.080118	-1.46	181.06 (6.79)
423.769	2.00	0.080118	-1.47	180.69 (6.39)
423.776	2.00	0.14899	-2.75	180.00 (3.35)
423.769	2.00	0.14899	-2.67	182.36 (4.72)
423.770	2.01	0.28786	-5.09	182.97 (2.47)
423.770	2.01	0.28786	-5.18	181.54 (2.00)
423.773	2.01	0.59173	-10.23	184.08 (0.76)
423.773	2.01	0.59173	-10.19	184.39 (0.93)
423.775	2.03	1.21477	-19.51	188.84 (0.61)
423.775	2.03	1.21477	-19.39	189.27 (0.59)
$T_{average}$ = 447.746 K; $p_{average}$ = 10.30 MPa; $c_{p,w\ average}$ = 4.3465 J·g^{-1}·K^{-1}				
447.742	10.29	0.080118	-1.58	178.15 (17.50)
447.742	10.29	0.080118	-1.60	177.14 (9.33)
447.744	10.26	0.14899	-3.00	176.08 (6.75)
447.744	10.26	0.14899	-2.97	176.94 (6.98)
447.745	10.31	0.28786	-5.69	177.34 (3.64)
447.748	10.32	0.28786	-5.72	176.89 (2.79)
447.748	10.31	0.59173	-11.36	179.18 (1.90)
447.748	10.31	0.59173	-11.29	179.70 (1.89)
447.749	10.33	1.21477	-21.76	183.98 (0.78)
447.749	10.33	1.21477	-21.81	183.78 (0.84)
$T_{average}$ = 473.799 K; $p_{average}$ = 5.62 MPa; $c_{p,w\ average}$ = 4.4760 J·g^{-1}·K^{-1}				
473.801	5.62	0.080118	-1.74	173.18 (12.56)
473.801	5.62	0.080118	-1.78	171.19 (11.58)
473.800	5.60	0.14899	-3.24	173.15 (7.26)
473.800	5.60	0.14899	-3.26	172.52 (5.83)

T K	p MPa	m mol·kg^{-1}	$(f \cdot \Delta W / W) \cdot 10^3$	$C_{p,\phi}$ J·mol^{-1}·K^{-1}
473.800	5.60	0.28786	-6.17	174.06 (4.53)
473.800	5.60	0.28786	-6.17	174.03 (3.44)
473.797	5.61	0.59173	-12.33	175.81 (2.16)
473.797	5.61	0.59173	-12.36	175.63 (1.91)
473.796	5.67	1.21477	-23.29	182.28 (1.13)
473.794	5.67	1.21477	-23.30	182.26 (1.01)
$T_{average}$ = 323.168 K; $p_{average}$ = 29.77 MPa; $c_{p,w\ average}$ = 4.1186 J·g^{-1}·K^{-1}				
323.168	29.70	0.080118	-1.55	174.62 (4.17)
323.167	29.71	0.14899	-2.83	175.86 (1.98)
323.167	29.71	0.14899	-2.85	175.08 (2.38)
323.168	29.90	0.28786	-5.41	176.21 (1.42)
323.168	29.90	0.28786	-5.51	174.77 (0.98)
323.168	29.59	0.59173	-10.91	177.12 (0.58)
323.168	29.59	0.59173	-10.87	177.40 (0.78)
323.168	29.91	1.21477	-21.29	180.26 (0.48)
323.168	29.91	1.21477	-21.16	180.72 (0.44)
$T_{average}$ = 373.543 K; $p_{average}$ = 30.03 MPa; $c_{p,w\ average}$ = 4.1527 J·g^{-1}·K^{-1}				
373.541	29.89	0.080118	-1.33	187.22 (5.93)
373.541	29.89	0.080118	-1.27	190.76 (5.09)
373.542	29.98	0.14899	-2.44	188.24 (2.62)
373.542	29.98	0.14899	-2.39	189.61 (2.99)
373.543	30.08	0.28786	-4.61	189.47 (1.66)
373.543	30.08	0.28786	-4.62	189.37 (1.46)
373.543	30.11	0.59173	-9.12	191.72 (0.94)
373.543	30.11	0.59173	-9.27	190.66 (0.74)
373.544	30.11	1.21477	-17.86	194.42 (0.61)
373.544	30.11	1.21477	-17.77	194.76 (0.48)
$T_{average}$ = 423.769 K; $p_{average}$ = 30.56 MPa; $c_{p,w\ average}$ = 4.2217 J·g^{-1}·K^{-1}				
423.770	30.50	0.080118	-1.42	185.97 (4.97)
423.770	30.50	0.080118	-1.39	187.26 (6.10)

T K	p MPa	m mol·kg^{-1}	$(f \cdot \Delta W / W) \cdot 10^3$	$C_{p,\phi}$ J·mol^{-1}·K^{-1}
423.770	30.60	0.14899	-2.51	189.47 (3.58)
423.769	30.58	0.28786	-4.80	189.99 (1.65)
423.769	30.58	0.28786	-4.85	189.27 (1.97)
423.768	30.51	0.59173	-9.45	192.54 (0.92)
423.768	30.51	0.59173	-9.36	193.21 (1.08)
423.769	30.61	1.21477	-17.62	198.66 (0.62)
423.769	30.61	1.21477	-17.61	198.69 (0.49)
$T_{average}$ = 447.857 K; $p_{average}$ = 30.22 MPa; $c_{p,w\ average}$ = 4.2777 J·g^{-1}·K^{-1}				
447.860	30.30	0.080118	-1.46	186.13 (5.40)
447.860	30.30	0.080118	-1.46	185.86 (9.21)
447.858	30.21	0.14899	-2.70	186.43 (3.05)
447.858	30.21	0.14899	-2.70	186.42 (3.56)
447.857	30.19	0.28786	-5.15	187.07 (1.94)
447.857	30.19	0.28786	-5.13	187.48 (1.76)
447.856	30.21	0.59173	-10.12	190.00 (0.86)
447.856	30.21	0.59173	-10.16	189.71 (0.90)
447.856	30.20	1.21477	-19.10	195.61 (0.60)
447.856	30.20	1.21477	-19.08	195.66 (0.95)
$T_{average}$ = 473.818 K; $p_{average}$ = 30.19 MPa; $c_{p,w\ average}$ = 4.3584 J·g^{-1}·K^{-1}				
473.817	30.04	0.080118	-1.52	186.08 (7.01)
473.817	30.04	0.080118	-1.49	188.19 (9.85)
473.817	30.19	0.080118	-1.48	188.42 (7.47)
473.817	30.19	0.080118	-1.46	189.35 (7.01)
473.820	30.29	0.14899	-2.91	183.81 (7.16)
473.820	30.29	0.14899	-2.87	184.91 (9.34)
473.817	30.20	0.28786	-5.50	185.30 (2.57)
473.817	30.20	0.28786	-5.49	185.45 (2.15)
473.818	30.20	0.59173	-10.81	188.31 (0.77)
473.818	30.20	0.59173	-10.84	188.09 (1.07)
473.819	30.22	1.21477	-20.36	194.42 (0.57)
473.819	30.22	1.21477	-20.23	194.91 (0.64)

Table 3.3.2 Apparent molar heat capacities $C_{p,\phi}$ of aqueous β-alanine as a function of molality m.

T / K	p / MPa	m / mol·kg^{-1}	$(f \cdot \Delta W / W) \cdot 10^3$	$C_{p,\phi}$ / J·mol^{-1}·K^{-1}
$T_{average}$ = 323.172 K; $p_{average}$ = 0.10 MPa; $c_{p,w\ average}$ = 4.1814 J·g^{-1}·K^{-1}				
323.170	0.10	0.081666	-2.56	112.19 (3.15)
323.170	0.10	0.081666	-2.58	111.00 (3.10)
323.171	0.10	0.15025	-4.73	111.27 (1.92)
323.173	0.10	0.15025	-4.72	111.62 (1.94)
323.173	0.10	0.30585	-9.46	113.07 (0.99)
323.173	0.10	0.30585	-9.45	113.08 (1.03)
323.173	0.10	0.64458	-19.19	116.80 (0.63)
323.173	0.10	0.64458	-19.22	116.56 (0.62)
323.173	0.10	1.33941	-37.38	123.12 (0.46)
323.173	0.10	1.33941	-37.37	123.16 (0.46)
$T_{average}$ = 373.554 K; $p_{average}$ = 2.02 MPa; $c_{p,w\ average}$ = 4.2117 J·g^{-1}·K^{-1}				
373.556	2.07	0.081666	-2.00	142.28 (7.62)
373.556	2.07	0.081666	-2.11	136.62 (8.30)
373.554	1.99	0.15025	-3.66	142.87 (4.05)
373.553	1.99	0.30585	-7.54	141.07 (1.83)
373.553	1.99	0.30585	-7.54	141.05 (1.88)
373.553	2.00	0.64458	-14.79	147.88 (1.15)
373.553	2.00	0.64458	-14.94	146.87 (0.86)
373.554	2.02	1.33941	-29.09	152.52 (0.51)
373.554	2.02	1.33941	-29.43	151.39 (0.45)
$T_{average}$ = 423.778 K; $p_{average}$ = 2.02 MPa; $c_{p,w\ average}$ = 4.3037 J·g^{-1}·K^{-1}				
423.777	2.01	0.081666	-1.80	156.22 (7.64)
423.777	2.01	0.081666	-1.77	157.67 (6.63)
423.777	2.01	0.15025	-3.31	156.01 (4.54)
423.777	2.01	0.15025	-3.29	156.65 (3.72)
423.778	2.01	0.30585	-6.66	156.75 (1.70)
423.778	2.01	0.30585	-6.70	156.30 (2.00)

T / K	p / MPa	m / mol·kg^{-1}	$(f \cdot \Delta W / W) \cdot 10^3$	$C_{p,\phi}$ / J·mol^{-1}·K^{-1}
423.779	2.02	0.64458	-13.79	157.99 (1.07)
423.779	2.02	0.64458	-13.30	161.40 (0.85)
423.779	2.03	1.33941	-25.30	169.03 (0.77)
423.779	2.03	1.33941	-25.24	169.24 (0.60)
$T_{average}$ = 323.169 K; $p_{average}$ = 29.77 MPa; $c_{p,w\ average}$ = 4.1186 J·g^{-1}·K^{-1}				
323.167	29.80	0.081666	-2.48	120.82 (3.27)
323.167	29.80	0.081666	-2.48	120.64 (3.38)
323.170	29.79	0.15025	-4.49	122.27 (1.96)
323.170	29.79	0.15025	-4.55	120.68 (1.87)
323.170	29.72	0.30585	-9.04	123.12 (0.97)
323.170	29.72	0.30585	-9.19	120.98 (0.96)
323.170	29.73	0.64458	-18.46	125.82 (0.65)
323.170	29.73	0.64458	-18.46	125.81 (0.61)
323.170	29.80	1.33941	-36.06	131.46 (0.46)
323.170	29.80	1.33941	-36.01	131.62 (0.46)
$T_{average}$ = 373.557 K; $p_{average}$ = 30.23 MPa; $c_{p,w\ average}$ = 4.1524 J·g^{-1}·K^{-1}				
373.562	30.25	0.081666	-1.95	148.64 (4.65)
373.562	30.25	0.081666	-1.95	148.78 (4.36)
373.557	30.29	0.15025	-3.53	150.32 (2.80)
373.557	30.29	0.15025	-3.55	149.71 (2.61)
373.556	30.37	0.30585	-7.15	150.37 (1.32)
373.556	30.37	0.30585	-7.19	149.78 (1.41)
373.556	30.28	0.64458	-14.70	152.14 (0.85)
373.556	30.28	0.64458	-14.56	153.08 (0.72)
373.556	29.97	1.33941	-28.28	158.70 (0.49)
373.556	29.97	1.33941	-28.28	158.67 (0.48)
$T_{average}$ = 423.765 K; $p_{average}$ = 30.34 MPa; $c_{p,w\ average}$ = 4.2222 J·g^{-1}·K^{-1}				
423.763	30.39	0.081666	-1.71	164.00 (6.88)
423.763	30.39	0.081666	-1.72	163.18 (11.02)
423.764	30.30	0.15025	-3.20	161.99 (6.67)

T K	p MPa	m mol·kg^{-1}	$(f \cdot \Delta W / W) \cdot 10^3$	$C_{p,\phi}$ J·mol^{-1}·K^{-1}
423.764	30.30	0.15025	-3.15	163.63 (5.58)
423.765	30.41	0.30585	-6.22	165.92 (2.74)
423.765	30.41	0.30585	-6.30	164.85 (2.81)
423.766	30.31	0.64458	-12.54	169.42 (1.37)
423.766	30.31	0.64458	-12.50	169.68 (1.43)
423.767	30.30	1.33941	-23.77	176.79 (0.94)
423.767	30.30	1.33941	-23.74	176.88 (0.54)

Table 3.3.3 Apparent molar heat capacities $C_{p,\phi}$ of aqueous glycine as a function of molality m.

T / K	p / MPa	m / mol·kg^{-1}	$(f \cdot \Delta W / W) \cdot 10^3$	$C_{p,\phi}$ / J·mol^{-1}·K^{-1}
$T_{average}$ = 323.170 K; $p_{average}$ = 0.10 MPa; $c_{p,w\ average}$ = 4.1814 J·g^{-1}·K^{-1}				
323.173	0.10	0.096677	-2.58	69.59 (4.26)
323.173	0.10	0.096677	-2.55	70.82 (2.52)
323.173	0.10	0.25394	-6.56	72.66 (1.08)
323.173	0.10	0.25394	-6.55	72.78 (1.06)
323.173	0.10	0.51960	-13.06	74.93 (0.69)
323.167	0.10	0.51960	-13.08	74.72 (0.70)
323.167	0.10	1.07965	-25.56	80.04 (0.49)
323.167	0.10	1.07965	-25.56	80.01 (0.51)
323.169	0.10	2.26847	-47.73	90.19 (0.38)
323.169	0.10	2.26847	-47.73	90.17 (0.38)
$T_{average}$ = 373.560 K; $p_{average}$ = 2.09 MPa; $c_{p,w\ average}$ = 4.2116 J·g^{-1}·K^{-1}				
373.560	2.10	0.096677	-2.24	84.87 (6.22)
373.560	2.10	0.096677	-1.97	96.89 (3.23)
373.560	2.10	0.25394	-5.49	91.23 (2.14)
373.560	2.10	0.25394	-5.34	93.77 (2.29)
373.561	2.07	0.51960	-10.90	93.63 (1.16)
373.561	2.07	0.51960	-10.67	95.48 (0.96)
373.560	2.07	1.07965	-21.17	98.79 (0.65)
373.560	2.07	1.07965	-20.86	100.06 (0.63)
373.561	2.11	2.26847	-39.65	107.63 (0.40)
373.561	2.11	2.26847	-39.91	107.09 (0.42)
$T_{average}$ = 423.780 K; $p_{average}$ = 2.03 MPa; $c_{p,w\ average}$ = 4.3037 J·g^{-1}·K^{-1}				
423.781	2.04	0.096677	-2.18	89.64 (4.94)
423.772	1.98	0.096677	-2.23	87.47 (6.30)
423.771	2.02	0.25394	-5.65	90.63 (2.31)
423.784	2.05	0.25394	-5.84	87.25 (2.17)
423.786	2.01	0.51960	-11.65	89.31 (1.16)

T K	p MPa	m mol·kg^{-1}	$(f \cdot \Delta W / W) \cdot 10^3$	$C_{p,\phi}$ J·mol^{-1}·K^{-1}
423.786	2.01	0.51960	-11.44	91.08 (1.19)
423.787	2.09	1.07965	-21.22	100.74 (0.69)
423.787	2.09	1.07965	-21.59	99.18 (0.73)
423.773	2.01	2.26847	-39.86	109.53 (0.44)
423.773	2.01	2.26847	-39.63	110.02 (0.44)
$T_{average}$ = 473.810 K; $p_{average}$ = 5.56 MPa; $c_{p,\,w\ average}$ = 4.4763 J·g^{-1}·K^{-1}				
473.810	5.51	0.096677	-2.65	71.92 (7.19)
473.810	5.51	0.096677	-2.65	72.02 (5.77)
473.810	5.59	0.25394	-6.73	75.46 (2.62)
473.810	5.59	0.25394	-6.72	75.57 (2.48)
473.810	5.51	0.51960	-13.14	80.20 (2.35)
473.810	5.51	0.51960	-13.14	80.26 (1.46)
473.810	5.61	1.07965	-24.89	89.35 (0.72)
473.810	5.61	1.07965	-24.85	89.54 (0.91)
473.810	5.59	2.26847	-44.64	104.07 (0.53)
473.810	5.59	2.26847	-44.68	104.00 (0.57)
$T_{average}$ = 499.099 K; $p_{average}$ = 5.55 MPa; $c_{p,\,w\ average}$ = 4.6315 J·g^{-1}·K^{-1}				
499.100	5.60	0.096677	-2.84	65.01 (6.27)
499.100	5.60	0.096677	-2.88	63.09 (9.48)
499.100	5.59	0.096677	-2.90	62.19 (8.54)
499.101	5.59	0.25394	-7.33	67.03 (3.13)
499.101	5.59	0.25394	-7.35	66.65 (2.74)
499.100	5.59	0.51960	-14.42	71.37 (1.32)
499.100	5.59	0.51960	-14.40	71.50 (1.39)
499.096	5.47	1.07965	-26.89	83.48 (1.07)
499.096	5.47	1.07965	-26.90	83.45 (0.80)
499.095	5.47	2.26847	-46.55	103.38 (0.54)
499.095	5.47	2.26847	-46.53	103.43 (0.53)
$T_{average}$ = 323.166 K; $p_{average}$ = 30.12 MPa; $c_{p,\,w\ average}$ = 4.1179 J·g^{-1}·K^{-1}				
323.165	30.22	0.096677	-2.37	81.12 (3.35)
323.165	30.22	0.096677	-2.36	81.65 (2.91)

T / K	p / MPa	m / mol·kg^{-1}	$(f \cdot \Delta W / W) \cdot 10^3$	$C_{p,\phi}$ / J·mol^{-1}·K^{-1}
323.166	30.15	0.25394	-6.15	82.07 (1.10)
323.166	30.15	0.25394	-6.10	82.95 (1.39)
323.167	30.12	0.51960	-12.20	84.59 (0.94)
323.167	30.12	0.51960	-12.24	84.25 (0.88)
323.167	30.19	1.07965	-24.07	88.72 (0.58)
323.167	30.19	1.07965	-24.07	88.73 (0.59)
323.167	29.90	2.26847	-45.15	98.06 (0.38)
323.167	29.90	2.26847	-45.19	97.99 (0.39)
$T_{average}$ = 373.540 K; $p_{average}$ = 30.11 MPa; $c_{p,w\ average}$ = 4.1526 J·g^{-1}·K^{-1}				
373.540	30.11	0.096677	-2.03	96.33 (4.21)
373.540	30.11	0.096677	-2.01	97.60 (4.08)
373.539	30.08	0.25394	-5.16	99.17 (1.49)
373.539	30.08	0.25394	-5.18	98.82 (1.50)
373.540	30.09	0.51960	-10.41	99.92 (0.88)
373.540	30.09	0.51960	-10.64	98.04 (1.01)
373.540	30.02	1.07965	-20.10	105.44 (0.57)
373.540	30.02	1.07965	-20.53	103.73 (0.53)
373.540	30.23	2.26847	-38.57	112.21 (0.44)
373.540	30.23	2.26847	-38.66	112.03 (0.38)
$T_{average}$ = 423.761 K; $p_{average}$ = 30.34 MPa; $c_{p,w\ average}$ = 4.2222 J·g^{-1}·K^{-1}				
423.762	30.39	0.096677	-2.25	88.32 (4.79)
423.762	30.39	0.096677	-2.32	85.39 (4.36)
423.755	30.40	0.096677	-2.16	92.53 (8.60)
423.755	30.40	0.096677	-2.28	87. 27 (12.88)
423.762	30.23	0.25394	-5.39	96.99 (3.31)
423.762	30.23	0.25394	-5.44	96.13 (1.61)
423.762	30.39	0.51960	-10.47	101.13 (1.03)
423.762	30.39	0.51960	-10.36	102.12 (1.02)
423.762	30.21	1.07965	-19.99	107.69 (0.61)
423.762	30.21	1.07965	-19.87	108.19 (0.59)
423.761	30.39	2.26847	-36.88	117.60 (0.49)
423.761	30.39	2.26847	-36.77	117.83 (0.44)

T K	p MPa	m mol·kg^{-1}	$(f \cdot \Delta W / W) \cdot 10^3$	$C_{p,\phi}$ J·mol^{-1}·K^{-1}
$T_{average}$ = 447.842 K; $p_{average}$ = 30.09 MPa; $c_{p,w\ average}$ = 4.2781 J·g^{-1}·K^{-1}				
447.840	29.99	0.096677	-2.21	91.52 (6.08)
447.840	29.99	0.096677	-2.22	91.07 (4.82)
447.842	30.03	0.25394	-5.49	96.54 (2.00)
447.842	30.03	0.25394	-5.49	96.46 (2.20)
447.841	30.12	0.51960	-10.86	99.18 (1.19)
447.841	30.12	0.51960	-10.79	99.77 (1.17)
447.843	30.11	1.07965	-20.58	106.67 (0.58)
447.843	30.11	1.07965	-20.60	106.56 (0.58)
447.845	30.19	2.26847	-36.30	120.32 (0.39)
447.845	30.19	2.26847	-36.64	119.62 (0.43)
$T_{average}$ = 473.438 K; $p_{average}$ = 30.20 MPa; $c_{p,w\ average}$ = 4.3570 J·g^{-1}·K^{-1}				
473.814	30.02	0.096677	-2.22	92.72 (6.88)
473.814	30.02	0.096677	-2.18	94.72 (5.80)
473.815	30.03	0.25394	-5.72	94.37 (2.82)
473.815	30.03	0.25394	-5.72	94.33 (2.54)
472.493	30.60	0.25394	-5.77	93.35 (2.49)
472.493	30.60	0.25394	-5.77	93.43 (1.76)
473.816	30.07	0.51960	-11.20	98.16 (1.29)
473.816	30.07	0.51960	-11.24	97.79 (1.24)
473.817	30.09	1.07965	-21.48	104.84 (0.69)
473.817	30.09	1.07965	-21.42	105.11 (1.09)
473.816	30.06	2.26847	-38.74	117.41 (0.43)
473.816	30.06	2.26847	-38.74	117.42 (0.42)
472.495	30.53	2.26847	-38.91	116.93 (0.39)
472.495	30.53	2.26847	-38.93	116.89 (0.42)
$T_{average}$ = 499.096 K; $p_{average}$ = 30.58 MPa; $c_{p,w\ average}$ = 4.4620 J·g^{-1}·K^{-1}				
499.096	30.51	0.096677	-2.23	94.73 (5.86)
499.096	30.51	0.096677	-2.17	97.47 (3.28)
499.096	30.58	0.096677	-2.19	96.33 (4.04)
499.096	30.58	0.25394	-5.99	91.85 (1.92)

T / K	p / MPa	m / mol·kg^{-1}	$(f \cdot \Delta W / W) \cdot 10^3$	$C_{p,\phi}$ / J·mol^{-1}·K^{-1}
499.097	30.60	0.25394	-5.98	91.98 (1.94)
499.096	30.59	0.51960	-11.70	96.16 (0.79)
499.096	30.59	0.51960	-11.64	96.66 (0.77)
499.096	30.59	1.07965	-22.00	105.15 (0.51)
499.096	30.59	1.07965	-21.98	105.24 (0.52)
499.096	30.60	2.26847	-38.26	121.31 (0.47)
499.096	30.60	2.26847	-38.28	121.27 (0.48)

Table 3.3.4 Apparent molar heat capacities $C_{p,\phi}$ of aqueous proline as a function of molality m.

T / K	p / MPa	m / mol·kg^{-1}	$(f \cdot \Delta W / W) \cdot 10^3$	$C_{p,\phi}$ / J·mol^{-1}·K^{-1}
$T_{average}$ = 323.173 K; $p_{average}$ = 0.10 MPa; $c_{p,w\ average}$ = 4.1814 J·g^{-1}·K^{-1}				
323.173	0.10	0.097407	-3.07	212.68 (3.17)
323.173	0.10	0.097407	-3.06	213.41 (2.82)
323.173	0.10	0.25341	-7.93	212.15 (1.07)
323.173	0.10	0.25341	-7.92	212.27 (1.11)
323.173	0.10	0.52171	-15.93	212.55 (0.70)
323.173	0.10	0.52171	-15.92	212.60 (0.73)
323.173	0.10	1.19912	-34.59	213.68 (0.50)
323.173	0.10	1.19912	-34.60	213.64 (0.47)
323.174	0.10	1.78992	-49.28	215.17 (0.45)
323.174	0.10	1.78992	-49.27	215.22 (0.54)
$T_{average}$ = 373.567 K; $p_{average}$ = 2.10 MPa; $c_{p,w\ average}$ = 4.2116 J·g^{-1}·K^{-1}				
373.566	2.01	0.097407	-2.67	232.09 (6.42)
373.565	2.06	0.097407	-2.58	236.24 (6.19)
373.567	2.11	0.25341	-6.33	241.18 (2.47)
373.567	2.11	0.25341	-6.61	236.44 (1.74)
373.567	2.11	0.52171	-13.16	237.81 (1.03)
373.567	2.11	0.52171	-13.06	238.64 (1.08)
373.568	2.11	1.19912	-28.59	238.87 (0.63)
373.568	2.11	1.19912	-28.60	238.83 (0.62)
373.568	2.12	1.78992	-39.32	244.10 (0.55)
373.568	2.12	1.78992	-39.96	242.37 (0.51)
$T_{average}$ = 423.765 K; $p_{average}$ = 2.00 MPa; $c_{p,w\ average}$ = 4.3038 J·g^{-1}·K^{-1}				
423.767	2.02	0.097407	-2.46	246.78 (6.76)
423.767	2.02	0.097407	-2.43	248.22 (5.65)
423.767	1.98	0.25341	-6.26	247.67 (2.17)
423.767	1.98	0.25341	-6.27	247.42 (2.12)
423.765	2.01	0.52171	-12.60	247.79 (1.16)

T K	p MPa	m mol·kg^{-1}	$(f \cdot \Delta W / W) \cdot 10^3$	$C_{p,\phi}$ J·mol^{-1}·K^{-1}
423.765	2.01	0.52171	-12.50	248.67 (1.19)
423.763	2.02	1.19912	-26.90	250.72 (0.69)
423.763	2.02	1.19912	-26.93	250.60 (0.64)
423.765	1.99	1.78992	-37.87	253.43 (0.55)
423.765	1.99	1.78992	-37.94	253.23 (0.52)
$T_{average}$ = 473.795 K; $p_{average}$ = 5.60 MPa; $c_{p,w\ average}$ = 4.4760 J·g^{-1}·K^{-1}				
473.793	5.59	0.097407	-2.85	239.23 (9.71)
473.793	5.59	0.097407	-2.88	237.90 (10.27)
473.794	5.59	0.097407	-2.83	240.17 (7.15)
473.794	5.59	0.097407	-2.85	239.47 (5.87)
473.794	5.59	0.25341	-7.37	238.39 (4.35)
473.794	5.59	0.25341	-7.47	236.68 (4.25)
473.795	5.53	0.52171	-14.94	237.64 (2.00)
473.795	5.53	0.52171	-14.91	237.94 (2.26)
473.796	5.59	1.19912	-31.35	233.36 (0.92)
473.796	5.59	1.19912	-31.35	233.38 (0.95)
473.797	5.68	1.78992	-43.45	238.42 (0.63)
473.797	5.68	1.78992	-43.43	238.50 (0.73)
$T_{average}$ = 499.101 K; $p_{average}$ = 5.57 MPa; $c_{p,w\ average}$ = 4.6314 J·g^{-1}·K^{-1}				
499.101	5.53	0.097407	-3.27	227.47 (8.57)
499.100	5.58	0.097407	-3.24	229.17 (6.83)
499.101	5.54	0.25341	-8.44	226.79 (2.76)
499.101	5.54	0.25341	-8.47	226.08 (2.97)
499.101	5.57	0.52171	-17.30	224.03 (1.52)
499.101	5.57	0.52171	-17.23	224.72 (1.59)
499.100	5.59	1.19912	-36.03	231.94 (0.75)
499.100	5.59	1.19912	-36.03	231.92 (0.86)
499.100	5.58	1.78992	-49.41	239.33 (0.68)
499.100	5.58	1.78992	-49.37	239.45 (0.68)

T K	p MPa	m mol·kg^{-1}	$(f \cdot \Delta W / W) \cdot 10^3$	$C_{p,\phi}$ J·mol^{-1}·K^{-1}
$T_{average}$ = 323.166 K; $p_{average}$ = 29.83 MPa; $c_{p,w\ average}$ = 4.1184 J·g^{-1}·K^{-1}				
323.166	30.11	0.097407	-3.02	218.36 (3.23)
323.166	30.11	0.097407	-2.99	219.57 (4.18)
323.165	29.68	0.25341	-7.79	217.57 (1.27)
323.165	29.68	0.25341	-7.80	217.33 (1.46)
323.166	29.78	0.52171	-15.64	218.12 (0.76)
323.166	29.78	0.52171	-15.70	217.65 (0.71)
323.166	29.78	1.19912	-34.03	219.10 (0.49)
323.166	29.78	1.19912	-33.98	219.26 (0.47)
323.167	29.82	1.78992	-48.31	221.11 (0.50)
323.167	29.82	1.78992	-48.31	221.11 (0.45)
$T_{average}$ = 373.559 K; $p_{average}$ = 30.35 MPa; $c_{p,w\ average}$ = 4.1521 J·g^{-1}·K^{-1}				
373.558	30.29	0.097407	-2.45	244.50 (4.26)
373.558	30.29	0.097407	-2.52	241.73 (4.81)
373.558	30.23	0.25341	-6.59	239.49 (1.90)
373.558	30.23	0.25341	-6.19	246.29 (1.43)
373.558	30.37	0.52171	-12.94	242.48 (0.83)
373.558	30.37	0.52171	-12.93	242.56 (0.76)
373.559	30.35	1.19912	-27.85	244.56 (0.57)
373.559	30.35	1.19912	-27.90	244.37 (0.61)
373.560	30.53	1.78992	-39.87	245.61 (0.49)
373.560	30.53	1.78992	-39.90	245.52 (0.56)
$T_{average}$ = 423.768 K; $p_{average}$ = 30.48 MPa; $c_{p,w\ average}$ = 4.2219 J·g^{-1}·K^{-1}				
423.768	30.40	0.097407	-2.40	251.02 (6.08)
423.768	30.40	0.097407	-2.40	251.06 (4.66)
423.767	30.52	0.25341	-6.10	251.87 (1.95)
423.767	30.52	0.25341	-6.08	252.33 (2.11)
423.766	30.57	0.52171	-12.20	252.83 (1.37)
423.766	30.57	0.52171	-12.13	253.40 (1.21)
423.768	30.53	1.19912	-26.06	255.64 (0.75)
423.768	30.53	1.19912	-26.09	255.52 (0.91)

T K	p MPa	m mol·kg^{-1}	$(f \cdot \Delta W / W) \cdot 10^3$	$C_{p,\phi}$ J·mol^{-1}·K^{-1}
423.769	30.40	1.78992	-36.64	258.50 (0.59)
423.769	30.40	1.78992	-36.59	258.64 (0.49)
$T_{average}$ = 447.846 K; $p_{average}$ = 30.18 MPa; $c_{p,w\ average}$ = 4.2778 J·g^{-1}·K^{-1}				
447.846	30.08	0.097407	-2.49	250.22 (5.86)
447.846	30.08	0.097407	-2.45	252.04 (4.99)
447.845	30.11	0.25341	-6.23	252.91 (2.06)
447.845	30.11	0.25341	-6.31	251.60 (1.94)
447.845	30.19	0.52171	-12.56	253.00 (1.10)
447.846	30.29	0.52171	-12.65	252.19 (1.17)
447.847	30.23	1.19912	-26.90	255.67 (0.69)
447.847	30.23	1.19912	-26.66	256.63 (0.99)
447.846	30.22	1.78992	-37.63	259.14 (0.51)
447.846	30.22	1.78992	-37.67	259.03 (0.60)
$T_{average}$ = 473.438 K; $p_{average}$ = 30.39 MPa; $c_{p,w\ average}$ = 4.3562 J·g^{-1}·K^{-1}				
473.818	30.50	0.097407	-2.57	251.22 (4.91)
473.818	30.50	0.097407	-2.58	250.65 (4.21)
473.818	30.49	0.25341	-6.67	250.05 (1.63)
473.818	30.49	0.25341	-6.62	250.82 (1.84)
472.481	30.21	0.25341	-6.76	248.19 (1.58)
472.481	30.21	0.25341	-6.71	249.12 (1.81)
473.818	30.51	0.52171	-13.42	250.23 (1.36)
473.818	30.51	0.52171	-13.45	249.98 (0.92)
473.818	30.20	1.19912	-28.34	254.74 (0.63)
473.818	30.20	1.19912	-28.23	255.18 (0.58)
473.817	30.23	1.78992	-39.36	259.18 (0.50)
473.817	30.23	1.78992	-39.45	258.93 (0.49)
472.495	30.57	1.78992	-39.86	257.49 (0.57)
472.495	30.57	1.78992	-39.83	257.56 (0.50)

T / K	p / MPa	m / mol·kg^{-1}	$(f \cdot \Delta W / W) \cdot 10^3$	$C_{p,\phi}$ / J·mol^{-1}·K^{-1}
$T_{average}$ = 499.098 K; $p_{average}$ = 30.61 MPa; $c_{p,w\ average}$ = 4.4619 J·g^{-1}·K^{-1}				
499.100	30.59	0.25341	-7.10	248.41 (1.62)
499.098	30.59	0.25341	-7.12	247.97 (1.56)
499.098	30.61	0.52171	-14.54	246.32 (0.76)
499.098	30.61	0.52171	-14.56	246.13 (0.86)
499.098	30.63	1.19912	-30.88	250.45 (0.63)
499.098	30.63	1.19912	-30.89	250.42 (0.52)
499.098	30.59	1.78992	-42.95	255.12 (0.45)
499.098	30.59	1.78992	-43.25	254.27 (0.46)

Table 3.3.5 Values of C_p^o, b, and c obtained by fitting either equation (3.3.1) or equation (3.3.2) to each set of isothermal calorimetric data for each amino acid.

T / (K)	p / (MPa)	C_p^o / (J·mol^{-1}·K^{-1})	b / (J·kg·mol^{-2}·K^{-1})	c / (J·kg^2·mol^{-3}·K^{-1})
		α-Alanine		
298.10	0.10	140.52 ± 0.49	9.01 ± 0.93	—
323.173	0.10	167.76 ± 0.25	4.86 ± 0.26	—
373.563	2.08	181.67 ± 0.59	4.65 ± 0.66	—
423.772	2.01	180.01 ± 0.35	7.42 ± 0.37	—
447.746	10.30	175.50 ± 0.31	6.86 ± 0.33	—
473.799	5.62	170.94 ± 0.37	9.22 ± 0.39	—
323.168	29.77	174.25 ± 0.31	5.13 ± 0.33	—
373.543	30.03	188.04 ± 0.38	5.38 ± 0.41	—
423.769	30.56	187.00 ± 0.35	9.64 ± 0.36	—
447.857	30.22	184.79 ± 0.15	8.89 ± 0.16	—
473.818	30.19	182.47 ± 0.27	10.00 ± 0.28	—
		β-Alanine		
323.172	0.10	110.34 ± 0.16	9.58 ± 0.16	—
373.554	2.02	140.20 ± 1.12	8.95 ± 1.07	—
423.778	2.02	153.16 ± 0.95	11.76 ± 0.92	—
323.169	29.77	119.94 ± 0.38	8.69 ± 0.37	—
373.557	30.23	147.76 ± 0.34	8.10 ± 0.32	—
423.765	30.34	162.11 ± 0.33	11.04 ± 0.32	—
		Glycine		
323.17	0.10	69.88 ± 0.27	9.81 ± 0.49	-0.38 ± 0.17
373.56	2.09	89.89 ± 1.74	9.77 ± 3.17	-0.91 ± 1.11
423.78	2.03	83.93 ± 1.80	17.03 ± 3.27	-2.48 ± 1.15
473.81	5.56	70.35 ± 0.14	20.27 ± 0.25	-2.39 ± 0.09
499.10	5.55	60.74 ± 0.51	22.77 ± 0.94	-1.74 ± 0.35
323.17	30.12	80.61 ± 0.21	7.35 ± 0.39	0.15 ± 0.14
373.54	30.11	95.75 ± 1.18	8.60 ± 2.16	-0.61 ± 0.76
423.76	30.34	92.75 ± 0.79	17.18 ± 1.42	-2.72 ± 0.49

T / (K)	p / (MPa)	C_p^o / (J·mol^{-1}·K^{-1})	b / (J·kg·mol^{-2}·K^{-1})	c / (J·kg^2·mol^{-3}·K^{-1})
447.84	30.09	91.92 ± 0.76	14.90 ± 1.38	-1.12 ± 0.49
473.44	30.20	90.68 ± 0.50	14.59 ± 0.97	-1.29 ± 0.35
499.10	30.58	87.52 ± 0.21	17.73 ± 0.37	-1.25 ± 0.13
		Proline		
323.17	0.10	212.44 ± 0.22	-0.14 ± 0.46	0.94 ± 0.20
373.57	2.10	238.37 ± 1.90	-3.36 ± 4.00	3.37 ± 1.79
423.77	2.00	247.05 ± 0.35	1.92 ± 0.75	0.89 ± 0.33
473.80	5.60	237.35 ± 0.82	1.48 ± 1.80	2.67 ± 0.83
499.10	5.57	225.54 ± 1.53	-1.25 ± 3.21	5.07 ± 1.44
323.17	29.83	217.95 ± 0.40	-0.64 ± 0.84	1.35 ± 0.38
373.56	30.35	242.25 ± 1.50	1.38 ± 3.15	0.28 ± 1.41
423.77	30.48	251.30 ± 0.28	2.76 ± 0.59	0.72 ± 0.26
447.85	30.18	250.80 ± 0.67	3.87 ± 1.41	0.43 ± 0.63
473.82	30.39	248.37 ± 1.05	4.61 ± 2.34	0.53 ± 1.06
499.10	30.61	246.87 ± 1.41	-0.65 ± 2.83	2.82 ± 1.23

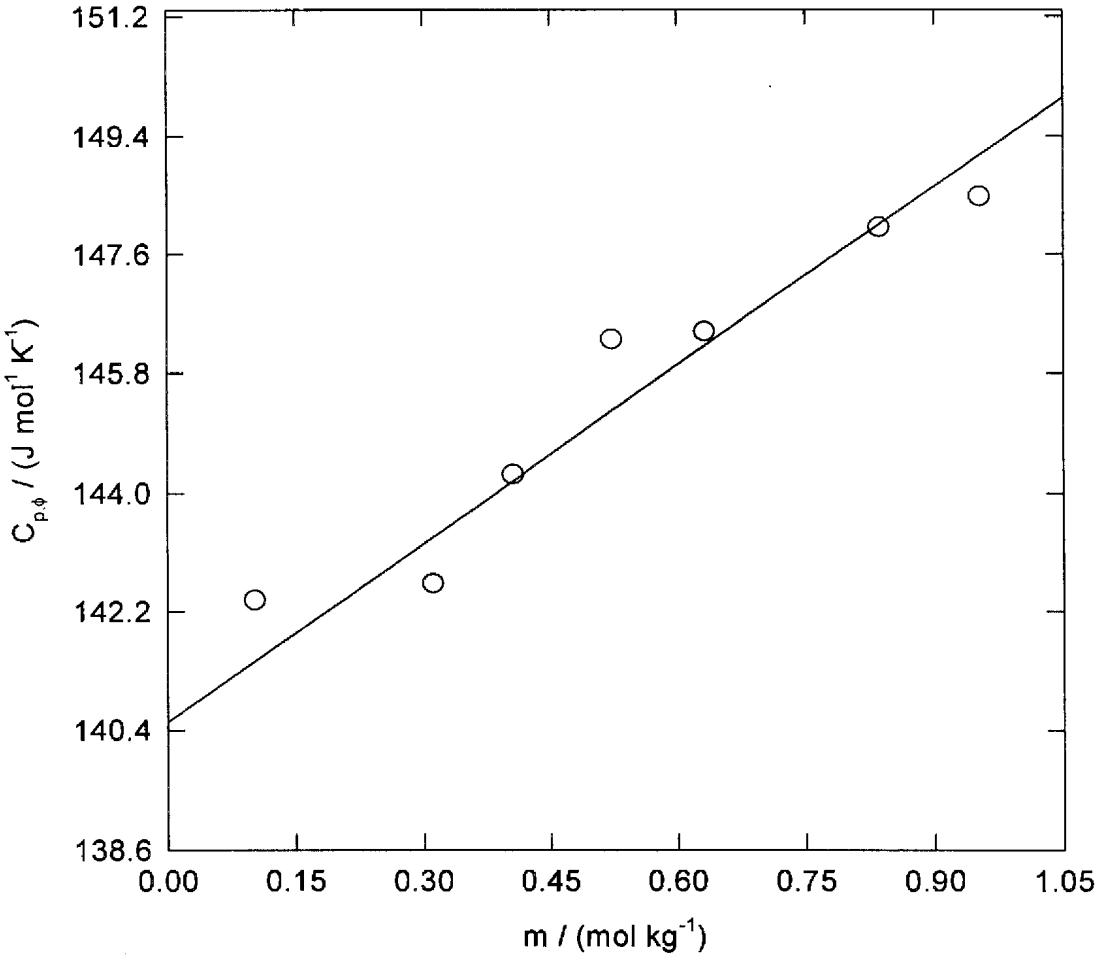

Figure 3.3.1 The apparent molar heat capacities $C_{p,\phi}$ of α-alanine at 298.10 K and 0.10 MPa plotted against molality. Symbols are experimental results: ○, 298.10 K. The line is the isothermal fit to the experimental data.

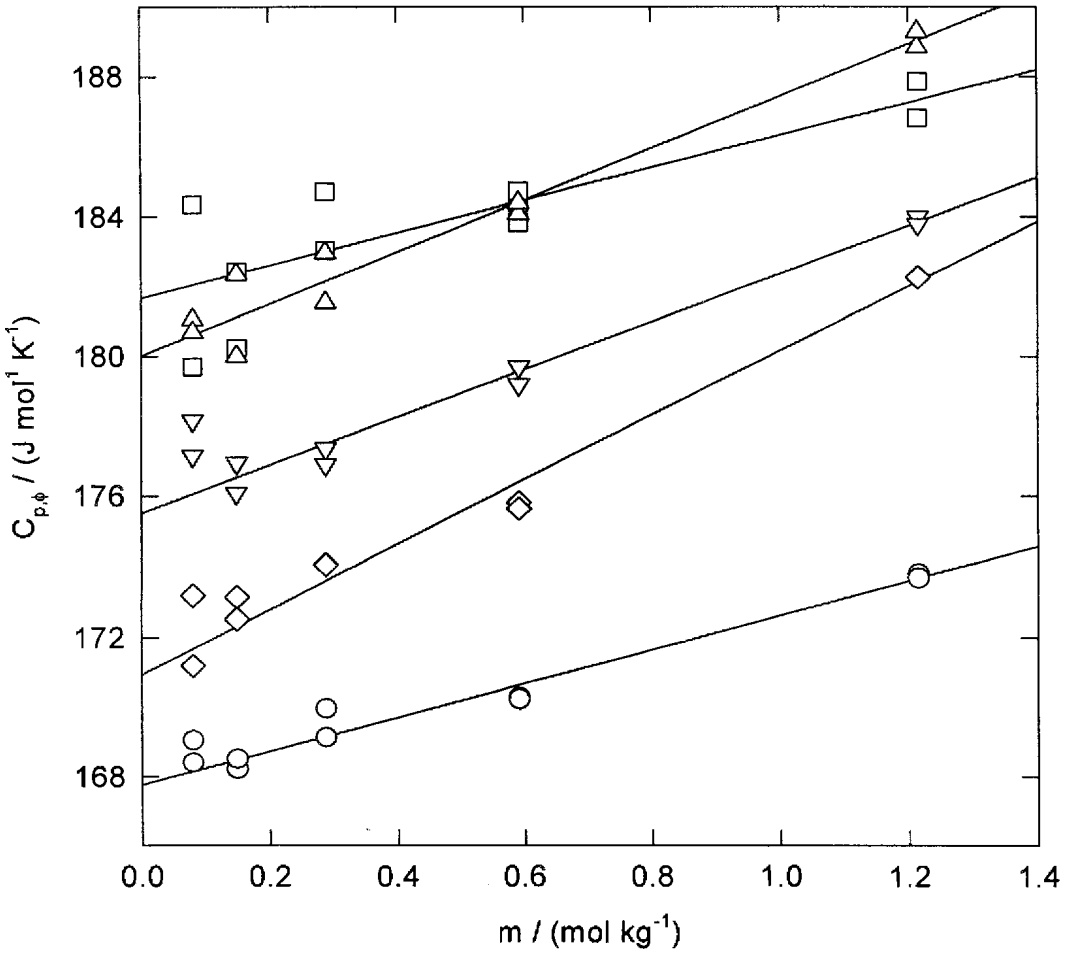

Figure 3.3.2 The apparent molar heat capacities $C_{p,\phi}$ of α-alanine from 323.2 to 473.8 K at steam saturation plotted against molality. Symbols are experimental results: ○, 323.17 K, 0.10 MPa; □, 373.56 K, 2.08 MPa; Δ, 423.77 K, 2.01 MPa; ▽, 447.75 K, 10.30 MPa; ◇, 473.80 K, 5.62 MPa. Lines are the isothermal fits to the experimental data.

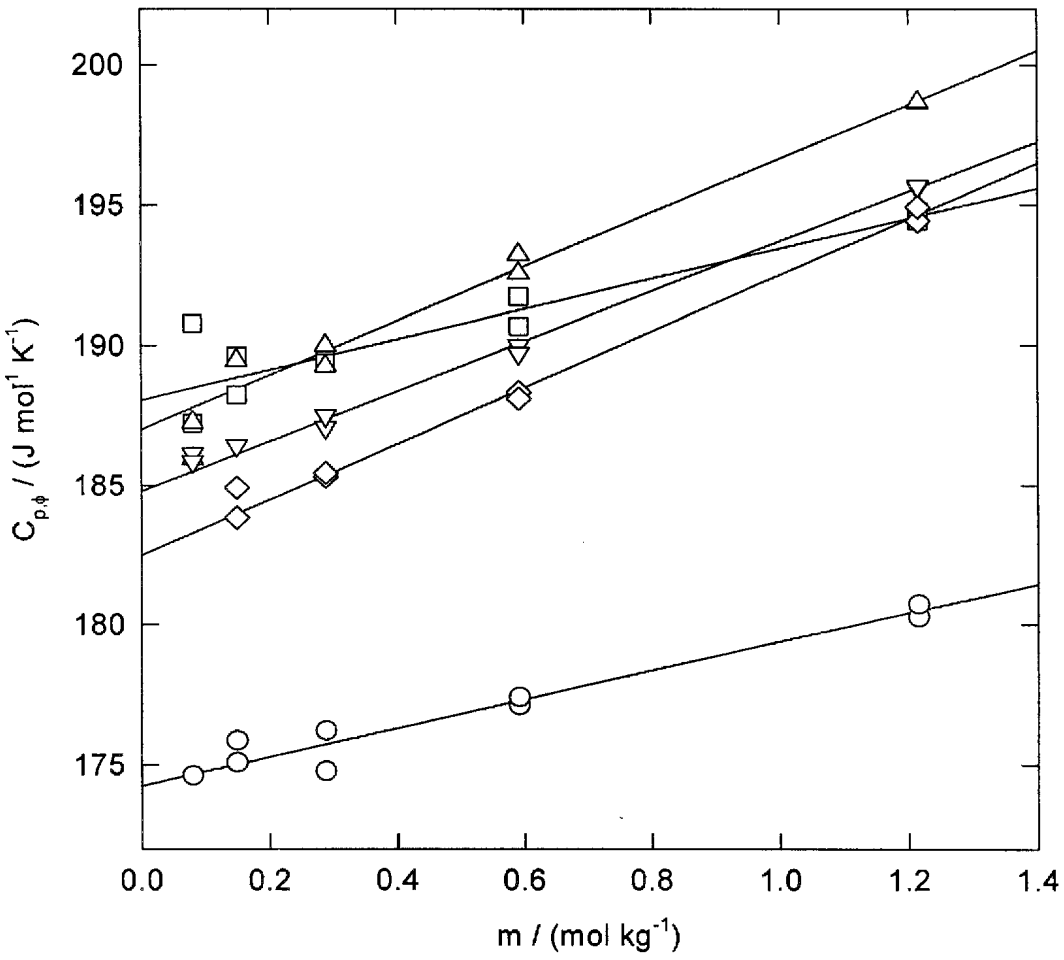

Figure 3.3.3 The apparent molar heat capacities $C_{p,\phi}$ of α-alanine from 323.2 to 473.8 K at 30.15 MPa plotted against molality. Symbols are experimental results: ○, 323.19 K; □, 373.54 K; Δ, 423.77 K; ∇, 447.86 K; ◇, 473.82 K. Lines are the isothermal fits to the experimental data.

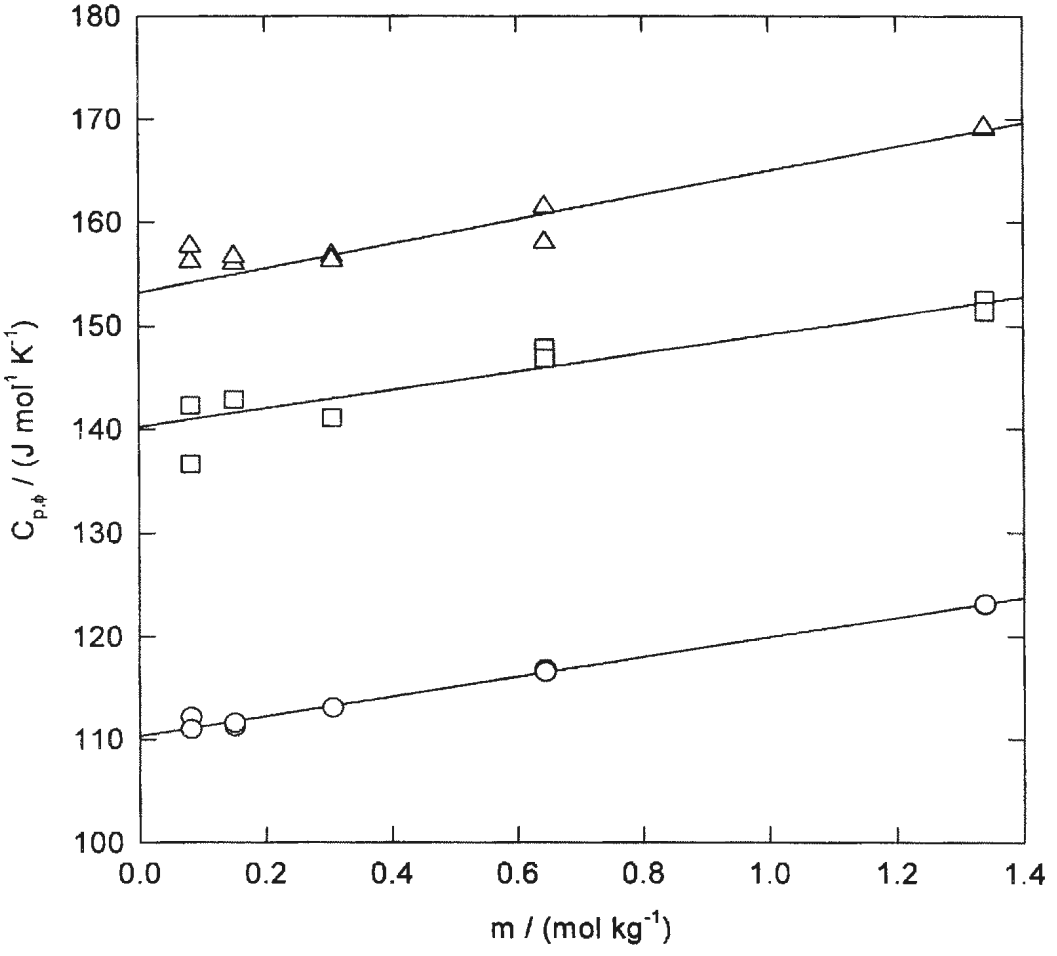

Figure 3.3.4 The apparent molar heat capacities $C_{p,\phi}$ of β-alanine from 323.2 to 423.8 K at steam saturation plotted against molality. Symbols are experimental results: ○, 323.17 K, 0.10 MPa; □, 373.55 K, 2.02 MPa K; Δ, 423.78 K, 2.02 MPa. Lines are the isothermal fits to the experimental data.

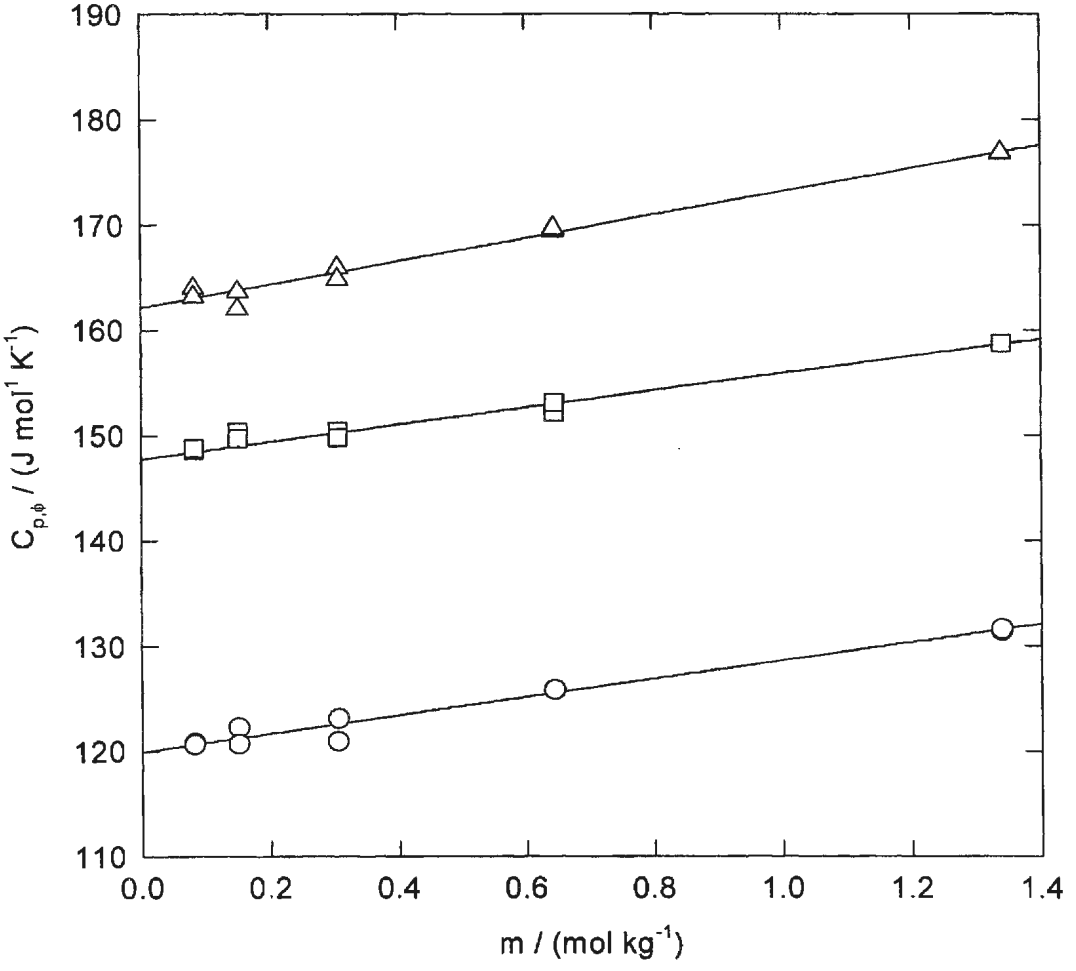

Figure 3.3.5 The apparent molar heat capacities $C_{p,\phi}$ of β-alanine from 323.2 to 423.8 K at 30.11 MPa plotted against molality. Symbols are experimental results: ○, 323.17 K; □, 373.56 K; Δ, 423.77 K. Lines are the isothermal fits to the experimental data.

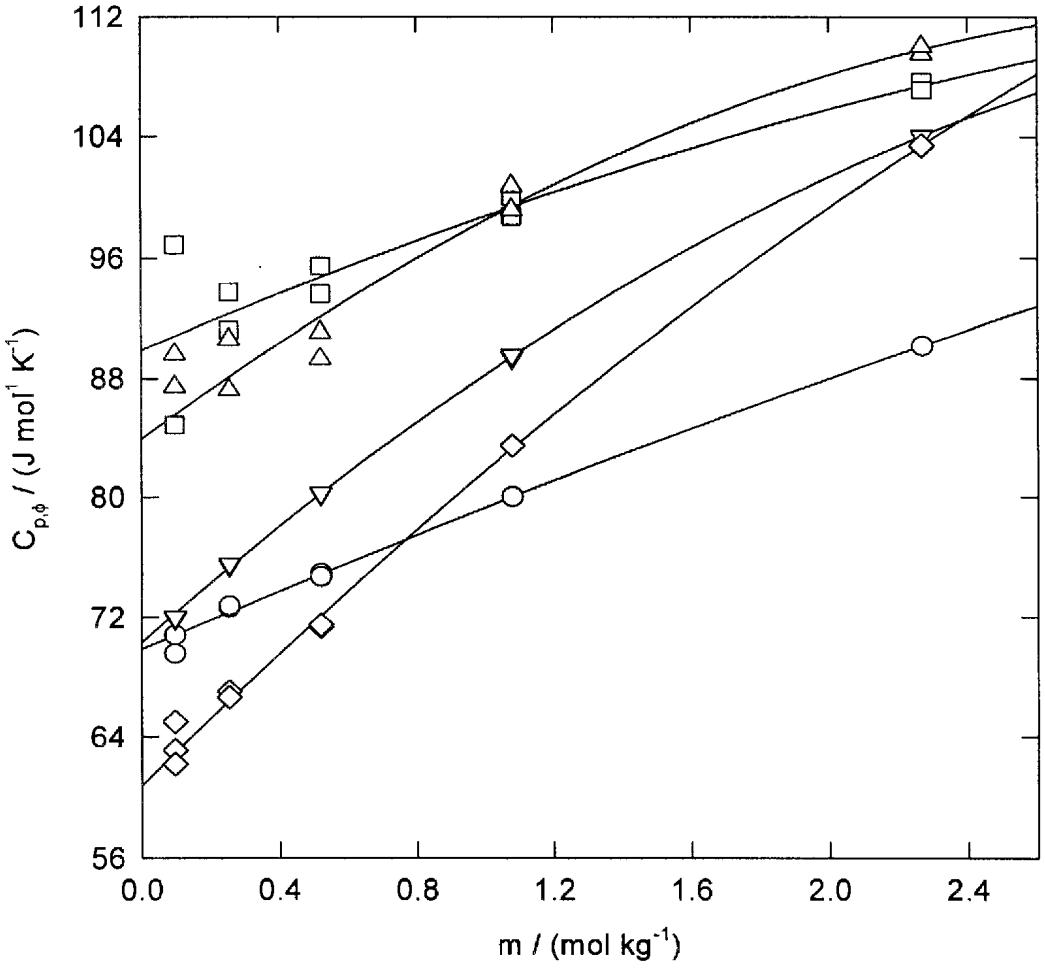

Figure 3.3.6 The apparent molar heat capacities $C_{p,\phi}$ of glycine from 323.2 to 499.1 K at steam saturation plotted against molality. Symbols are experimental results: ○, 323.17 K, 0.10 MPa; □, 373.56 K, 2.09 MPa; Δ, 423.78 K, 2.03 MPa; ∇, 473.81 K, 5.56 MPa; ◇, 499.10 K, 5.55 MPa. Lines are the isothermal fits to the experimental data.

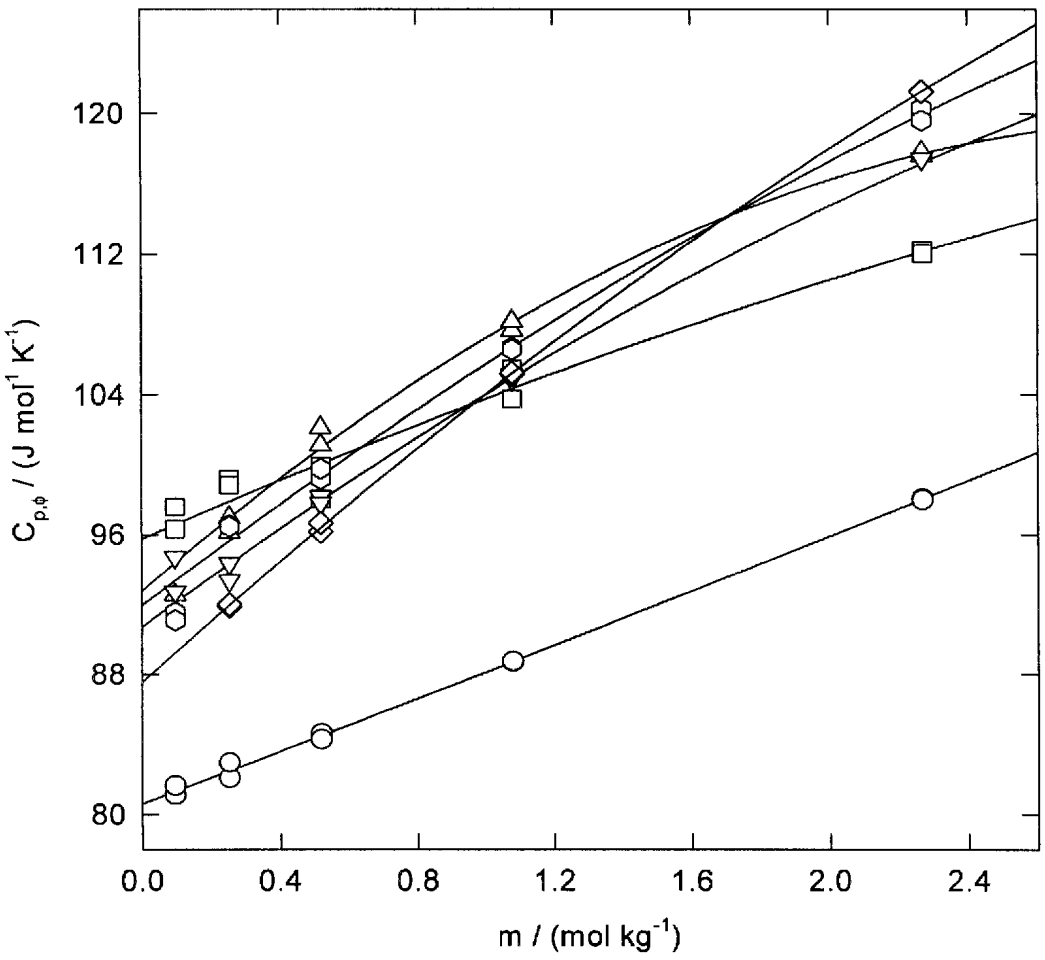

Figure 3.3.7 The apparent molar heat capacities $C_{p,\phi}$ of glycine from 323.2 to 499.1 K at 30.24 MPa plotted against molality. Symbols are experimental results: ○, 323.17 K; □, 373.54 K; Δ, 423.76 K; ⬯, 447.84 K; ▽, 473.44 K; ◇, 499.10 K. Lines are the isothermal fits to the experimental data.

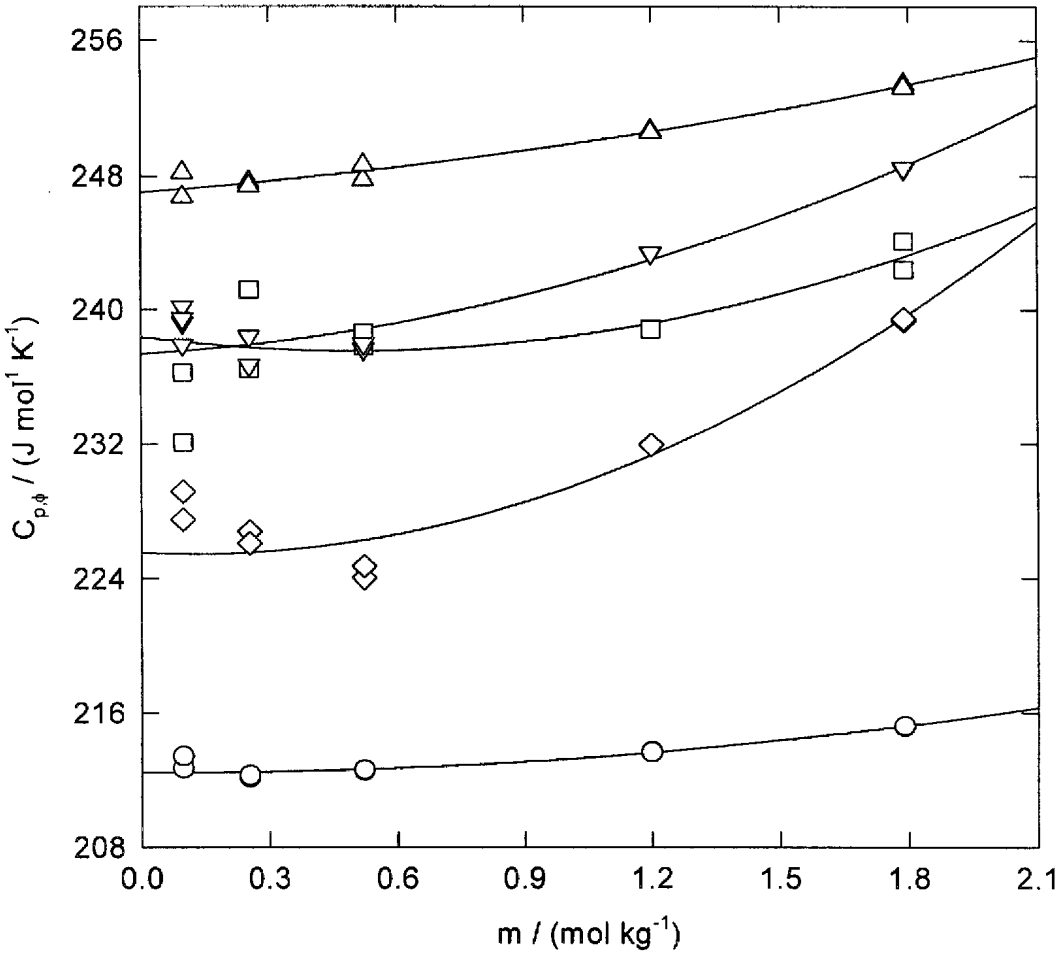

Figure 3.3.8 The apparent molar heat capacities $C_{p,\phi}$ of proline from 323.2 to 499.1 K at steam saturation plotted against molality. Symbols are experimental results: ○, 323.17 K, 0.10 MPa; □, 373.57 K, 2.10 MPa; Δ, 423.77 K, 2.00 MPa; ∇, 473.80 K, 5.60 MPa; ◇, 499.10 K, 5.57 MPa. Lines are the isothermal fits to the experimental data.

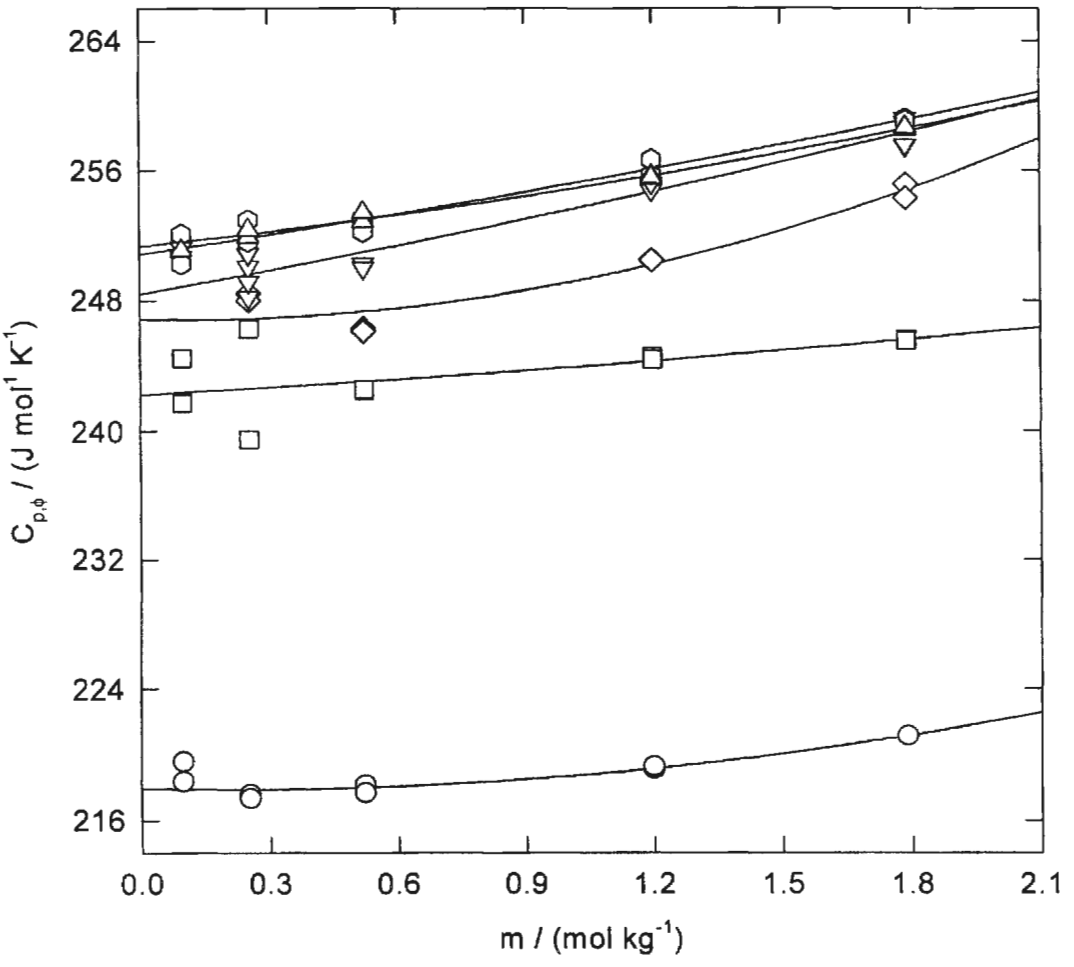

Figure 3.3.9 The apparent molar heat capacities $C_{p,\phi}$ of proline from 323.2 to 499.1 K at 30.24 MPa plotted against molality. Symbols are experimental results: ○, 323.17 K; □, 373.56 K; Δ, 423.77 K; ◊, 447.85 K; ▽, 473.44 K; ◇, 499.10 K. Lines are the isothermal fits to the experimental data.

3.4 Equations of State for V° and C_p°.

3.4.1 Background and Strategy.

An equation of state is the most convenient method of representing the temperature, pressure, and molality dependence of the experimentally determined apparent molar volumes V_ϕ and heat capacities $C_{p,\phi}$. In our initial attempt to model the experimentally determined data both the density model and the revised HKF model were used as fitting functions. Since the apparent molar volumes were measured first, the data set was limited to the $V_\phi(m, T, p)$ results and selected values of κ_T° found in the literature. Section 3.4.2 describes the representation of $V_\phi(m, T, p)$ by both the revised HKF and density models.

Although, the density model reproduced the V_ϕ data better than the revised HKF model, the density model could not simultaneously represent $V_\phi(m, T, p)$ and $C_{p,\phi}(m, T, p)$ with sufficient accuracy. In its final form the density model was extended to include a number of additional temperature and/or pressure dependent terms. As well, the data set was restricted to the values of $V^\circ(T, p)$ and $C_p^\circ(T, p)$ determined in Sections 3.2 and 3.3. Section 3.4.3 describes the representation of $V^\circ(T, p)$ and $C_p^\circ(T, p)$ by the extended density model.

3.4.2 Representation of $V_\phi(m, T, p)$ by Both the Revised HKF and Density Models.

The revised Helgeson Kirkham Flowers (HKF) model and the density model have both been used to fit the thermodynamic properties of aqueous species as a function of temperature and pressure.

The revised Helgeson Kirkham Flowers model, as adapted to organic species by Shock and Helgeson (1990), yields the following expressions for $V°$ and $\kappa_T°$:

$$V^o = a_1 + \left[a_3 + \left(\frac{a_4}{(p+\Psi)} \right) \right] \left(\frac{1}{(T-\Theta)} \right) - \omega_e Q \qquad (3.4.2.1)$$

$$\kappa_T^o = \left(\frac{a_4}{(p+\Psi)^2} \right) \left(\frac{1}{(T-\Theta)} \right) + \omega_e \left(\frac{\partial Q}{\partial p} \right)_T \qquad (3.4.2.2)$$

The molality dependence of V_ϕ was described by the expressions:

$$V_\phi = V^o + bm + cm^2 \qquad (3.4.2.3)$$

$$b = b_1 + \left(\frac{b_2}{(T-\Theta)} \right) - b_3 Q \qquad (3.4.2.4)$$

$$c = c_1 + \left(\frac{c_2}{(T-\Theta)} \right) \qquad (3.4.2.5)$$

Here Ψ is a solvent parameter equal to 260.0 MPa, Θ is a solvent parameter equal to 228 K, and $Q = (1/\varepsilon_r^2)(\partial\varepsilon_r/\partial p)_T$ is a Born function where ε_r is the dielectric constant of water. a_1, a_3, a_4, b_1, b_2, b_3, c_1, and c_2 are fitting parameters. It was necessary to use the effective Born coefficient ω_e as a fitting parameter although Shock and Helgeson (1990) gave an expression for its estimation. An expression for $\kappa_T°$ was included in this model to ensure a good fit to the small pressure dependence observed in the measured apparent molar volumes. The statistical standard deviation associated with equations (3.4.2.1), (3.4.2.2), (3.4.2.3), (3.4.2.4), and (3.4.2.5) can be estimated from equations (3.4.2.1a), (3.4.2.2a), (3.4.2.3a),

(3.4.2.4a), and (3.4.2.5a), respectively.

$$(\sigma_{V^o})^2 = (\sigma_{a_1})^2 + \left[(\sigma_{a_3})^2 + \left(\frac{(\sigma_{a_4})^2}{(p+\Psi)^2}\right)\right]\left(\frac{1}{(T-\Theta)^2}\right) + Q^2(\sigma_{\omega_e})^2 \qquad (3.4.2.1a)$$

$$(\sigma_{\kappa^o_T})^2 = \left(\frac{(\sigma_{a_4})^2}{(p+\Psi)^4}\right)\left(\frac{1}{(T-\Theta)^2}\right) + (\sigma_{\omega_e})^2\left(\frac{\partial Q}{\partial p}\right)^2_T \qquad (3.4.2.2a)$$

$$(\sigma_{V_\phi})^2 = (\sigma_{V^o})^2 + [(\sigma_b)^2 m^2] + [(\sigma_c)^2 m^4] \qquad (3.4.2.3a)$$

$$(\sigma_b)^2 = (\sigma_{b_1})^2 + \left(\frac{(\sigma_{b_2})^2}{(T-\Theta)^2}\right) + Q^2(\sigma_{b_3})^2 \qquad (3.4.2.4a)$$

$$(\sigma_c)^2 = (\sigma_{c_1})^2 + \left(\frac{(\sigma_{c_2})^2}{(T-\Theta)^2}\right) \qquad (3.4.2.5a)$$

The density model discussed in Section 1.2.4 is an alternative to the revised HKF model for describing the dependence of V_ϕ on T and p. The model was developed by Mesmer *et al.* (1988) to describe the temperature and pressure dependence of log K under hydrothermal conditions and yields the following expressions for V° and $\kappa_T{}^\circ$:

$$V^o = (d_0) - (RT\beta_w)\left(d_5 + \frac{d_6}{T} + \frac{d_7}{T^2}\right) \qquad (3.4.2.6)$$

$$\kappa^o{}_T = RT\left(d_5 + \frac{d_6}{T} + \frac{d_7}{T^2}\right)\left(\frac{d\beta_w}{dp}\right)_T \qquad (3.4.2.7)$$

The molality dependence of V_ϕ was described by the expressions:

$$V_\phi = V^o + bm + cm^2 \tag{3.4.2.8}$$

$$b = b_1 + (b_2 R T \beta_w) \tag{3.4.2.9}$$

$$c = c_1 + (c_2 R T \beta_w) \tag{3.4.2.10}$$

Here $\beta_w = -(1/V_w)(\partial V_w/\partial p)_T$ is the compressibility of water. The terms d_0, d_5, d_6, d_7, b_1, b_2, c_1, and c_2 are fitting parameters. The addition of the term d_0, absent in the original model, increases the flexibility of the functions thereby improving their ability to reproduce the temperature and pressure dependence of the experimental data at temperatures below 373 K. An expression for κ_T° was included in this model to ensure a good fit to the small pressure dependence observed in the measured apparent molar volumes. The statistical standard deviation associated with equations (3.4.2.6), (3.4.2.7), (3.4.2.8), (3.4.2.9), and (3.4.2.10) can be estimated from equations (3.4.2.6a), (3.4.2.7a), (3.4.2.8a), (3.4.2.9a), and (3.4.2.10a), respectively:

$$(\sigma_{V^o})^2 = (\sigma_{d_0})^2 + (R T \beta_w)^2 \left((\sigma_{d_5})^2 + \frac{(\sigma_{d_6})^2}{T^2} + \frac{(\sigma_{d_7})^2}{T^4} \right) \tag{3.4.2.6a}$$

$$(\sigma_{\kappa_T^o})^2 = (R T)^2 \left((\sigma_{d_5})^2 + \frac{(\sigma_{d_6})^2}{T^2} + \frac{(\sigma_{d_7})^2}{T^4} \right) \left(\frac{d\beta_w}{dp} \right)_T^2 \tag{3.4.2.7a}$$

$$(\sigma_{V_\phi})^2 = (\sigma_{V^o})^2 + [(\sigma_b)^2 m^2] + [(\sigma_c)^2 m^4] \tag{3.4.2.8a}$$

$$(\sigma_b)^2 = (\sigma_{b_1})^2 + (R T \beta_w)^2 (\sigma_{b_2})^2 \tag{3.4.2.9a}$$

$$(\sigma_c)^2 = (\sigma_{c_1})^2 + (RT\beta_w)^2(\sigma_{c_2})^2 \qquad (3.4.2.10a)$$

To increase the temperature range and accuracy of the fitting parameters obtained from each model, a number of complementary data sets were included, along with the values of V_ϕ measured in this work. The literature sources used for complementary data are listed in Table 3.4.2.1. The diversity of this data requires that each data point be assigned a weight. As discussed in Section 3.2, the uncertainty associated with experimental apparent molar volumes increases as the molality of the sample solution decreases. Therefore, the apparent molar volumes measured in this work and those measured by Hakin *et al.* (1997) were given a weight equal to the molality of the solution. At each temperature and pressure the combined weight of the α-alanine solutions was approximately equal to 3.0. Therefore, the standard partial molar volume obtained by Hakin *et al.* (1994) at 298.15 K and the standard partial molar isothermal compressibilities obtained by Chalikian *et al.* (1994) were assigned a weight of 3.0. Weights were assigned to the other standard partial molar volumes obtained by Hakin *et al.* (1994) using the following expression:

$$weight = 3.0\left(\frac{\sigma_{V^o_{298}}}{\sigma_{V^o_T}}\right)^2 \qquad (3.4.2.11)$$

where $\sigma_{V^o_{298}}$ is the uncertainty associated with V° at 298.15 K and $\sigma_{V^o_T}$ is the uncertainty associated with V° at temperatures other than 298.15 K. For each temperature and pressure the combined weight of the proline solutions was approximately equal to 5.5. Therefore the standard partial molar isothermal compressibilities obtained by Kharakoz (1991) were

assigned a weight of 5.5.

The fitting parameters obtained using the revised HKF model and the density model are tabulated in Tables 3.4.2.2 and 3.4.2.3, respectively, along with their standard deviations. The fitted apparent molar volumes V_ϕ for α-alanine are plotted in Figures 3.4.2.1 and 3.4.2.2, while those for proline are plotted in Figures 3.4.2.3 and 3.4.2.4. Figures 3.4.2.5 and 3.4.2.6 compare the standard partial molar volumes V° obtained using equation (3.4.2.1) from the revised HKF model and equation (3.4.2.6) from the density model with the fitted isotherms obtained for α-alanine and proline in Section 3.2. Figures 3.4.2.7 and 3.4.2.8 compare the molality fit coefficients obtained using equations (3.4.2.4) and (3.4.2.5) from the revised HKF model and equations (3.4.2.9) and (3.4.2.10) from the density model with the isothermal molality fit coefficients obtained for α-alanine and proline in Section 3.2. Figures 3.4.2.9 and 3.4.2.10 compare the fitted values of κ_T° with those measured by Chalikian *et al.* (1994) for α-alanine and Kharakoz (1991) for proline.

Table 3.4.2.1 Literature data sources used in fitting parameters for both the revised HKF and density models.

Data	α-alanine	proline
V_ϕ	—	Hakin *et al.* (1997)
V°	Hakin *et al.* (1994)†	—
κ_T°	Chalikian *et al.* (1994)‡	Kharakoz (1991)‡

† Values are listed in Table 1.6.3.1. ‡ Values are listed in Table 1.6.3.2.

Table 3.4.2.2 Fitting parameters obtained by fitting the revised HKF model to $V_\phi(m, T, p)$.‡

	α-Alanine	Proline
a_1 / ($cm^3 \cdot mol^{-1}$)	65.483 (0.179)	91.213 (0.258)
$a_3 \cdot 10^{-2}$ / ($K \cdot cm^3 \cdot mol^{-1}$)	1.91 (1.39)	-10.21 (1.67)
$a_4 \cdot 10^{-5}$ / ($MPa \cdot K \cdot cm^3 \cdot mol^{-1}$)	-1.224 (0.350)	1.164 (0.415)
$\omega_e \cdot 10^{-4}$ / ($MPa \cdot cm^3 \cdot mol^{-1}$)	17.388 (0.246)	7.506 (0.387)
b_1 / ($cm^3 \cdot kg \cdot mol^{-2}$)	3.082 (0.500)	1.296 (0.432)
$b_2 \cdot 10^{-1}$ / ($K \cdot cm^3 \cdot kg \cdot mol^{-2}$)	-18.83 (6.20)	-9.72 (3.74)
$b_3 \cdot 10^{-3}$ / ($kg \cdot mol^{-1}$)	-46.06 (3.49)	-7.22 (6.88)
c_1 / ($cm^3 \cdot kg^2 \cdot mol^{-3}$)	-2.514 (0.451)	—
$c_2 \cdot 10^{-2}$ / ($K \cdot cm^3 \cdot kg^2 \cdot mol^{-3}$)	1.987 (0.631)	—
σ	0.08	0.18

‡ The standard deviation for each parameter is given in parentheses; σ is the overall weighted standard deviation.

Table 3.4.2.3 Fitting parameters obtained by fitting the density model to $V_\phi(m, T, p)$.‡

	α-Alanine	Proline
d_0 / ($cm^3 \cdot mol^{-1}$)	68.419 (0.342)	88.146 (0.449)
d_5	6.163 (0.562)	18.112 (0.093)
$d_6 \cdot 10^{-3}$ / (K)	-4.327 (0.423)	-15.886 (0.708)
$d_7 \cdot 10^{-6}$ / (K^2)	1.3735 (0.0571)	3.5752 (0.0965)
$b_1 \cdot 10^2$ / ($cm^3 \cdot kg \cdot mol^{-2}$)	59.0 (29.3)	-5.2 (13.7)
$b_2 \cdot 10$ / ($kg \cdot mol^{-1}$)	9.49 (1.16)	3.164 (0.509)
$c_1 \cdot 10$ / ($cm^3 \cdot kg^2 \cdot mol^{-3}$)	-5.15 (2.47)	—
$c_2 \cdot 10$ / ($kg^2 \cdot mol^{-2}$)	-2.666 (0.909)	—
σ	0.07	0.13

‡ The standard deviation for each parameter is given in parentheses; σ is the overall weighted standard deviation.

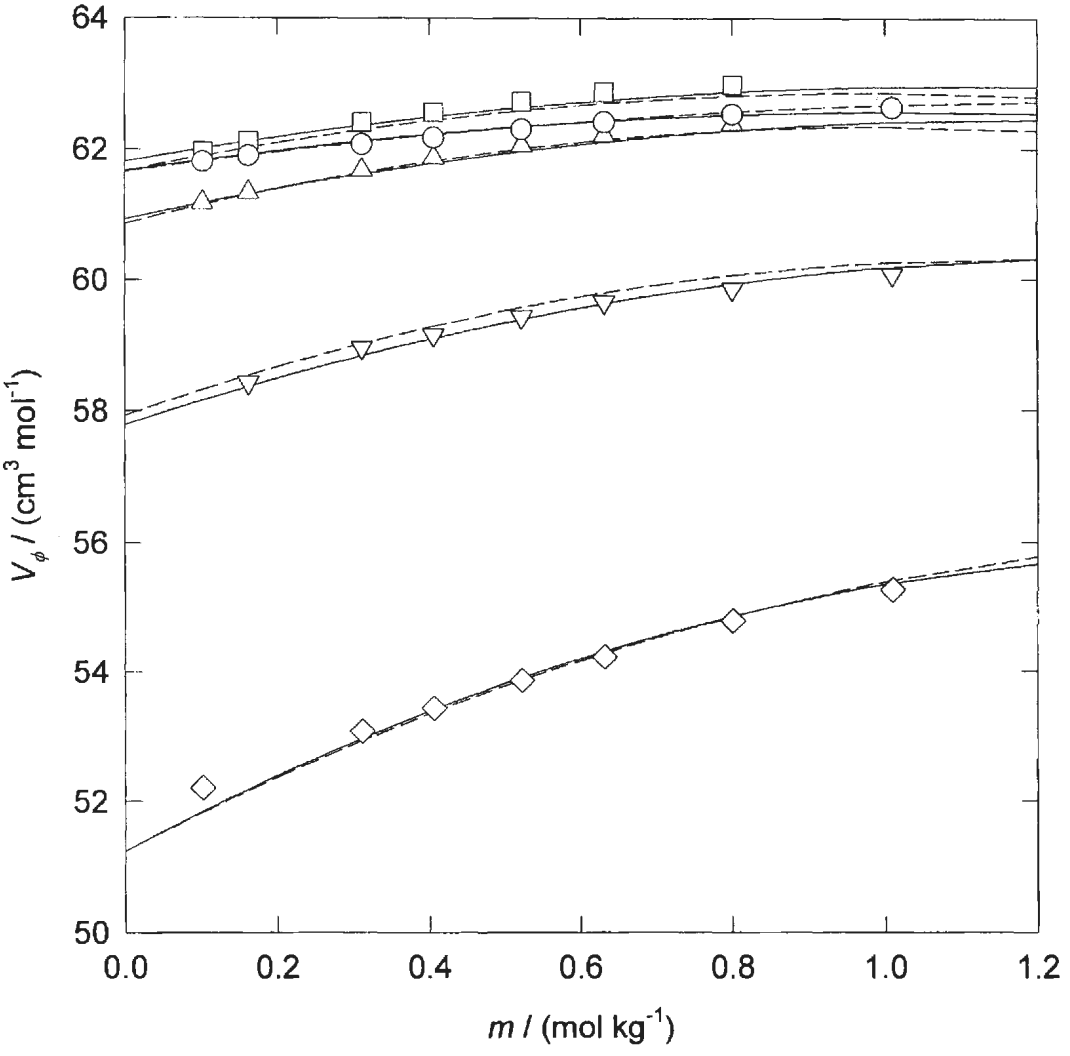

Figure 3.4.2.1 The apparent molar volumes V_ϕ of α-alanine from 333.2 K to 523.4 K at 10.05 MPa plotted against molality. Symbols are experimental results: □, 381.7 K; ○, 333.2 K; Δ, 422.4 K; ∇, 477.2 K; ◊, 523.4 K. Lines are fitted values: -----, revised HKF model; ——, density model.

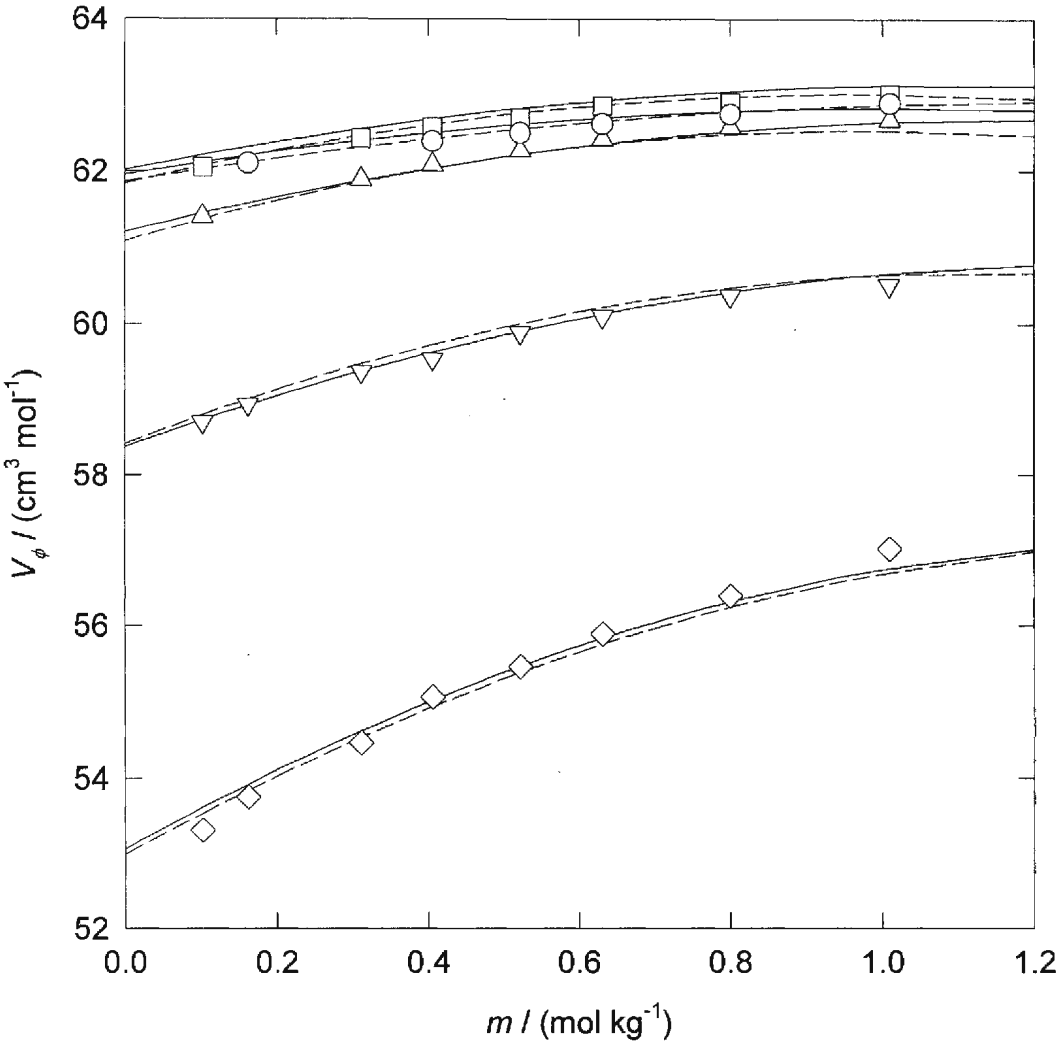

Figure 3.4.2.2 The apparent molar volumes V_ϕ of α-alanine from 334.6 K to 523.4 K at 19.96 MPa plotted against molality. Symbols are experimental results: □, 383.2 K; ○, 334.6 K; Δ, 423.5 K; ▽, 478.7 K; ◇, 523.4 K. Lines are fitted values: -----, revised HKF model; ———, density model.

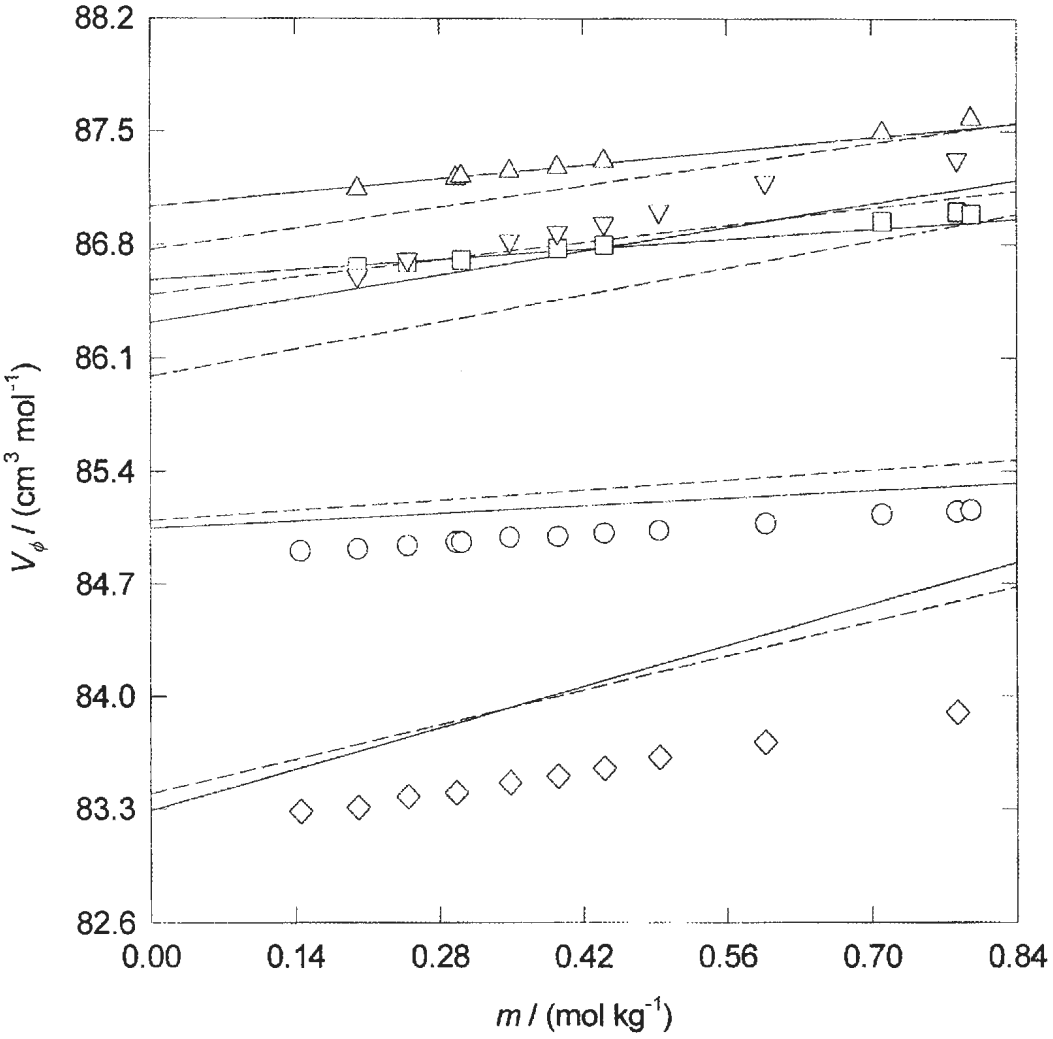

Figure 3.4.2.3 The apparent molar volumes V_ϕ of proline from 334.6 K to 524.1 K at 10.14 MPa plotted against molality. Symbols are experimental results: Δ, 423.7 K; ∇, 479.0 K; □, 383.4 K; ○, 334.6 K; ◇, 524.1 K. Lines are fitted values: -----, revised HKF model; ———, density model.

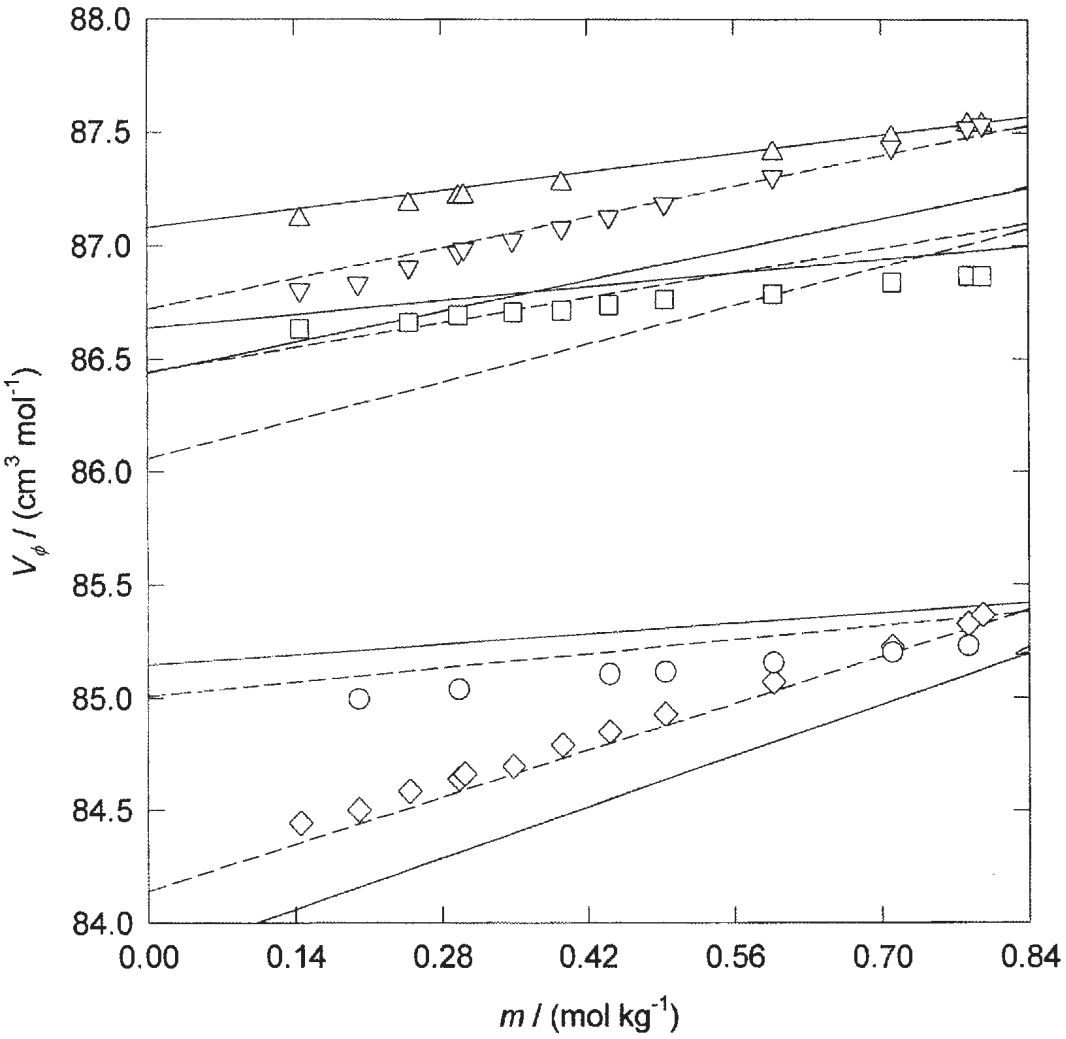

Figure 3.4.2.4 The apparent molar volumes V_ϕ of proline from 334.9 K to 524.0 K at 10.14 MPa plotted against molality. Symbols are experimental results: Δ, 423.9 K; ∇, 479.1 K; □, 383.7 K; ○, 334.9 K; ◊, 524.0 K. Lines are fitted values: -----, revised HKF model; ———, density model.

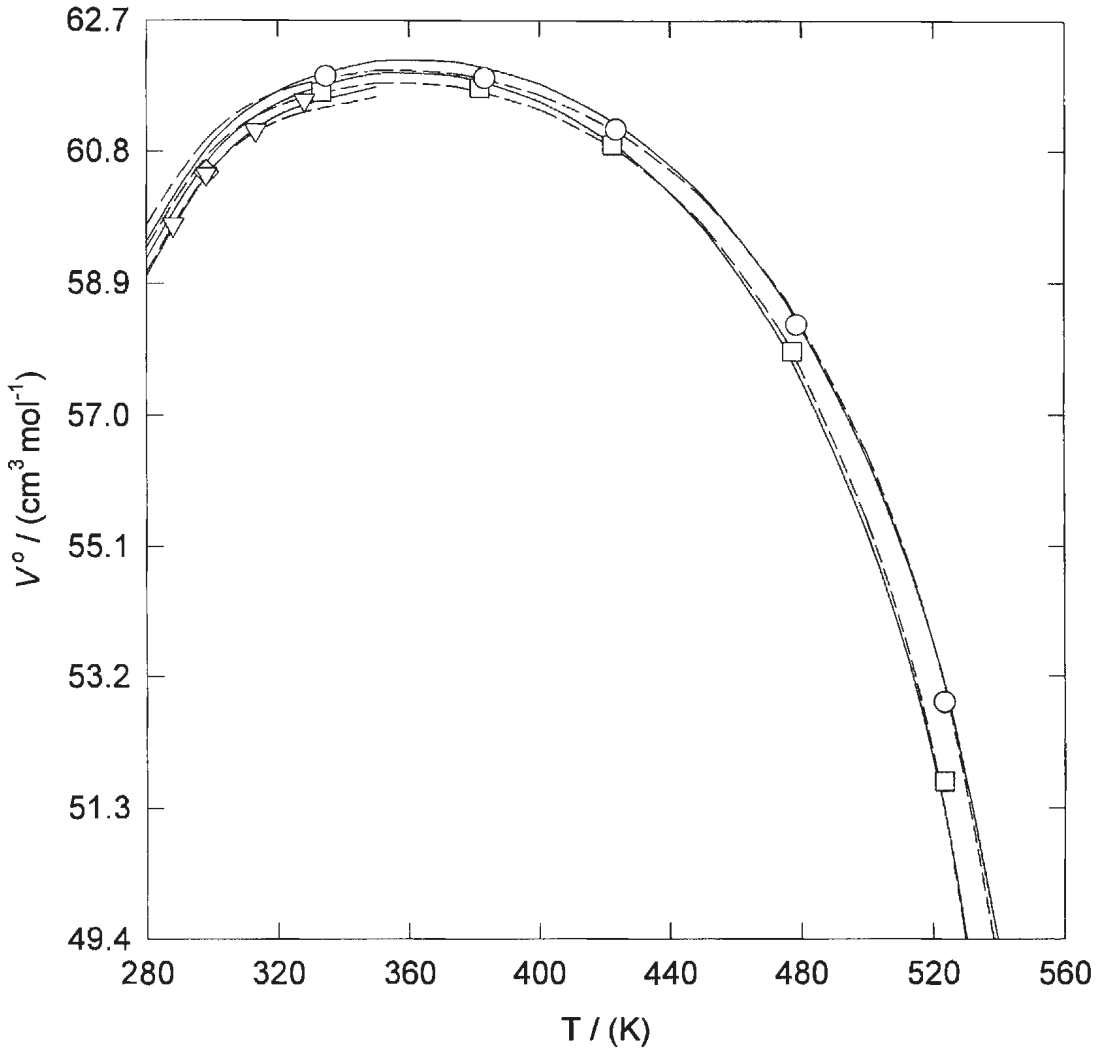

Figure 3.4.2.5 The standard partial molar volumes $V°$ of α-alanine from 0.1 MPa to 19.96 MPa plotted against temperature. Symbols are the fitted isotherms obtained in Section 3.2: ○, 19.96 MPa; □, 10.05 MPa; ◇, 0.1 MPa. ▽, 0.1 MPa represents the standard partial molar volumes obtained by Hakin *et al.* (1994). Lines are fitted values: -----, revised HKF model; ——, density model.

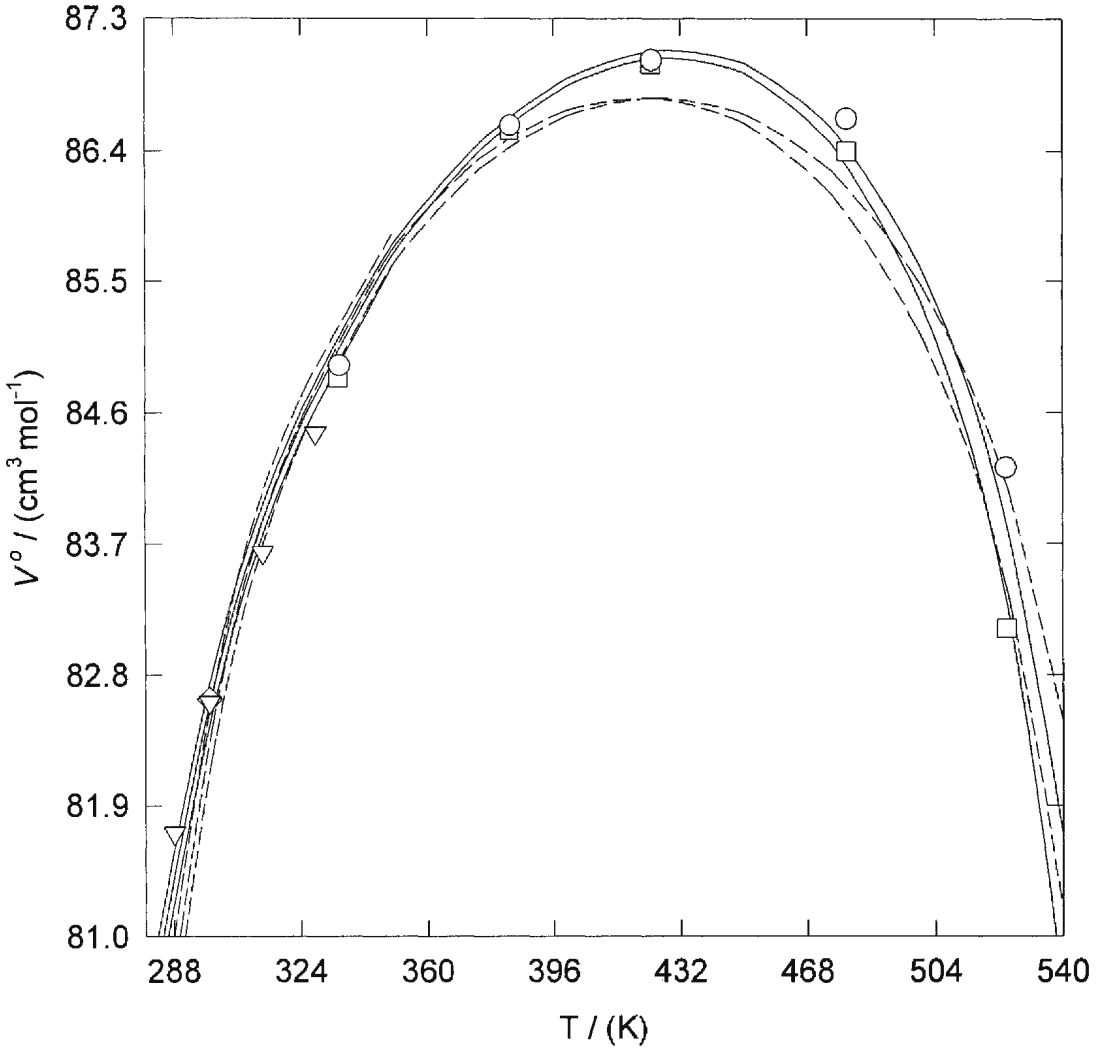

Figure 3.4.2.6 The standard partial molar volumes $V°$ of proline from 0.1 MPa to 20.20 MPa plotted against temperature. Symbols are the fitted isotherms obtained in Section 3.2: ○, 20.20 MPa; □, 10.14 MPa; ◇, 0.1 MPa. ▽, 0.1 MPa represents the standard partial molar volumes obtained by Hakin *et al.* (1997). Lines are fitted values: -----, revised HKF model; ——, density model.

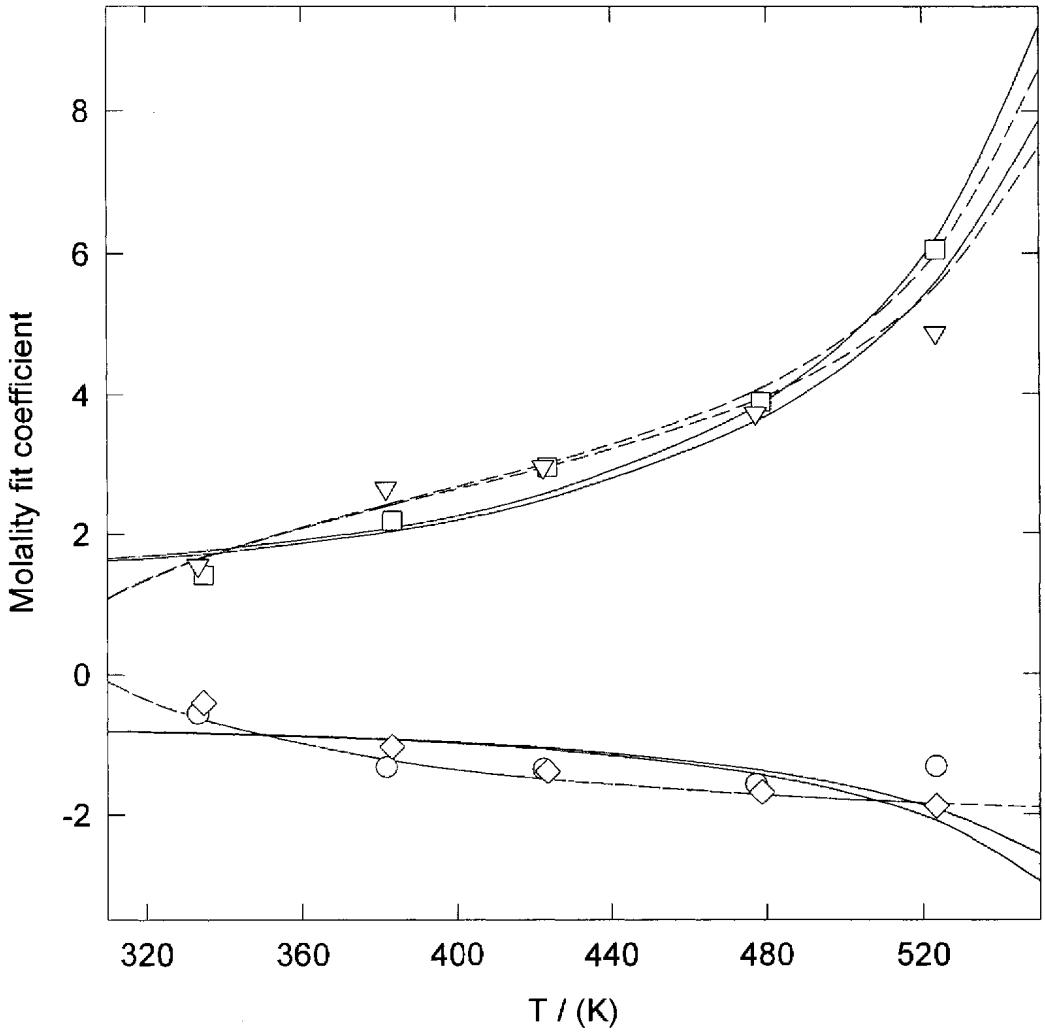

Figure 3.4.2.7 The molality fit coefficients *b* and *c* of α-alanine at 10.05 MPa and 19.96 MPa plotted against temperature. Symbols are the isothermal molality fit coefficients obtained in Section 3.2: ∇, b, 10.05 MPa; ○, c, 10.05 MPa; □, b, 19.96 MPa; ◇, c, 19.96 MPa. Lines are fitted values: -----, revised HKF model; ———, density model.

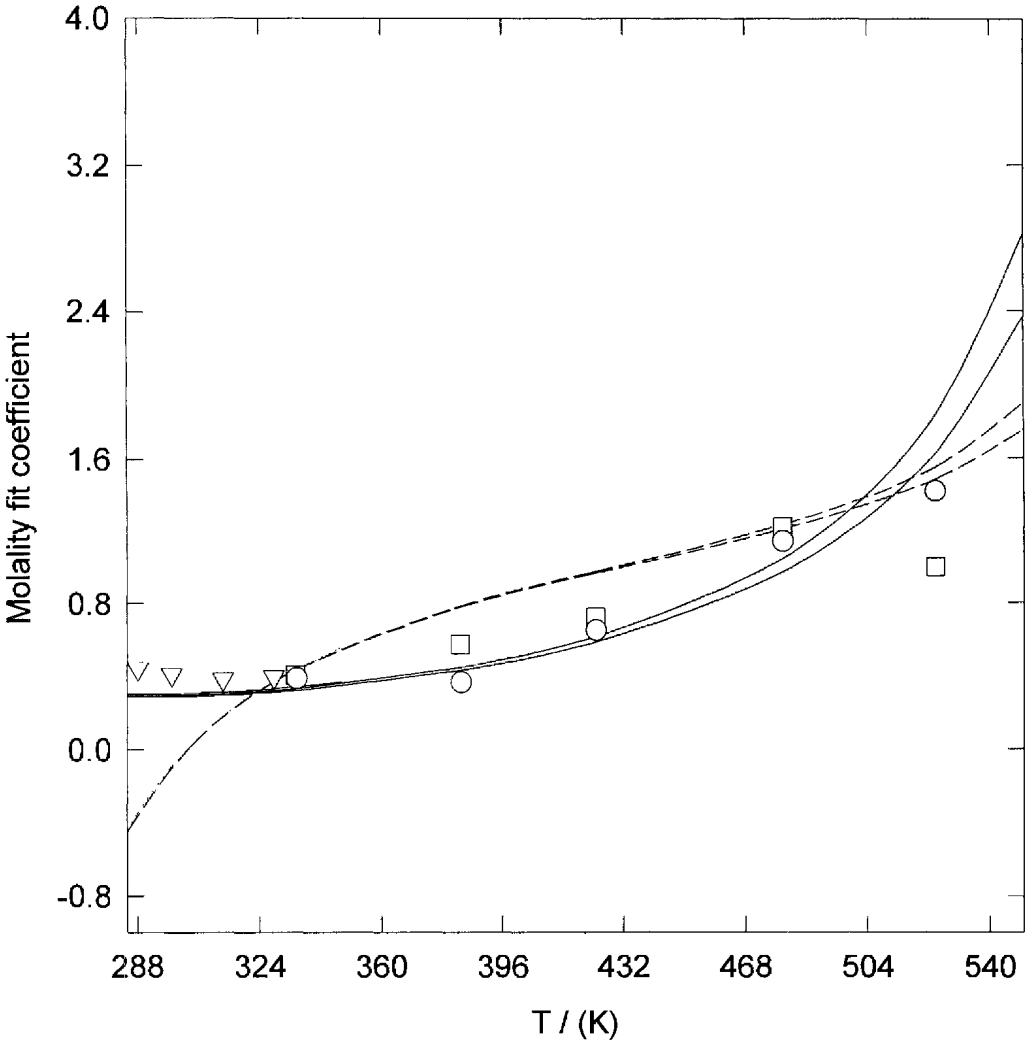

Figure 3.4.2.8 The molality fit coefficient *b* of proline from 0.1 MPa to 20.20 MPa plotted against temperature. Symbols are the isothermal molality fit coefficients obtained in Section 3.2: ○, 20.20 MPa; □, 10.14 MPa. ▽, 0.1 MPa represents the isothermal molality fit coefficients obtained using the V_ϕ data of Hakin *et al.* (1997). Lines are fitted values: -----, revised HKF model; ——, density model.

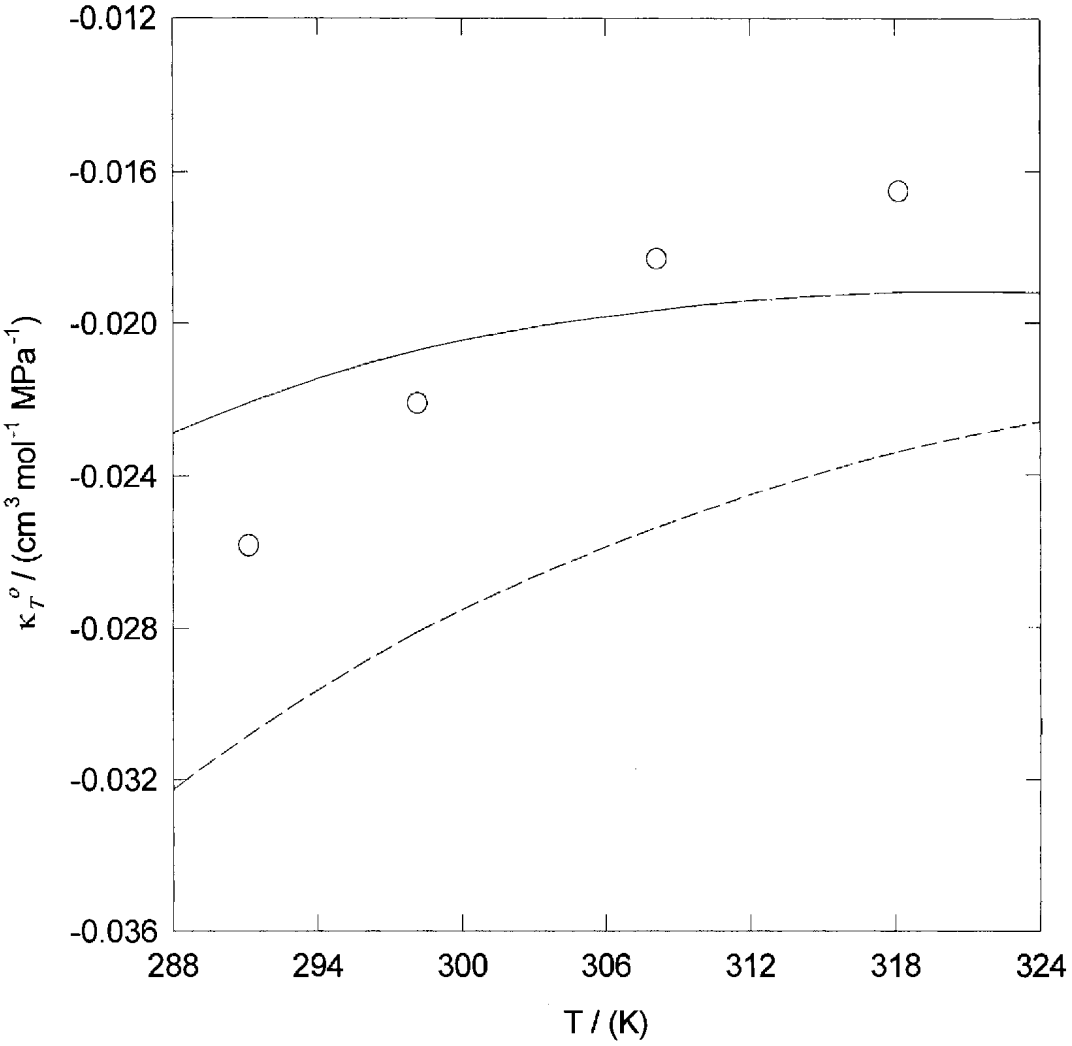

Figure 3.4.2.9 The standard partial molar isothermal compressibilities κ_T° of α-alanine at 0.1 MPa plotted against temperature. Symbols are the experimental values of Chalikian *et al.* (1994). Lines are fitted values: -----, revised HKF model; ——, density model.

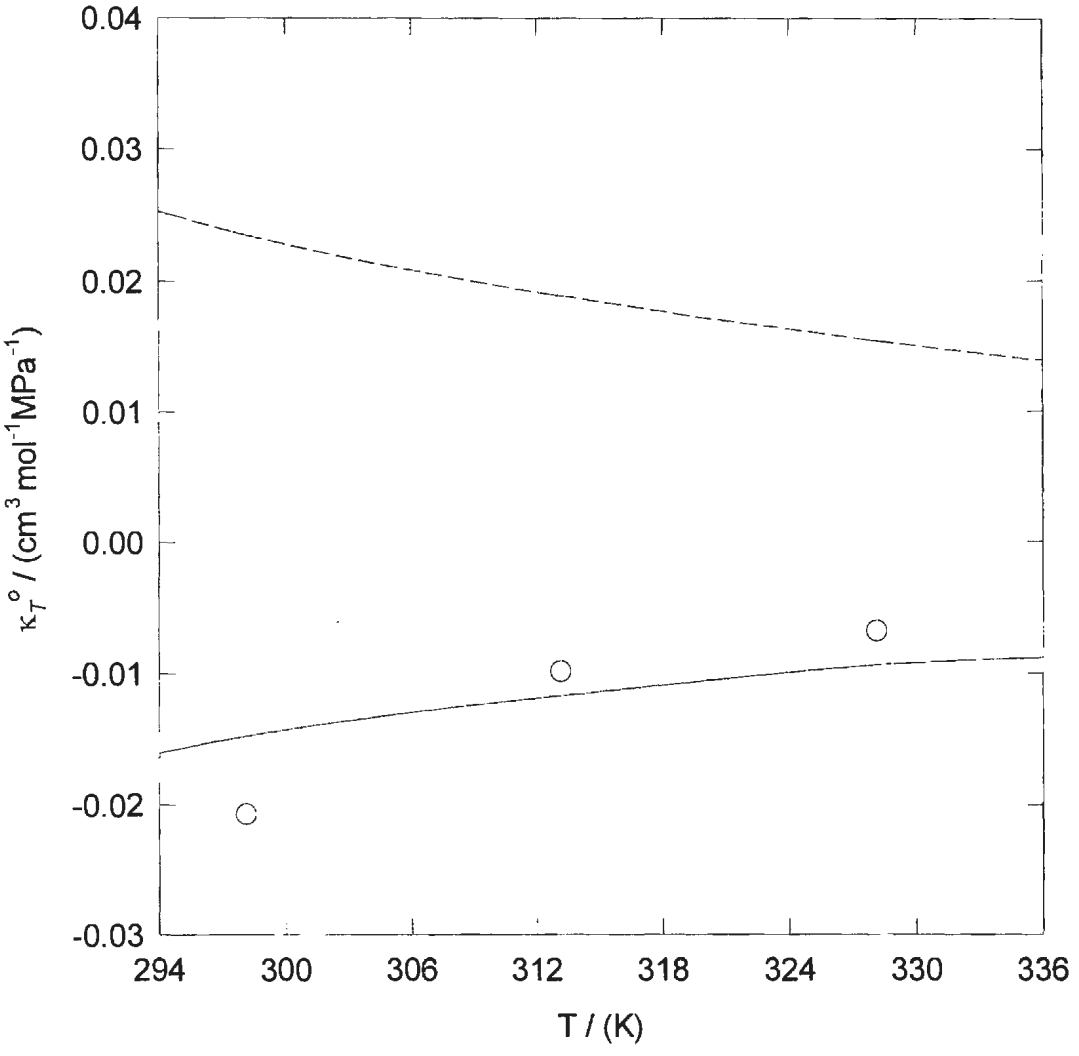

Figure 3.4.2.10 The standard partial molar isothermal compressibilities κ_T° of proline at 0.1 MPa plotted against temperature. Symbols are the experimental values of Kharakoz (1991). Lines are fitted values: -----, revised HKF model; ——, density model.

3.4.3 Representation of $V^{\circ}(T, p)$ and $C_p^{\circ}(T, p)$ by the Extended Density Model.

As seen in Section 3.4.2, the density model reproduced the thermodynamic properties (V_{ϕ}, V°, $\kappa_T{}^{\circ}$) of aqueous α-alanine and proline better than the revised HKF model. However, neither model was able to fit the entire set of experimental data for $V_{\phi}(m, T, p)$ and $C_{p,\phi}(m, T, p)$ in a self consistent manner. Therefore, we chose to use an extended version of the density model to represent the temperature and pressure dependencies of the standard partial molar volumes reported in Section 3.2 and the standard partial molar heat capacities reported in Section 3.3. This model takes the form:

$$\Delta G^{o} = p(A_o + A_1 T_R) + 2.303R\left[\left(\frac{A_2}{T_R^2} + \frac{A_3}{T_R} + A_4 + A_5 T_R + A_6 T_R^2\right)\log\rho_o\right]$$

$$+ 2.303R\left(\frac{A_7}{T_R^4} + \frac{A_8}{T_R^3} + \frac{A_9}{T_R^2} + \frac{A_{10}}{T_R} + A_{11} + A_{12} T_R + A_{13} T_R^2 + A_{14} T_R^3\right) \qquad (3.4.3.1)$$

$$\Delta V^{o} = (A_o + A_1 T_R) + R\beta_w\left(\frac{A_2}{T_R^2} + \frac{A_3}{T_R} + A_4 + A_5 T_R + A_6 T_R^2\right) \qquad (3.4.3.2)$$

$$\Delta\kappa_T{}^{o} = -R\left(\frac{A_2}{T_R^2} + \frac{A_3}{T_R} + A_4 + A_5 T_R + A_6 T_R^2\right)\left(\frac{\partial\beta_w}{\partial p}\right)_T \qquad (3.4.3.3)$$

$$\Delta C_p{}^{o} = -2.303R\left[\left(\frac{6A_2}{T_R^3} + \frac{2A_3}{T_R^2} + 2A_6 T_R\right)\log\rho_o\right] + R\alpha_w\left(\frac{-4A_2}{T_R^2} + \frac{-2A_3}{T_R} + 2A_5 T_R + 4A_6 T_R^2\right)$$

$$-2.303R\left(\frac{20A_7}{T_R^5}+\frac{12A_8}{T_R^4}+\frac{6A_9}{T_R^3}+\frac{2A_{10}}{T_R^2}+2A_{13}T_R+6A_{14}T_R^2\right)$$

$$+R\left(\frac{A_2}{T_R}+A_3+A_4T_R+A_5T_R^2+A_6T_R^3\right)\left(\frac{\partial\alpha_w}{\partial T}\right)_p \qquad (3.4.3.4)$$

where β_w and α_w are the compressibility and the expansitivity coefficient of water, respectively, and $T_R=(T/373.15\ \mathrm{K})$. T was replaced with T_R in equations (3.4.3.1), (3.4.3.2), (3.4.3.3), and (3.4.3.4) to increase the accuracy of the fitting parameters obtained. The terms A_0 to A_{14} are fitting parameters. Not all fitting parameters were used for a given amino acid. The additional terms, absent in the original model, increase the flexibility of the fitting functions thereby improving their ability to reproduce the temperature and pressure dependence of the experimental data. An expression for the standard partial molar compressibility was included in this model to ensure a good fit to the small pressure dependence observed in the standard partial molar volumes reported in Section 3.2. The statistical standard deviation associated with equations (3.4.3.2), (3.4.3.3), and (3.4.3.4) can be estimated from equations (3.4.3.2a), (3.4.3.3a), and (3.4.3.4a), respectively:

$$(\sigma_{\Delta V^\circ})^2=(\sigma_{A_0})^2+(\sigma_{A_1})^2T_R^2$$

$$+R^2\beta_w^2\left[\frac{(\sigma_{A_2})^2}{T_R^4}+\frac{(\sigma_{A_3})^2}{T_R^2}+(\sigma_{A_4})^2+(\sigma_{A_5})^2T_R^2+(\sigma_{A_6})^2T_R^4\right] \qquad (3.4.3.2a)$$

$$(\sigma_{\Delta\kappa_T{}^o})^2 = R^2\left[\frac{(\sigma_{A_2})^2}{T_R^{\,4}} + \frac{(\sigma_{A_3})^2}{T_R^{\,2}} + (\sigma_{A_4})^2 + (\sigma_{A_5})^2 T_R^{\,2} + (\sigma_{A_6})^2 T_R^{\,4}\right]\left(\frac{\partial\beta_w}{\partial p}\right)_T^2 \qquad (3.4.3.3a)$$

$$(\sigma_{\Delta C_p{}^o})^2 = (2.303\,R\log\rho_o)^2\left[\frac{36(\sigma_{A_2})^2}{T_R^{\,6}} + \frac{4(\sigma_{A_3})^2}{T_R^{\,4}} + 4(\sigma_{A_6})^2 T_R^{\,2}\right]$$

$$+(R\alpha_w)^2\left[\frac{16(\sigma_{A_2})^2}{T_R^{\,4}} + \frac{4(\sigma_{A_3})^2}{T_R^{\,2}} + 4(\sigma_{A_5})^2 T_R^{\,2} + 16(\sigma_{A_6})^2 T_R^{\,4}\right]$$

$$+(2.303\,R)^2\left[\frac{400(\sigma_{A_7})^2}{T_R^{\,10}} + \frac{144(\sigma_{A_8})^2}{T_R^{\,8}} + \frac{36(\sigma_{A_9})^2}{T_R^{\,6}} + \frac{4(\sigma_{A_{10}})^2}{T_R^{\,4}}\right]$$

$$+(2.303\,R)^2\left[4(\sigma_{A_{13}})^2 T_R^{\,2} + 36(\sigma_{A_{14}})^2 T_R^{\,4}\right]$$

$$+R^2\left[\frac{(\sigma_{A_2})^2}{T_R^{\,2}} + (\sigma_{A_3})^2 + (\sigma_{A_4})^2 T_R^{\,2} + (\sigma_{A_5})^2 T_R^{\,4} + (\sigma_{A_6})^2 T_R^{\,6}\right]\left(\frac{\partial\alpha_w}{\partial T}\right)_p^2 \qquad (3.4.3.4a)$$

To increase the temperature range and accuracy of the fitting parameters obtained using the extended density model, a number of complementary data sets were included, along with the values of V° and C_p° measured in this work. The literature sources used for complementary data are listed in Table 3.4.3.1. The fitting parameters obtained using the extended density model are tabulated in Table 3.4.3.2, along with their standard deviations. The standard partial molar volumes V° obtained using the extended density model are plotted in Figures 3.4.3.1, 3.4.3.4, 3.4.3.7, and 3.4.3.10 for α-alanine, β-alanine, glycine, and proline, respectively. The standard partial molar heat capacities C_p° obtained using the extended

density model are plotted in Figures 3.4.3.2, 3.4.3.5, 3.4.3.8, and 3.4.3.11 for α-alanine, β-alanine, glycine, and proline, respectively. The standard partial molar isothermal compressibilities κ_T° obtained using the extended density model are plotted in Figures 3.4.3.3, 3.4.3.6, 3.4.3.9, and 3.4.3.12 for α-alanine, β-alanine, glycine, and proline, respectively.

Table 3.4.3.1 Literature data sources used in fitting parameters for the extended density model.

Data	V°	C_p°	$\kappa_T{}^\circ$
α-alanine	Hakin *et al.* (1994)†	Hakin *et al.* (1994)†	Kikuchi *et al.* (1995)‡ Kharakoz (1991)‡
β-alanine	Chalikian *et al.* (1993)†	Gucker and Allen (1942)†	Chalikian *et al.* (1993)‡
glycine	Hakin *et al.* (1994)†	Hakin *et al.* (1994)†	Kikuchi *et al.* (1995)‡ Kharakoz (1991)‡
proline	Hakin *et al.* (1997)†	Hakin *et al.* (1997)†	Kikuchi *et al.* (1995)‡ Kharakoz (1991)‡

† Values are listed in Table 1.6.3.1. ‡ Values are listed in Table 1.6.3.2.

Table 3.4.3.2 Fitting parameters obtained by fitting the extended density model to $V^{\circ}(T, p)$ and $C_p^{\circ}(T, p)$.[‡]

	α-Alanine	β-Alanine	Glycine	Proline
A_0 / ($cm^3 \cdot mol^{-1}$)	61.89 (1.98)	56.216 (0.913)	30.77 (1.94)	71.98 (2.96)
A_1 / ($cm^3 \cdot mol^{-1}$)	6.97 (3.12)	14.25 (1.20)	21.92 (2.89)	18.48 (4.47)
A_2 / (K)	—	—	—	-117.1 (39.7)
A_3 / (K)	-42.34 (3.70)	-33.486 (0.826)	-27.37 (3.26)	467 (152)
A_4 / (K)	-1763 (293)	-1652 (337)	1904 (612)	-1376 (407)
A_5 / (K)	-18.8 (12.8)	-990 (187)	-4034 (287)	—
A_6 / (K)	—	—	—	-118.9 (27.8)
A_7	—	—	—	-1.959 (0.783)
A_8	—	—	—	8.49 (3.04)
A_9	2.0820 (0.0937)	1.2190 (0.0540)	5.322 (0.230)	—
A_{10}	-8.691 (0.439)	-3.828 (0.253)	-24.03 (1.18)	-58.9 (18.3)
A_{13}	-2.987 (0.203)	-4.398 (0.140)	15.17 (1.22)	57.2 (18.0)
A_{14}	—	—	-3.737 (0.259)	-12.08 (3.36)
σ	1.28	0.18	0.94	1.77

[‡]The standard deviation for each parameter is given in parentheses; σ is the overall weighted standard deviation.

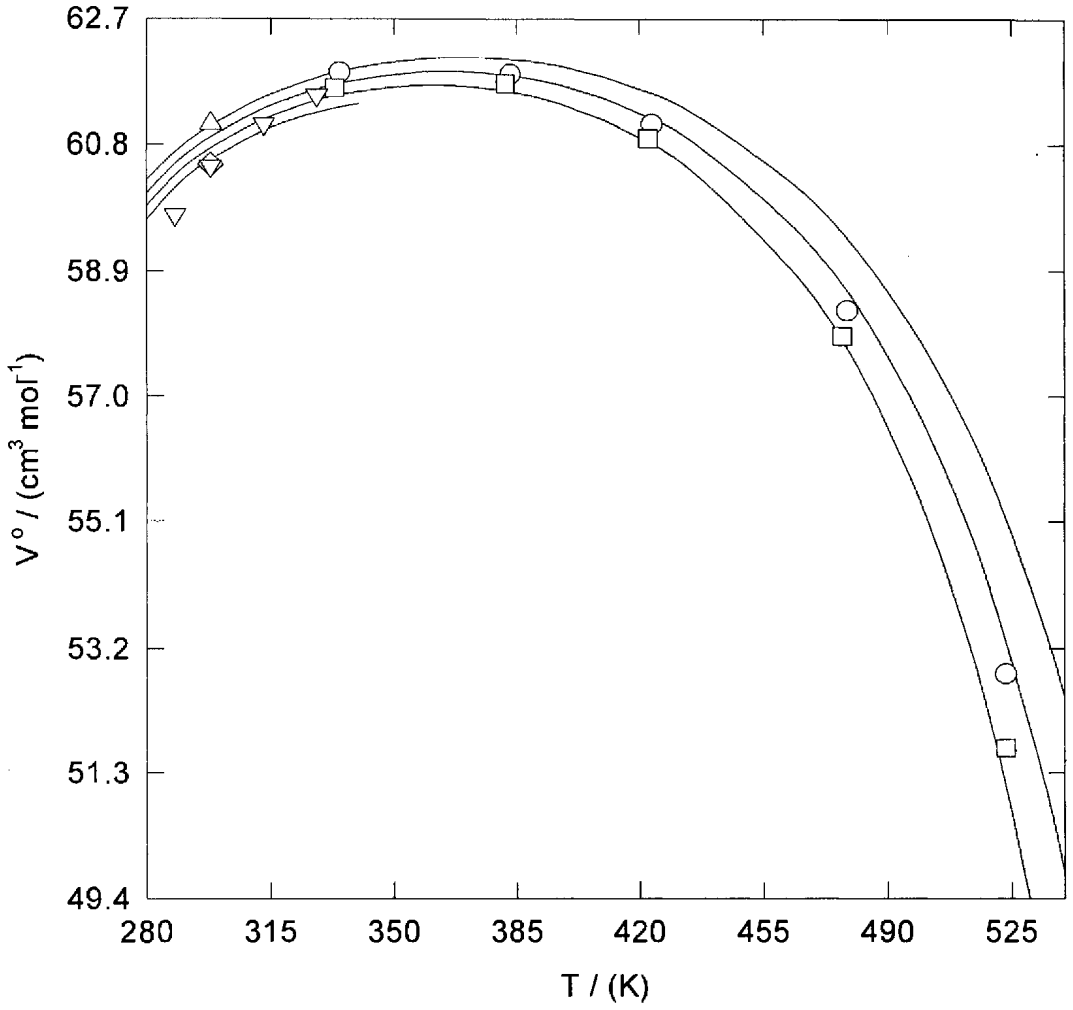

Figure 3.4.3.1 The standard partial molar volumes $V°$ of α-alanine from 0.1 MPa to 30.77 MPa plotted against temperature. Symbols are the fitted isotherms obtained in Section 3.2: Δ, 30.77 MPa; ○, 19.96 MPa; □, 10.05 MPa; ◇, 0.1 MPa. ▽, 0.1 MPa represents the standard partial molar volumes obtained by Hakin *et al.* (1994). Lines are fitted values obtained using the extended density model.

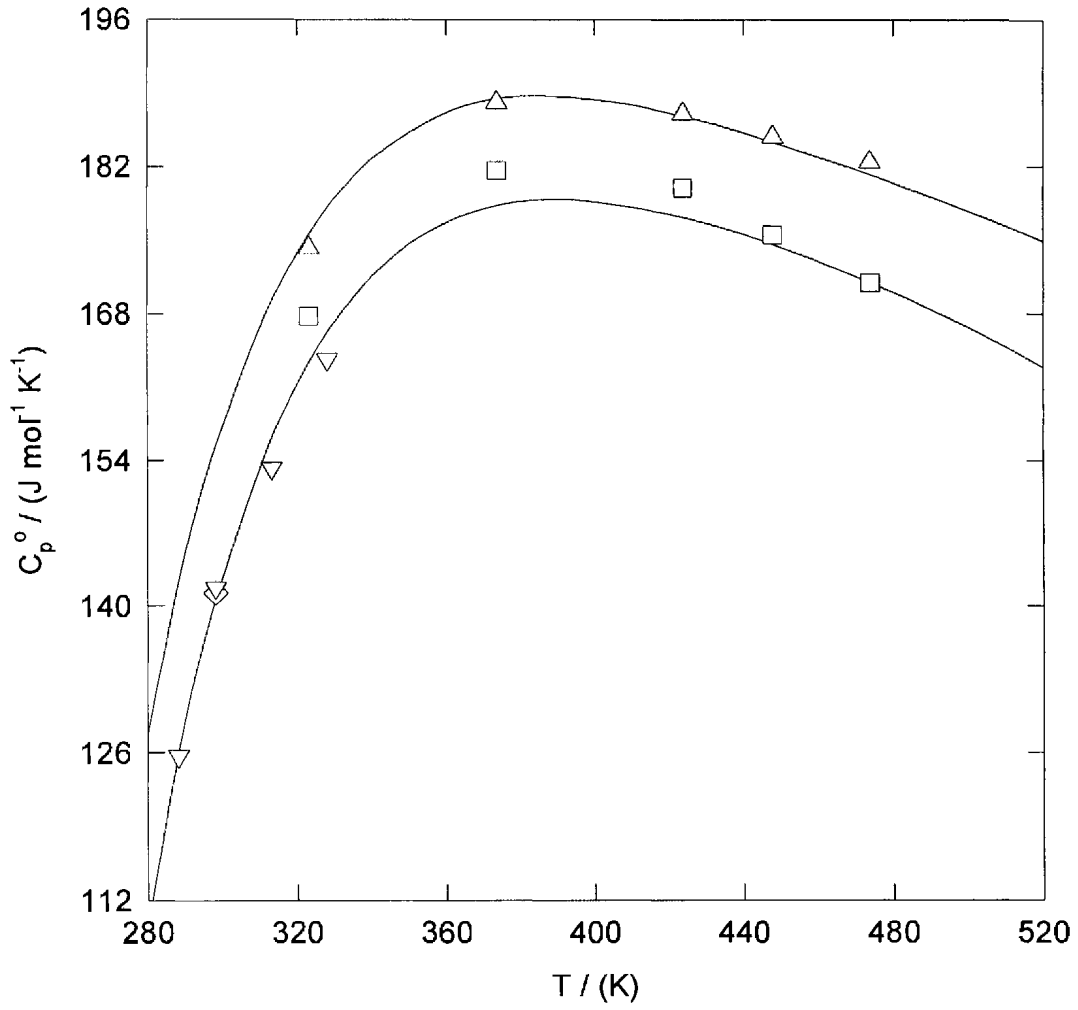

Figure 3.4.3.2 The standard partial molar heat capacities C_p° of α-alanine from 0.1 MPa to 30.15 MPa plotted against temperature. Symbols are the fitted isotherms obtained in Section 3.3: Δ, 30.15 MPa; □, steam saturation pressure; ◇, 0.1 MPa. ∇, 0.1 MPa represents the standard partial molar volumes obtained by Hakin *et al.* (1994). Lines are fitted values obtained using the extended density model.

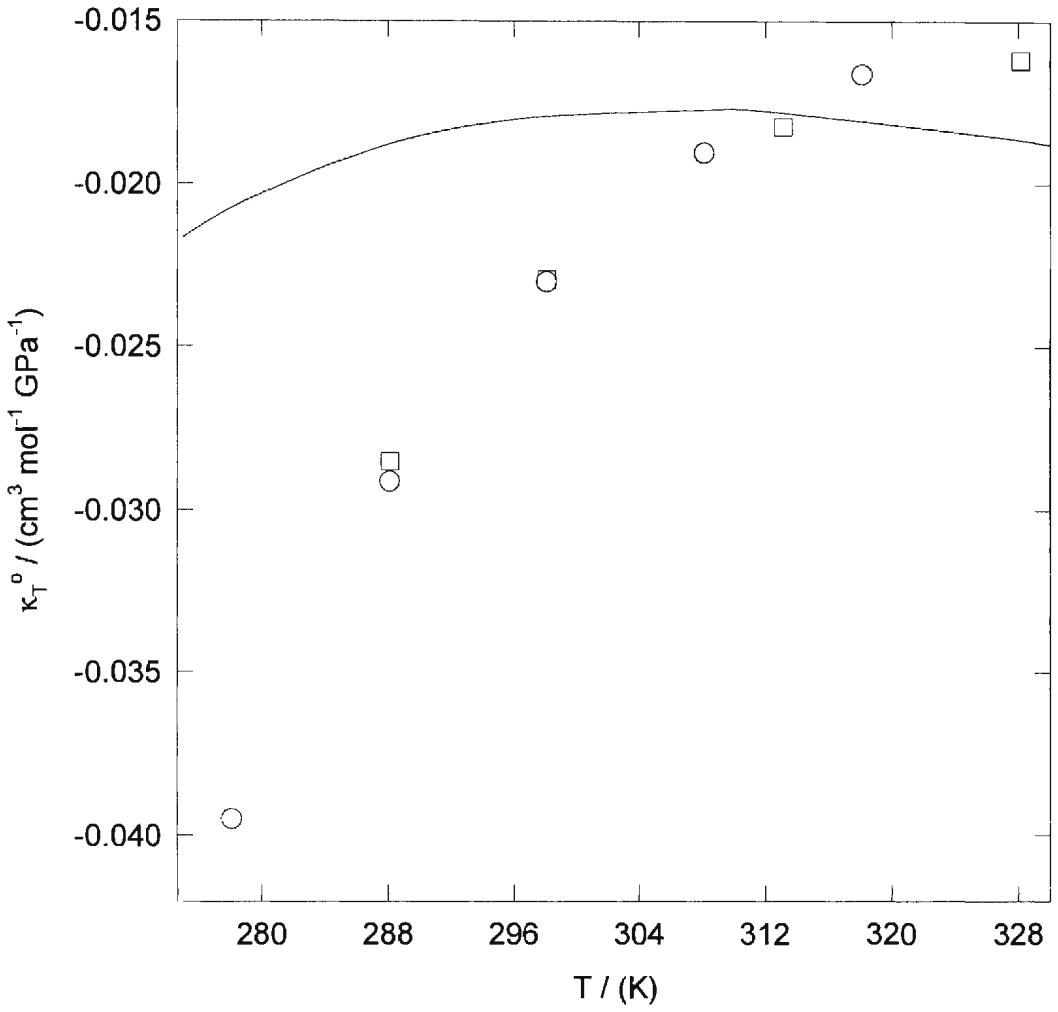

Figure 3.4.3.3 The standard partial molar isothermal compressibilities κ_T° of α-alanine at 0.1 MPa plotted against temperature. Symbols are the experimental values of: ○, Kikuchi *et al.* (1995); □, Kharakoz (1991). The line represents the fitted values obtained using the extended density model.

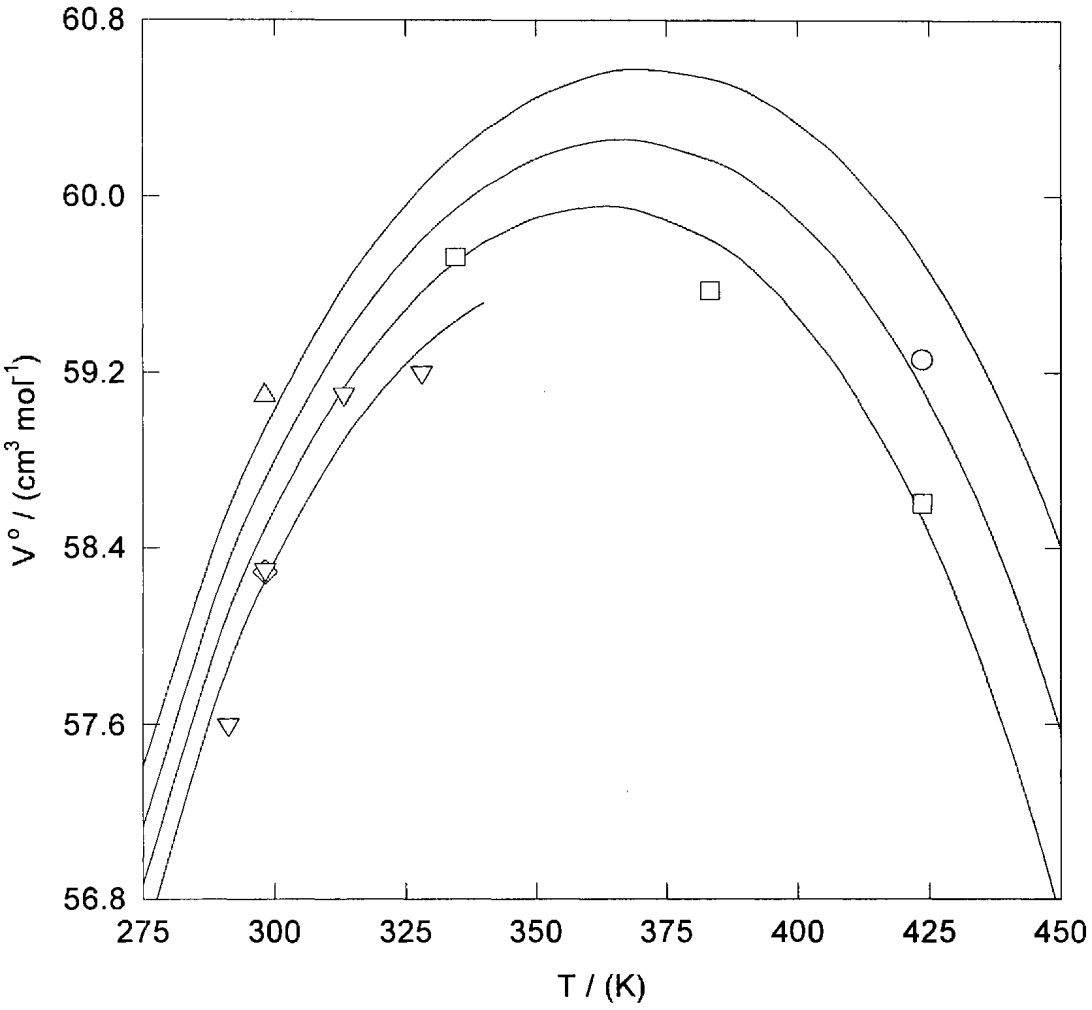

Figure 3.4.3.4 The standard partial molar volumes $V°$ of β-alanine from 0.1 MPa to 30.90 MPa plotted against temperature. Symbols are the fitted isotherms obtained in Section 3.2: Δ, 30.90 MPa; ○, 20.53 MPa; □, 10.32 MPa; ◇, 0.1 MPa. ▽, 0.1 MPa represents the standard partial molar volumes obtained by Chalikian *et al.* (1993). Lines are fitted values obtained using the extended density model.

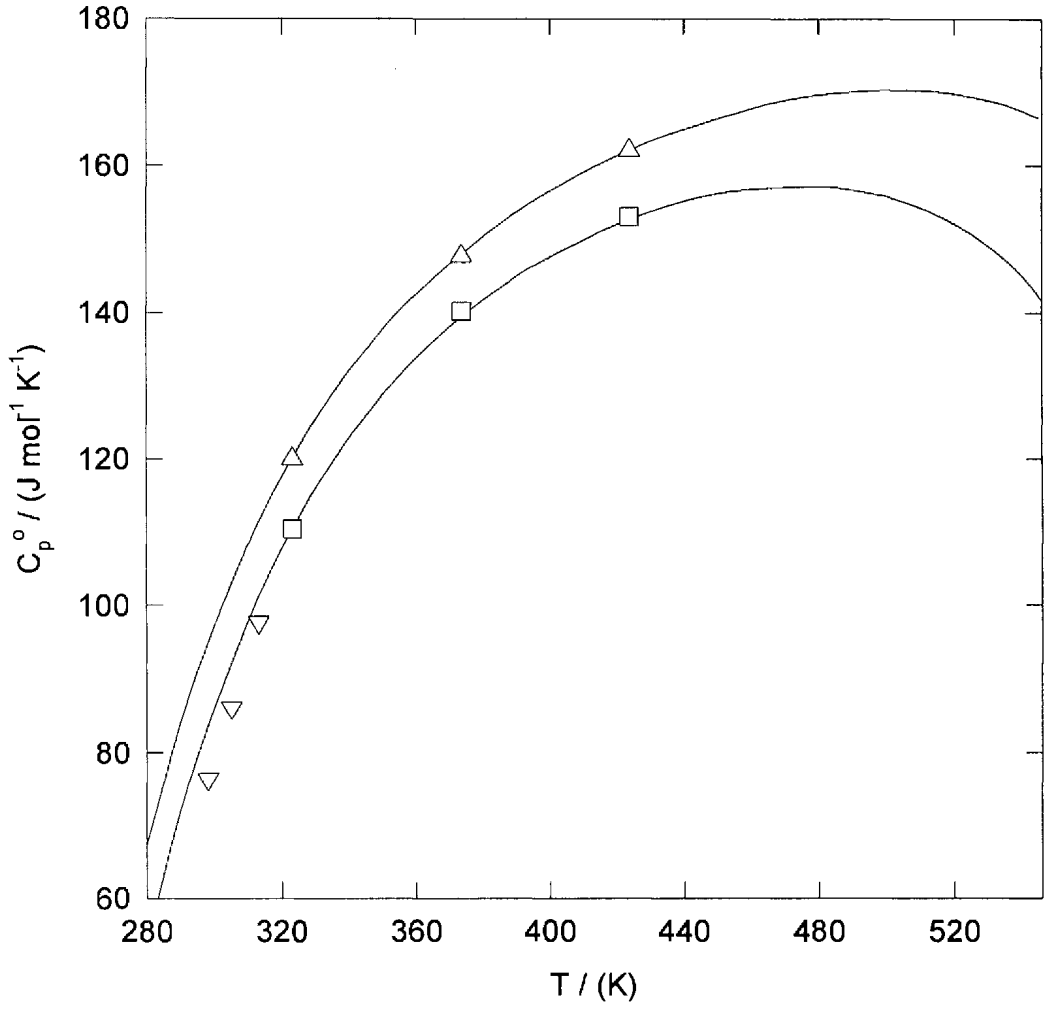

Figure 3.4.3.5 The standard partial molar heat capacities C_p° of β-alanine from 0.1 MPa to 30.11 MPa plotted against temperature. Symbols are the fitted isotherms obtained in Section 3.3: Δ, 30.11 MPa; □, steam saturation pressure. ∇, 0.1 MPa represents the standard partial molar volumes obtained by Gucker and Allen (1942). Lines are fitted values obtained using the extended density model.

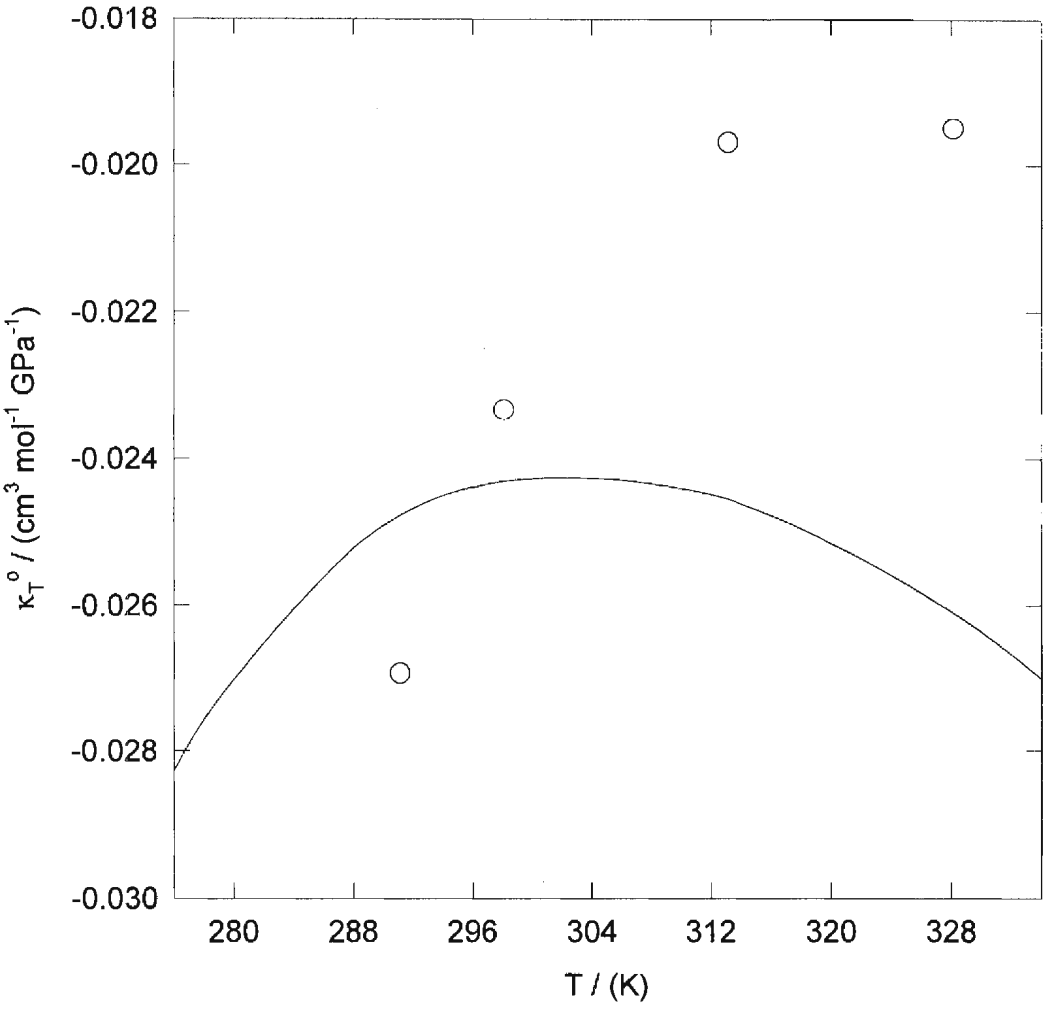

Figure 3.4.3.6 The standard partial molar isothermal compressibilities κ_T° of β-alanine at 0.1 MPa plotted against temperature. Symbols are the experimental values of: ○, Chalikian *et al.* (1993). The line represents the fitted values obtained using the extended density model.

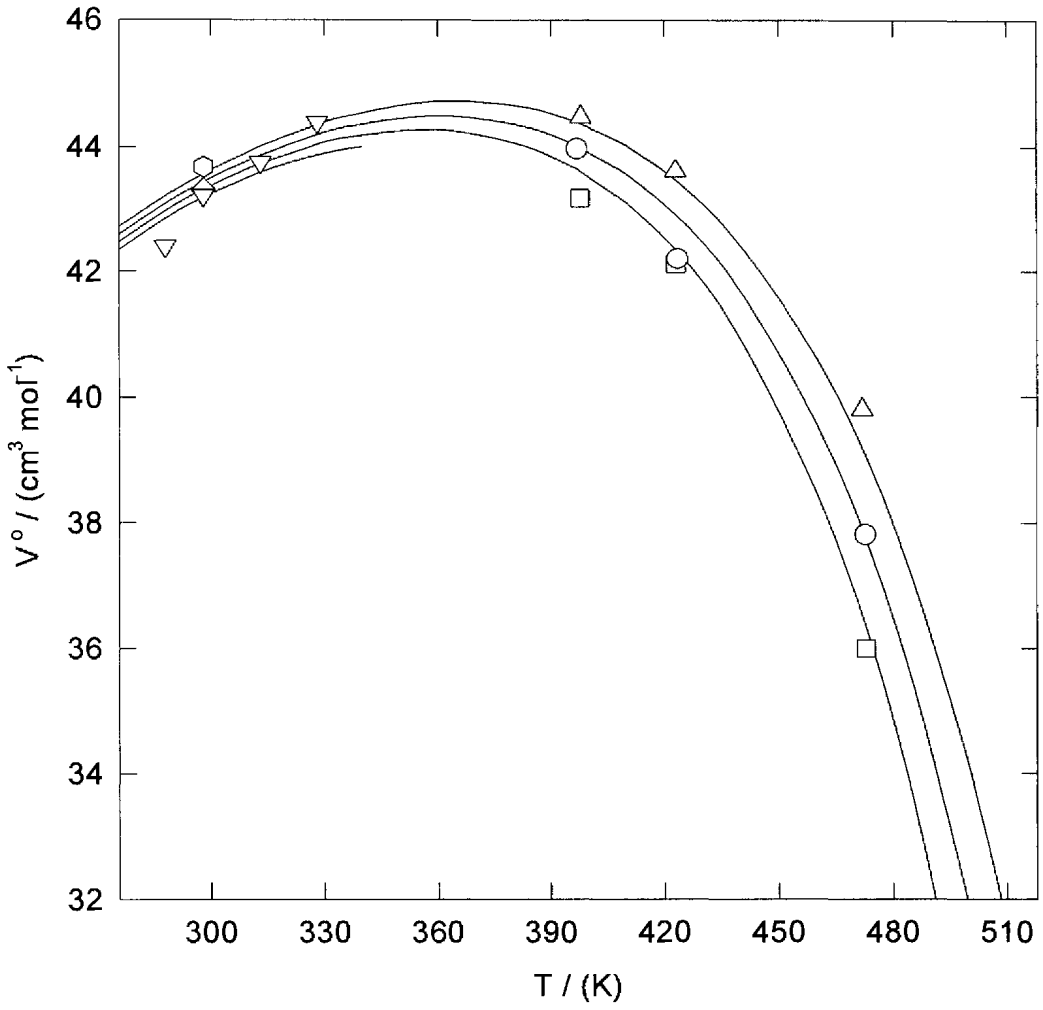

Figure 3.4.3.7 The standard partial molar volumes $V°$ of glycine from 0.1 MPa to 30.83 MPa plotted against temperature. Symbols are the fitted isotherms obtained in Section 3.2: [], 30.83 MPa; ◇, 0.1 MPa. Δ, 30.21 MPa; ○, 20.00 MPa; □, 10.00 MPa represent the standard partial molar volumes obtained by Hakin *et al.* (1998). ▽, 0.1 MPa represents the standard partial molar volumes obtained by Hakin *et al.* (1994). Lines are fitted values obtained using the extended density model.

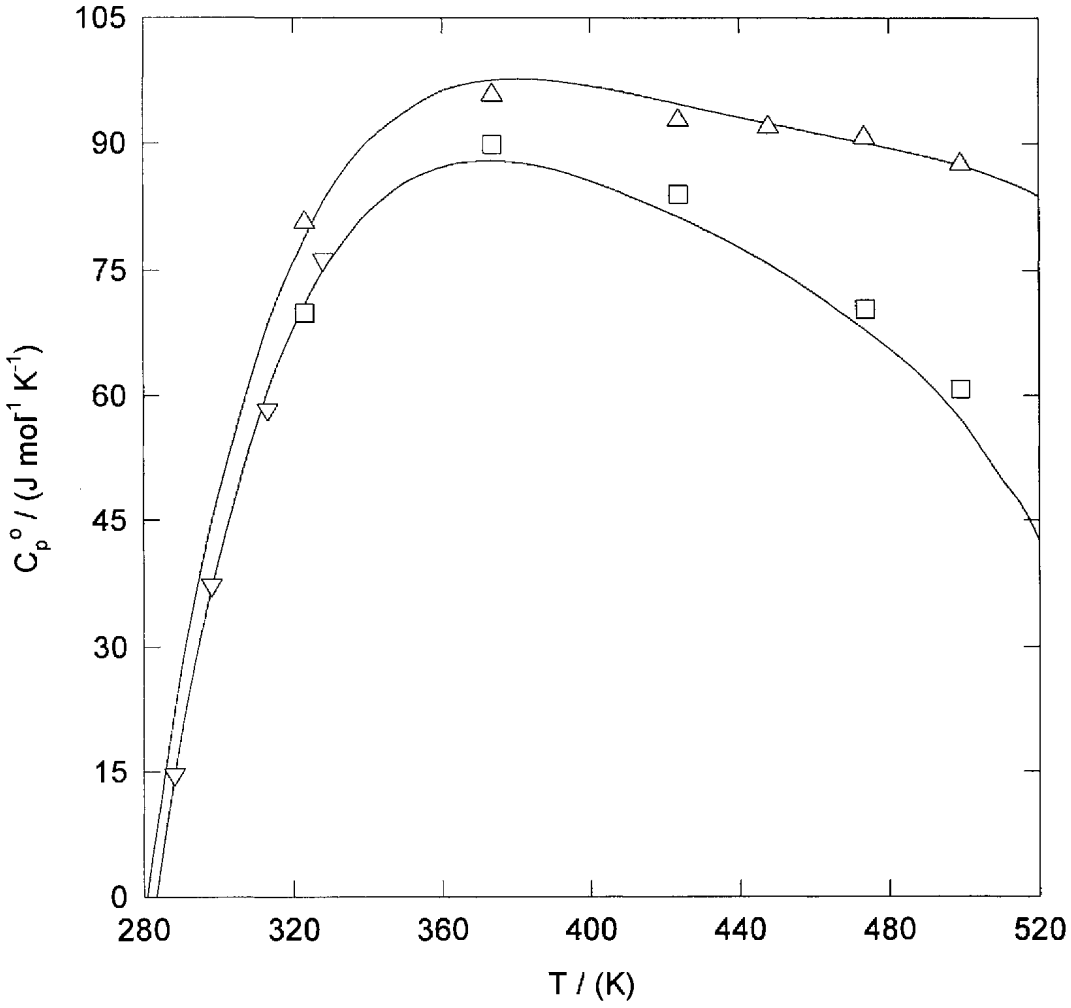

Figure 3.4.3.8 The standard partial molar heat capacities C_p° of glycine from 0.1 MPa to 30.24 MPa plotted against temperature. Symbols are the fitted isotherms obtained in Section 3.3: Δ, 30.24 MPa; □, steam saturation pressure. ∇, 0.1 MPa represents the standard partial molar volumes obtained by Hakin *et al.* (1994). Lines are fitted values obtained using the extended density model.

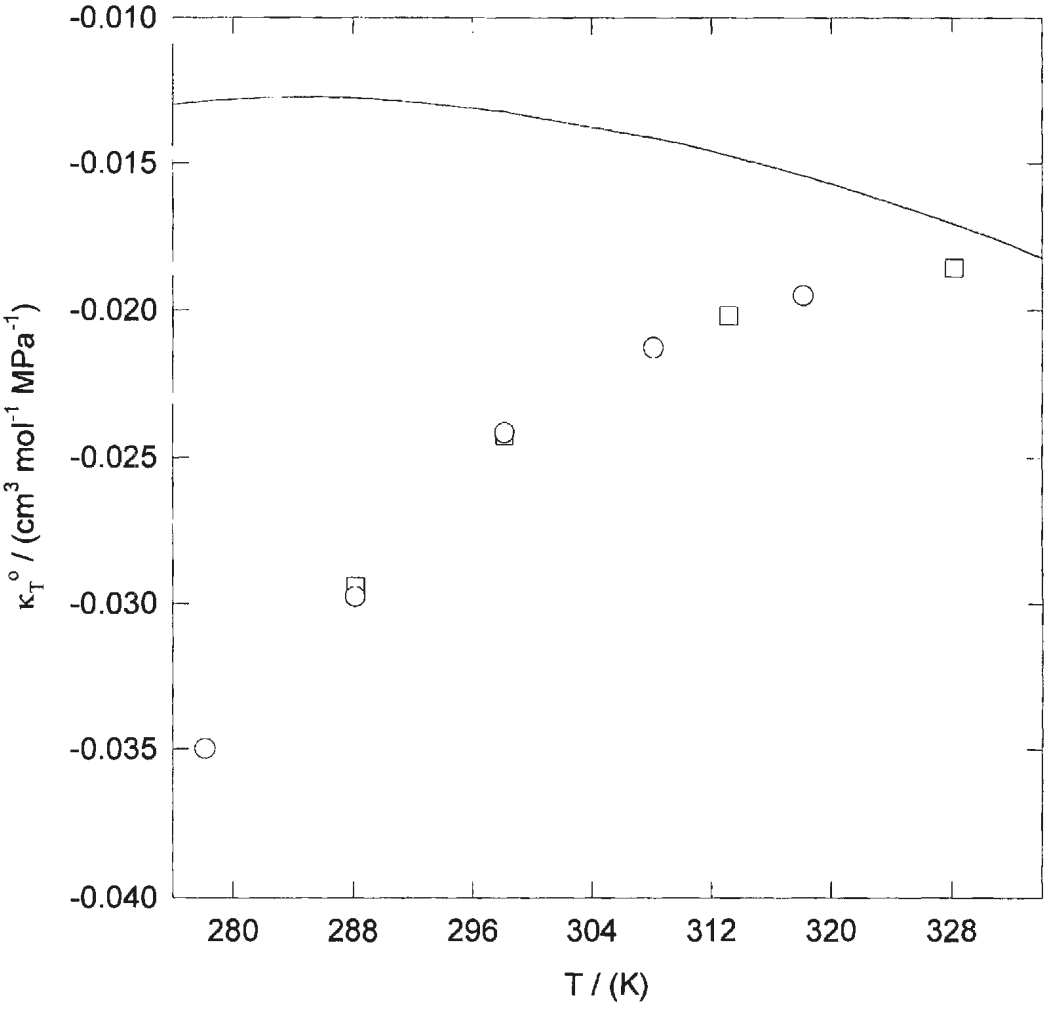

Figure 3.4.3.9 The standard partial molar isothermal compressibilities κ_T° of glycine at 0.1 MPa plotted against temperature. Symbols are the experimental values of: ○, Kikuchi *et al.* (1995); □, Kharakoz (1991). The line represents the fitted values obtained using the extended density model.

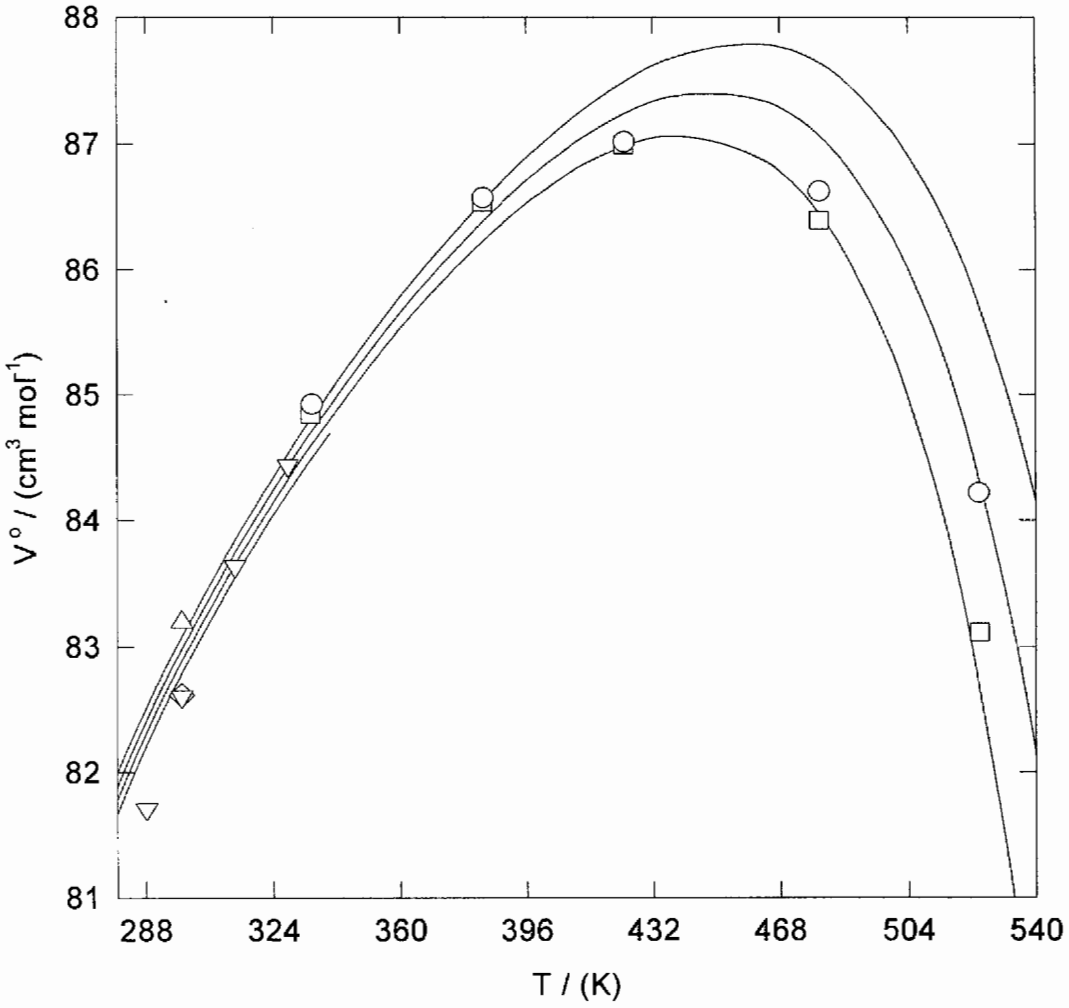

Figure 3.4.3.10 The standard partial molar volumes $V°$ of proline from 0.1 MPa to 30.80 MPa plotted against temperature. Symbols are the fitted isotherms obtained in Section 3.2: Δ, 30.80 MPa; ○, 20.20 MPa; □, 10.14 MPa; ◇, 0.1 MPa. ▽, 0.1 MPa represents the standard partial molar volumes obtained by Hakin *et al.* (1997). Lines are fitted values obtained using the extended density model.

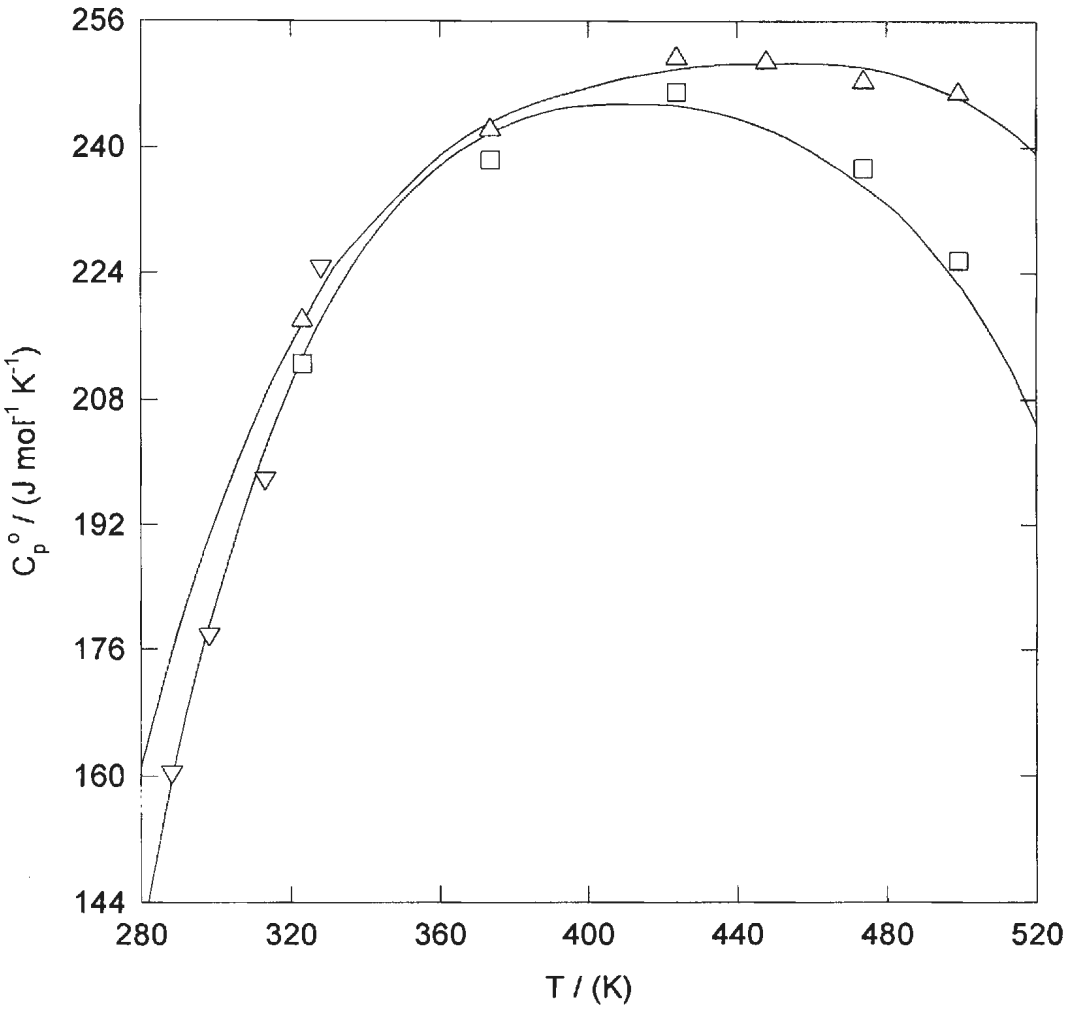

Figure 3.4.3.11 The standard partial molar heat capacities C_p° of proline from 0.1 MPa to 30.31 MPa plotted against temperature. Symbols are the fitted isotherms obtained in Section 3.3: Δ, 30.31 MPa; □, steam saturation pressure. ∇, 0.1 MPa represents the standard partial molar volumes obtained by Hakin *et al.* (1997). Lines are fitted values obtained using the extended density model.

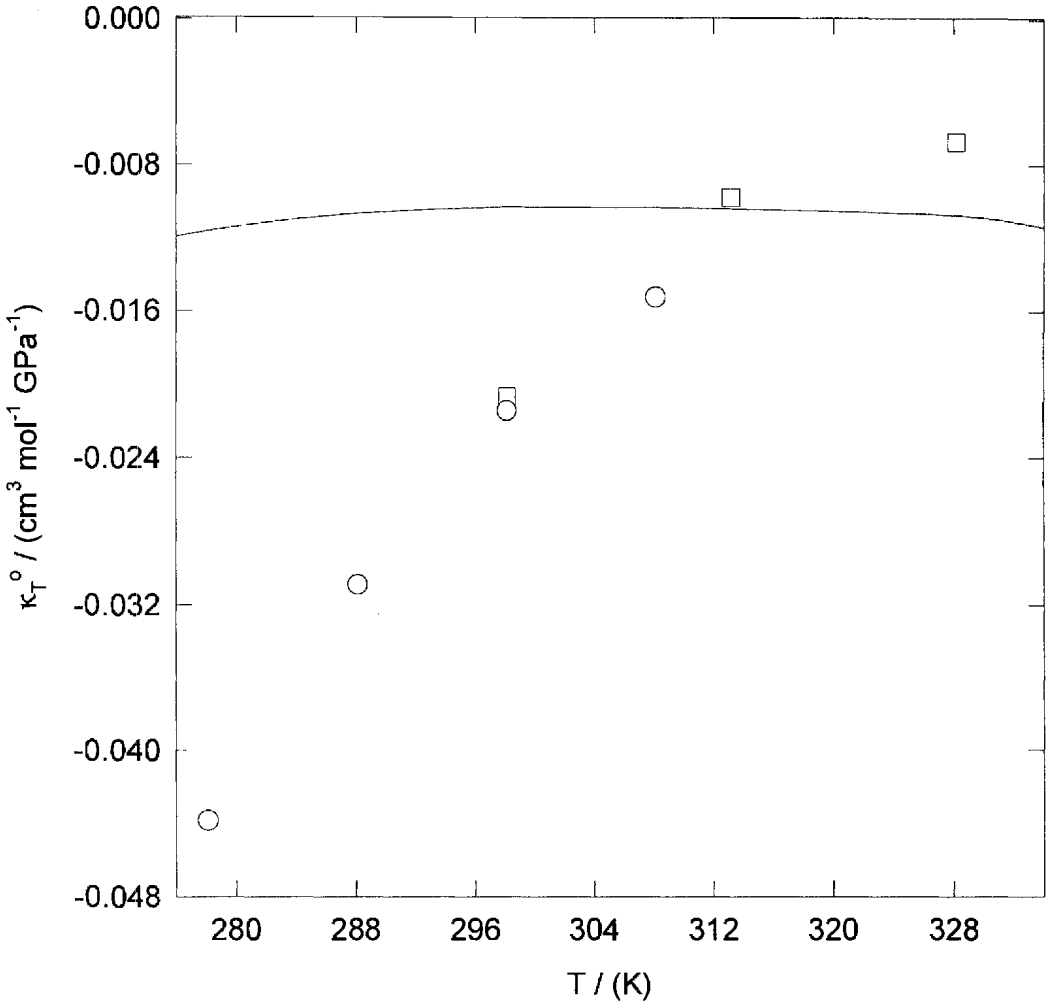

Figure 3.4.3.12 The standard partial molar isothermal compressibilities κ_T° of proline at 0.1 MPa plotted against temperature. Symbols are the experimental values of: ○, Kikuchi *et al.* (1995); □, Kharakoz (1991). The line represents the fitted values obtained using the extended density model.

3.5 Equilibrium Constants from UV-Visible Spectroscopy.

Figures 3.5.1 to 3.5.8 illustrate the temperature-dependent UV-visible absorption spectra obtained for acridine and β-naphthoic acid in the triflic acid solution, the sodium hydroxide solution, the α-alanine buffer solution, and the phosphoric acid or acetic acid buffer solution, respectively. The UV-visible absorption spectrum for each solution is the average of five spectra taken over a period of about 15 minutes. At each temperature a UV-visible absorption spectrum was obtained for each solution in the absence of colorimetric indicators. The absorbance due to these blank solutions remained small throughout the range of wavelengths under consideration and was subtracted from the absorbance measured for the solutions containing the colorimetric indicators.

Figures 3.5.1, 3.5.2, 3.5.5, and 3.5.6 show the spectra of acridine and β-naphthoic acid in triflic acid and in sodium hydroxide. Triflate is a non-oxidizing anion that is stable at elevated temperatures (Fabes and Swaddle, 1975). The relative concentrations of AcH^+ / Ac and NapH / Nap were obtained by fitting linear combinations of the "pure" spectra to the spectra of the buffer solutions over the wavelength range 310 - 450 nm (1 nm intervals) for the acridine solutions and 270 - 400 nm (1 nm intervals) for the β-naphthoic acid solutions. Because they contained different concentrations of indicator, the UV-visible absorption spectra of the buffer solutions in Figures 3.5.3, 3.5.4, 3.5.7, and 3.5.8 were normalised to either an acridine molality of $3.49 \cdot 10^{-5}$ mol·kg^{-1} or a β-naphthoic acid molality of $1.43 \cdot 10^{-4}$ mol·kg^{-1}. Equation (1.5.3.5) was fitted to the UV-visible absorption spectra measured for

acridine in the phosphoric acid buffer solution and in the α-alanine buffer solution ($HA^{\pm}$ / H_2A^+) to obtain the molality of protonated AcH^+ and deprotonated acridine Ac in each buffer solution. The molal ratio of AcH^+ to Ac at each temperature and pressure is given in Table 3.5.1. Equation (1.5.3.5) was also fitted to the spectra measured for β-naphthoic acid in the acetic acid buffer solution and in the α-alanine buffer solution ($HA^{\pm}$ / A^-) to obtain the molality of protonated NapH and deprotonated β-naphthoic acid Nap^- in each buffer solution. Table 3.5.1 lists the molal ratio of NapH to Nap^- at each temperature and pressure.

The values of $K_{Indicator}$ for acridine and β-naphthoic acid were calculated using equations (1.5.3.6) and (1.5.3.7), respectively. At each temperature and pressure the value of K_1 for α-alanine was determined from equation (2.7.2.5) and the known molalities of H_2A^+, $HA^{\pm}$, AcH^+, and Ac. The value of K_{a1} for phosphoric acid was determined from equation (2.7.2.11) and the known molalities of $H_2PO_4^-$, H_3PO_4, AcH^+, and Ac. The value of K_2 for α-alanine was determined from equation (2.7.2.6) and the known molalities of A^-, $HA^{\pm}$, NapH, and Nap^-. The value of K_a for acetic acid was determined from equation (2.7.2.12) and the known molalities of CH_3COO^-, CH_3COOH, NapH, and Nap^-. The values of pK_1, pK_{a1}, pK_2, and pK_a obtained at each temperature and pressure are given in Table 3.5.1. Error limits were taken to be one standard deviation of the least squares fit of equation (1.5.3.5) to the spectroscopic data. Figure 3.5.9 compares the experimentally determined values of pK_{a1} to those obtained from Mesmer and Baes (1974). Figure 3.5.10 compares the experimentally determined values of pK_a to those obtained by Mesmer *et al.* (1989).

As illustrated in Figure 3.5.9 the experimentally determined values of pK_{a1} for phosphoric acid are 0.7 to 0.4 units lower than those determined by Mesmer and Baes (1974) which contain uncertainties of no more than ± 0.04 units. The accuracy of our values increases with increasing temperature since the values of pK_{a1} from Mesmer and Baes (1974) move into the indicator range of acridine at temperatures above 425 K (Figure 2.7.3). As illustrated in Figure 3.5.10 the experimental values of pK_a for acetic acid are 0.3 to 0.9 units higher than those determined by Mesmer *et al.* (1989) which contain uncertainties of no more than ± 0.04 units. The accuracy of the experimental values decreases with increasing temperature. This is unexpected since the values of pK_a as obtained by Mesmer *et al.* (1989) lie within the indicator range of β-naphthoic acid over the entire temperature range under consideration, as shown in Figure 2.7.4.

Johnston and Chlistunoff (1998) used acridine to determine pH in a titration of hydrochloric acid with aqueous sodium chloride (653 K, 34 MPa). The experimentally determined values of pH were found to be within 0.4 units of the predicted values. Similarly, β-naphthoic acid was used to determine pH in a titration of ammonia with acetic acid (623K, 34 MPa). The experimental values of pH were found to be within 0.5 units of the predicted values. Johnston and Chlistunoff (1998) consider the uncertainty in the colorimetric technique to be in the range ± 0.3 - 0.5 log units. Therefore, the differences between the experimentally determined values and the literature values of pK_{a1} for phosphoric acid and pK_a for acetic acid are only slightly higher than those expected from this technique.

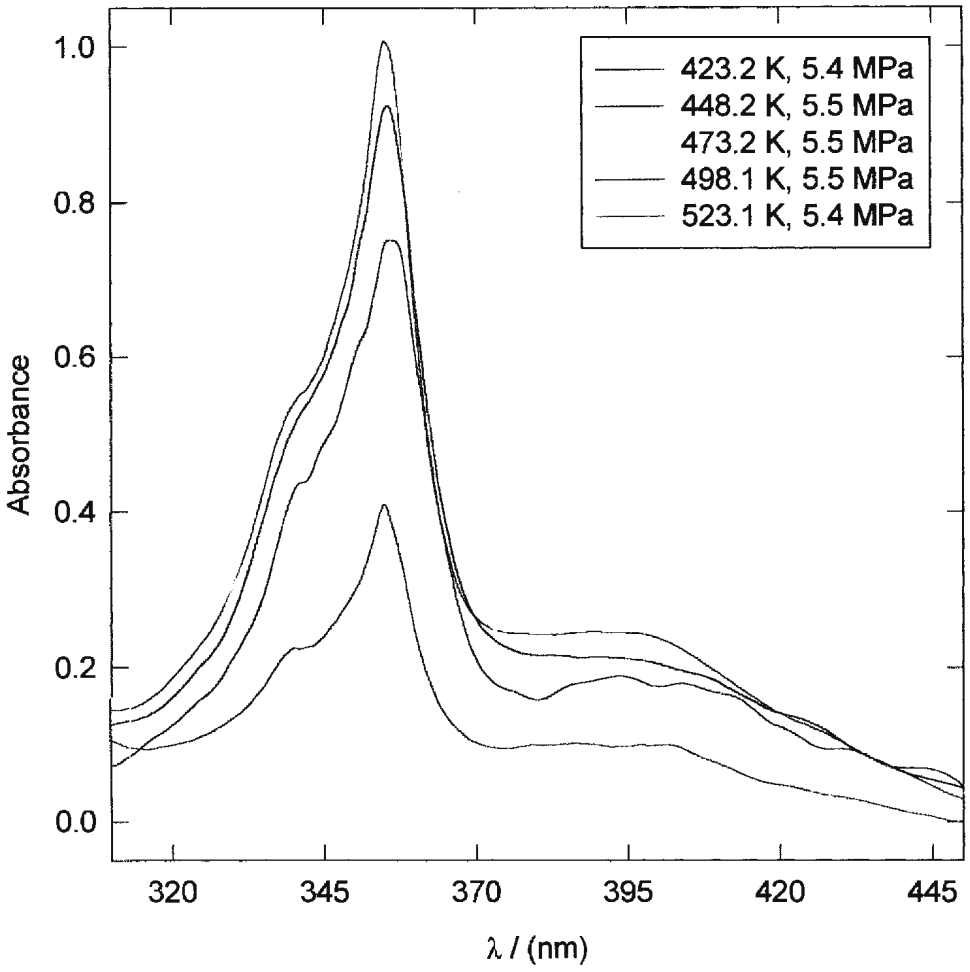

Figure 3.5.1 Absorbance as a function of wavelength for acridine in a 0.0203 mol·kg^{-1} solution of triflic acid.

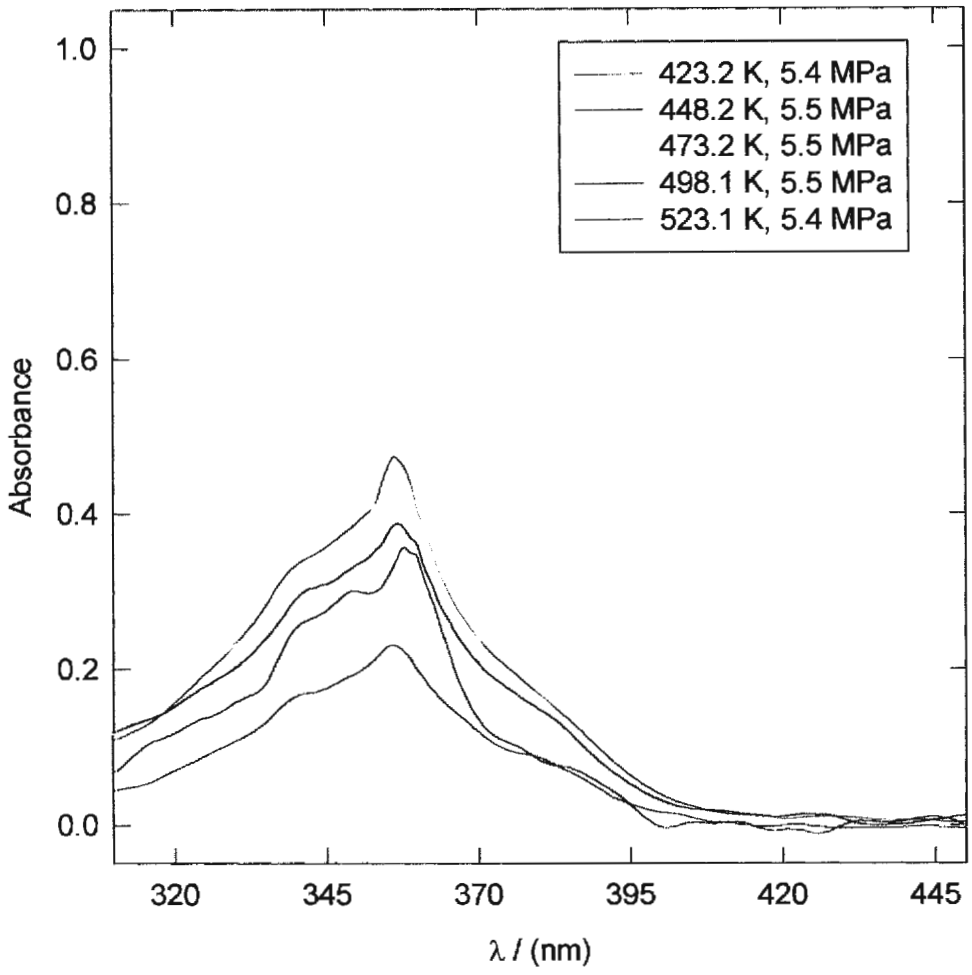

Figure 3.5.2 Absorbance as a function of wavelength for acridine in a 0.0981 mol·kg^{-1} solution of sodium hydroxide.

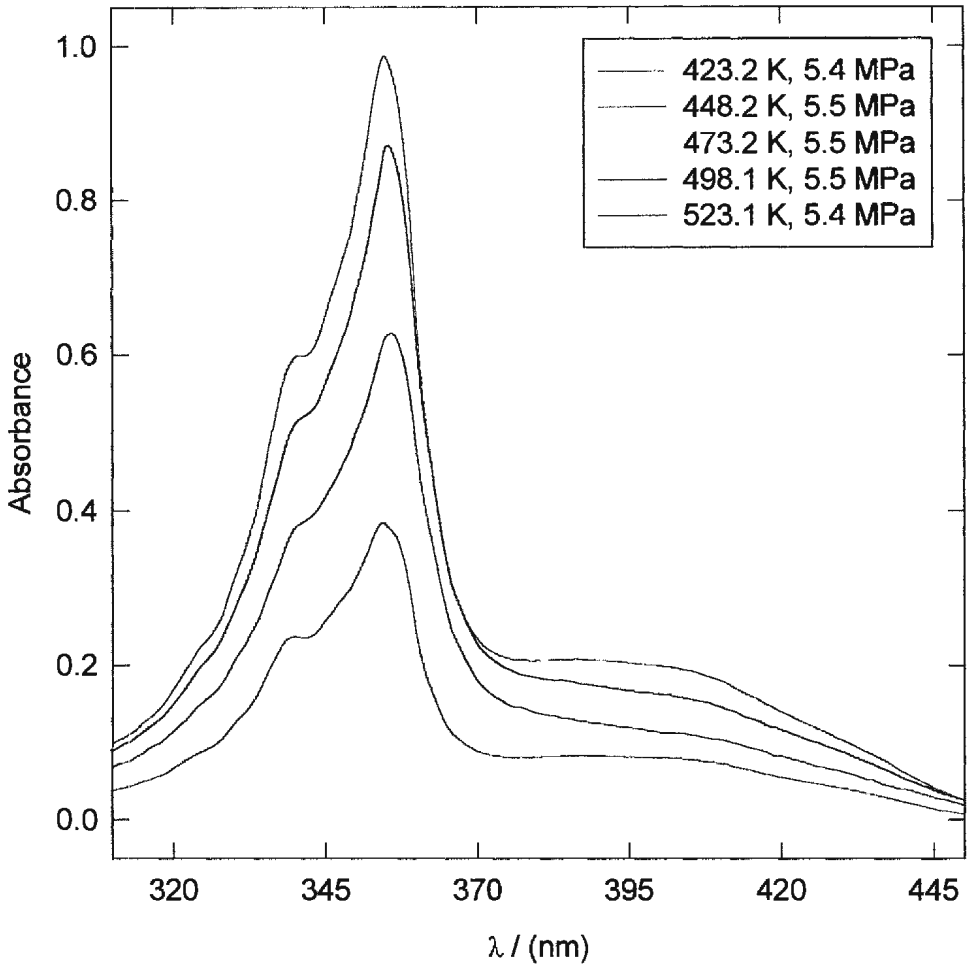

Figure 3.5.3 Absorbance as a function of wavelength for acridine in a buffer solution of α-alanine $m(H_2A^+)$ = 0.048974 mol·kg^{-1} and $m(HA^{\pm})$ = 0.050483 mol·kg^{-1}.

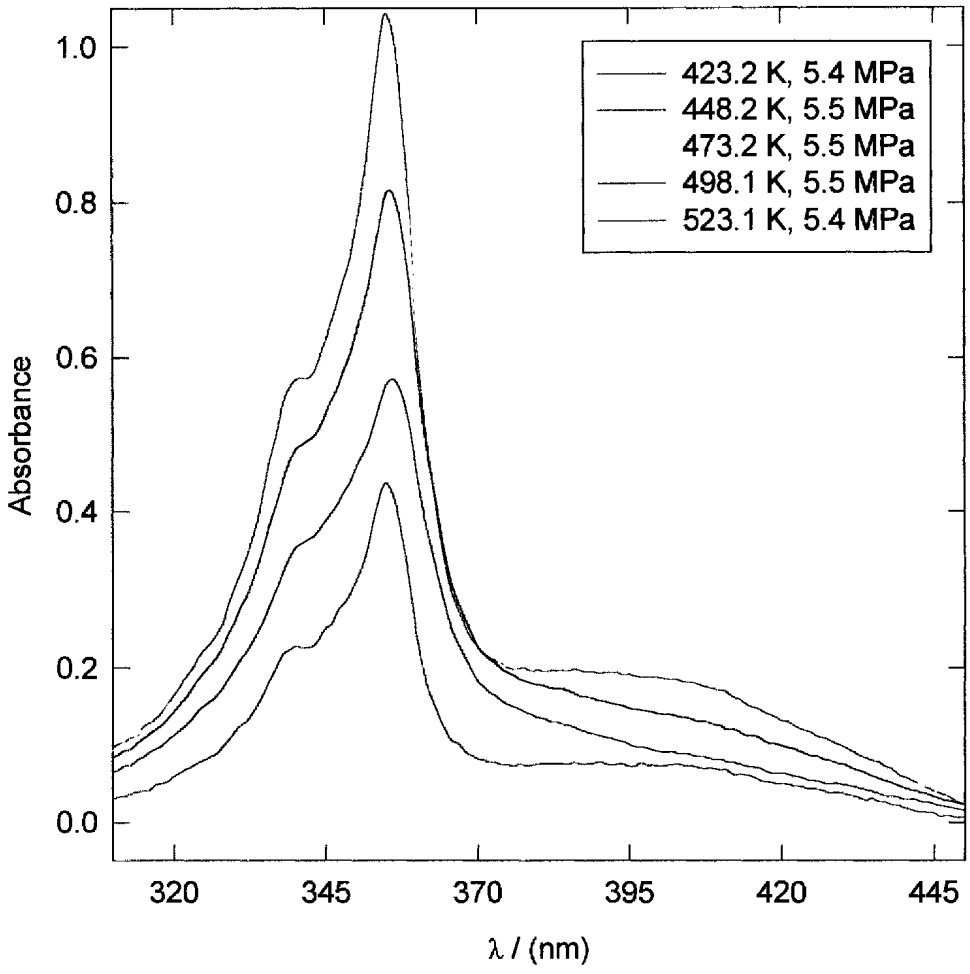

Figure 3.5.4 Absorbance as a function of wavelength for acridine in a buffer solution containing 0.049279 mol·kg^{-1} of H_3PO_4 and 0.049293 mol·kg^{-1} of $H_2PO_4^-$.

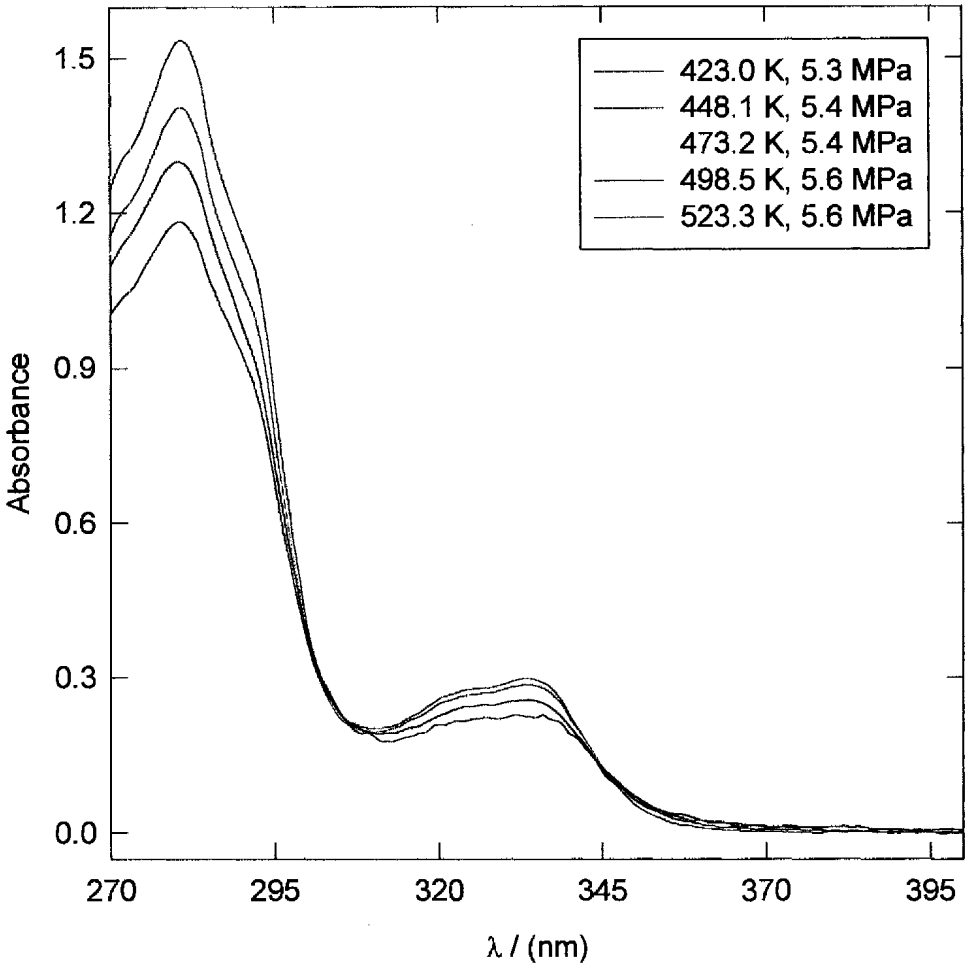

Figure 3.5.5 Absorbance as a function of wavelength for β-naphthoic acid in a 0.100 mol·kg^{-1} solution of triflic acid.

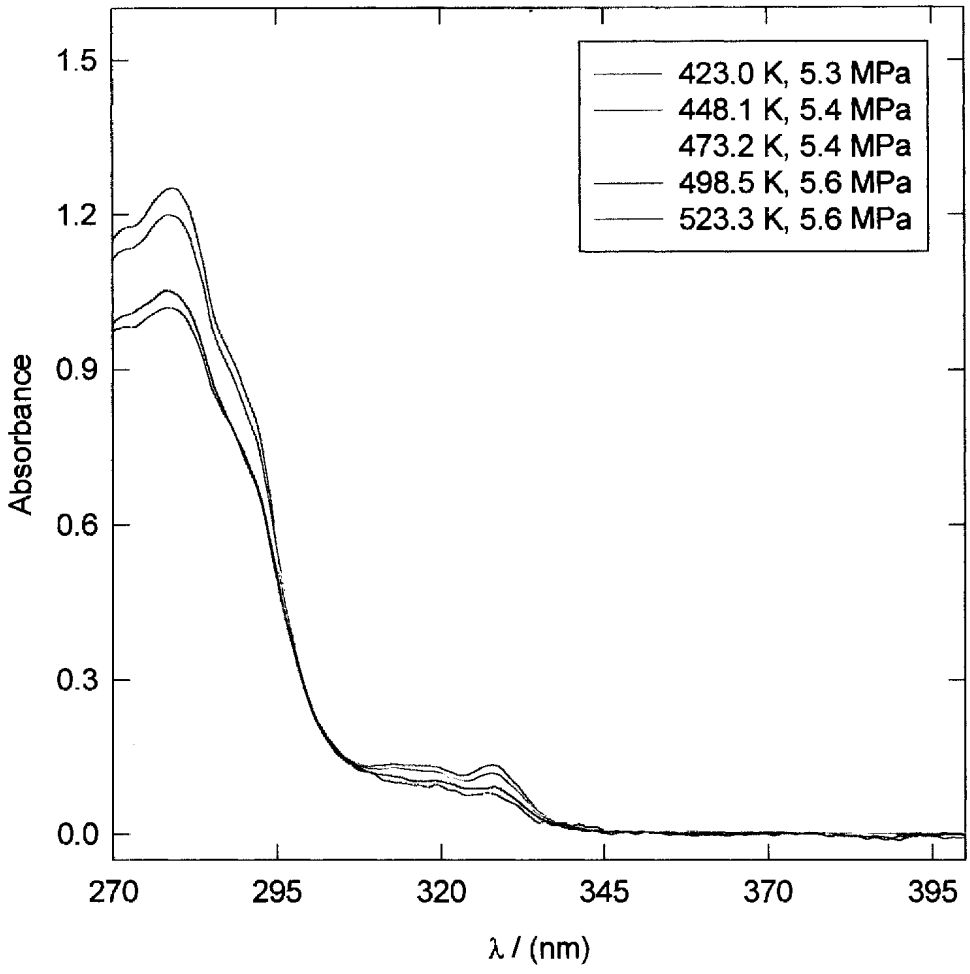

Figure 3.5.6 Absorbance as a function of wavelength for β-naphthoic acid in a 0.0123 mol·kg^{-1} solution of sodium hydroxide.

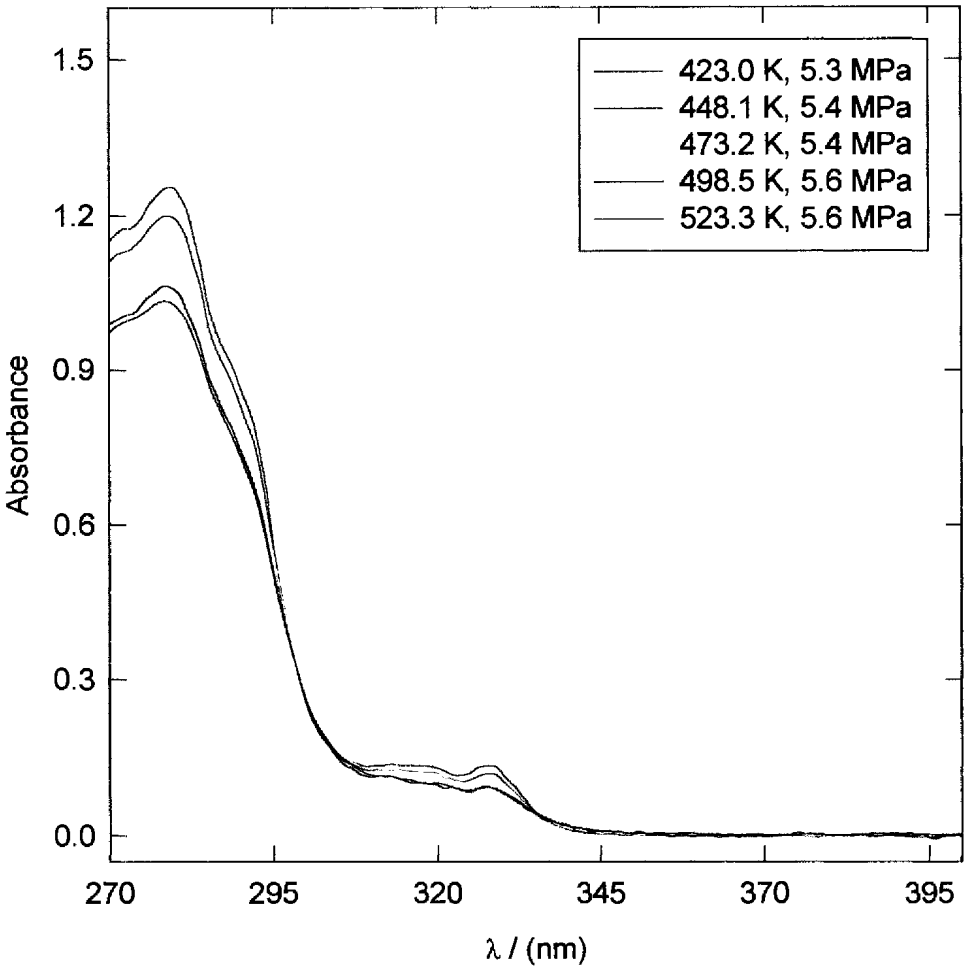

Figure 3.5.7 Absorbance as a function of wavelength for β-naphthoic acid in a buffer solution of α-alanine $m(A^-) = 0.049658$ mol·kg^{-1} and $m(HA^{\pm}) = 0.049680$ mol·kg^{-1}.

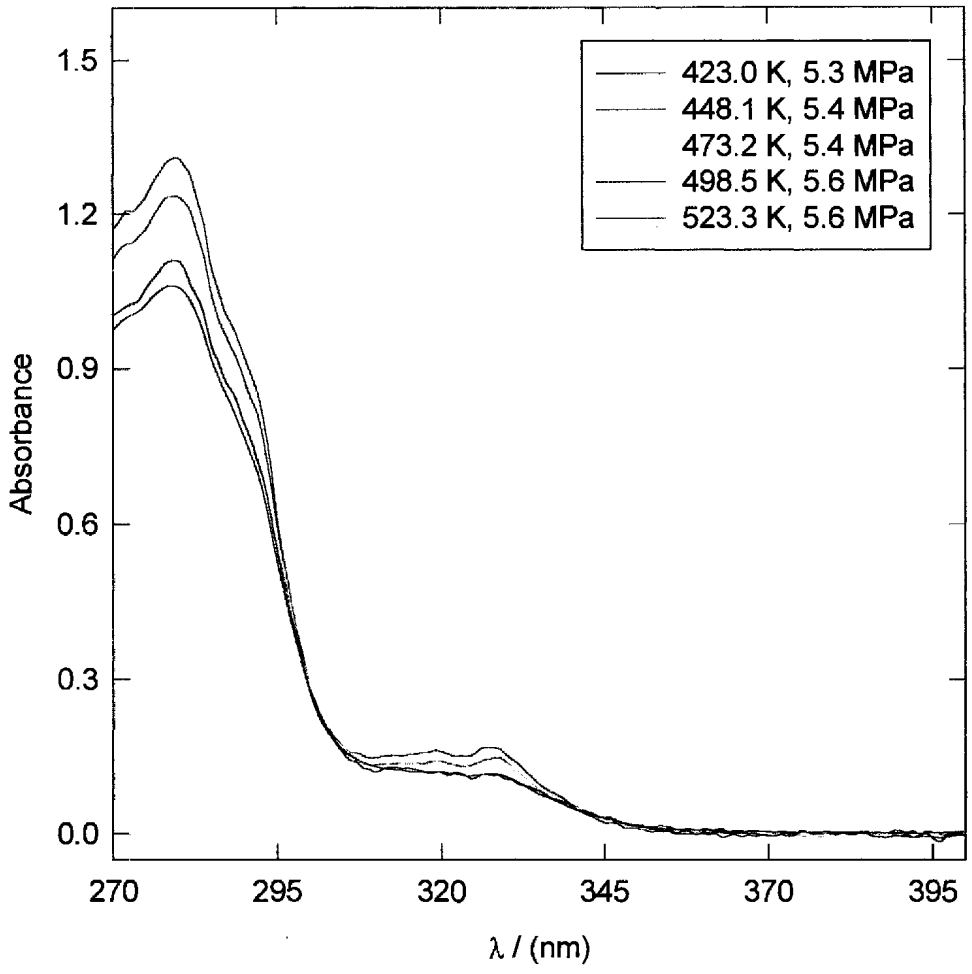

Figure 3.5.8 Absorbance as a function of wavelength for β-naphthoic acid in a buffer solution containing 0.049776 mol·kg^{-1} of CH_3COOH and 0.049838 mol·kg^{-1} of CH_3COO^-.

Table 3.5.1 Experimentally determined values of pK_1, pK_2, pK_{a1}, and pK_a as a function of temperature.

		Indicator: Acridine			
		α-Alanine ($HA^{\pm}$ / H_2A^+) Buffer Solution		H_3PO_4 / $H_2PO_4^-$ Buffer Solution	
T / (K)	p / (MPa)	[AcH^+] / [Ac]	pK_1	[AcH^+] / [Ac]	pK_{a1}
423.2	5.4	56.6	2.23 ± 0.97	—	—
448.2	5.5	24.7	2.41 ± 0.41	23.3	2.44 ± 0.49
473.2	5.5	12.6	2.56 ± 0.21	10.3	2.64 ± 0.23
498.1	5.5	6.80	2.70 ± 0.09	3.15	3.03 ± 0.05
523.1	5.4	1.88	3.15 ± 0.03	1.09	3.38 ± 0.03

		Indicator: β-naphthoic acid			
		α-Alanine ($HA^{\pm}$ / A^-) Buffer Solution		CH_3COOH / CH_3COO^- Buffer Solution	
T / (K)	p / (MPa)	[NapH] / [Nap^-]	pK_2	[NapH] / [Nap^-]	pK_a
423.0	5.3	0.00336	7.19 ± 0.21	0.263	5.29 ± 0.01
448.1	5.4	—	—	0.232	5.67 ± 0.01
473.2	5.4	—	—	0.245	5.99 ± 0.01
498.5	5.6	0.0297	7.27 ± 0.06	0.263	6.32 ± 0.01
523.3	5.6	0.0474	7.45 ± 0.07	0.288	6.66 ± 0.01

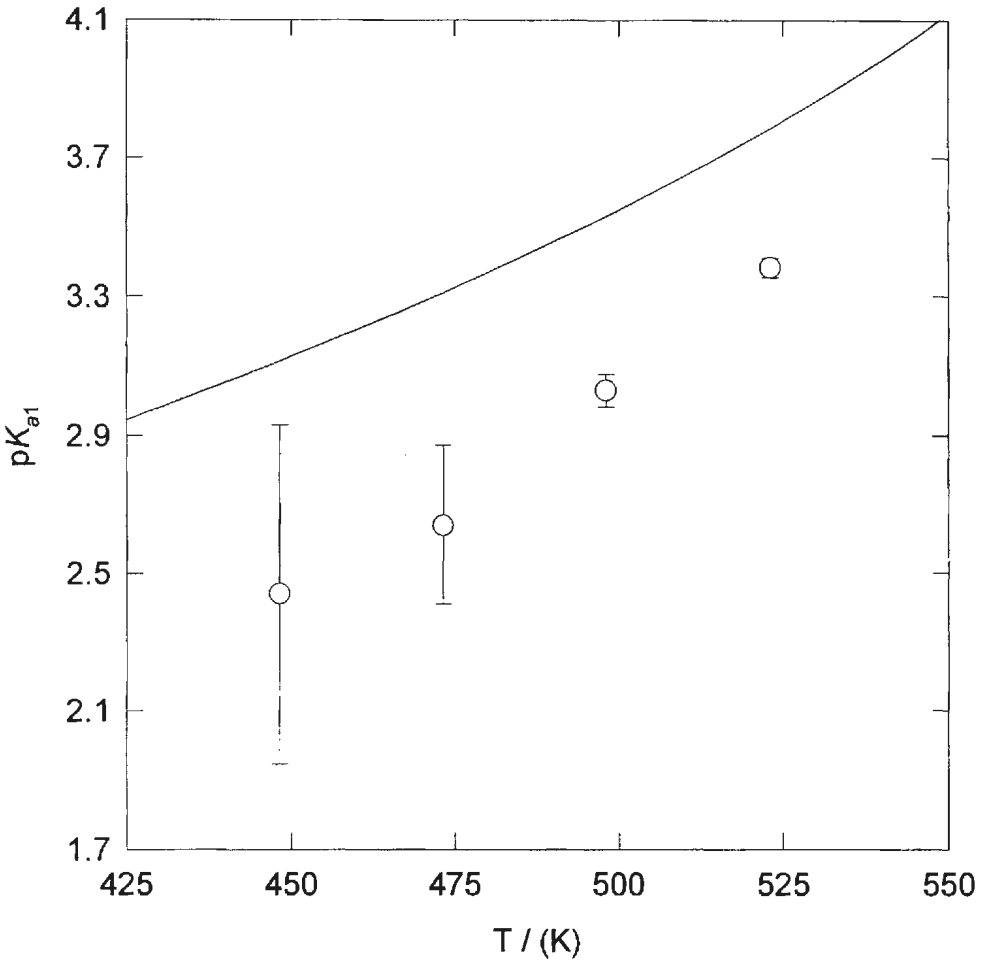

Figure 3.5.9 Comparison of the experimentally determined values of pK_{a1} for phosphoric acid with those determined from the work of Mesmer and Baes (1974) at I = 0.05 mol·kg^{-1}. The solid line represents the work of Mesmer and Baes. The symbols represent the experimental results obtained at 5.5 MPa.

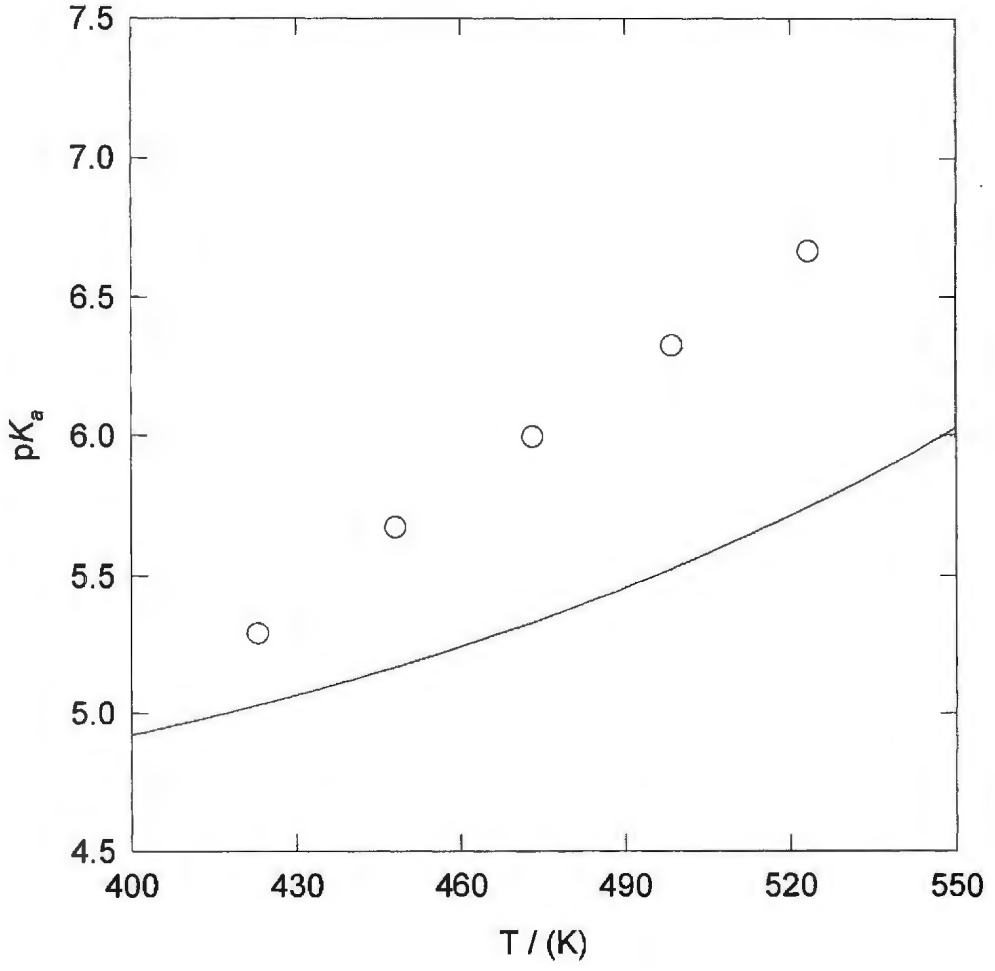

Figure 3.5.10 Comparison of the experimentally determined values of pK_a for acetic acid with those determined from the work of Mesmer *et al.* (1989) at I = 0.05 mol·kg^{-1}. The solid line represents the work of Mesmer and Baes. The symbols represent the experimental results obtained at 5.5 MPa.

CHAPTER 4.0 DISCUSSION

4.1 Comparison of Experimental Results with Literature Data.

4.1.1 Apparent Molar Volumes.

Except for the measurements made by Hakin *et al.* (1998) on glycine, there are no experimental values of V_ϕ for aqueous amino acids above 348 K in the literature with which to compare the results obtained in this work. However, our results are completely consistent with the literature reports of measurements made at lower temperatures. The literature data at 0.1 MPa follow the trend in pressure dependence established by the isothermally determined standard partial molar volumes V° for α-alanine, β-alanine, glycine, and proline obtained in Section 3.2 and shown in Figures 3.4.3.1, 3.4.3.4, 3.4.3.7, and 3.4.3.10, respectively. Considering the pressure difference between the literature data and the experimentally determined data, the values of V° appear to have a relatively smooth temperature dependence over a temperature range that includes both literature and experimental conditions.

Table 4.1.1.1 compares the experimentally determined values of V° obtained for α-alanine, β-alanine, glycine, and proline at 298.15 K and 0.1 MPa with those obtained from literature. The values of V° obtained in this work agree with the literature values within the combined experimental uncertainties.

Table 4.1.1.1 Comparison of the experimentally determined values of V° obtained at 298.15 K and 0.1 MPa with those obtained from literature.

Amino Acid	V° (this work) $cm^3 \cdot mol^{-1}$	V° (literature) $cm^3 \cdot mol^{-1}$	
α-Alanine	60.50 ± 0.02	60.52 ± 0.01	Kikuchi *et al.* (1995)
	60.49 ± 0.05	60.5 ± 0.1	Chalikian *et al.* (1994)
		60.47 ± 0.03	Hakin *et al.* (1994)
		60.4 ± 0.1	Kharakoz (1989)
		60.50 ± 0.02	Ogawa *et al.* (1984)
		60.54 ± 0.09	Cabani *et al.* (1981)
		60.50 ± 0.07	Millero *et al.* (1978)
		60.47 ± 0.1	Ahluwalia *et al.* (1977)
		60.3 ± 0.2	Shahidi and Farell (1978)
β-Alanine	58.29 ± 0.02	58.3 ± 0.2	Chalikian *et al.* (1993)
		58.25 ± 0.02	Ogawa *et al.* (1984)
		58.63 ± 0.48	Cabani *et al.* (1981)
		58.28 ± 0.1	Ahluwalia *et al.* (1977)
		58.5 ± 0.3	Shahidi and Farell (1978)
Glycine	43.31 ± 0.05	43.4 ± 0.1	Chalikian *et al.* (1994)
		43.3 ± 0.1	Kharakoz (1989)
		43.33 ± 0.12	Cabani *et al.* (1981)
		43.25 ± 0.01	Jolicoeur and Boileau (1978)
		43.5 ± 0.2	Shahidi and Farell (1978)
		43.3	Kirchnerova *et al.* (1976)
Proline	82.63 ± 0.02	82.61 ± 0.02	Hakin *et al.* (1997)
		82.5 ± 0.2	Kharakoz (1989)
		82.65 ± 0.03	Jolicoeur *et al.* (1986)
		82.63 ± 0.05	Mishra and Ahluwalia (1984)

4.1.2 Apparent Molar Heat Capacities.

There are no experimental values of $C_{p,\,\phi}$ for any aqueous amino acid above 328 K in the literature with which to compare the results obtained in this work. However, our results are again completely consistent with the literature reports of measurements made at lower temperatures. The literature data at 0.1 MPa follow the trend in pressure dependence established by the isothermally determined standard partial molar heat capacities C_p° obtained in Section 3.3 and shown in Figures 3.4.3.2, 3.4.3.5, 3.4.3.8, and 3.4.3.11 for α-alanine, β-alanine, glycine, and proline, respectively. The literature data at 0.1 MPa also follow the trend in temperature dependence established by the experimental data at steam saturation pressure.

Table 4.1.2.1 compares the experimentally determined value of C_p° obtained for α-alanine at 298.15 K and 0.1 MPa with those obtained from literature. The value of C_p° obtained in this work agrees with the literature values within the combined experimental uncertainties.

Table 4.1.2.1 Comparison of the experimentally determined value of C_p° obtained for α-alanine at 298.15 K and 0.1 MPa with those obtained from literature.

C_p° (this work) $J \cdot K^{-1} \cdot mol^{-1}$	C_p° (literature) $J \cdot K^{-1} \cdot mol^{-1}$	
140.52 ± 0.49	141.2	Hakin *et al.* (1994)
	141.4 ± 0.2	Jolicoeur and Boileau (1978)
	141 ± 4	Spink and Wadsö (1975)
	140.96	Gucker and Allen (1942)

4.2 Relative Success of the Revised HKF Model Versus the Density Model.

In Section 3.4.2 the revised HKF model and the density model were fitted to the apparent molar volumes measured in this work. The overall weighted standard deviation σ for each model is included in Tables 3.4.2.2 and 3.4.2.3. For aqueous α-alanine, the revised HKF model gave a weighted standard deviation of 0.08 which is only slightly higher than the value of 0.07 obtained using the density model. For aqueous proline, the revised HKF model gave a weighted standard deviation of 0.18, significantly higher than the value of 0.13 obtained using the density model. From these results it is clear that the density model performs better than the revised HKF model as a fitting function.

Figures 3.4.2.1, 3.4.2.2, 3.4.2.5, and 3.4.2.7 illustrate the near equality of the fits obtained for α-alanine using both the revised HKF model and the density model. The fitting functions obtained using both models agree relatively well with the isothermal values. The advantage in using the density model as compared to the revised HKF model is illustrated in Figure 3.4.2.9. Both models produce fitting functions for κ_T° that are very similar in shape. However, the function obtained using the revised HKF model lies well below the data of Chalikian *et al.* (1994). The function obtained using the density model lies nearer to the centre of the set of compressibility data points.

In Figures 3.4.2.3 and 3.4.2.4 it is evident that neither model fits the experimental V_ϕ data for proline as well as they do for α-alanine. The fitted function for V_ϕ obtained using the density model represents the experimental data better than that obtained from the revised

HKF model. Figure 3.4.2.6 illustrates the lack of agreement between the fit obtained using the revised HKF model and the isothermal values of V° reported in Section 3.2 throughout the temperature range under consideration. The revised HKF model produced a fitted function for V° with an inverted pressure dependence at low temperatures. The correct pressure dependence is given only at temperatures above 425 K. The fitted function obtained for V° using the density model closely followed the isothermal values of V° and it gives the correct pressure dependence throughout the temperature range under consideration. Figure 3.4.2.10 exemplifies the worst failure of the revised HKF model. The fitted function obtained for κ_T° using the revised HKF model completely failed to reproduce the isothermal values. This function also had a temperature dependence opposite to that exhibited by the κ_T° values of Kharakoz (1991). The fitted function obtained for κ_T° using the density model agreed with the isothermal values relatively well over most of the temperature range. Figure 3.4.2.8 illustrates the excessive deviation of the fit obtained for b using the revised HKF model from the isothermal values of b at both the low and midrange temperatures in this figure. The fitted function obtained for b using the density model agrees with the isothermal values over most of the temperature range.

It is apparent from the preceding discussion that the density model performs better as a fitting function for the thermodynamic properties (V_ϕ, V°, κ_T°) of aqueous amino acids than does the HKF model. However, to fit the standard partial molar heat capacities in addition to the standard partial molar volumes, the density model must be modified to

include several additional terms. These additional terms, absent in the original model, increase the flexibility of the functions thereby improving their ability to reproduce the temperature and pressure dependence of the diverse experimental data. Therefore, an extended version of the density model was used in Section 3.4.3 to represent the temperature and pressure dependencies of the standard partial molar volumes reported in Section 3.2 and the standard partial molar heat capacities reported in Section 3.3.

4.3 Comparison of the Standard Partial Molar Properties Predicted by the Revised HKF Model with the Experimental Results.

Amend and Helgeson (1997) have used the revised HKF model, with the correlations derived for neutral organic species, to predict the standard partial molar volumes V° and standard partial molar heat capacities C_p° of aqueous α-alanine, glycine, and proline as a function of temperature. The predicted values of V° for aqueous α-alanine at 19.96 MPa, aqueous glycine at 20.00 MPa, and aqueous proline at 20.20 MPa are compared to the experimental values of V° in Figures 4.3.1, 4.3.2, and 4.3.3, respectively. The predicted values of C_p° for aqueous α-alanine at 30.15 MPa, aqueous glycine at 30.24 MPa, and aqueous proline at 30.31 MPa are compared to the experimental values of C_p° in Figures 4.3.4, 4.3.5, and 4.3.6, respectively. These figures illustrate the gross error in the prediction made by Amend and Helgeson (1997) for aqueous α-amino acids. The temperature dependence of the experimental values of V° and C_p° for aqueous α-alanine, glycine, and proline suggests that both approach negative infinity as the temperature approaches the

critical temperature of water. However, the predicted values of V° and C_p° approach positive infinity. Criss and Wood (1996) and Shvedov and Tremaine (1997) have also found quantitative errors arising from the very limited high temperature database upon which the extension of the revised HKF model to organic species was based. However, it appears that the discrepancy between the predicted and experimental behaviour of V° and C_p° in Figures 4.3.1 to 4.3.6 also reflects the neglect of the zwitterionic nature of the aqueous amino acids.

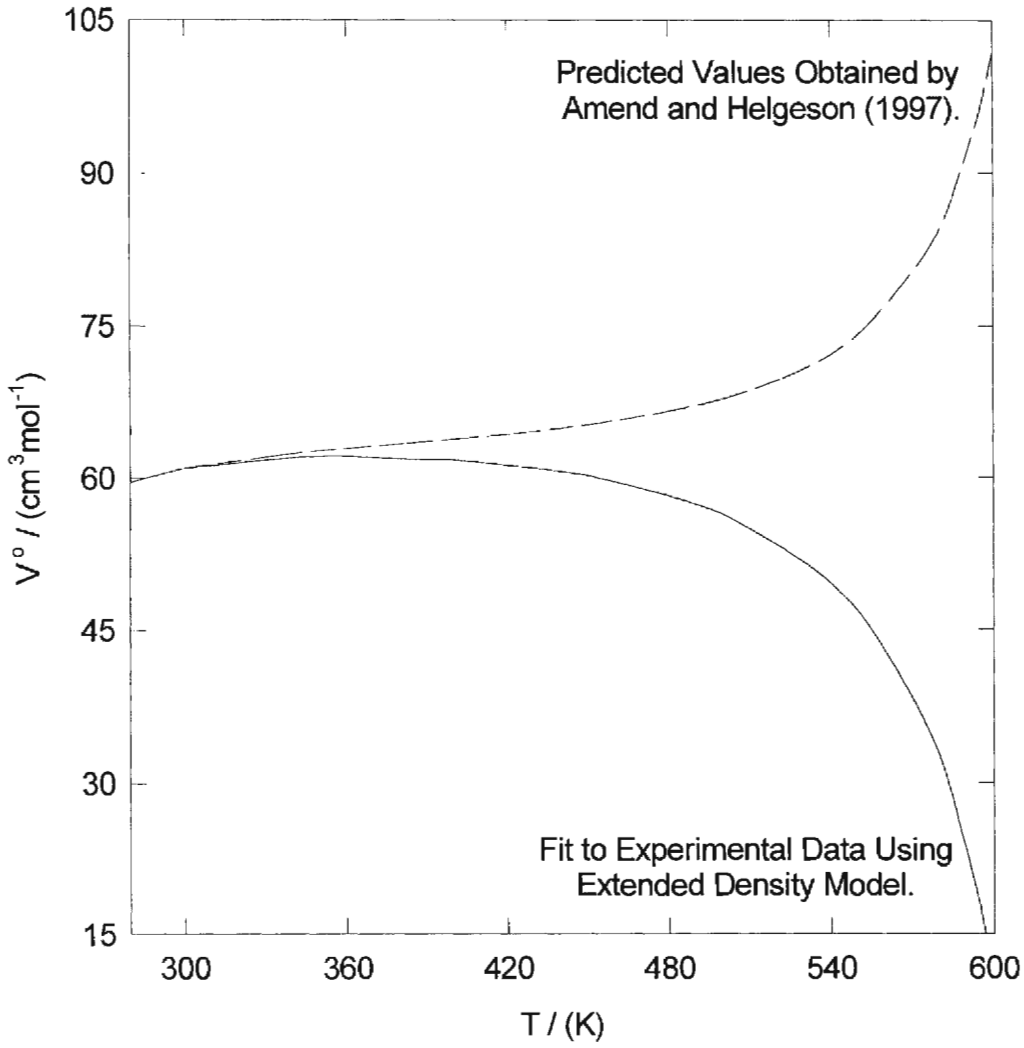

Figure 4.3.1 The predicted and experimental standard partial molar volumes V° of α-alanine at 19.96 MPa.

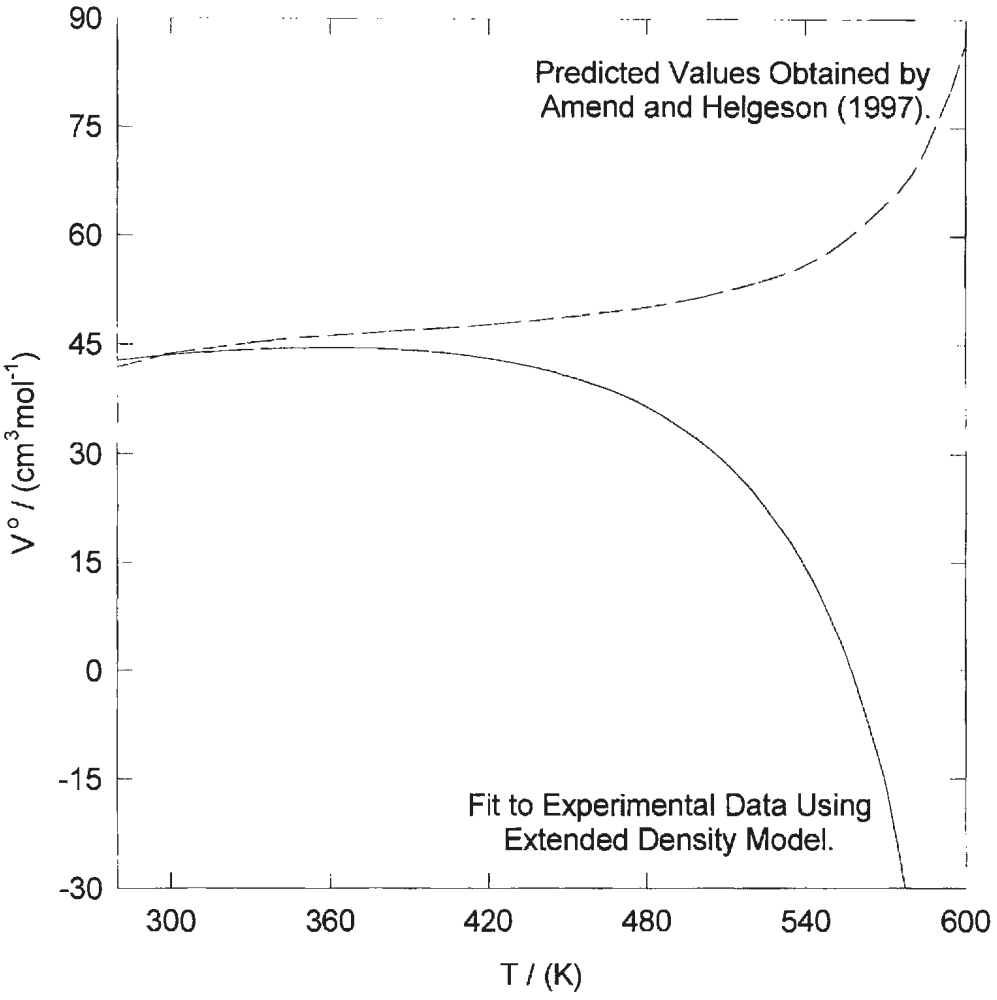

Figure 4.3.2 The predicted and experimental standard partial molar volumes $V°$ of glycine at 20.00 MPa.

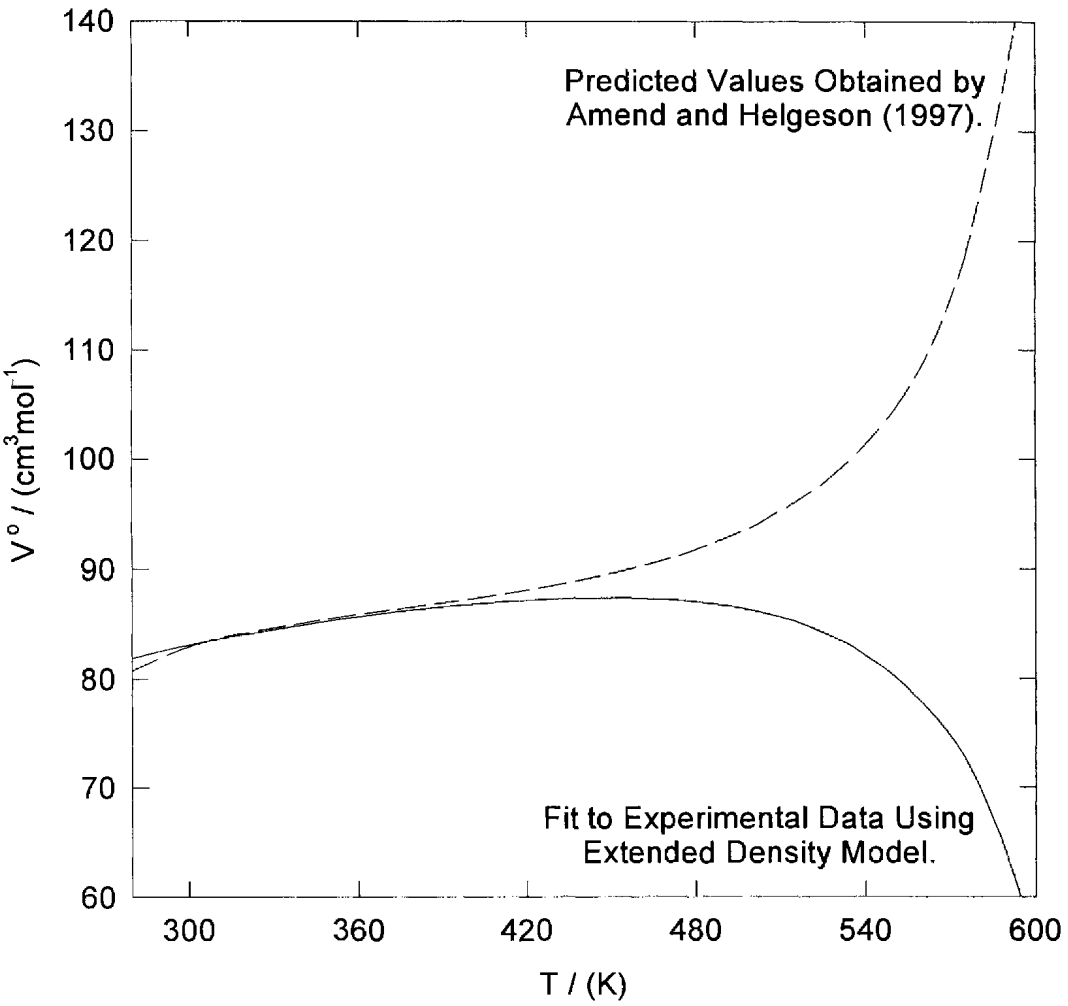

Figure 4.3.3 The predicted and experimental standard partial molar volumes $V°$ of proline at 20.20 MPa.

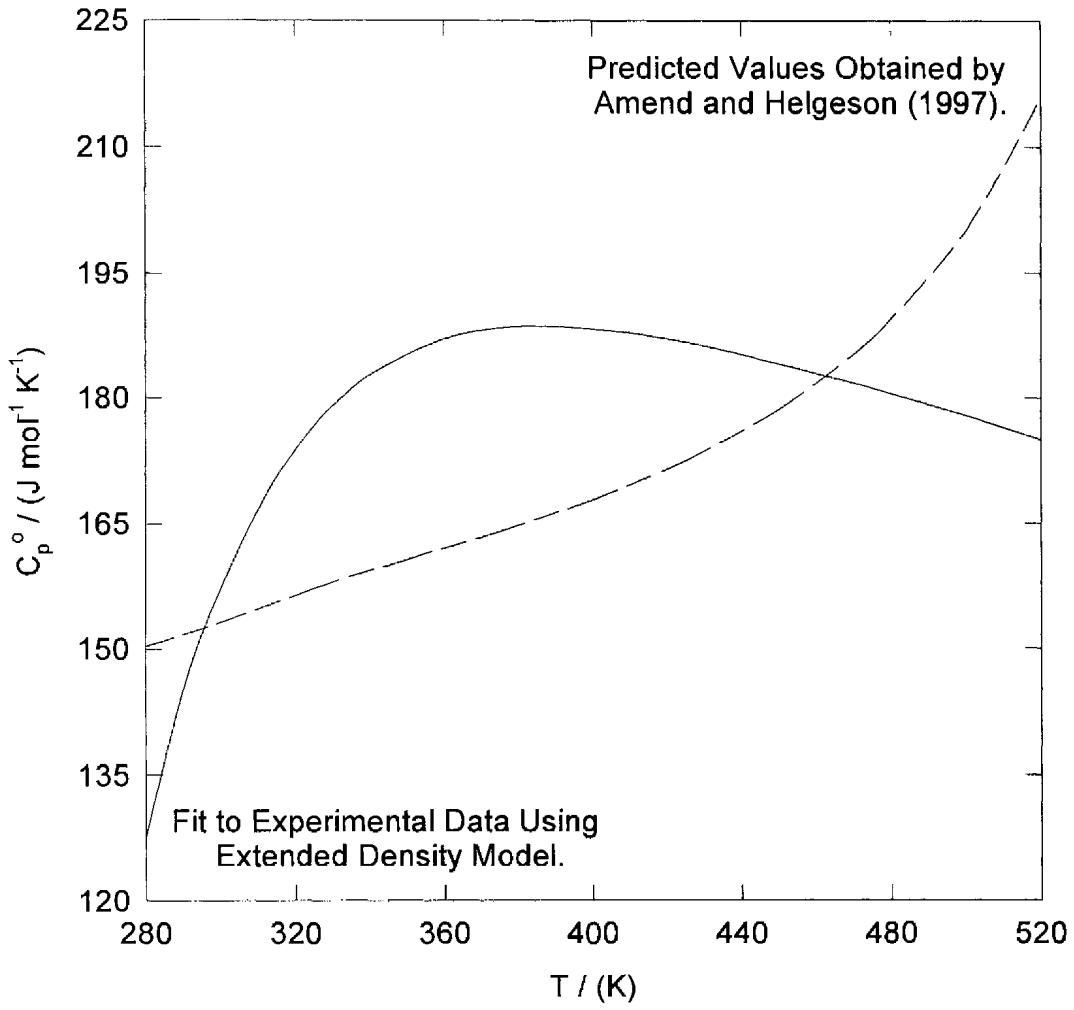

Figure 4.3.4 The predicted and experimental standard partial molar heat capacities C_p° of α-alanine at 30.15 MPa.

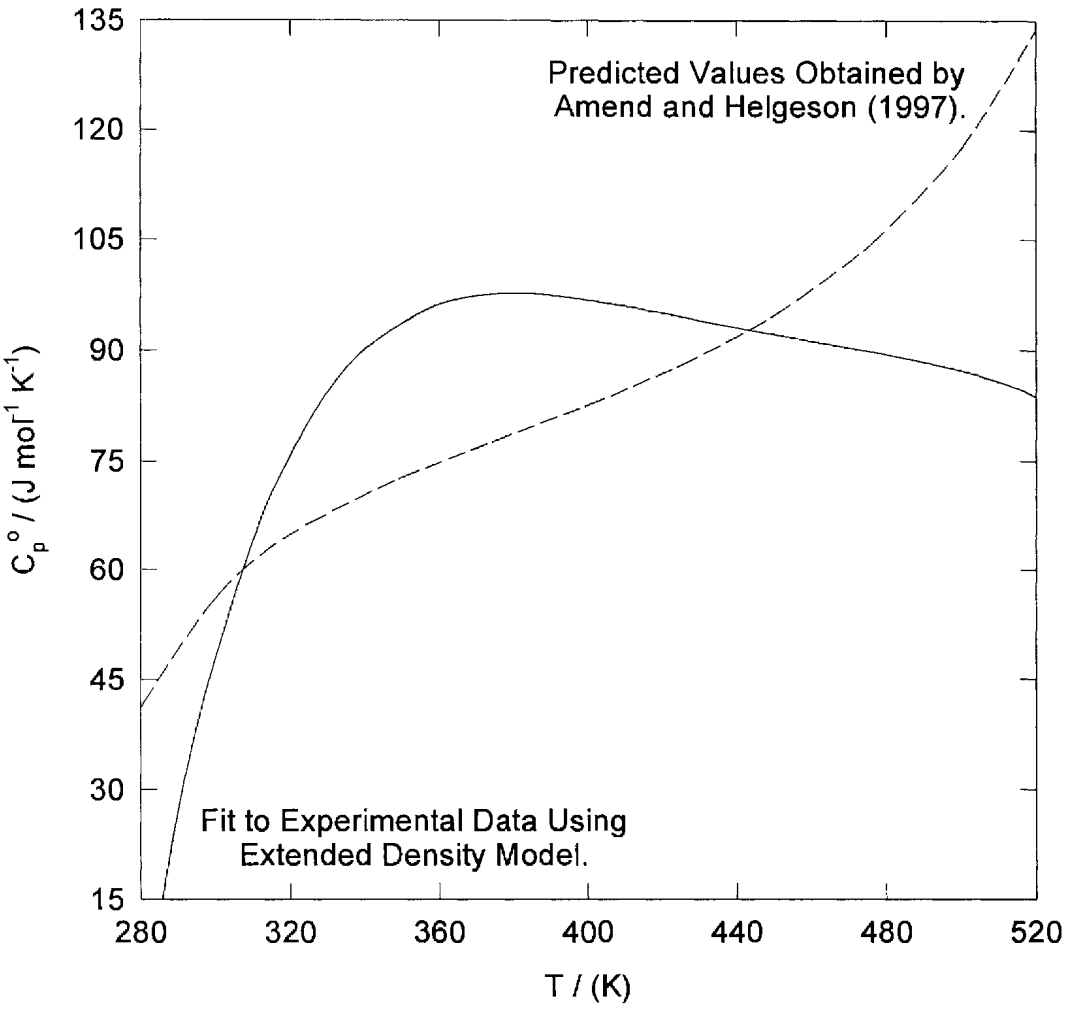

Figure 4.3.5 The predicted and experimental standard partial molar heat capacities C_p° of glycine at 30.24 MPa.

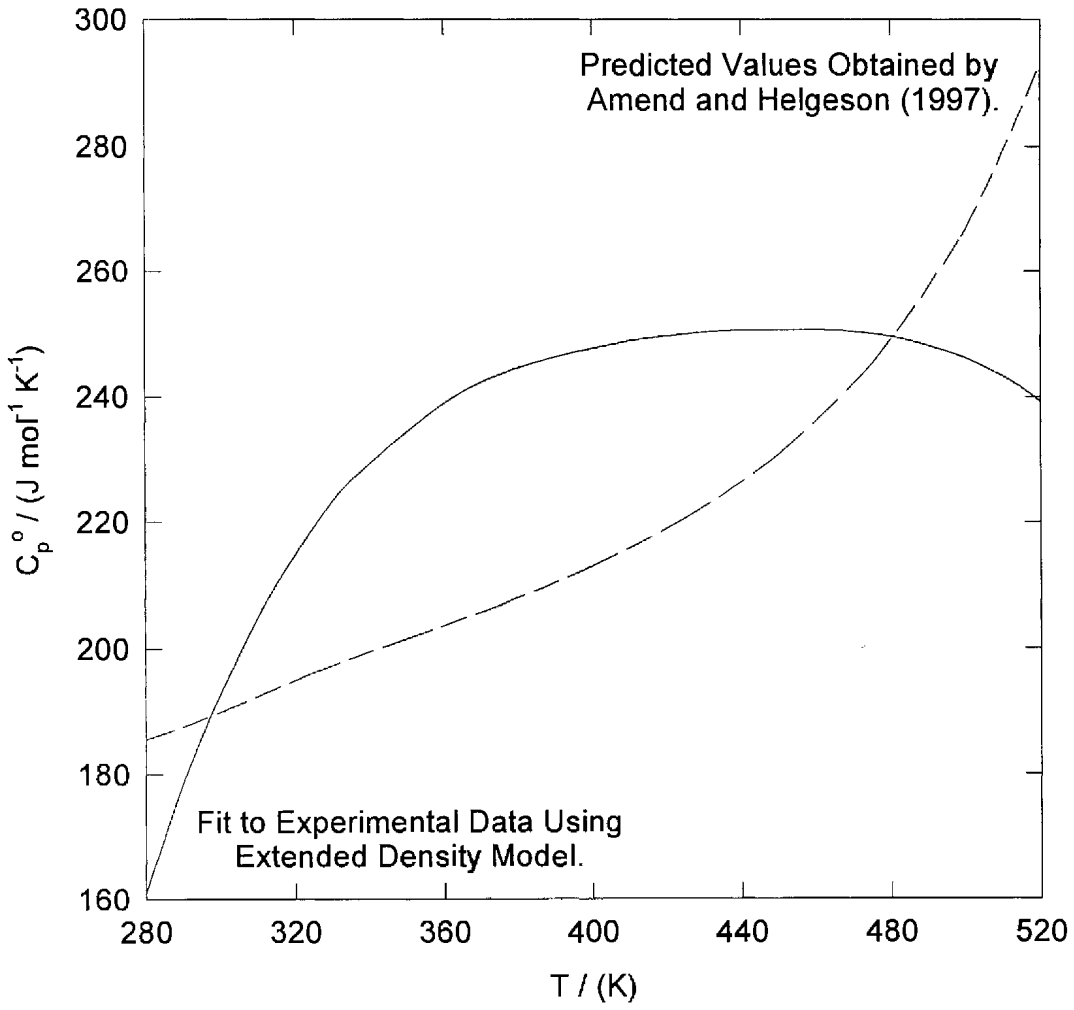

Figure 4.3.6 The predicted and experimental standard partial molar heat capacities C_p^o of proline at 30.31 MPa.

4.4 The Yezdimer-Sedlbauer-Wood Functional Group Additivity Model

4.4.1 Predicted Behaviour of the Standard Partial Molar Properties.

Yezdimer *et al.* (2000) have used the equations-of-state developed by Sedlbauer *et al.* (2000) to develop a functional group additivity model for aqueous organic species that is capable of predicting the standard partial molar properties of aqueous α-alanine and glycine as a function of temperature. The predicted values of V° for aqueous α-alanine and glycine are compared to the experimentally determined values of V° in Figures 4.4.1.1 and 4.4.1.2, respectively. The predicted values of C_p° for aqueous α-alanine and glycine are compared to the experimentally determined values of C_p° in Figures 4.4.1.3 and 4.4.1.4, respectively.

As the temperature approaches the critical temperature of water, the predicted values of V° and C_p° for aqueous α-alanine and glycine deviate toward negative values in a manner similar to the experimental values of V° and C_p°. However, as can be seen in Figures 4.4.1.1 to 4.4.1.4, the agreement is not quantitative. The discrepancy between the predicted and experimental behaviour of V° and C_p° undoubtedly arises as a result of the limited data set used to determine the parameters for the amino acid functional group. The only experimental data for aqueous amino acids to be included in the Yezdimer-Sedlbauer-Wood functional group additivity model were limited to temperatures below 328 K. Therefore, it is not unexpected that the greatest deviation of the predicted values from the experimental results occurs at the highest temperatures at which measurements were made.

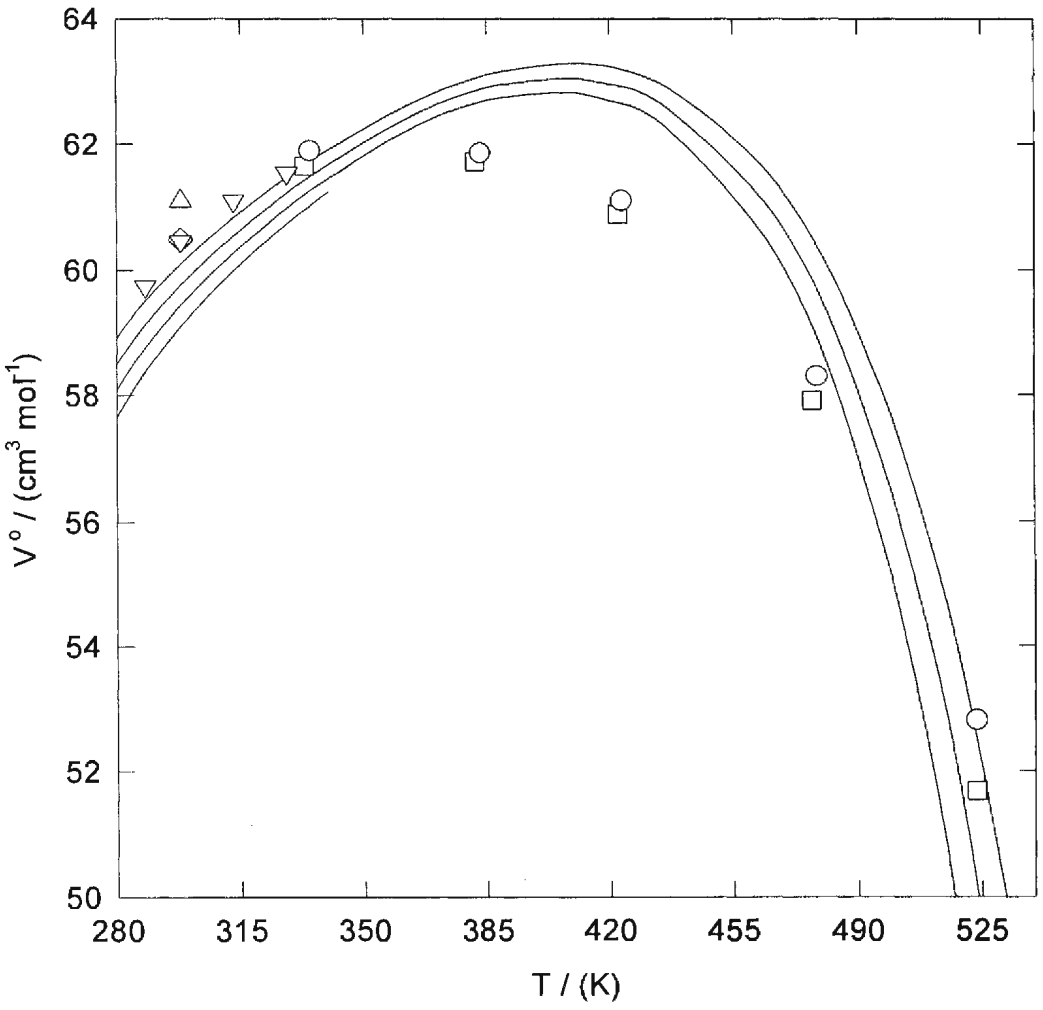

Figure 4.4.1.1 The predicted and experimental standard partial molar volumes $V°$ of α-alanine from 0.1 MPa to 30.77 MPa plotted against temperature. Symbols are the fitted isotherms obtained in Section 3.2: Δ, 30.77 MPa; ○, 19.96 MPa; □, 10.05 MPa; ◇, 0.1 MPa. ▽, 0.1 MPa represents the standard partial molar volumes obtained by Hakin *et al.* (1994). Lines are values obtained using the functional group additivity model of Yezdimer *et al.* (2000).

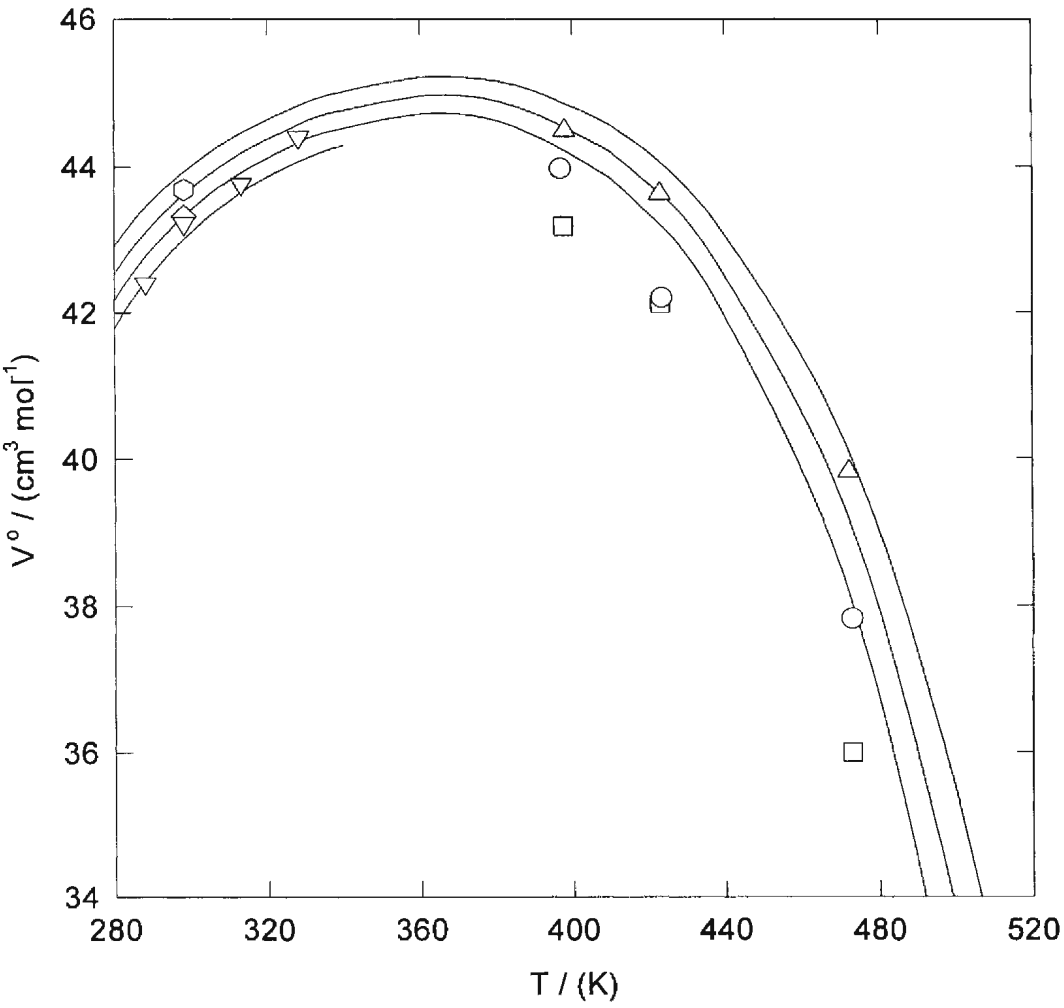

Figure 4.4.1.2 The predicted and experimental standard partial molar volumes $V°$ of glycine from 0.1 MPa to 30.83 MPa plotted against temperature. Symbols are the fitted isotherms obtained in Section 3.2: ⬡, 30.83 MPa; ◇, 0.1 MPa. Δ, 30.21 MPa; ○, 20.00 MPa; □, 10.00 MPa represent the standard partial molar volumes obtained by Hakin *et al.* (1998). ▽, 0.1 MPa represents the standard partial molar volumes obtained by Hakin *et al.* (1994). Lines are values obtained using the functional group additivity model of Yezdimer *et al.* (2000).

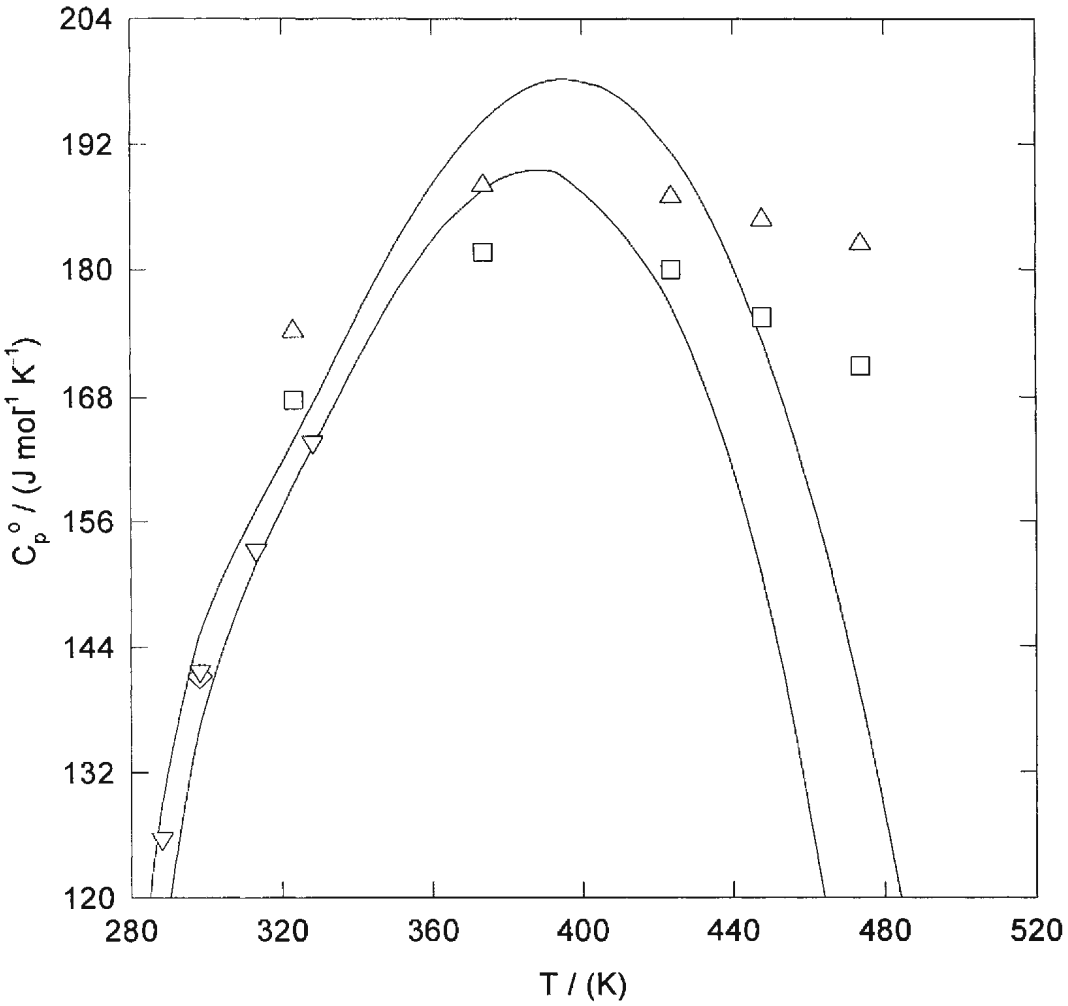

Figure 4.4.1.3 The predicted and experimental standard partial molar heat capacities C_p° of α-alanine from 0.1 MPa to 30.15 MPa plotted against temperature. Symbols are the fitted isotherms obtained in Section 3.3: Δ, 30.15 MPa; □, steam saturation pressure; ◊, 0.1 MPa. ∇, 0.1 MPa represents the standard partial molar volumes obtained by Hakin *et al.* (1994). Lines are values obtained using the functional group additivity model of Yezdimer *et al.* (2000).

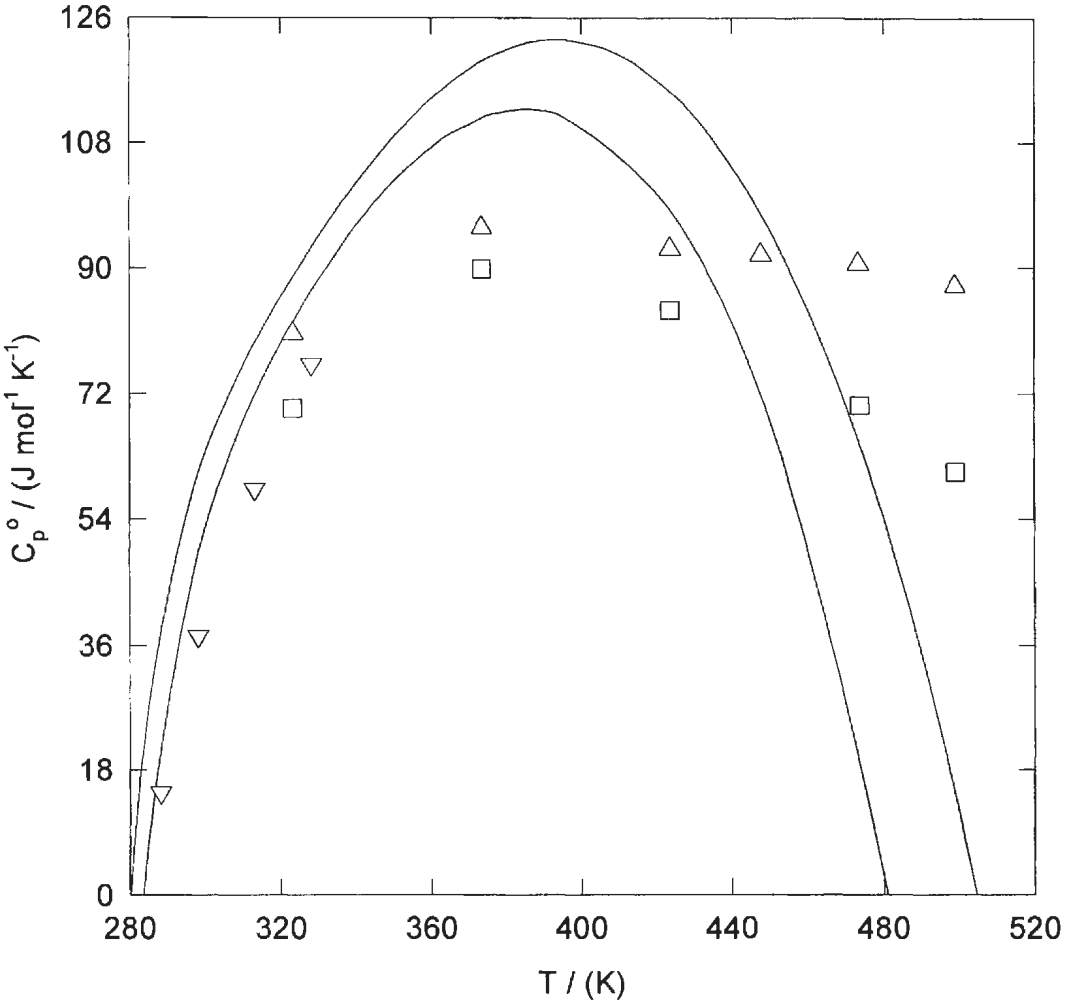

Figure 4.4.1.4 The predicted and experimental standard partial molar heat capacities C_p° of glycine from 0.1 MPa to 30.24 MPa plotted against temperature. Symbols are the fitted isotherms obtained in Section 3.3: Δ, 30.24 MPa; □, steam saturation pressure; ◊, 0.1 MPa. ∇, 0.1 MPa represents the standard partial molar volumes obtained by Hakin *et al.* (1994). Lines are values obtained using the functional group additivity model of Yezdimer *et al.* (2000).

4.4.2 Revision of the Amino Acid Functional Group Parameters Used in the Yezdimer-Sedlbauer-Wood Functional Group Additivity Model.

The experimentally determined standard partial molar volumes V° and standard partial molar heat capacities C_p° have been combined with the existing literature data for aqueous glycine and α-alanine in an attempt to improve the parameters for the amino acid functional group used in the Yezdimer-Sedlbauer-Wood functional group additivity model. The standard-state term and the contributions due to the other functional groups present in the amino acid were subtracted from the experimental values of V° and C_p° to determine the contribution to the standard partial molar volume and heat capacity from the amino acid functional group, V°_{Amino} and $C^\circ_{p,\,Amino}$, respectively. The values of V°_{Amino} and $C^\circ_{p,\,Amino}$ are illustrated in Figures 4.4.2.1 and 4.4.2.2. The parameters for the amino acid functional group were obtained by simultaneously fitting equations (1.4.4) and (1.4.9) to the V°_{Amino} and $C^\circ_{p\,Amino}$ data, respectively. These parameters are tabulated in Table 4.4.2.1 along with their standard deviations. The fitted values of V°_{Amino} and $C^\circ_{p,\,Amino}$ are plotted in Figures 4.4.2.1 and 4.4.2.2. For comparative purposes, the values of V°_{Amino} and $C^\circ_{p,\,Amino}$ obtained by Yezdimer *et al.* (2000) are also included in Figures 4.4.2.1 and 4.4.2.2.

It is evident from Figure 4.4.2.2 that the representation of the experimental values of $C^\circ_{p,\,Amino}$ is greatly improved by the revision of the parameters for the amino acid functional group. However, as can be seen in Figure 4.4.2.1 this improvement is partially offset by a deterioration in the representation of the experimental values of V°_{Amino}. The values of V°_{Amino} obtained by Yezdimer *et al.* (2000) represent the temperature dependence of the experimental

results better than the fitted values of V°_{Amino}. The fitted values of V°_{Amino} exhibit an inversion in pressure dependence at T=365 K. The correct pressure dependence is given only at $T \geq$ 360 K. The values of V°_{Amino} obtained by Yezdimer *et al.* give the correct pressure dependence throughout the temperature range under consideration. As can be seen in Figure 4.4.2.2 the fitted values of $C^{\circ}_{p,\,Amino}$ represent the temperature dependence of the experimental results significantly better than the values of $C^{\circ}_{p,\,Amino}$ obtained by Yezdimer *et al.* (2000). The fitted values of $C^{\circ}_{p,\,Amino}$ slowly decline in the range 423 K $\geq T \geq$ 523 K in a manner similar to the experimental results. The values of $C^{\circ}_{p,\,Amino}$ obtained by Yezdimer *et al.* deviate strongly toward negative values in the same temperature range.

Although the parameters for the amino acid functional group were redetermined using the experimental values of V° and C°_{p} obtained in this work and the values of V° obtained by Hakin *et al.* (1998), there was little improvement in the ability of the Yezdimer-Sedlbauer-Wood functional group additivity model to predict the thermodynamic properties of aqueous amino acids at high temperatures and pressures. This suggests that there is insufficient flexibility in the equations-of-state developed by Sedlbauer *et al.* (2000) upon which Yezdimer *et al.* (2000) have developed their model. Figures 4.4.2.1 and 4.4.2.2 illustrate the difference in temperature dependence exhibited by V°_{Amino} and $C^{\circ}_{p,\,Amino}$. The values of V°_{Amino} increase slowly until they reach their maximum value at T = 398 K and then deviate toward negative values at $T \geq$ 398 K. The values of $C^{\circ}_{p,\,Amino}$ increase sharply until they reach their maximum value and then slowly decline in the range 423 - 523 K.

Table 4.4.2.1 Revised amino acid functional group parameters for use in the Yezdimer-Sedlbauer-Wood functional group additivity model.[†]

	Amino Group
$a_i \cdot 10^{-1}$ / ($m^3 \cdot kg^{-1} \cdot mol^{-1}$)	-6.4716 (0.0065)
$b_i \cdot 10^{4}$ / ($m^3 \cdot kg^{-1} \cdot mol^{-1}$)	-1.842 (0.419)
$c_i \cdot 10^{5}$ / ($m^3 \cdot kg^{-1} \cdot mol^{-1}$)	3.025 (0.556)
d_i	3.256 (0.385)
$e_i \cdot 10^{-2}$ / ($J \cdot K^{-2} \cdot mol^{-1}$)	-2.624 (0.509)
f_i / ($J \cdot K^{-2} \cdot mol^{-1}$)	1.003 (0.164)
σ	6.76

[†] The standard deviation for each parameter is given in parentheses; σ is the overall standard deviation.

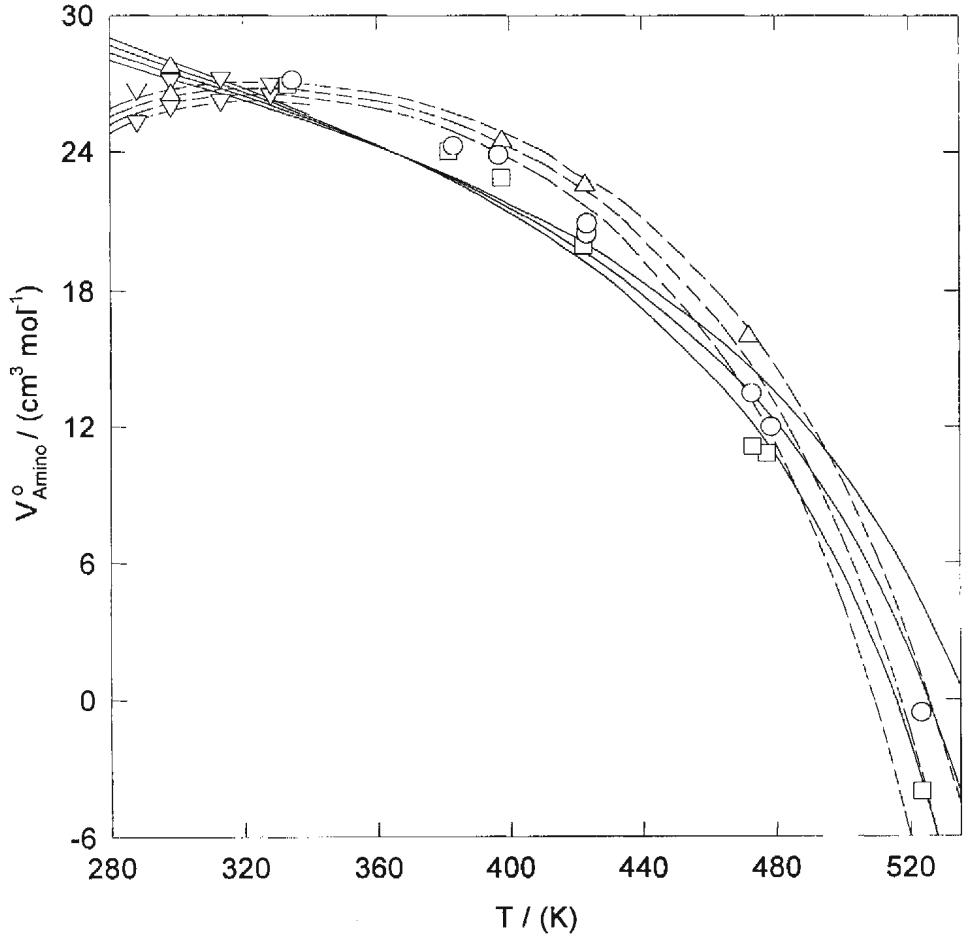

Figure 4.4.2.1 Contribution to the standard partial molar volume of aqueous amino acids due to the amino acid functional group V°_{Amino} plotted against temperature. Symbols are the values of V°_{Amino} derived from experimental data: Δ, 30 MPa; ○, 20 MPa; □, 10 MPa; ∇, 0.1 MPa. Lines are fitted values of V°_{Amino}: -----, Yezdimer *et al.* (2000); ——, this work.

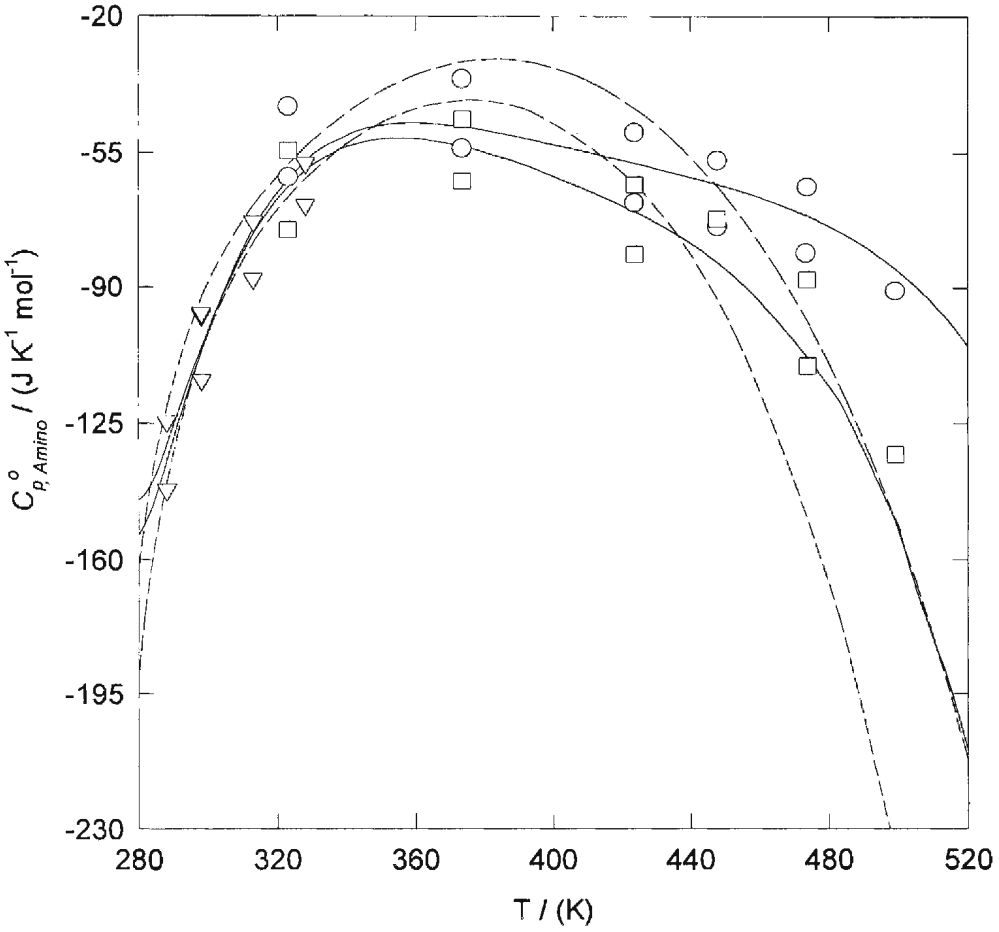

Figure 4.4.2.2 Contribution to the standard partial molar heat capacity of aqueous amino acids due to the amino acid functional group $C^{\circ}_{p,Amino}$ plotted against temperature. Symbols are the values of $C^{\circ}_{p,Amino}$ derived from experimental data: ○, 30 MPa; □, steam saturation pressure; ▽, 0.1 MPa. Lines are fitted values of $C^{\circ}_{p,Amino}$: -----, Yezdimer *et al.* (2000); ——, this work.

4.5 Aqueous Amino Acid Speciation as a Function of Temperature.

4.5.1 Speciation Equilibria.

In aqueous solution an amino acid can exist in either the zwitterionic form $HA^{\pm}$, the neutral form HA^{o}, the deprotonated form A^{-}, or the protonated form H_2A^{+}. The equilibria between the zwitterionic, neutral, and ionic forms of an amino acid can be summarized as follows:

$$H_2A^{+} \underset{\rightleftharpoons}{K_1} HA^{\pm} + H^{+} \qquad (4.5.1.1)$$

$$HA^{\pm} \underset{\rightleftharpoons}{K_2} A^{-} + H^{+} \qquad (4.5.1.2)$$

$$HA^{o} \underset{\rightleftharpoons}{K_3} HA^{\pm} \qquad (4.5.1.3)$$

where K_1, K_2, and K_3 are equilibrium constants. K_3 was assumed to be approximately equal to (K_1 / K_2). A better estimate of the high temperature values for K_2 can often be obtained from the corresponding isocoulombic reaction:

$$HA^{\pm} + OH^{-} \underset{\rightleftharpoons}{K_4} A^{-} + H_2O \qquad (4.5.1.4)$$

where $K_4 = (K_2 / K_w)$ and K_w is the dissociation constant of water. Once K_4 is obtained at the temperature and pressure of interest, K_2 can be calculated from it using the appropriate value of K_w.

Values of K_1, K_2, and K_3 can be used to determine the speciation of the aqueous

amino acids. From equations (4.5.1.1), (4.5.1.2), and (4.5.1.3) the following expressions are obtained for the molality of H_2A^+, A^-, and HA°:

$$[H_2A^+] = ([HA^\pm] [H^+]) / K_1 \qquad (4.5.1.5)$$

$$[A^-] = ([HA^\pm] K_2) / [H^+] \qquad (4.5.1.6)$$

$$[HA^\circ] = [HA^\pm] / K_3 \qquad (4.5.1.7)$$

Combining the charge balance equation, $[H^+] + [H_2A^+] - [A^-] - [OH^-] = 0$, with equations (4.5.1.5) and (4.5.1.6) yields the following expression for $[H^+]$:

$$[H^+]^2 = (K_1 K_2 [HA^+] + K_1 K_w) / (K_1 + [HA^\pm]) \qquad (4.5.1.8)$$

Combining the mass balance equation, $[HA^\pm] + [H_2A^+] + [A^-] + [HA^\circ] = m$, with equations (4.5.1.5), (4.5.1.6), and (4.5.1.7) yields the following expression for $[HA^\pm]$:

$$[HA^\pm] = (K_1 K_3 [H^+] m) / (K_1 [H^+] + K_1 K_3 [H^+] + K_1 K_2 K_3 + K_3 [H^+]^2) \qquad (4.5.1.9)$$

To obtain the equilibrium values for $[HA^\pm]$, $[H_2A^+]$, $[A^-]$, and $[HA^\circ]$ an iterative process was employed. The first step assumed that $[HA^\pm]$ was to equal m. In the second step equation (4.5.1.8) was used to calculate $[H^+]$. Equations (4.5.1.5), (4.5.1.6), and (4.5.1.7) were used in the third step to calculate $[H_2A^+]$, $[A^-]$, and $[HA^\circ]$, respectively. In the fourth step equation (4.5.1.9) was used to calculate $[HA^\pm]$. At this point the process returned to the second step where a new value of $[H^+]$ was calculated. This process was repeated until the values of $[HA^\pm]$, $[H_2A^+]$, $[A^-]$, and $[HA^\circ]$ remained constant.

Two independent methods were used to estimate the values of K_1, K_2, and K_3 at

elevated temperatures and pressures. These methods are described in Sections 4.5.2 and 4.5.3. The speciation of the aqueous amino acids has been determined under our experimental conditions using each of the two methods. To confirm the accuracy of these calculations, the speciation of α-alanine was also determined as a function of temperature using the experimental equilibrium constants determined in Section 3.5. These calculations are described in Section 4.5.5.

4.5.2 Isocoulombic Extrapolation of Room Temperature Data.

For a constant pressure p the temperature dependent equilibrium constant $K_{T,p}$ for a reaction can be determined from the expression:

$$\left(\frac{\partial \ln K_{T,p}}{\partial T}\right)_p = \left(\frac{\Delta_r H^o_{T,p}}{RT^2}\right) \qquad (4.5.2.1)$$

where R is the universal gas constant. The following expression can be used to determine the standard partial molar enthalpy of reaction $\Delta_r H^\circ_{T,p}$:

$$\left(\frac{\partial \Delta_r H^o_{T,p}}{\partial T}\right)_p = \Delta_r C_p{}^o \qquad (4.5.2.2)$$

where $\Delta_r C_p^o$ is the standard partial molar heat capacity of the reaction at T and p. If $\Delta_r C_p^o$ is assumed to be temperature independent, then integration of equation (4.5.2.2) gives:

$$\Delta_r H^o_{T,p} = \Delta_r H^o_{Tr,pr} + (\Delta_r C_p{}^o)(T - T_r) \qquad (4.5.2.3)$$

where $\Delta_r H^\circ_{Tr,pr}$ is the standard partial molar enthalpy of reaction at a reference temperature

T_r and a reference pressure p_r. Therefore, integration of equation (4.5.2.1) gives:

$$\ln K_{T,p} = \ln K_{Tr,pr} + \left(\frac{\Delta_r H^o_{Tr,pr}}{R}\right)\left(\frac{1}{T_r} - \frac{1}{T}\right)$$

$$+ (lnT - lnT_r)\left(\frac{\Delta_r C_p{}^o}{R}\right) - \left(\frac{(\Delta_r C_p{}^o)(T - T_r)}{RT}\right) \qquad (4.5.2.4)$$

where $K_{Tr,pr}$ is the equilibrium constant for the reaction at T_r and p_r. The effect of pressure is given by the expression:

$$\left(\frac{\partial \ln K_{T,p}}{\partial p}\right)_T = -\left(\frac{\Delta_r V^o}{RT}\right) \qquad (4.5.2.5)$$

where $\Delta_r V°$ is the standard partial molar volume of the reaction at T and p.

Table 4.5.2.1 lists the values of $K_{Tr,pr}$, $\Delta_r H°_{Tr,pr}$, and $\Delta_r C_p^o$ required to calculate K_1 and K_4 using equation (4.5.2.4). The values of K_1, K_2, and K_3 are plotted as a function of temperature in Figures 4.5.2.1, 4.5.2.2, 4.5.2.3, and 4.5.2.4 for α-alanine, β-alanine, glycine, and proline, respectively, ignoring the much smaller effect of pressure. The temperature dependent values of K_1, K_2, and K_3 were used to determine the temperature dependent speciation of the aqueous amino acids according to the method described in Section 4.5.1. The distribution of species as a function of temperature is plotted in Figures 4.5.2.5 to 4.5.2.8.

Table 4.5.2.1 Values of $K_{Tr,\,pr}$, $\Delta_r H^\circ{}_{Tr,\,pr}$, and $\Delta_r C_p^\circ$ for use in equation (4.5.2.4).

Thermodynamic Parameter	Value of Parameter	Source
	Water	
$\ln K_w$ / (10)	3.2228	Lide (1991)
$\Delta_{rw} H^\circ$ / (J·mol^{-1}·10^4)	-5.584	Atkins (1990)
$\Delta_{rw} C_p^\circ$ / (J·K^{-1}·mol^{-1}·10^2)	2.238	Atkins (1990)
	α-Alanine	
$\ln K_1$	-5.3944	Wang *et al.* (1996)
$\ln K_2$ / (10)	-2.2720	Martell and Smith (1974)
$\ln K_4$	9.508	($\ln K_2 + \ln K_w$)
$\Delta_{r1} H^\circ$ / (J·mol^{-1}·10^3)	3.2532	Wang *et al.* (1996)
$\Delta_{r2} H^\circ$ / (J·mol^{-1}·10^4)	4.52	Martell and Smith (1974)
$\Delta_{r4} H^\circ$ / (J·mol^{-1}·10^4)	-1.06	($\Delta_{r2} H^\circ + \Delta_{rw} H^\circ$)
$\Delta_{r1} C_p^\circ$ / (J·K^{-1}·mol^{-1}·10^2)	-1.2767	Wang *et al.* (1996)
$\Delta_{r2} C_p^\circ$ / (J·K^{-1}·mol^{-1}·10)	7.23†	Balakrishnan (1988)
$\Delta_{r4} C_p^\circ$ / (J·K^{-1}·mol^{-1}·10^2)	2.961	($\Delta_{r2} C_p^\circ + \Delta_{rw} C_p^\circ$)
	β-Alanine	
$\ln K_1$	-8.1578	Wang *et al.* (1996)
$\ln K_2$ / (10)	-2.3705	Martell and Smith (1974)
$\ln K_4$	8.520	($\ln K_2 + \ln K_w$)
$\Delta_{r1} H^\circ$ / (J·mol^{-1}·10^3)	4.3861	Wang *et al.* (1996)
$\Delta_{r2} H^\circ$ / (J·mol^{-1}·10^4)	4.73	Martell and Smith (1974)
$\Delta_{r4} H^\circ$ / (J·mol^{-1}·10^4)	-0.85	($\Delta_{r2} H^\circ + \Delta_{rw} H^\circ$)
$\Delta_{r1} C_p^\circ$ / (J·K^{-1}·mol^{-1}·10^2)	-1.3672	Wang *et al.* (1996)
$\Delta_{r2} C_p^\circ$ / (J·K^{-1}·mol^{-1}·10)	7.23†	Balakrishnan (1988)
$\Delta_{r4} C_p^\circ$ / (J·K^{-1}·mol^{-1}·10^2)	2.961	($\Delta_{r2} C_p^\circ + \Delta_{rw} C_p^\circ$)

Thermodynamic Parameter	Value of Parameter	Source
	Glycine	
$\ln K_1$	-5.4003	Wang *et al.* (1996)
$\ln K_2$ / (10)	-2.2515	Martell and Smith (1974)
$\ln K_4$	9.713	($\ln K_2 + \ln K_w$)
$\Delta_{r1} H°$ / (J·mol^{-1}·10^3)	3.9213	Wang *et al.* (1996)
$\Delta_{r2} H°$ / (J·mol^{-1}·10^4)	4.44	Martell and Smith (1974)
$\Delta_{r4} H°$ / (J·mol^{-1}·10^4)	-1.15	($\Delta_{r2} H° + \Delta_{rw} H°$)
$\Delta_{r1} C_p^o$ / (J·K^{-1}·mol^{-1}·10^2)	-1.1784	Wang *et al.* (1996)
$\Delta_{r2} C_p^o$ / (J·K^{-1}·mol^{-1}·10)	7.23†	Balakrishnan (1988)
$\Delta_{r4} C_p^o$ / (J·K^{-1}·mol^{-1}·10^2)	2.961	($\Delta_{r2} C_p^o + \Delta_{rw} C_p^o$)
	Proline	
$\ln K_1$	-4.495	Smith and Martell (1982)
$\ln K_2$ / (10)	-2.4500	Smith and Martell (1982)
$\ln K_4$	7.725	($\ln K_2 + \ln K_w$)
$\Delta_{r1} H°$ / (J·mol^{-1}·10^3)	1.3	Smith and Martell (1982)
$\Delta_{r2} H°$ / (J·mol^{-1}·10^4)	4.330	Smith and Martell (1982)
$\Delta_{r4} H°$ / (J·mol^{-1}·10^4)	-1.250	($\Delta_{r2} H° + \Delta_{rw} H°$)
$\Delta_{r1} C_p^o$ / (J·K^{-1}·mol^{-1}·10^2)	-1.1670‡	Wang *et al.* (1996)
$\Delta_{r2} C_p^o$ / (J·K^{-1}·mol^{-1}·10)	6.18‡‡	Balakrishnan (1988)
$\Delta_{r4} C_p^o$ / (J·K^{-1}·mol^{-1}·10^2)	2.856	($\Delta_{r2} C_p^o + \Delta_{rw} C_p^o$)

† Determined by averaging the $\Delta_r C_p^o$ values for the deprotonation of the NH_3^+ group in 3-methoxypropylamine and 2-amino-2-methyl-1-propanol reported by Balakrishnan (1988). ‡ Determined by averaging the $\Delta_r C_p^o$ values for the protonation of the COO^- group in alanine, glycine, and 2-aminobutyric acid reported by Wang *et al.* (1996). ‡‡ Assumed equal to the value of $\Delta_r C_p^o$ for the deprotonation of the NH_3^+ group in pyrrolidine reported by Balakrishnan (1988).

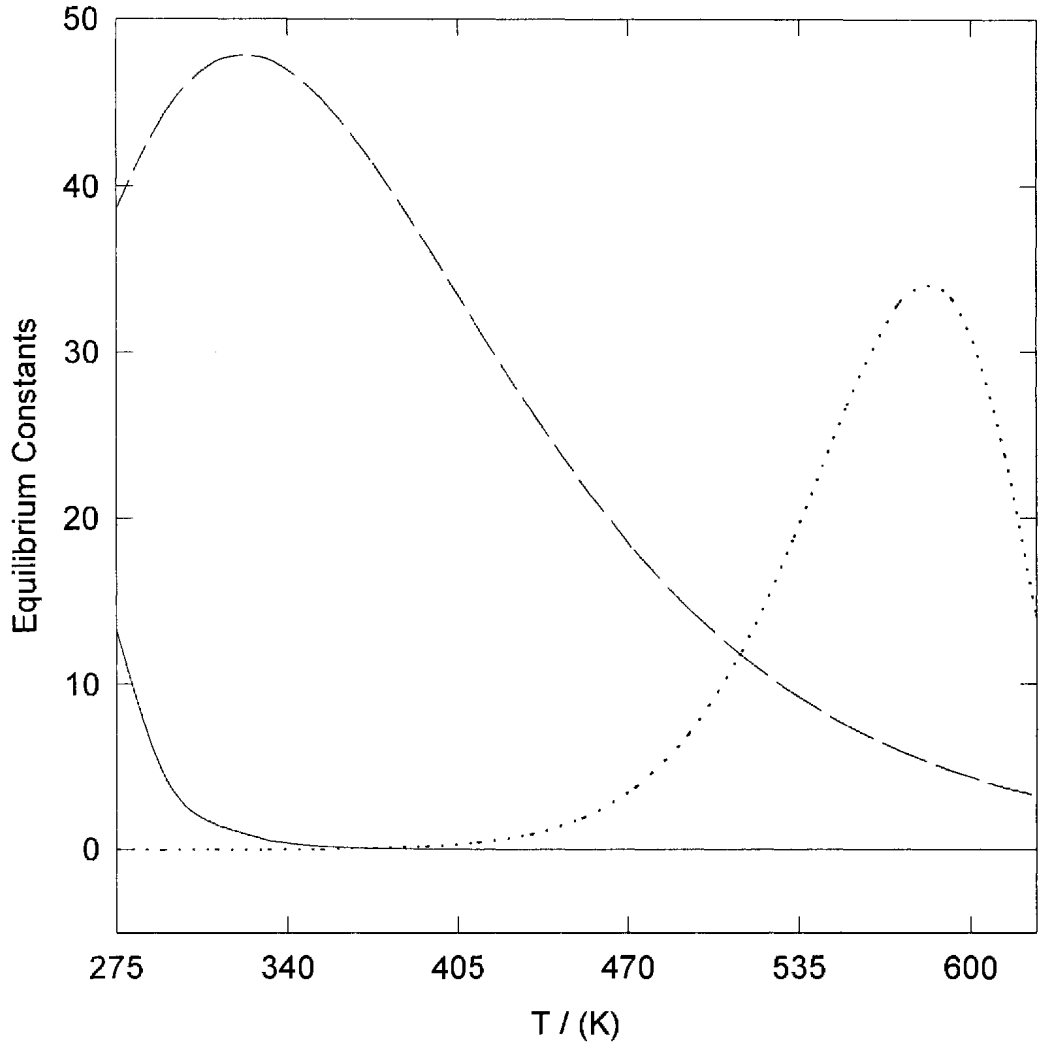

Figure 4.5.2.1 The values of K_1, K_2, and K_3 for α-alanine as a function of temperature. The lines represent: – – –, $K_1 \cdot 10^4$; ·····, $K_2 \cdot 10^7$; ———, $K_3 \cdot 10^{-7}$.

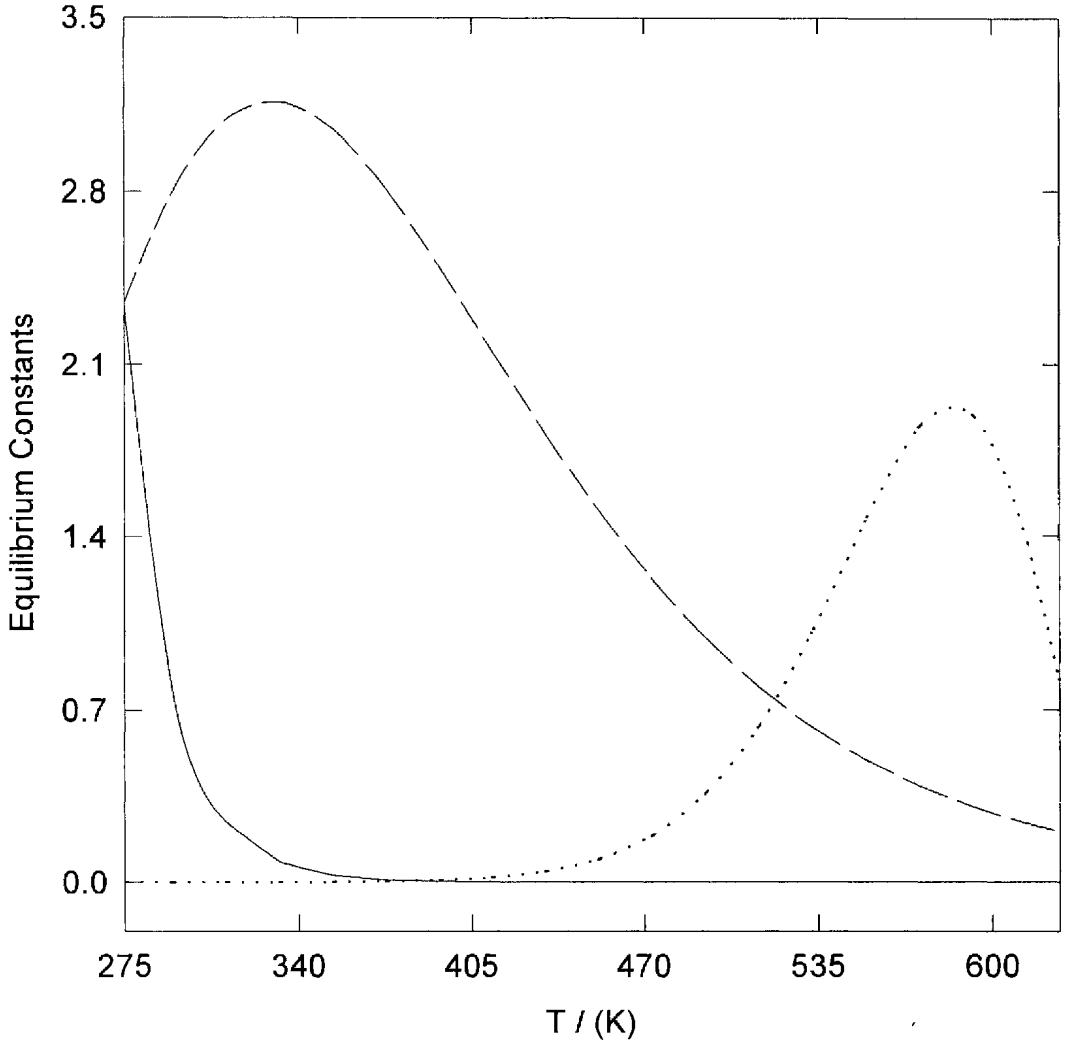

Figure 4.5.2.2 The values of K_1, K_2, and K_3 for β-alanine as a function of temperature. The lines represent: – – –, $K_1 \cdot 10^2$; ·····, $K_2 \cdot 10^6$; ——, $K_3 \cdot 10^{-9}$.

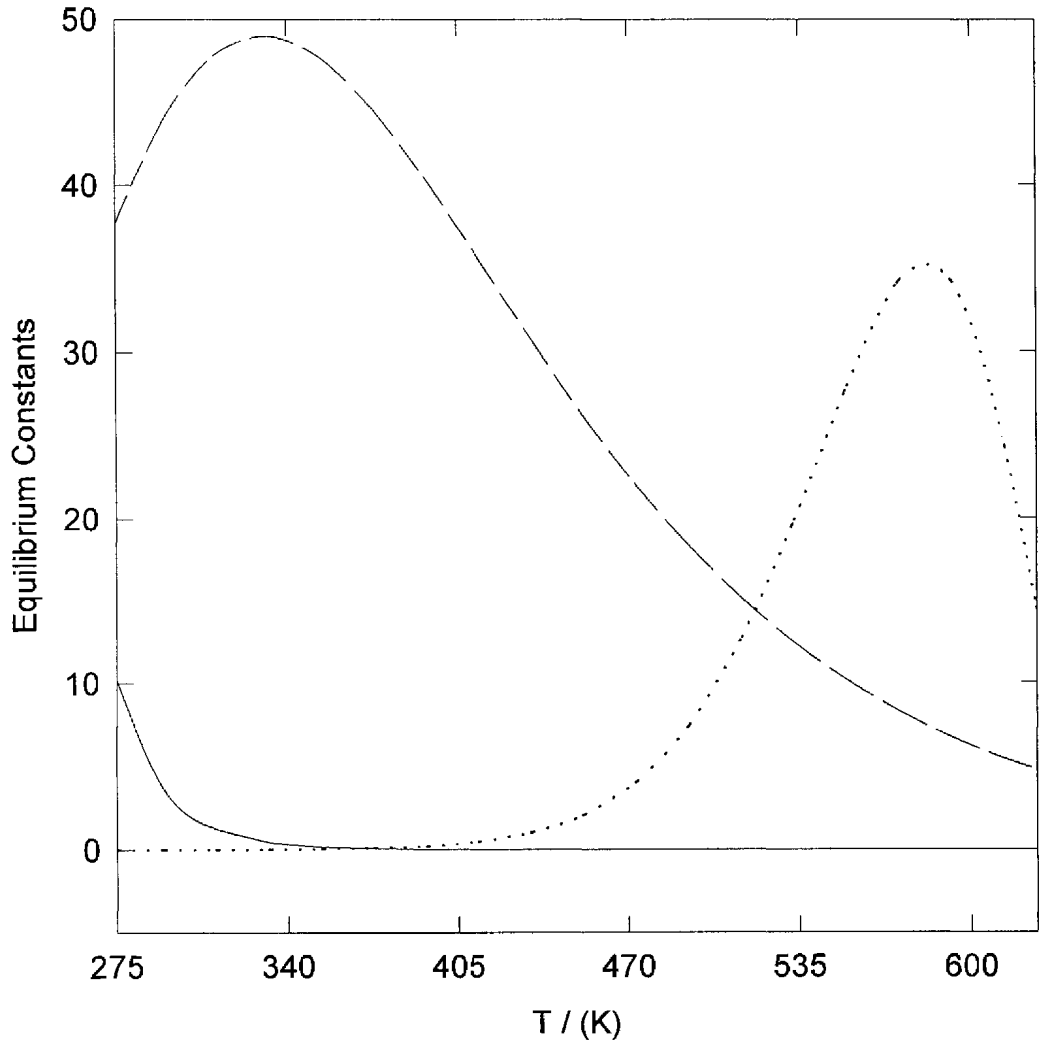

Figure 4.5.2.3 The values of K_1, K_2, and K_3 for glycine as a function of temperature. The lines represent: – – –, $K_1 \cdot 10^4$; ·····, $K_2 \cdot 10^7$; ——, $K_3 \cdot 10^{-7}$.

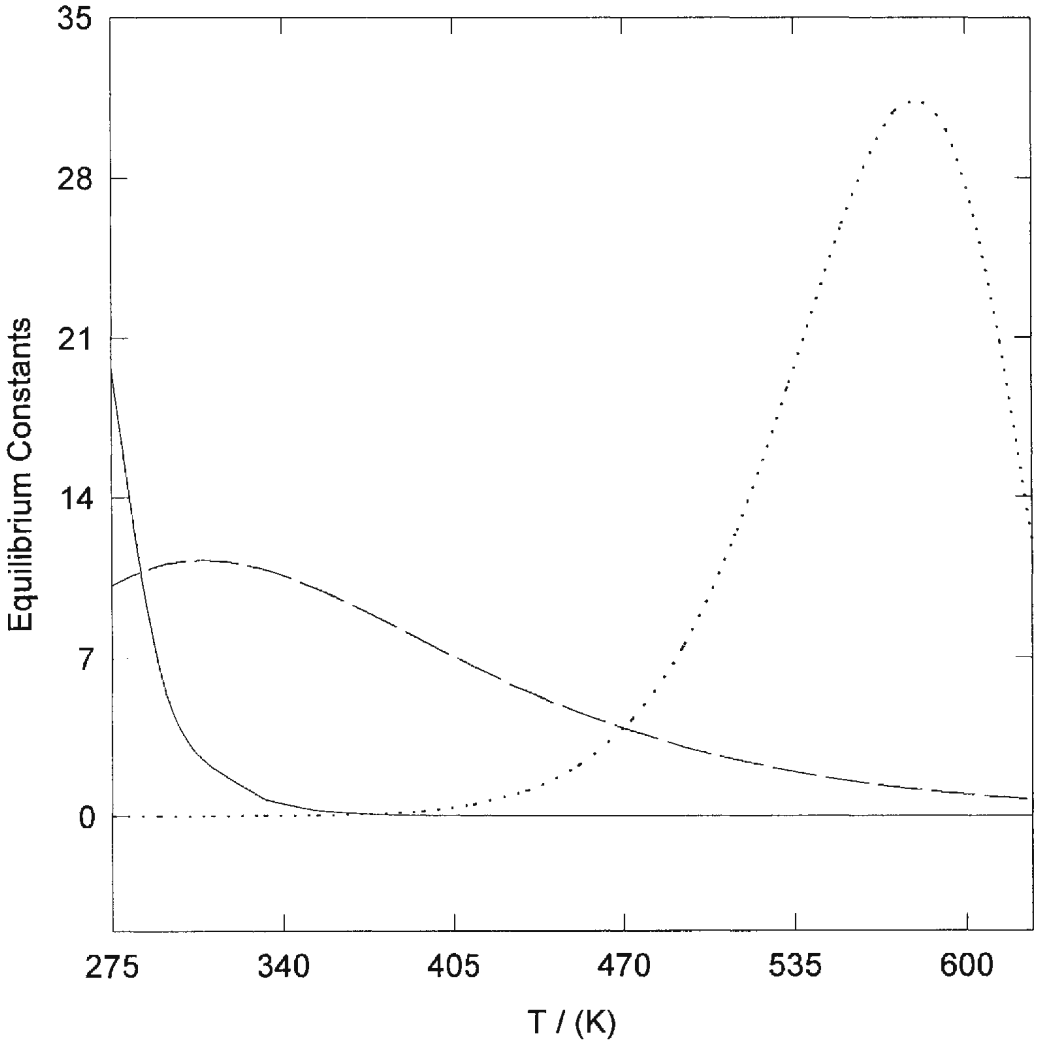

Figure 4.5.2.4 The values of K_1, K_2, and K_3 for proline as a function of temperature. The lines represent: – – –, $K_1 \cdot 10^3$; ·····, $K_2 \cdot 10^8$; ——, $K_3 \cdot 10^{-8}$.

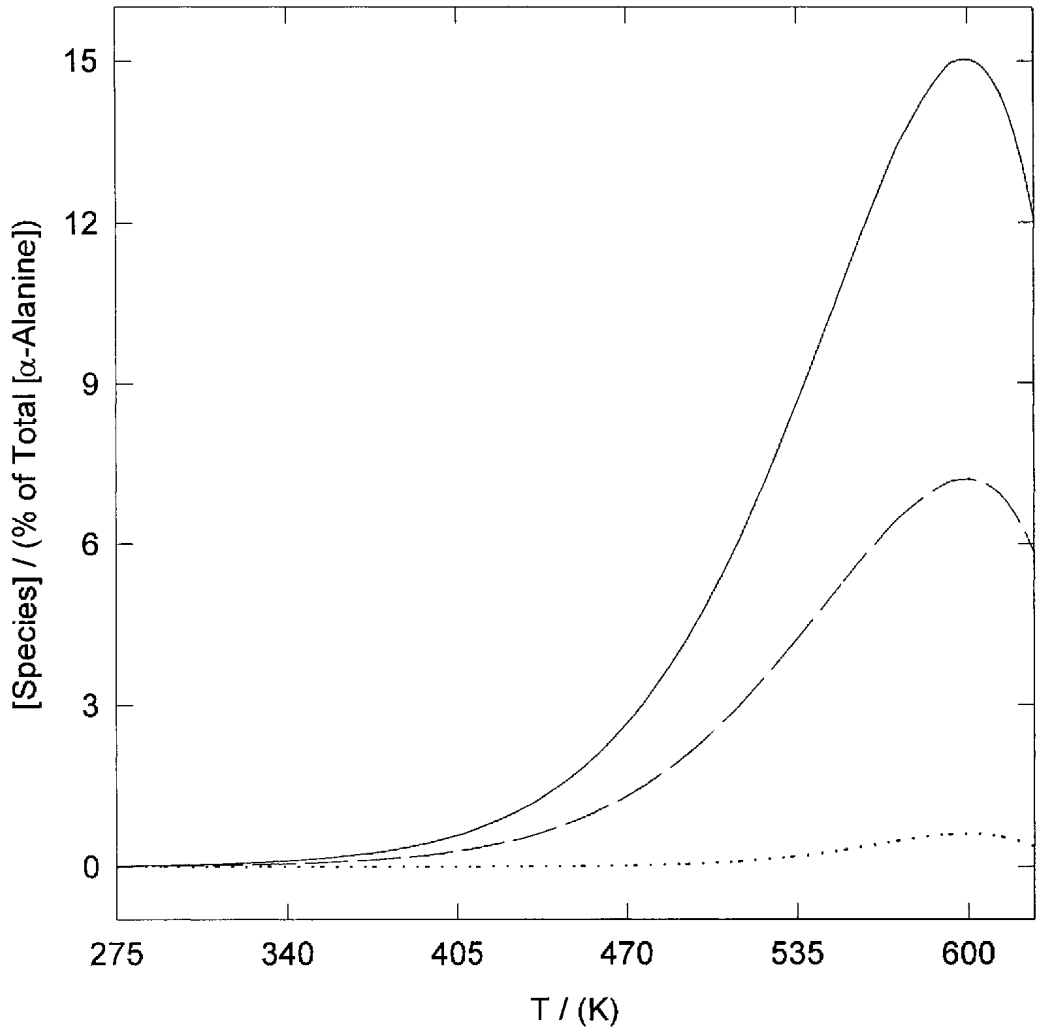

Figure 4.5.2.5 The values of $[H_2A^-]$, $[A^-]$, and $[HA^o]$ for α-alanine as a function of temperature, where the sum of $[HA^{\pm}]$, $[H_2A^+]$, $[A^-]$, and $[HA^o]$ is 1 mol·kg^{-1}. Lines represent the following: —, $[H_2A^+] + [A^-] + [HA^o]$; - - -, $[H_2A^+] = [A^-]$; ·····, $[HA^o]$.

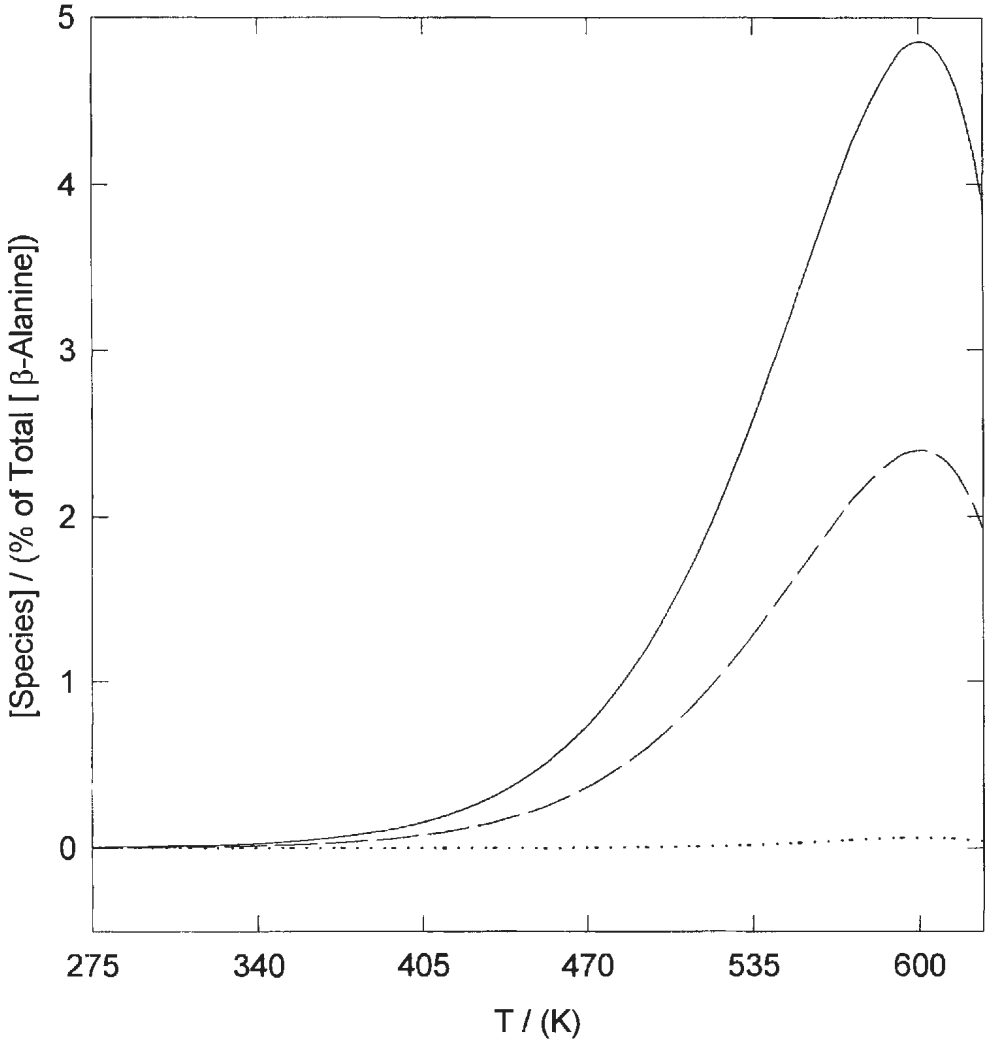

Figure 4.5.2.6 The values of $[H_2A^+]$, [A], and $[HA^o]$ for β-alanine as a function of temperature, where the sum of $[HA^{\pm}]$, $[H_2A^+]$, $[A^-]$, and $[HA^o]$ is 1 mol·kg^{-1}. Lines represent the following: —, $[H_2A^+] + [A^-] + [HA^o]$; - - -, $[H_2A^+] = [A^-]$; ·····, $[HA^o]$.

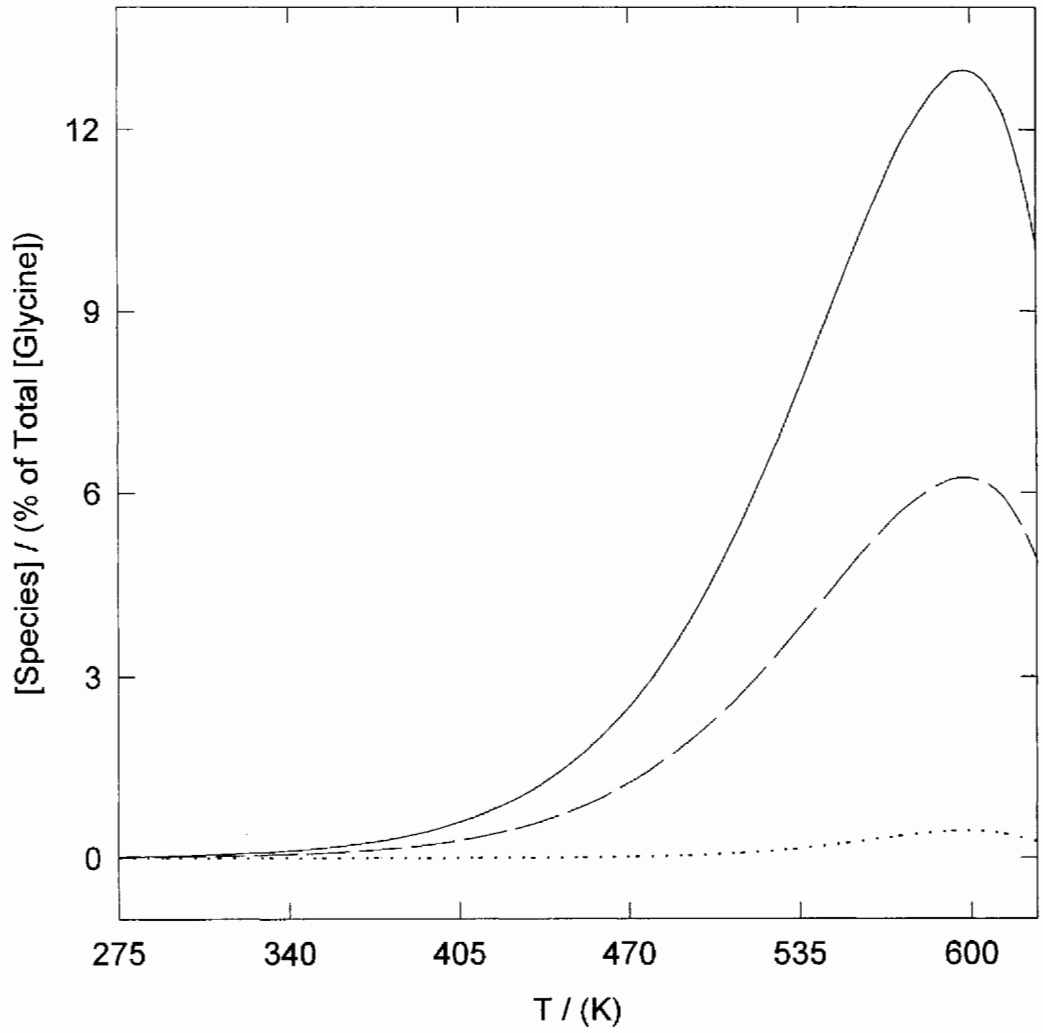

Figure 4.5.2.7 The values of $[H_2A^+]$, $[A^-]$, and $[HA^\circ]$ for glycine as a function of temperature, where the sum of $[HA^\pm]$, $[H_2A^+]$, $[A^-]$, and $[HA^\circ]$ is 1 mol·kg^{-1}. Lines represent the following: —, $[H_2A^+] + [A^-] + [HA^\circ]$; - - -, $[H_2A^+] = [A^-]$; ·····, $[HA^\circ]$.

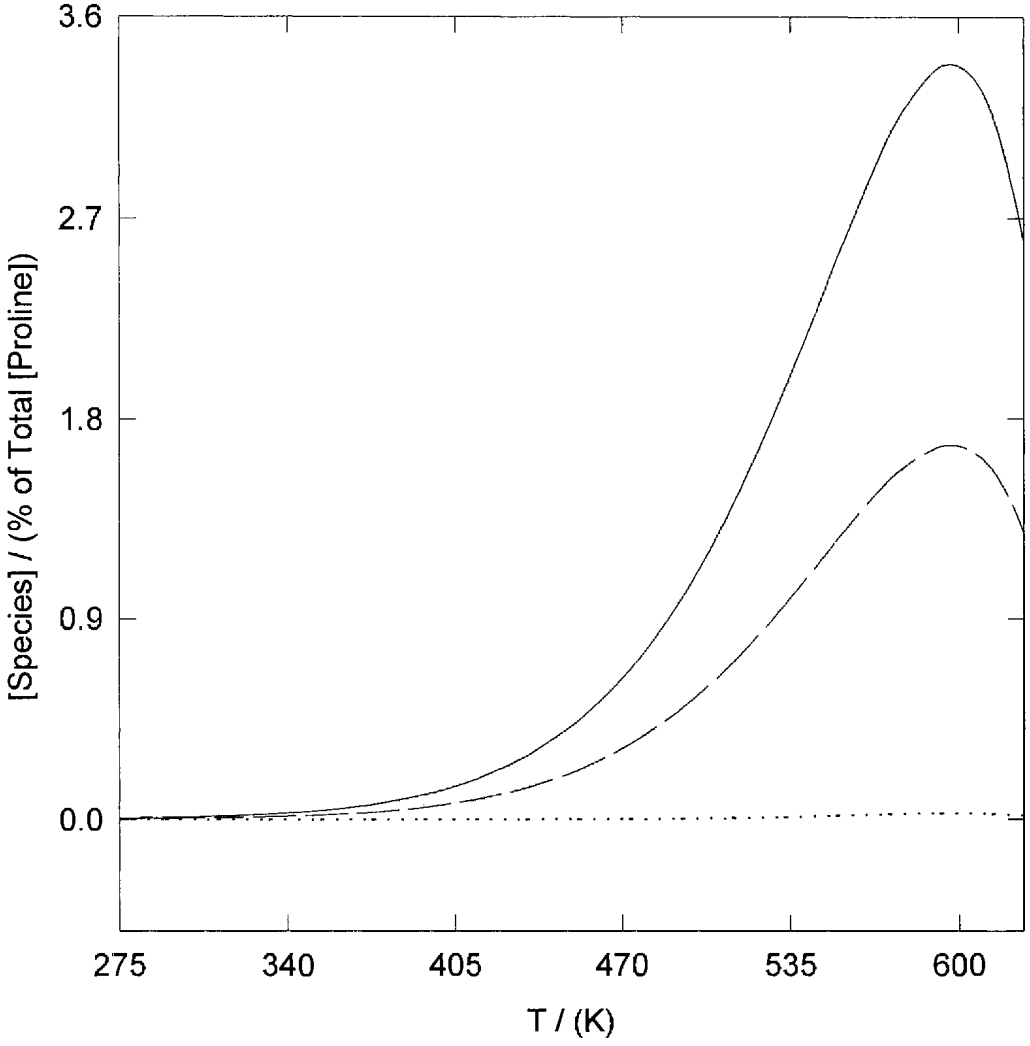

Figure 4.5.2.8 The values of $[H_2A^{\pm}]$, $[A^{-}]$, and $[HA^{o}]$ for proline as a function of temperature, where the sum of $[HA^{\pm}]$, $[H_2A^{+}]$, $[A^{-}]$, and $[HA^{o}]$ is 1 mol·kg^{-1}. Lines represent the following: —, $[H_2A^{+}] + [A^{-}] + [HA^{o}]$; - - -, $[H_2A^{+}] = [A^{-}]$; ·····, $[HA^{o}]$.

4.5.3 Estimates of Speciation from the Yezdimer-Sedlbauer-Wood Functional Group Additivity Model.

The Yezdimer-Sedlbauer-Wood functional group additivity model was used to predict the standard partial molar Gibbs free energy of formation $\Delta_f G^\circ$ as a function of temperature and pressure for the zwitterionic and ionic forms of aqueous α-alanine and glycine. The values of $\Delta_f H^\circ$ and $\Delta_f S^\circ$ at 298.15 K and 0.1 MPa for α-alanine and glycine required to calculate $\Delta_f G^\circ$ were taken from the compilation of Amend and Helgeson (1997).

The standard partial molar Gibbs free energy of reaction $\Delta_r G^\circ$ was determined from the usual expression:

$$\Delta_r G^o = \sum_{products} \Delta_f G^o - \sum_{reactants} \Delta_f G^o \qquad (4.5.3.1)$$

The following expression was used to calculate the equilibrium constant for the reaction as a function of temperature and pressure:

$$\ln K = -\left(\frac{\Delta_r G^o}{RT} \right) \qquad (4.5.3.2)$$

K_3 was assumed to be approximately equal to (K_1 / K_2).

The values of K_1, K_2, and K_3 for α-alanine and glycine are plotted as a function of temperature in Figures 4.5.3.1 and 4.5.3.2, respectively. These temperature dependent values of K_1, K_2, and K_3 were used to determine the speciation of the aqueous amino acids according to the method described in Section 4.5.1. The distribution of species is plotted as a function of temperature in Figure 4.5.3.3 and 4.5.3.4 for α-alanine and glycine, respectively.

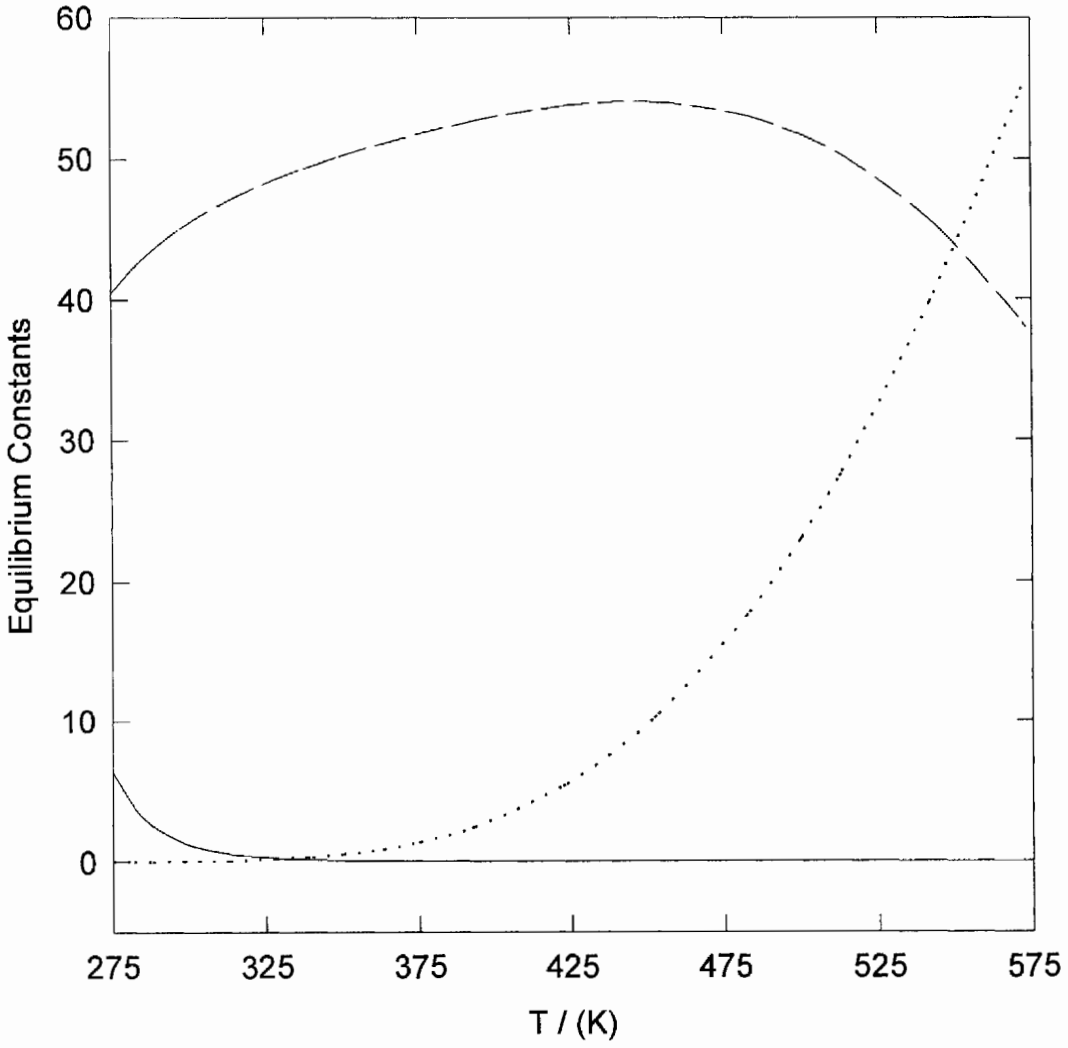

Figure 4.5.3.1 The values of K_1, K_2, and K_3 for α-alanine as a function of temperature. The lines represent: – – –, $K_1 \cdot 10^4$; ·····, $K_2 \cdot 10^7$; ——, $K_3 \cdot 10^{-6}$.

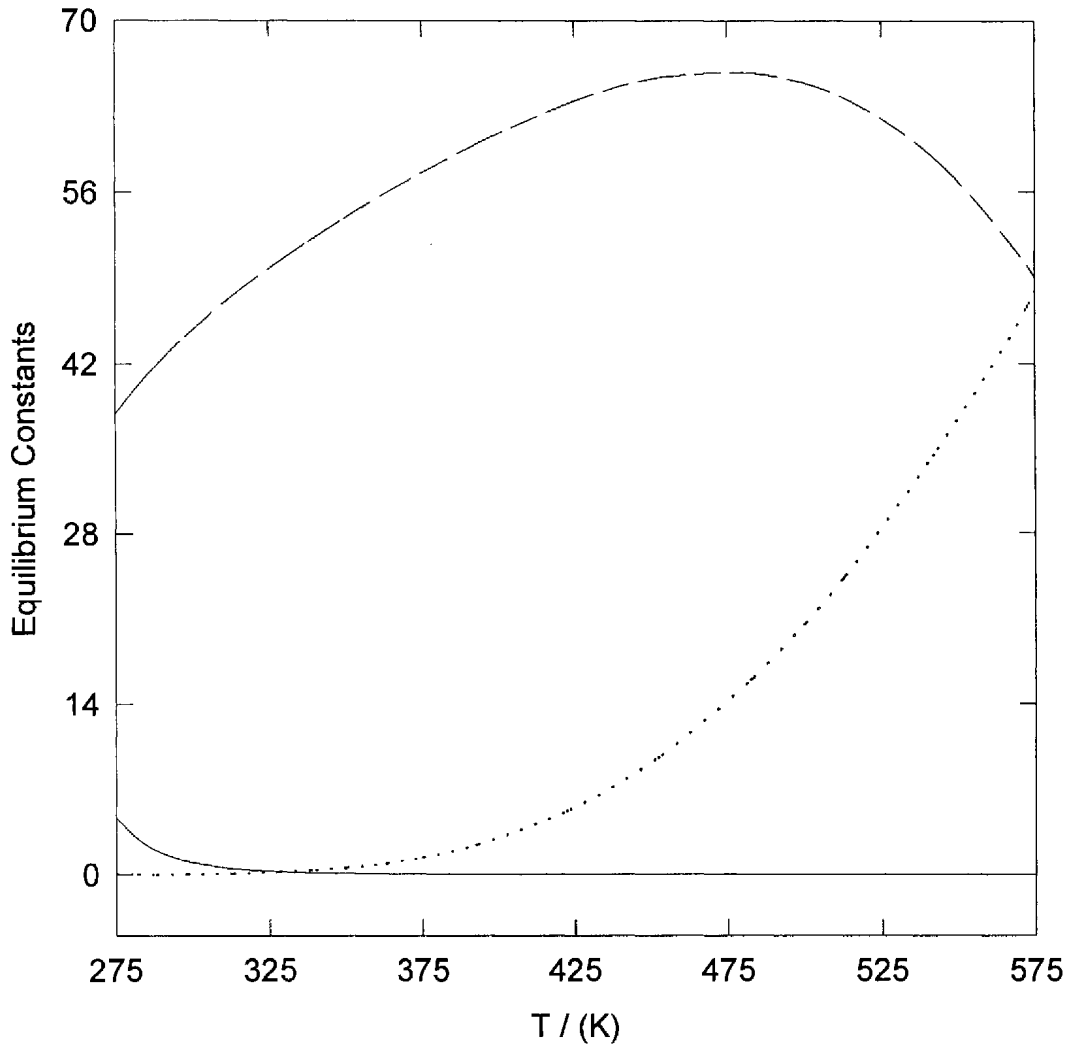

Figure 4.5.3.2 The values of K_1, K_2, and K_3 for glycine as a function of temperature. The lines represent: – – –, $K_1 \cdot 10^4$; ·····, $K_2 \cdot 10^7$; ——, $K_3 \cdot 10^{-6}$.

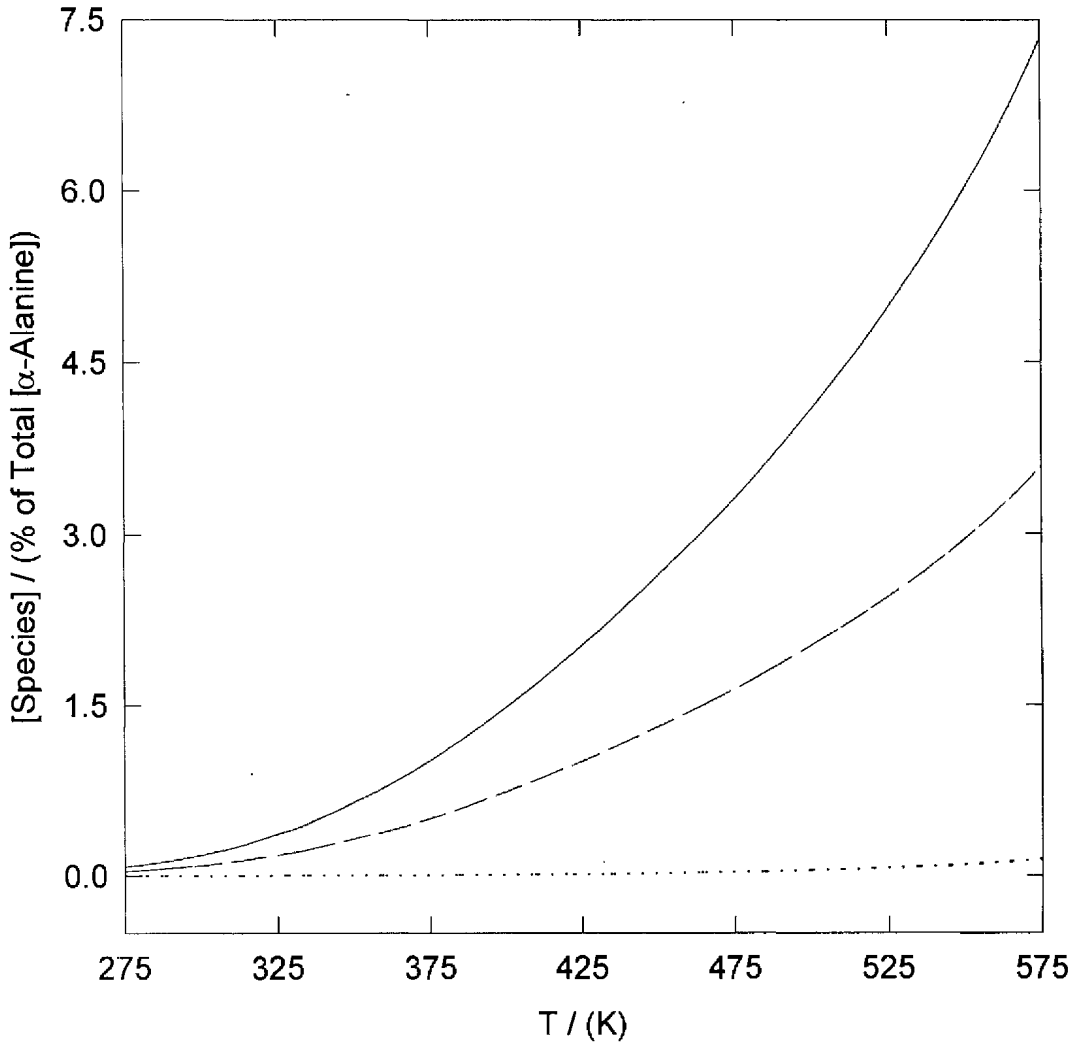

Figure 4.5.3.3 The values of $[H_2A^+]$, $[A^-]$, and $[HA^\circ]$ for α-alanine as a function of temperature, where the sum of $[HA^\pm]$, $[H_2A^+]$, $[A^-]$, and $[HA^\circ]$ is 1 mol·kg^{-1}. Lines represent the following: —, $[H_2A^+] + [A^-] + [HA^\circ]$; - - -, $[H_2A^+] = [A^-]$; ·····, $[HA^\circ]$.

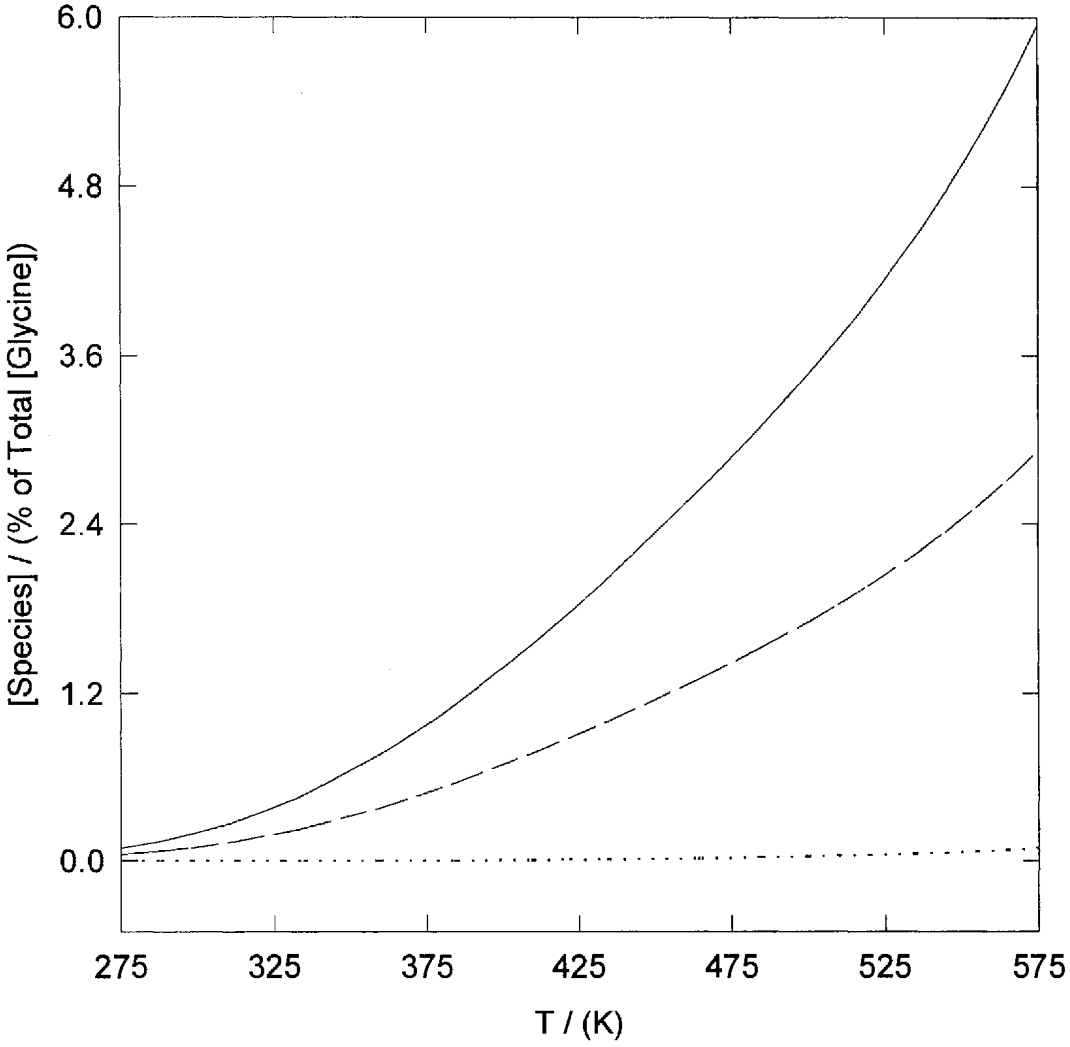

Figure 4.5.3.4 The values of $[H_2A^+]$, $[A^-]$, and $[HA^\circ]$ for glycine as a function of temperature, where the sum of $[HA^\pm]$, $[H_2A^-]$, $[A^-]$, and $[HA^\circ]$ is 1 mol·kg^{-1}. Lines represent the following: —, $[H_2A^+] + [A^-] + [HA^\circ]$; - - -, $[H_2A^+] = [A^-]$; ·····, $[HA^\circ]$.

4.5.4 Estimation of the Zwitterionic Contribution to the Experimentally Determined Values of V° and C_p° for Aqueous α-Alanine and Glycine.

As illustrated in Sections 4.5.2 and 4.5.3 the zwitterionic form of the aqueous amino acids is the predominant species at all temperature at which measurements were made. Although the percentage of aqueous amino acid in the neutral form is negligible at all temperatures, the percentage in the cationic and anionic forms is significant at the higher temperatures as shown in Figures 4.5.3.3 and 4.5.3.4. An estimate of the zwitterionic contribution to the experimentally determined values of V° and C_p° is required before solvation effects can be discussed in Sections 4.6 and 4.7.

In Section 4.5.3 the Yezdimer-Sedlbauer-Wood functional group additivity model was used to estimate the speciation of aqueous α-alanine and glycine. The standard partial molar volumes and standard partial molar heat capacities of the ionic and neutral forms of α-alanine and glycine were estimated using the Yezdimer-Sedlbauer-Wood functional group additivity model. Table 4.5.4.1 lists the estimated values of $V^\circ_{Anionic}$ (standard partial molar volume of A^-), $V^\circ_{Cationic}$ (standard partial molar volume of H_2A^+), and $V^\circ_{Neutral}$ (standard partial molar volume of HA°) at the temperatures and pressures corresponding to the experimentally determined values of V°. The uncertainties were assigned using the error estimates given by Yezdimer *et al.* (2000). The following expression was used to calculate the values of $V^\circ_{Zwitterionic}$ (standard partial molar volume of $HA^\pm$) listed in Table 4.5.4.1:

$$V^{o}_{Zwitterionic} = \frac{V^{o} - [A^{-}]V^{o}_{Anionic} - [H_2A^{+}]V^{o}_{Cationic} - [HA^{\circ}]V^{o}_{Neutral}}{[HA^{\pm}]} \qquad (4.5.4.1)$$

The uncertainty associated with equation (4.5.4.1) was estimated with the expression:

$$[HA^{\pm}]^2(\sigma_{V^{o}_{Zwitterionic}})^2 = (\sigma_{V^{o}})^2 + [A^{-}]^2(\sigma_{V^{o}_{Anionic}})^2$$

$$+ [H_2A^{+}]^2(\sigma_{V^{o}_{Cationic}})^2 + [HA^{\circ}]^2(\sigma_{V^{o}_{Neutral}})^2 \qquad (4.5.4.2)$$

The uncertainties associated with $[H_2A^+]$, $[A^-]$, and $[HA^o]$ were estimated from the uncertainties in K and ΔH° (Amend and Helgeson, 1997) and ΔC_p° (Yezdimer *et al.*, 2000). The effect of these is small relative to the uncertainty associated with $V^\circ_{Anionic}$, $V^\circ_{Cationic}$, and $V^\circ_{Neutral}$. Figures 4.5.4.1 and 4.5.4.2 illustrate the difference between the experimentally determined values of V° and the estimated values of $V^\circ_{Zwitterionic}$ for aqueous α-alanine and glycine, respectively. When the uncertainty associated with the values of $(V^\circ - V^\circ_{Zwitterionic})$ is considered, it is clear that only those values obtained for aqueous α-alanine at 423 K and 478 K are significantly different from zero. None of the values of $(V^\circ - V^\circ_{Zwitterionic})$ obtained for aqueous glycine are significantly different from zero.

The values of $C^\circ_{p,Anionic}$ (standard partial molar heat capacity of A^-), $C^\circ_{p,Cationic}$ (standard partial molar heat capacity of H_2A^+), and $C^\circ_{p,Neutral}$ (standard partial molar heat capacity of HA^o) at the temperatures and pressures corresponding to the experimentally determined values of C_p° are listed in Table 4.5.4.2. The following expression was used to calculate the values of $C^\circ_{p,Zwitterionic}$ (standard partial molar heat capacity of $HA^\pm$) listed in Table 4.5.4.2:

$$C^{o}_{p,\,Zwitterionic} = \frac{C^{o}_{p} - [A^{-}]C^{o}_{p,\,Antonic} - [H_2A^{+}]C^{o}_{p,\,Cationic} - [HA^{\circ}]C^{o}_{p,\,Neutral}}{[HA^{\pm}]} \qquad (4.5.4.3)$$

$$[HA^{\pm}]^2(\sigma_{C^{o}_{p,\,Zwitterionic}})^2 = (\sigma_{C^{o}_{p}})^2 + [A^{-}]^2(\sigma_{C^{o}_{p,\,Anionic}})^2 + [H_2A^{+}]^2(\sigma_{C^{o}_{p,\,Cationic}})^2 + [HA^{\circ}]^2(\sigma_{C^{o}_{p,\,Neutral}})^2 \qquad (4.5.4.4)$$

The uncertainties associated with $[H_2A^+]$, $[A^-]$, and $[HA^\circ]$ were again neglected since they are small relative to the uncertainty associated with $C^\circ_{p,\,Anionic}$, $C^\circ_{p,\,Cationic}$, and $C^\circ_{p,\,Neutral}$. Figures 4.5.4.3 and 4.5.4.4 illustrate the difference between the experimentally determined values of C°_p and the estimated values of $C^\circ_{p,Zwitterionic}$ for aqueous α-alanine and glycine, respectively. Considering the uncertainty associated with the estimated values of $(C^\circ_p - C^\circ_{p,Zwitterionic})$, it is clear that only those values obtained for aqueous α-alanine at $T \geq 424$ K and those values obtained for aqueous glycine at $T \geq 474$ K are significantly different from zero.

In all cases where the values of $(V^\circ - V^\circ_{Zwitterionic})$ and $(C^\circ_p - C^\circ_{p,Zwitterionic})$ were significantly different from zero, the differences remained small when compared with the values of V° and C°_p, respectively. The error introduced by ignoring the speciation of the aqueous amino acids at the temperatures corresponding to the experimental results is less than ± 0.15 $cm^3 \cdot mol^{-1}$ and ± 2.4 $J \cdot K^{-1} \cdot mol^{-1}$.

Table 4.5.4.1 Values of $V^{\circ}_{Cationic}$, $V^{\circ}_{Anionic}$, $V^{\circ}_{Neutral}$, and $V^{\circ}_{Zwitterionic}$ for aqueous α-alanine and glycine at the temperatures and pressures corresponding to the experimentally determined values of V°.

T (K)	p (MPa)	$V^{\circ}_{Cationic}$ ($cm^3 \cdot mol^{-1}$)	$V^{\circ}_{Anionic}$ ($cm^3 \cdot mol^{-1}$)	$V^{\circ}_{Neutral}$ ($cm^3 \cdot mol^{-1}$)	$V^{\circ}_{Zwitterionic}$ ($cm^3 \cdot mol^{-1}$)	$V^{\circ}-V^{\circ}_{Zwitterionic}$ ($cm^3 \cdot mol^{-1}$)
			α-Alanine			
288.15	0.10	67.59 ± 1.50	59.52 ± 1.31	70.86 ± 0.85	59.74 ± 0.06	0.01 ± 0.09
298.10	0.10	68.15 ± 1.50	60.38 ± 1.33	72.01 ± 0.86	60.48 ± 0.01	0.01 ± 0.02
298.14	0.10	68.15 ± 1.50	60.38 ± 1.33	72.02 ± 0.86	60.49 ± 0.05	0.01 ± 0.07
298.15	0.10	68.15 ± 1.50	60.38 ± 1.33	72.02 ± 0.86	60.46 ± 0.02	0.01 ± 0.03
313.15	0.10	69.01 ± 1.52	61.07 ± 1.34	73.48 ± 0.88	61.09 ± 0.03	0.01 ± 0.04
328.15	0.10	69.91 ± 1.54	61.26 ± 1.35	74.78 ± 0.90	61.52 ± 0.06	0.02 ± 0.09
333.21	10.047	70.25 ± 1.55	61.25 ± 1.35	75.03 ± 0.90	61.63 ± 0.01	0.02 ± 0.01
381.70	10.057	73.25 ± 1.61	59.64 ± 1.31	78.90 ± 0.95	61.67 ± 0.03	0.05 ± 0.04
422.42	10.036	75.72 ± 1.67	56.12 ± 1.23	82.41 ± 0.99	60.79 ± 0.02	0.10 ± 0.02
477.24	10.058	78.27 ± 1.72	45.77 ± 1.01	87.81 ± 1.05	57.76 ± 0.08	0.15 ± 0.10
523.36	10.063	77.91 ± 1.71	24.22 ± 0.70	92.96 ± 1.12	51.69 ± 0.08	-0.01 ± 0.11
334.65	19.977	70.38 ± 1.55	61.25 ± 1.35	74.97 ± 0.90	61.87 ± 0.02	0.02 ± 0.03
383.20	19.939	73.26 ± 1.61	59.79 ± 1.32	78.76 ± 0.95	61.81 ± 0.07	0.05 ± 0.10
423.47	19.976	75.60 ± 1.66	56.62 ± 1.25	82.12 ± 0.99	61.01 ± 0.02	0.10 ± 0.03
478.67	19.967	78.02 ± 1.72	47.45 ± 1.04	87.33 ± 1.05	58.14 ± 0.07	0.16 ± 0.09
523.39	19.934	77.88 ± 1.71	30.41 ± 0.70	92.05 ± 1.10	52.72 ± 0.12	0.09 ± 0.16
298.13	30.769	68.59 ± 1.51	60.15 ± 1.32	71.71 ± 0.86	61.10 ± 0.05	0.01 ± 0.07

T (K)	p (MPa)	$V^{\circ}_{Cationic}$ ($cm^3 \cdot mol^{-1}$)	$V^{\circ}_{Anionic}$ ($cm^3 \cdot mol^{-1}$)	$V^{\circ}_{Neutral}$ ($cm^3 \cdot mol^{-1}$)	$V^{\circ}_{Zwitterionic}$ ($cm^3 \cdot mol^{-1}$)	V°-$V^{\circ}_{Zwitterionic}$ ($cm^3 \cdot mol^{-1}$)
			Glycine			
288.15	0.10	51.64 ± 1.13	43.57 ± 0.96	54.92 ± 0.66	42.40 ± 0.01	0.01 ± 0.01
298.15	0.10	52.07 ± 1.15	44.30 ± 0.97	55.93 ± 0.67	43.21 ± 0.11	0.01 ± 0.16
298.15	0.10	52.07 ± 1.15	44.29 ± 0.97	55.93 ± 0.67	43.30 ± 0.05	0.01 ± 0.06
313.15	0.10	52.66 ± 1.16	44.72 ± 0.98	57.13 ± 0.69	43.74 ± 0.06	0.02 ± 0.09
328.15	0.10	53.24 ± 1.17	44.59 ± 0.98	58.11 ± 0.70	44.37 ± 0.06	0.02 ± 0.09
397.75	10.002	55.67 ± 1.22	39.95 ± 0.88	61.67 ± 0.74	43.13 ± 0.36	0.06 ± 0.51
423.02	10.006	56.30 ± 1.24	36.59 ± 0.80	63.01 ± 0.76	42.04 ± 0.24	0.08 ± 0.33
472.93	10.005	56.51 ± 1.24	25.33 ± 0.70	65.72 ± 0.79	35.85 ± 0.52	0.15 ± 0.73
397.00	20.001	55.64 ± 1.22	40.48 ± 0.89	61.43 ± 0.74	43.92 ± 0.16	0.06 ± 0.23
423.47	20.007	56.29 ± 1.24	37.31 ± 0.82	62.80 ± 0.75	42.12 ± 0.30	0.09 ± 0.43
472.85	19.996	56.57 ± 1.24	27.55 ± 0.70	65.48 ± 0.79	37.69 ± 0.58	0.13 ± 0.82
298.15	30.828	52.42 ± 1.15	43.97 ± 0.97	55.54 ± 0.67	43.67 ± 0.08	0.01 ± 0.11
398.00	30.009	55.67 ± 1.22	40.76 ± 0.90	61.27 ± 0.74	44.43 ± 0.25	0.05 ± 0.35
422.94	29.999	56.26 ± 1.24	38.06 ± 0.84	62.55 ± 0.75	43.56 ± 0.27	0.06 ± 0.38
472.03	29.989	56.59 ± 1.25	29.50 ± 0.70	65.22 ± 0.78	39.72 ± 0.32	0.09 ± 0.45

Table 4.5.4.2 Values of $C^{\circ}_{p,\,Cationic}$, $C^{\circ}_{p,\,Anionic}$, $C^{\circ}_{p,\,Neutral}$, and $C^{\circ}_{p,Zwitterionic}$ for aqueous α-alanine and glycine at the temperatures and pressures corresponding to the experimentally determined values of C°_{p}.

T (K)	p (MPa)	$C^{\circ}_{p,\,Cationic}$ (J·mol^{-1}·K^{-1})	$C^{\circ}_{p,\,Anionic}$ (J·mol^{-1}·K^{-1})	$C^{\circ}_{p,\,Neutral}$ (J·mol^{-1}·K^{-1})	$C^{\circ}_{p,Zwitterionic}$ (J·mol^{-1}·K^{-1})	C°_{p} - $C^{\circ}_{p,Zwitterionic}$ (J·mol^{-1}·K^{-1})
			α-Alanine			
288.15	0.10	184.80 ± 9.00	10.82 ± 9.00	173.34 ± 6.93	125.71 ± 0.74	-0.03 ± 1.04
298.10	0.10	182.60 ± 9.00	32.52 ± 9.00	181.14 ± 7.25	141.26 ± 0.57	-0.06 ± 0.80
298.15	0.10	182.58 ± 9.00	32.60 ± 9.00	181.16 ± 7.25	141.78 ± 0.44	-0.06 ± 0.63
313.15	0.10	177.63 ± 9.00	48.33 ± 9.00	183.95 ± 7.36	153.35 ± 1.16	-0.11 ± 1.64
328.15	0.10	177.78 ± 9.00	58.18 ± 9.00	190.63 ± 7.63	163.85 ± 2.26	-0.18 ± 3.20
323.173	0.10	177.17 ± 9.00	55.15 ± 9.00	187.76 ± 7.51	167.94 ± 0.25	-0.18 ± 0.35
373.563	2.08	194.00 ± 9.00	84.08 ± 9.00	235.33 ± 9.41	182.10 ± 0.59	-0.43 ± 0.84
423.772	2.01	202.16 ± 9.00	94.77 ± 9.00	287.55 ± 11.50	180.64 ± 0.36	-0.63 ± 0.51
447.746	10.30	197.81 ± 9.00	95.07 ± 9.00	305.30 ± 12.21	176.25 ± 0.34	-0.75 ± 0.46
473.799	5.62	180.42 ± 9.00	58.22 ± 9.00	320.72 ± 12.83	172.64 ± 0.40	-1.70 ± 0.55
323.168	29.77	175.07 ± 9.00	70.85 ± 9.00	191.32 ± 7.65	174.42 ± 0.31	-0.17 ± 0.44
373.543	30.03	194.00 ± 9.00	94.94 ± 9.00	234.06 ± 9.36	188.47 ± 0.38	-0.43 ± 0.54
423.769	30.56	205.07 ± 9.00	115.51 ± 9.00	284.61 ± 11.38	187.53 ± 0.36	-0.53 ± 0.51
447.857	30.22	201.57 ± 9.00	115.90 ± 9.00	303.07 ± 12.12	185.45 ± 0.20	-0.66 ± 0.25
473.818	30.19	189.86 ± 9.00	105.01 ± 9.00	317.59 ± 12.70	183.61 ± 0.31	-1.14 ± 0.41

T (K)	p (MPa)	$C^{\circ}_{p,\,Cationic}$ (J·mol^{-1}·K^{-1})	$C^{\circ}_{p,\,Anionic}$ (J·mol^{-1}·K^{-1})	$C^{\circ}_{p,\,Neutral}$ (J·mol^{-1}·K^{-1})	$C^{\circ}_{p,Zwitterionic}$ (J·mol^{-1}·K^{-1})	C°_{p} - $C^{\circ}_{p,Zwitterionic}$ (J·mol^{-1}·K^{-1})
			Glycine			
288.15	0.10	91.35 ± 9.00	-82.63 ± 9.00	79.89 ± 3.20	14.69 ± 0.75	-0.01 ± 1.06
298.15	0.10	95.47 ± 9.00	-54.51 ± 9.00	94.05 ± 3.76	37.38 ± 0.72	-0.03 ± 1.02
313.15	0.10	97.54 ± 9.00	-31.76 ± 9.00	103.86 ± 4.15	58.38 ± 1.63	-0.07 ± 2.31
328.15	0.10	101.24 ± 9.00	-18.36 ± 9.00	114.09 ± 4.56	76.38 ± 0.97	-0.14 ± 1.37
323.170	0.10	99.77 ± 9.00	-22.25 ± 9.00	110.36 ± 4.41	70.00 ± 0.27	-0.12 ± 0.38
373.560	2.09	118.10 ± 9.00	8.19 ± 9.00	159.43 ± 6.38	90.15 ± 1.74	-0.26 ± 2.46
423.780	2.03	124.10 ± 9.00	16.73 ± 9.00	209.49 ± 8.38	84.17 ± 1.80	-0.24 ± 2.55
473.810	5.56	102.25 ± 9.00	-20.11 ± 9.00	242.59 ± 9.70	71.17 ± 0.23	-0.82 ± 0.27
499.099	5.55	70.49 ± 9.00	-87.48 ± 9.00	249.71 ± 9.99	63.14 ± 0.55	-2.40 ± 0.75
323.166	30.12	99.72 ± 9.00	-4.32 ± 9.00	116.03 ± 4.64	80.73 ± 0.21	-0.12 ± 0.30
373.540	30.11	119.59 ± 9.00	20.57 ± 9.00	159.65 ± 6.39	95.99 ± 1.18	-0.24 ± 1.67
423.761	30.34	129.16 ± 9.04	39.52 ± 9.00	208.74 ± 8.35	92.89 ± 0.80	-0.15 ± 1.12
447.842	30.09	125.97 ± 9.00	40.21 ± 9.00	227.50 ± 9.10	92.11 ± 0.77	-0.19 ± 1.08
473.438	30.20	115.70 ± 9.00	30.87 ± 9.00	243.01 ± 9.72	91.16 ± 0.53	-0.47 ± 0.73
499.096	30.58	96.20 ± 9.00	5.74 ± 9.00	253.46 ± 10.14	88.75 ± 0.30	-1.24 ± 0.37

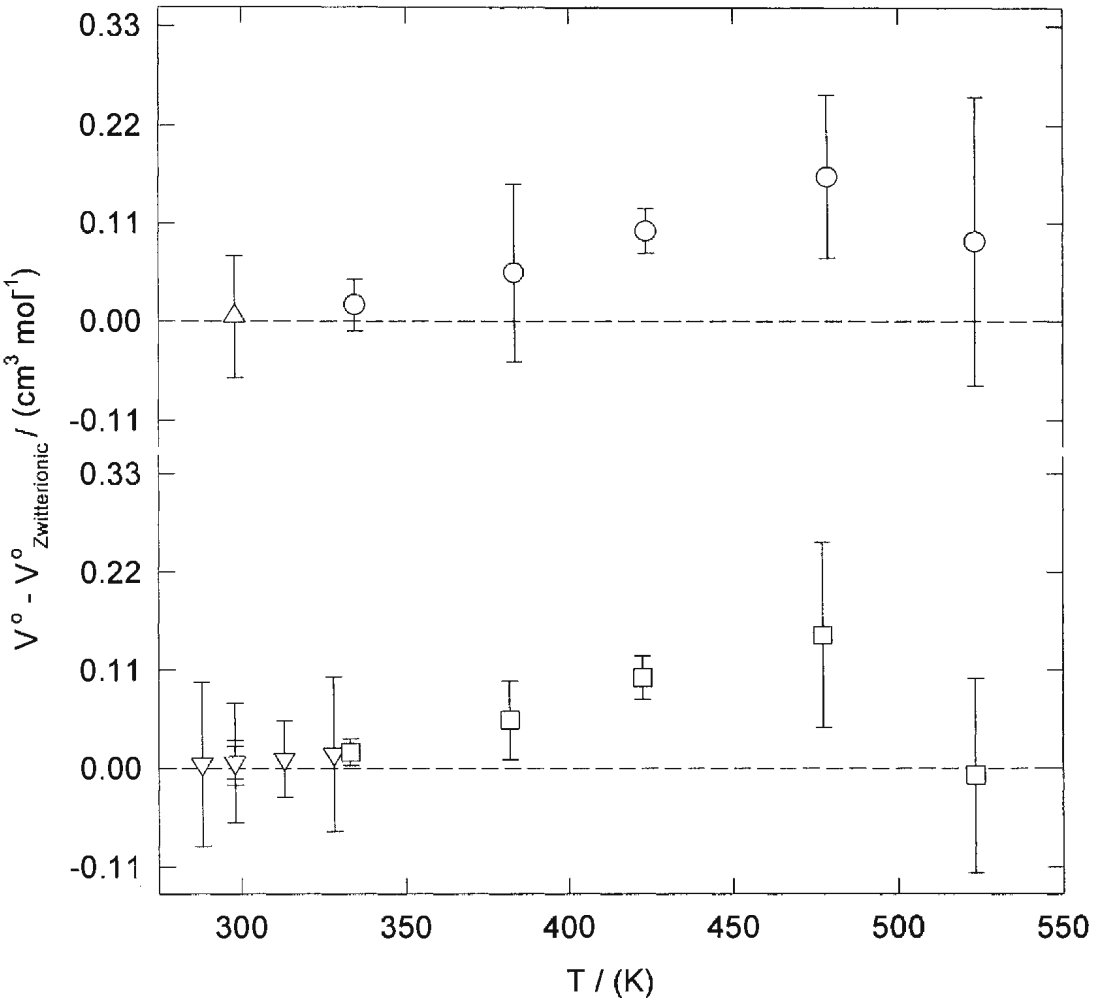

Figure 4.5.4.1 The difference between the experimental values of $V°$ and the estimated values of $V°_{Zwitterionic}$ for aqueous α-alanine. Symbols represent: Δ, 30.77 MPa; ○, 19.96 MPa; □, 10.05 MPa; ∇, 0.1 MPa.

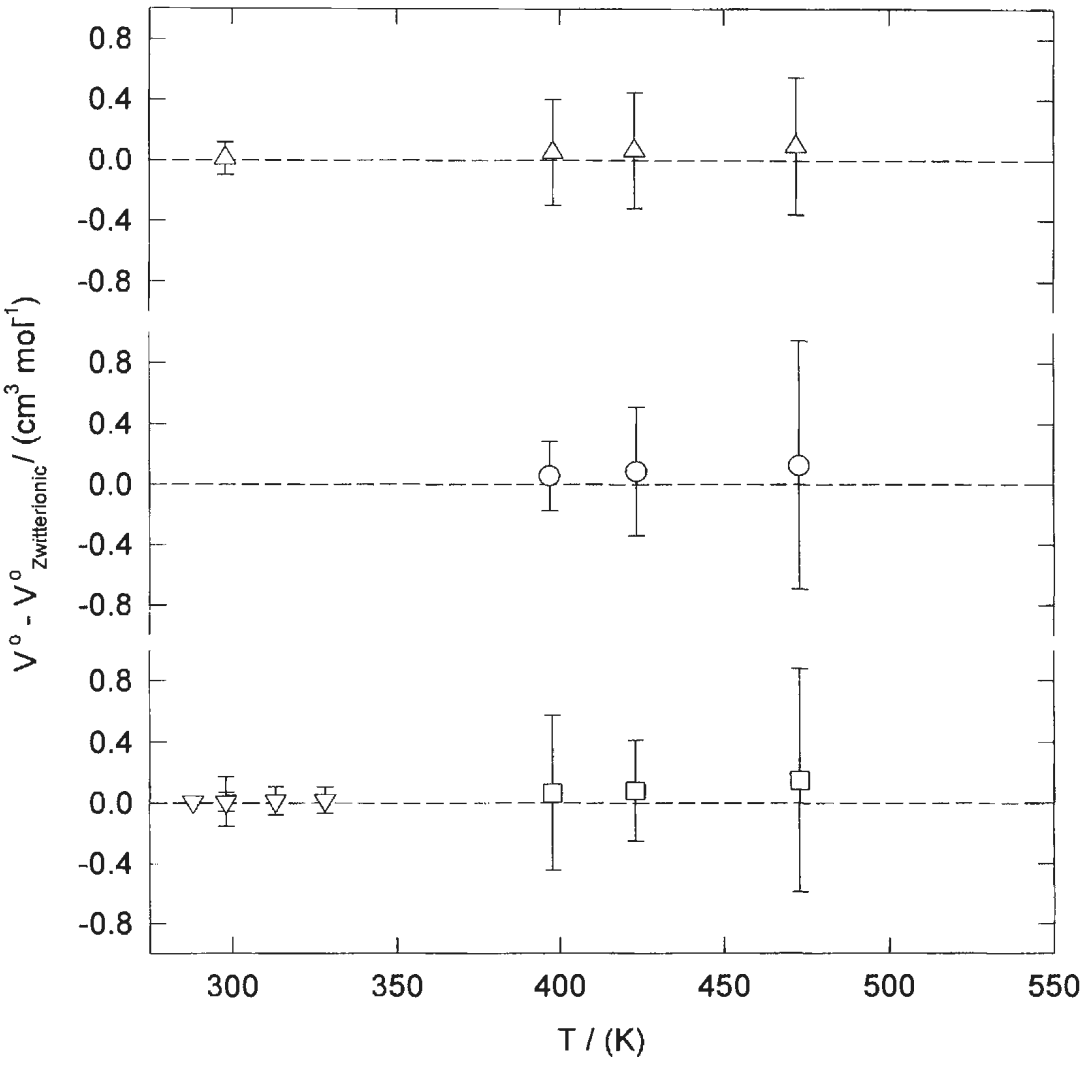

Figure 4.5.4.2 The difference between the experimental values of V° and the estimated values of $V^\circ_{Zwitterionic}$ for aqueous glycine. Symbols represent: Δ, 30.21 MPa; ○, 20.00 MPa; □, 10.00 MPa; ∇, 0.10 MPa

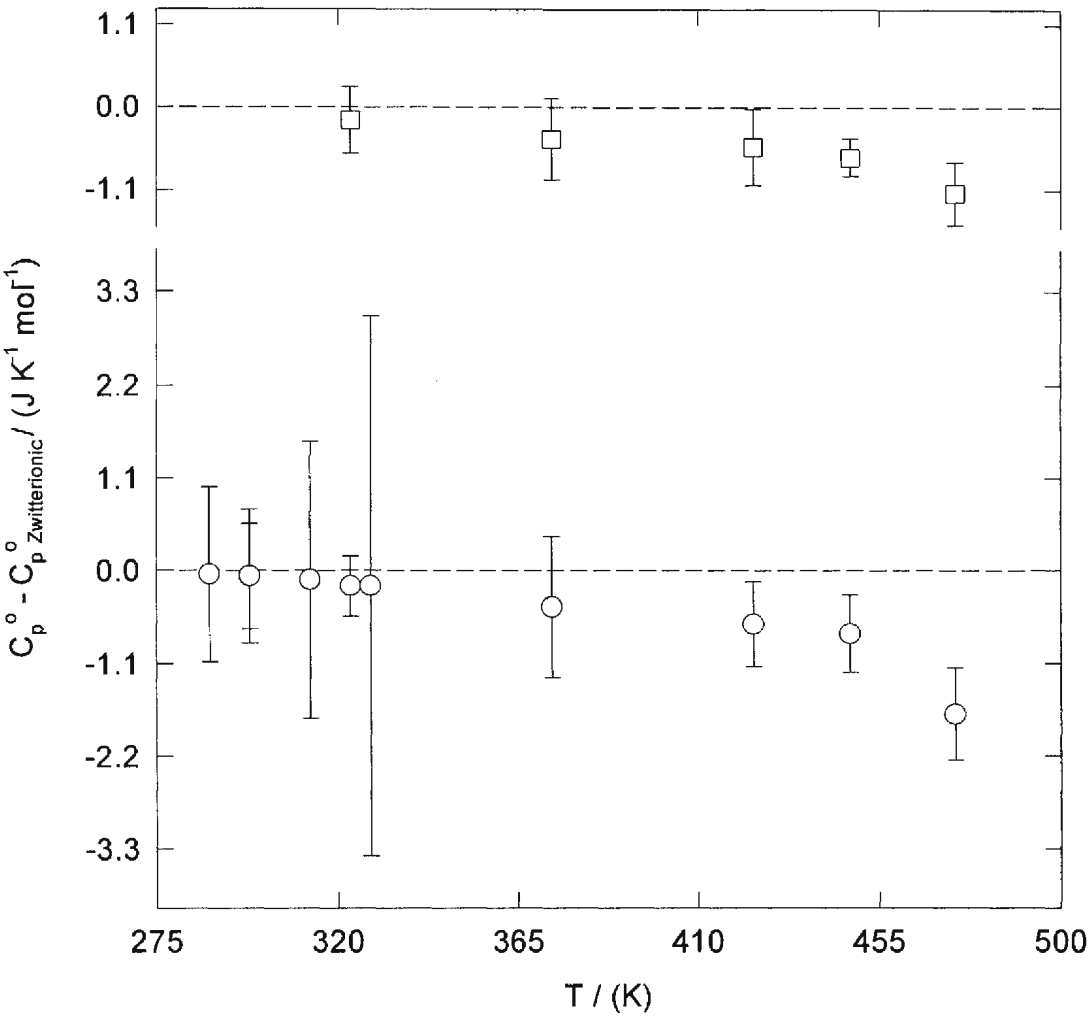

Figure 4.5.4.3 The difference between the experimental values of C_p° and the estimated values of $C^\circ_{p,Zwitterionic}$ for aqueous α-alanine. Symbols represent: ○, steam saturation pressure; □, 30.15 MPa.

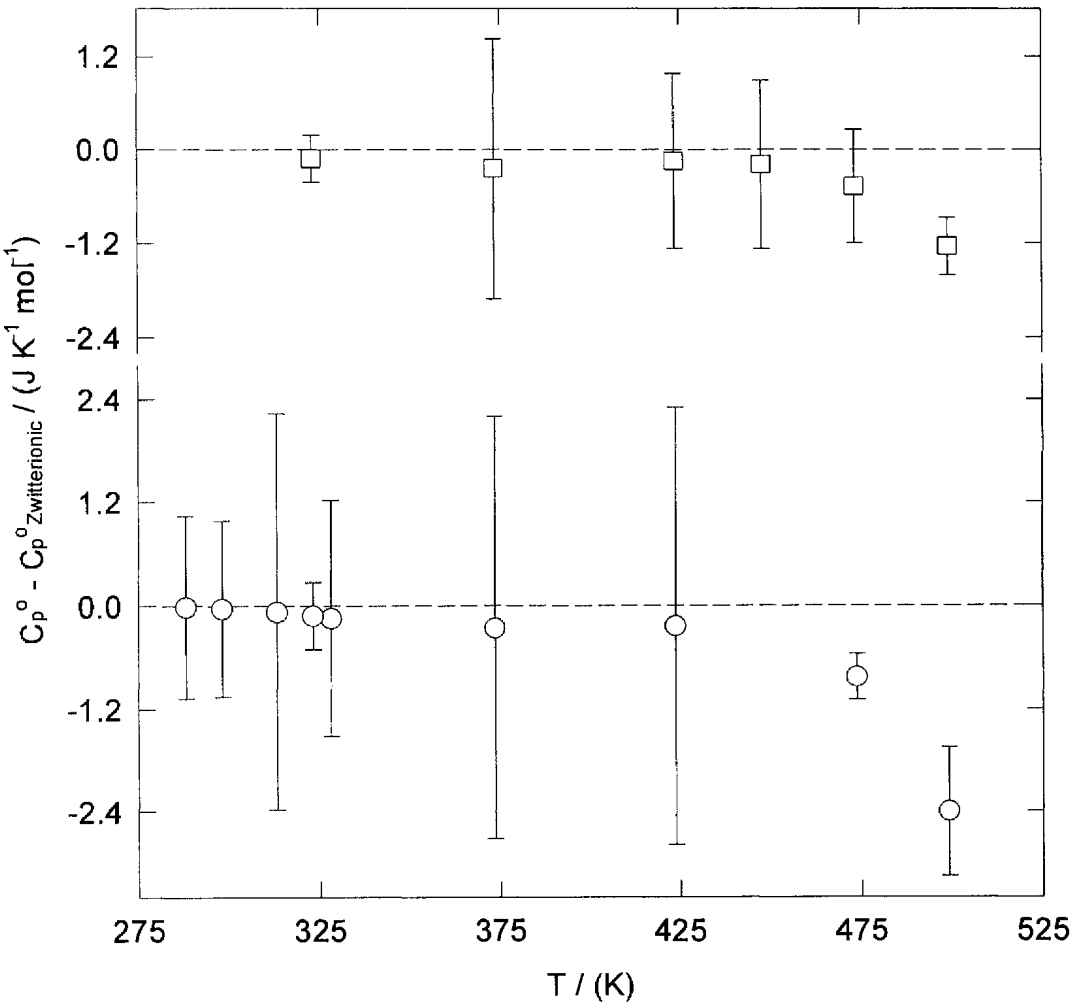

Figure 4.5.4.4 The difference between the experimental values of C_p° and the estimated values of $C^\circ_{p,Zwitterionic}$ for aqueous glycine. Symbols represent: ○, steam saturation pressure; □, 30.24 MPa.

4.5.5 Calculation of Speciation from the Equilibrium Constants Determined for Aqueous α-Alanine by UV-Visible Spectroscopy.

In order to confirm the speciation calculations from Sections 4.5.2 and 4.5.3, temperature dependent values of K_1 and K_2 were determined for aqueous α-alanine by UV-visible spectroscopy as described in Section 3.5. K_3 was assumed to be approximately equal to (K_1 / K_2). The equilibrium constants are plotted as a function of temperature in Figure 4.5.5.1. The speciation of aqueous α-alanine was calculated from these experimental values at 423.1 K and 5.4 MPa; 498.3 K and 5.6 MPa; 523.2 K and 5.5 MPa using the numerical method described in Section 4.5.1. The distribution of species for α-alanine is plotted as a function of temperature in Figure 4.5.5.2.

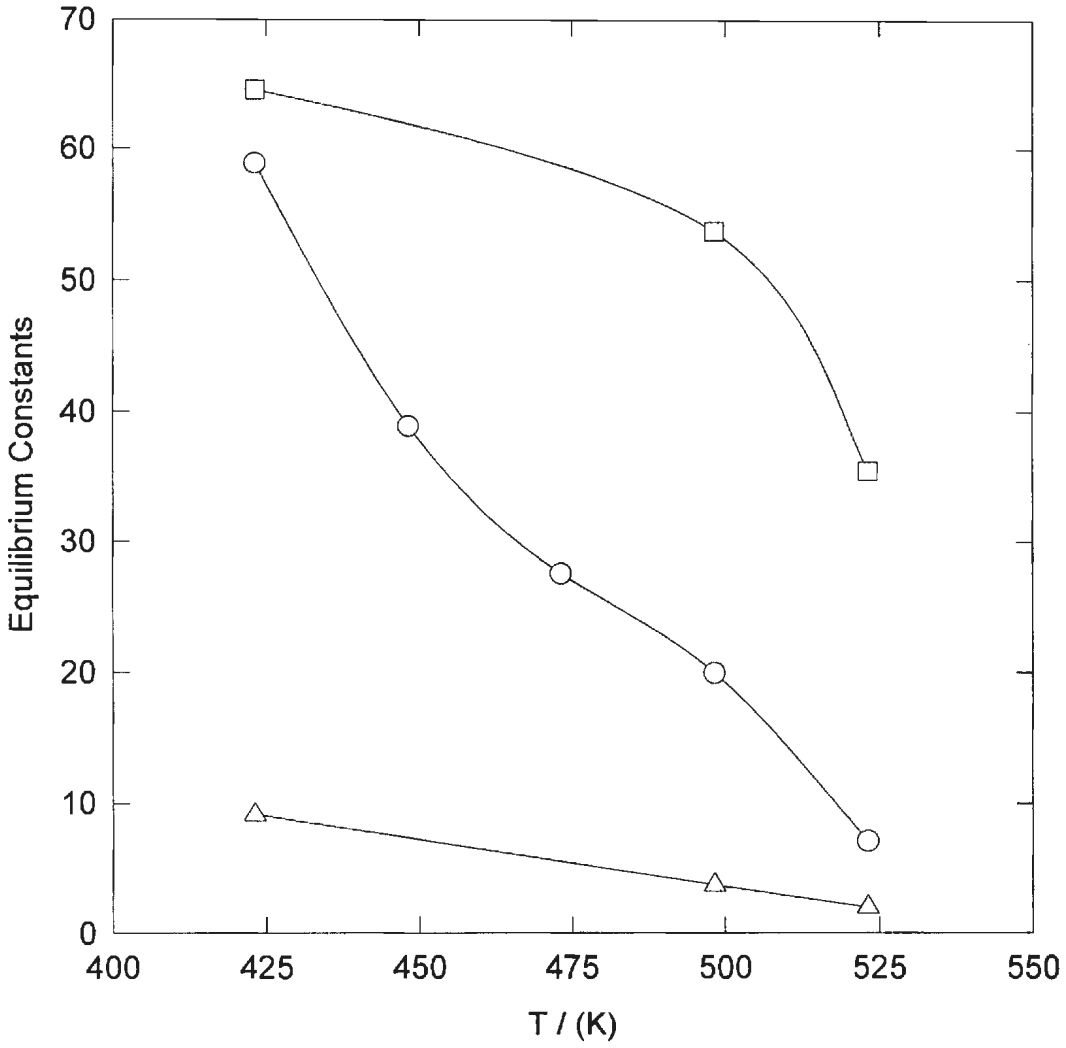

Figure 4.5.5.1 The values of K_1, K_2, and K_3 for α-alanine as a function of temperature. The symbols represent: ○, $K_1 \cdot 10^4$; □, $K_2 \cdot 10^9$; Δ, $K_3 \cdot 10^{-4}$.

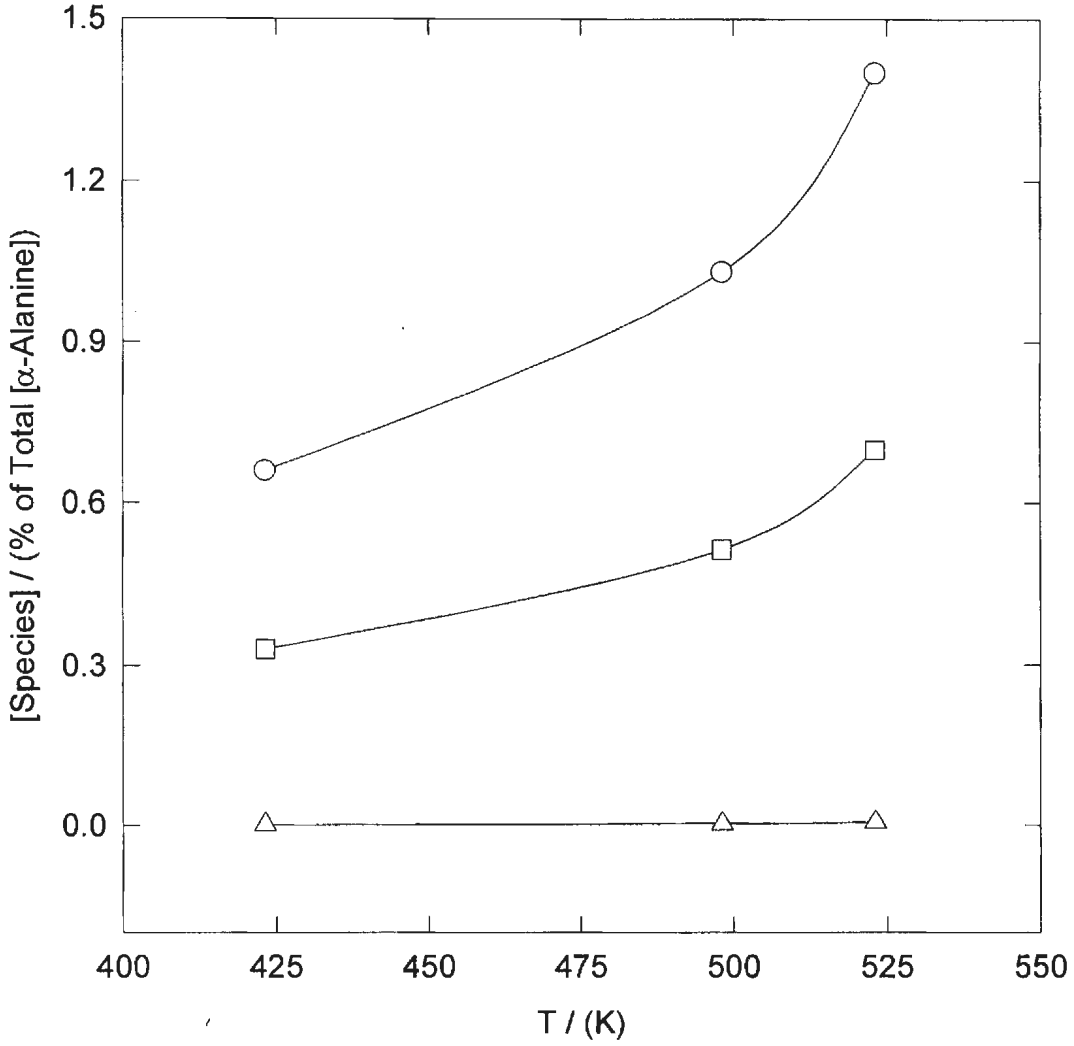

Figure 4.5.5.2 The values of $[H_2A^+]$, $[A^-]$, and $[HA^\circ]$ for α-alanine as a function of temperature, where the sum of $[HA^\pm]$, $[H_2A^+]$, $[A^-]$, and $[HA^\circ]$ is 1 mol·kg^{-1}. Symbols represent the following: ○, $[H_2A^+] + [A^-] + [HA^\circ]$; □, $[H_2A^+] = [A^-]$; Δ, $[HA^\circ]$.

4.5.6 Comparison of the Estimated Values of K_1, K_2, and $[H_2A^+] + [A^-] + [HA^o]$ with those Measured by UV-Visible Spectroscopy.

The temperature dependent values of K_1, K_2, and $[H_2A^+] + [A^-] + [HA^o]$ estimated for α-alanine in Sections 4.5.2 and 4.5.3 are compared with those obtained by UV-visible spectroscopy in Figures 4.5.6.1, 4.5.6.2, and 4.5.6.3. The temperature dependent values of K_1, K_2, and $[H_2A^+] + [A^-] + [HA^o]$ estimated for glycine in Sections 4.5.2 and 4.5.3 are compared in Figures 4.5.6.4, 4.5.6.5, and 4.5.6.6. Included in Figures 4.5.6.1 and 4.5.6.4 are the values of K_1 obtained from Wang *et al.* (1996). Wang *et al.* developed an equation to calculate K_1 as a function of temperature (298 K $\leq T \leq$ 398 K) by combining their experimental results (323 K $\leq T \leq$ 398 K) with existing literature values. The values of K_1 obtained by Wang *et al.* are the only experimental data under hydrothermal conditions with which to compare our experimental results.

The values of K_1 obtained for aqueous α-alanine and glycine by Wang *et al.* (1996) agree with the values estimated in both Sections 4.5.2 and 4.5.3 at $T \leq$ 350 K. Above 350 K the values of K_1 estimated with the Yezdimer-Sedlbauer-Wood functional group additivity model for aqueous α-alanine and glycine diverge from the values of K_1 obtained from the isocoulombic extrapolation of room temperature data. Only the values of K_1 obtained from the isocoulombic extrapolation of room temperature data reproduce the values determined by Wang *et al.* (1996) over the entire temperature range of their measurements. As the temperature increases from 425 to 525 K there is an increase in the agreement between the experimentally determined values of K_1 obtained for aqueous α-alanine by UV-visible

spectroscopy and those values obtained from the isocoulombic extrapolation of room temperature data.

The values of K_2 estimated for aqueous α-alanine and glycine in Section 4.5.2 agree with those estimated in Section 4.5.3 at $T \leq 350$ K. Above 350 K the values of K_2 estimated with the Yezdimer-Sedlbauer-Wood functional group additivity model for aqueous α-alanine and glycine diverge from the values of K_2 obtained from the isocoulombic extrapolation of room temperature data. There is agreement between the values of K_2 obtained for α-alanine by UV-visible spectroscopy and the values obtained from the isocoulombic extrapolation of room temperature data only at 423.0 K and 5.3 MPa. At temperatures above 425 K the estimated values of K_2 act as an upper limit for the experimentally determined values of K_2 obtained for α-alanine.

As expected from the comparison of the estimated values of K_1 and K_2, there is good agreement between the values of $[H_2A^+] + [A^-] + [HA^o]$ estimated in Sections 4.5.2 and 4.5.3 for both aqueous α-alanine and glycine. Above 350 K the values of $[H_2A^+] + [A^-] + [HA^o]$ estimated for aqueous α-alanine and glycine with the Yezdimer-Sedlbauer-Wood functional group additivity model diverge from the values obtained from the isocoulombic extrapolation of room temperature data. There is agreement between the values of $[H_2A^+] + [A^-] + [HA^o]$ obtained for α-alanine by UV-visible spectroscopy and the values obtained from the isocoulombic extrapolation of room temperature data only at 423.0 K and 5.3 MPa. At temperatures above 425 K the estimated values of $[H_2A^+] + [A^-] + [HA^o]$ act as an upper

limit for the experimentally determined values obtained for α-alanine.

As illustrated in Figures 4.5.6.3 and 4.5.6.6 the zwitterion is the predominant form of the amino acids in aqueous solution. Therefore, the assumption that the non-zwitterionic forms of the aqueous amino acids can be neglected in the volumetric and calorimetric measurements was a reasonable one.

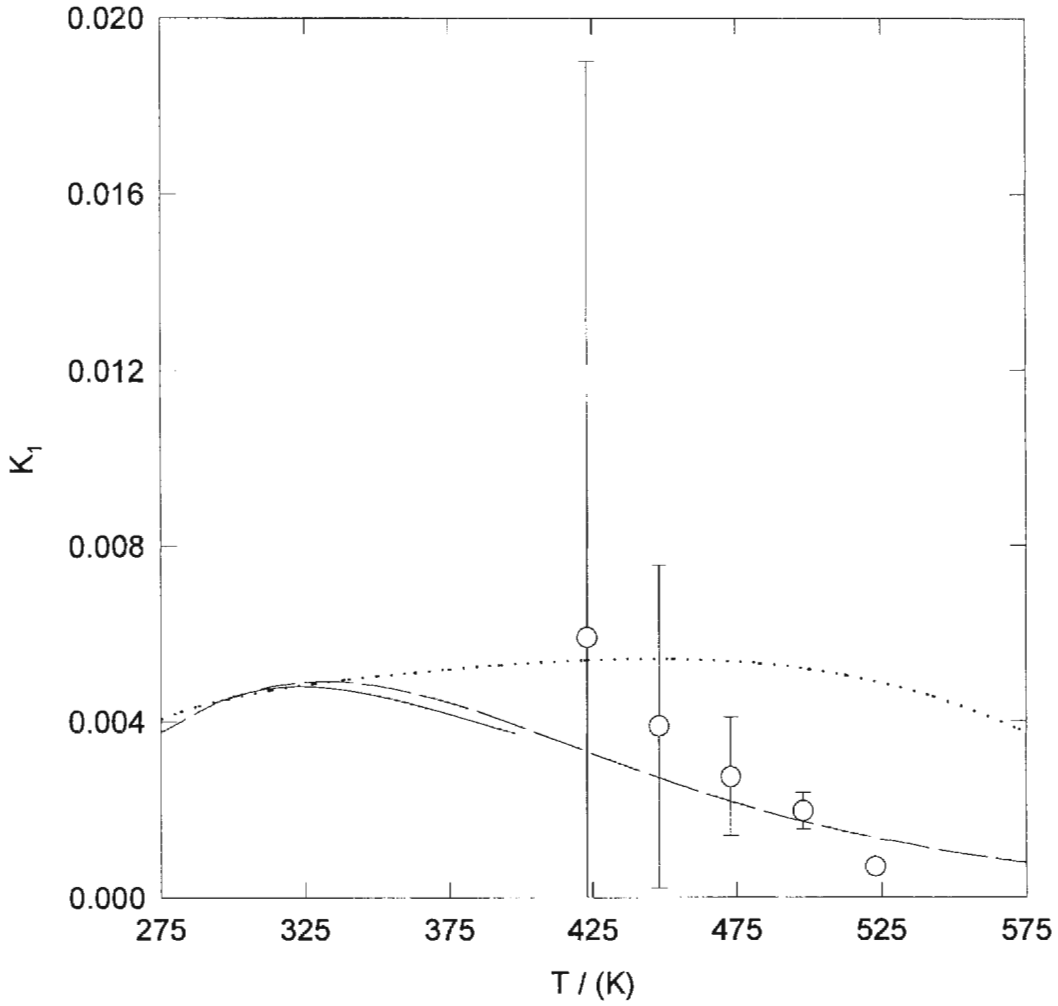

Figure 4.5.6.1 K_1 for α-alanine as a function of temperature. Symbols are the values obtained by UV-visible spectroscopy. Lines are the values obtained from: —, Wang *et al.* (1996); - - -, extrapolation of 298.15 K data; ·····, Yezdimer *et al.* (2000).

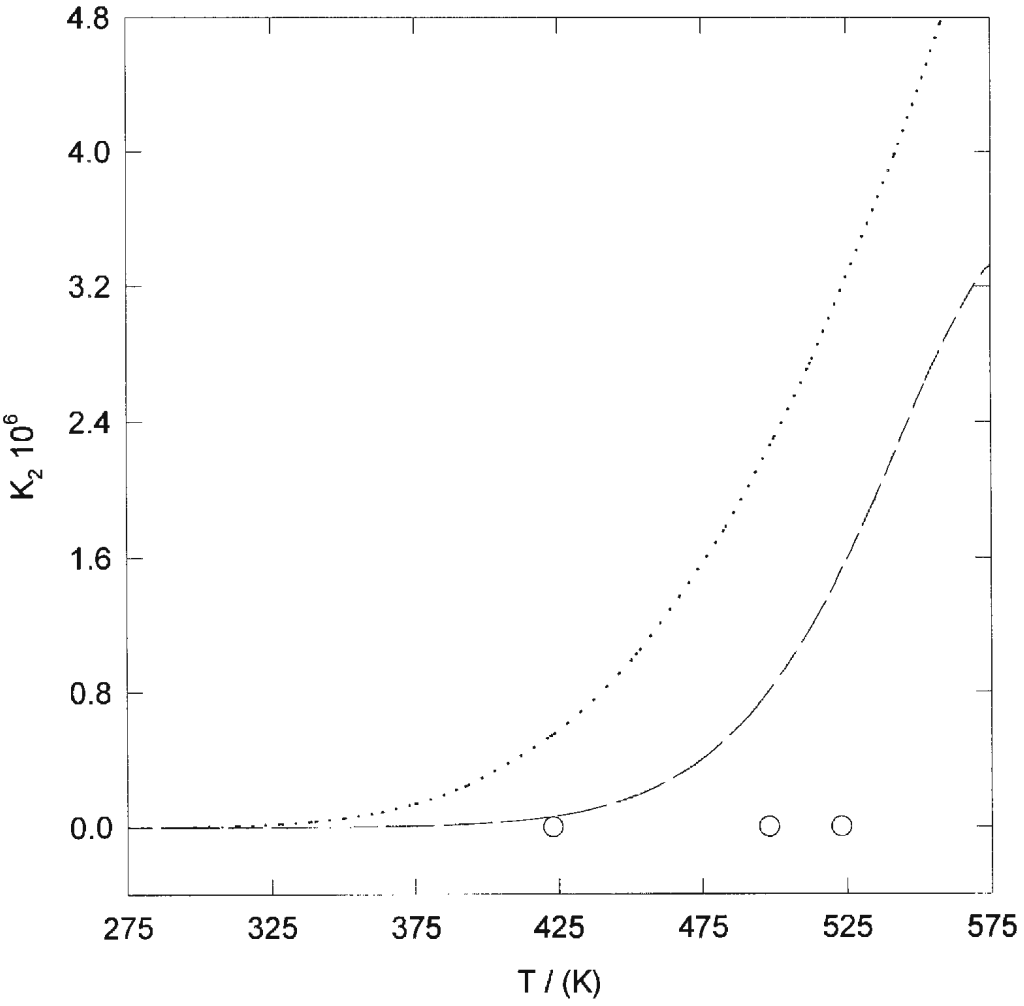

Figure 4.5.6.2 K_2 for α-alanine as a function of temperature. Symbols are the values obtained by UV-visible spectroscopy. Lines are the values obtained from: - - -, extrapolation of 298.15 K data; ·····, Yezdimer *et al.* (2000).

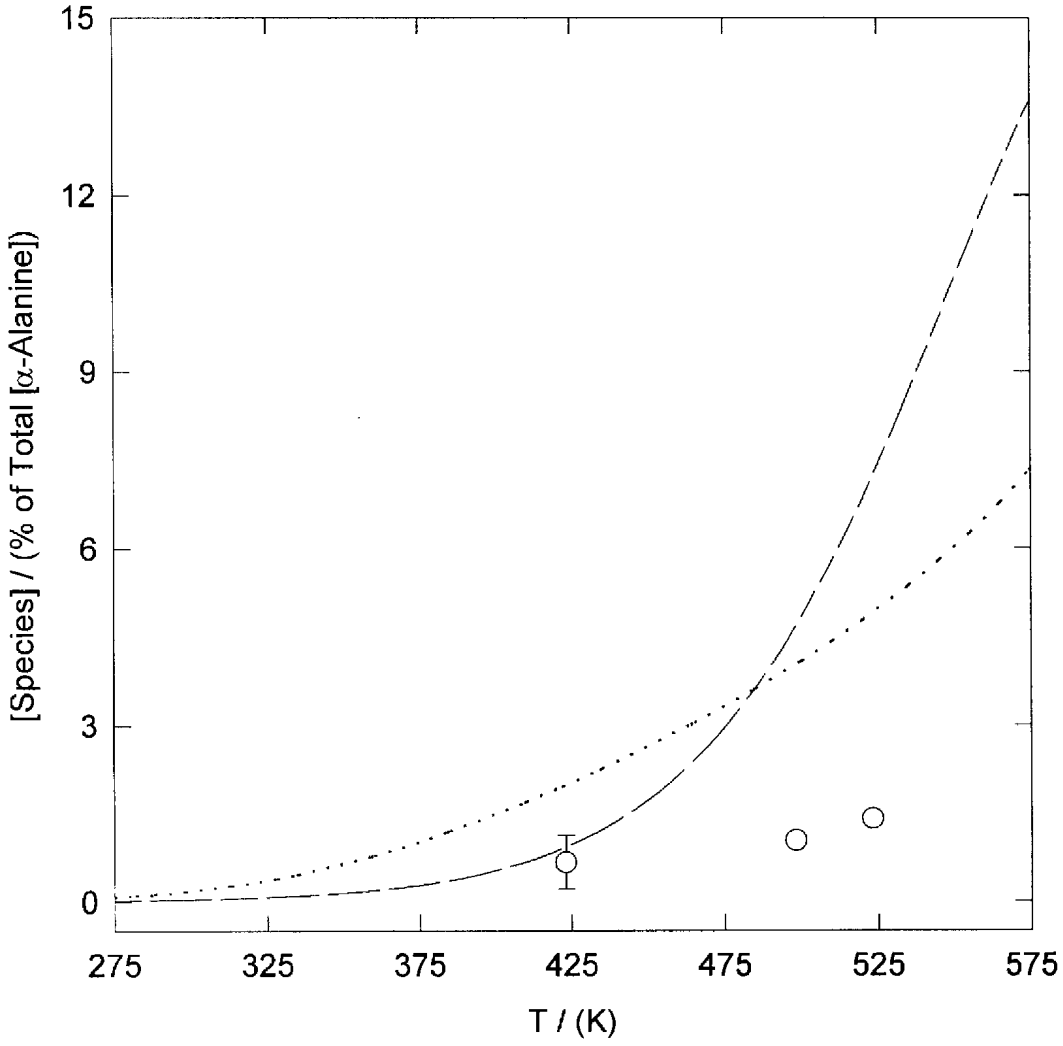

Figure 4.5.6.3 The sum of $[H_2A^+]$, $[A^-]$, and $[HA^o]$ for α-alanine as a function of temperature, where $[HA^\pm] + [H_2A^+] + [A^-] + [HA^o] = 1$ mol·kg^{-1}. Symbols are the values obtained from UV-visible spectroscopy. Lines are the values obtained from: - - -, extrapolation of 298.15 K data; ·····, Yezdimer *et al.* (2000).

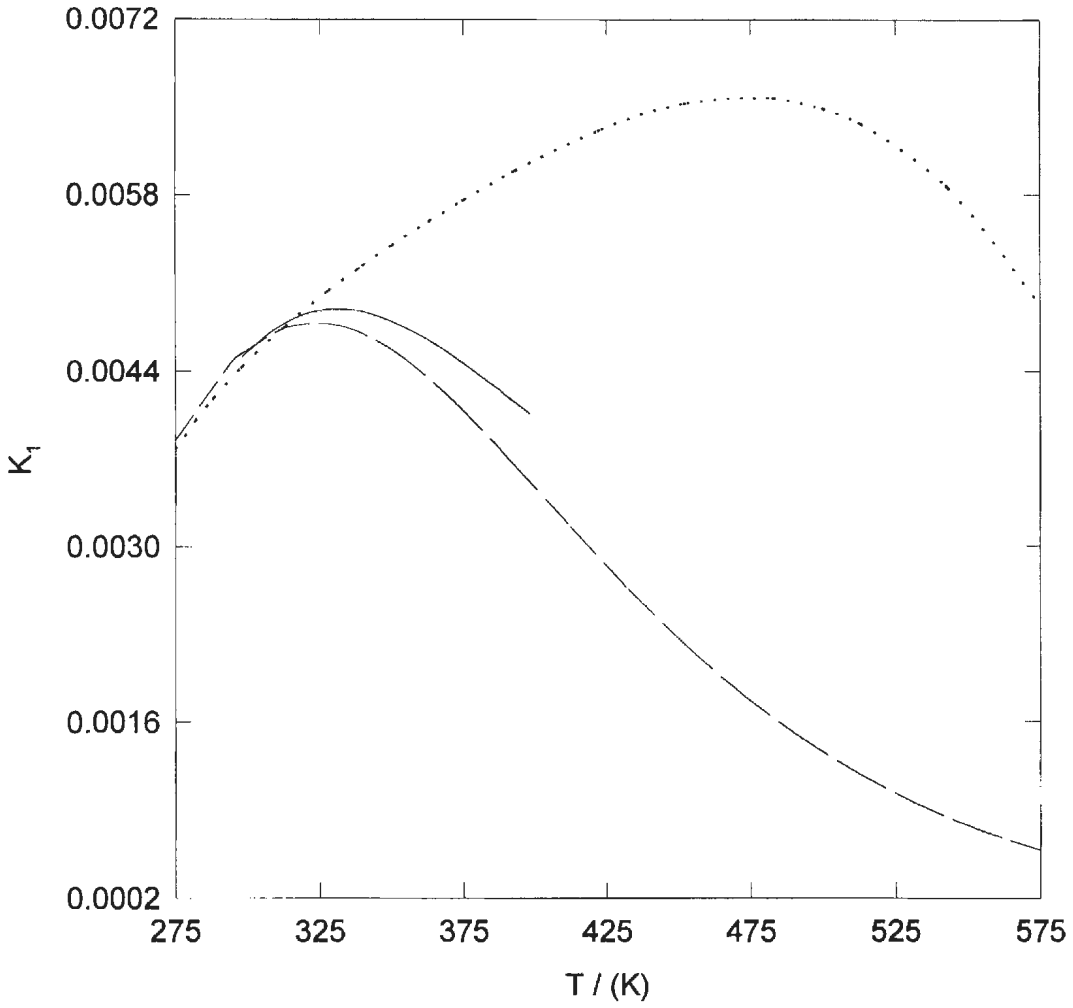

Figure 4.5.6.4 K_1 for glycine as a function of temperature. Lines are the values obtained from: —, Wang *et al.* (1996); - - -, extrapolation of 298.15 K data; ·····, Yezdimer *et al.* (2000).

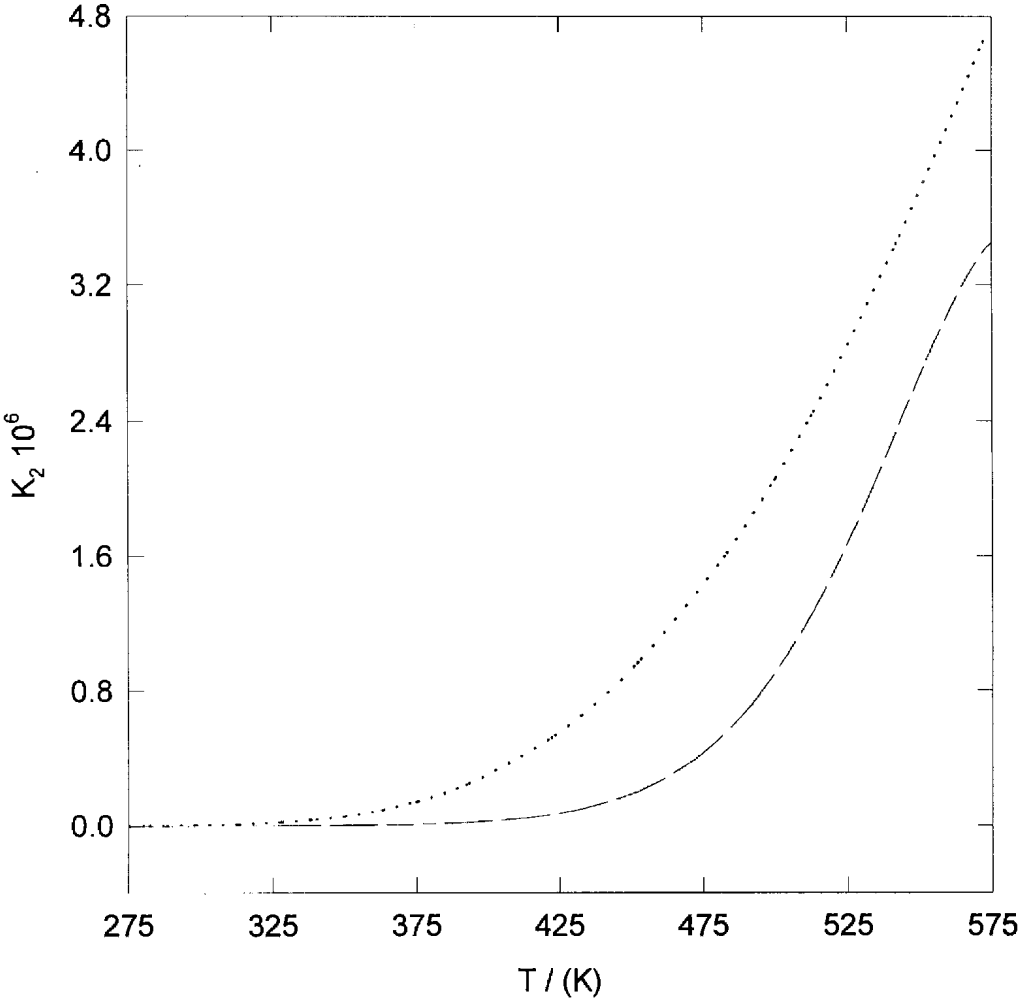

Figure 4.5.6.5 K_2 for glycine as a function of temperature. Lines are the values obtained from: - - -, extrapolation of 298.15 K data; ·····, Yezdimer *et al.* (2000).

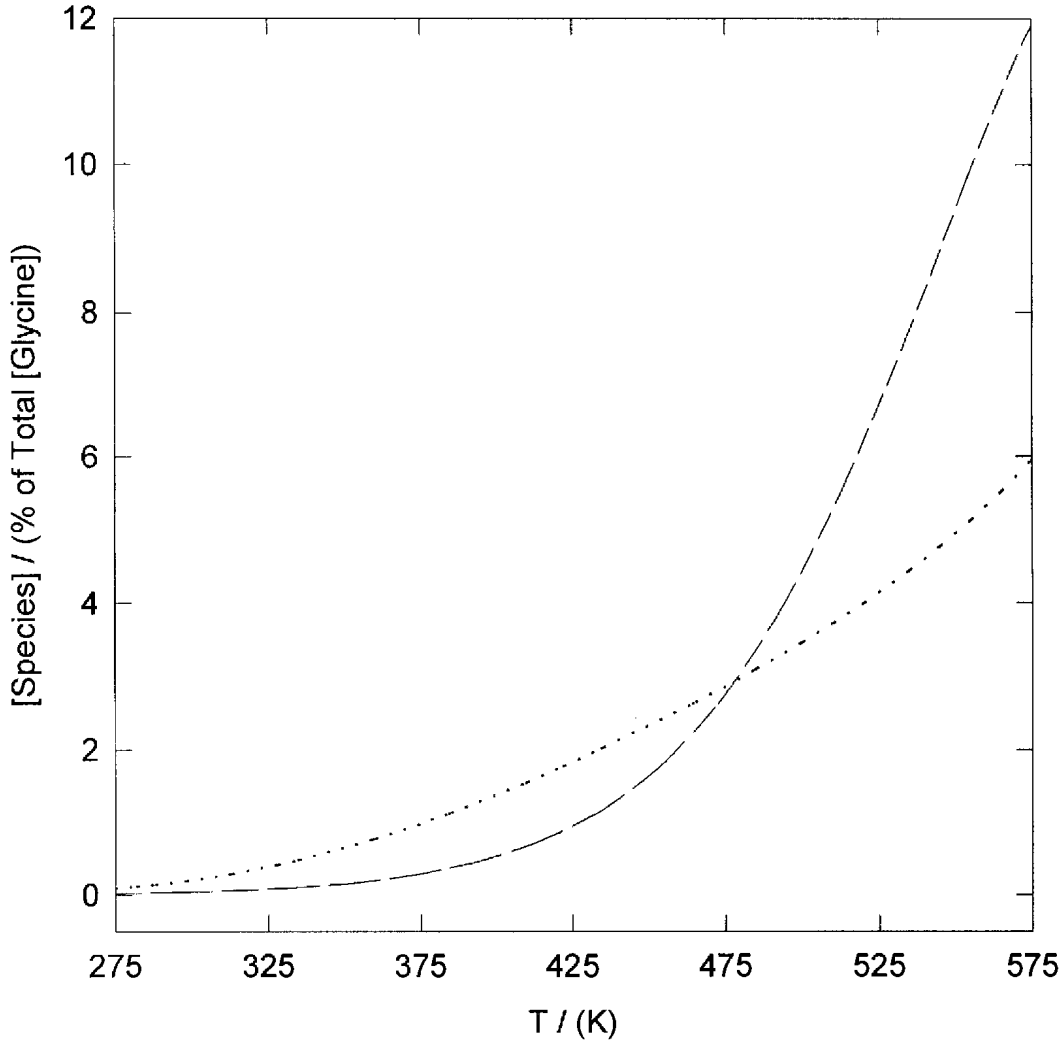

Figure 4.5.6.6 The sum of $[H_2A^+]$, $[A^-]$, and $[HA^\circ]$ for glycine as a function of temperature, where $[HA^\pm] + [H_2A^+] + [A^-] + [HA^\circ] = 1$ mol·kg^{-1}. Lines are the values obtained from: - - -, extrapolation of 298.15 K data; ·····, Yezdimer *et al.* (2000).

4.6 Contribution of Solvation Effects to $V°$.

4.6.1 Definition of Solvation Effects.

The standard partial molar volume $V°$ of an aqueous species is expressed as:

$$V^o = V^o_{intr} + \Delta_{solv} V^o_{ss} + \Delta_{solv} V^o_{pol} + \Delta_{solv} V^o_{hydr} \qquad (1.3.1.7)$$

Here V^o_{intr} is the intrinsic gas phase standard partial molar volume of the species (0.10 MPa, ideal gas), $\Delta_{solv}V^o_{ss}$ is the change in the standard partial molar volume arising from the difference in standard states between the gas phase (0.10 MPa, ideal gas) and solution (hypothetical 1 molal solution), $\Delta_{solv}V^o_{pol}$ is the standard partial molar volume due to the long-range polarization of water caused by the localized charge distribution within the solute, and $\Delta_{solv}V^o_{hydr}$ is the standard partial molar volume due to the short-range hydration effects arising from the hydrogen-bonded "structure" of water in the immediate vicinity of the solute. For a neutral aqueous species with a significant dipole moment $\Delta_{solv}V^o_{pol}$ is approximately equal to $\Delta_{solv}V^o_{dipole}$ and equation (1.3.1.7) becomes:

$$V^o = V^o_{intr} + \Delta_{solv} V^o_{ss} + \Delta_{solv} V^o_{dipole} + \Delta_{solv} V^o_{hydr} \qquad (4.6.1.1)$$

Values of V^o_{intr}, $\Delta_{solv}V^o_{ss}$, $\Delta_{solv}V^o_{dipole}$, and $\Delta_{solv}V^o_{hydr}$ were estimated for α-alanine, β-alanine, and proline in Sections 4.6.2, 4.6.3, and 4.6.4.

4.6.2 Intrinsic and Standard State Contributions.

The intrinsic gas phase standard partial molar volume of each amino acid V^o_{intr} was calculated using the expression for the volume of a hard sphere:

$$V_g^{\circ} = \left(\frac{4}{3}\right) N_A \pi r^3 \qquad (4.6.2.1)$$

r is the radius of the gaseous species. Crystallographic studies were used to estimate the gas phase radii. The values of r and V_{intr}° determined for α-alanine, β-alanine, and proline are summarized in Table 4.6.2.1.

The change in the standard partial molar volume of a dissolved neutral dipolar species arising from the difference in standard states between the gas phase (0.10 MPa, ideal gas) and solution (hypothetical 1 molal solution) was evaluated using the following expression:

$$\Delta_{solv} V_{ss}^{\circ} = RT\beta_w \qquad (4.6.2.2)$$

where $\beta_w = -(1 / V_w)(\partial V_w / \partial p)_T$ is the compressibility of water. Equation (4.6.2.2) was obtained from equation (1.3.1.2) through the following relationship:

$$\Delta_{solv} V_{ss}^{\circ} = \left(\frac{\partial \Delta_{solv} G_{ss}^{\circ}}{\partial p}\right)_T \qquad (4.6.2.3)$$

Table 4.6.2.2 summarizes the values of $\Delta_{solv} V_{ss}^{\circ}$ calculated for aqueous α-alanine, β-alanine, and proline at the temperatures and pressures associated with the experimentally determined values of V°.

Table 4.6.2.1 Gas phase radii r and intrinsic standard partial molar volumes V°_{intr} of α-alanine, β-alanine, and proline.

Amino Acid	V°_{intr} / ($cm^3 \cdot mol^{-1}$)	r / (Å)	Crystallographic Source
α-Alanine	33.5	2.37	Wyckoff (1966)
β-Alanine	59.8	2.87	Averbuch-Pouchot *et al.* (1988)
Proline	78.2	3.14	Padmanabhan *et al.* (1995)
Glycine	——	2.65	Bowen (1958)

Table 4.6.2.2 Change in the standard partial molar volumes arising from the difference in standard states between the gas phase and solution.

T K	p MPa	$\Delta_{solv}V_{ss}^{o}$ $cm^3 \cdot mol^{-1}$	T K	p MPa	$\Delta_{solv}V_{ss}^{o}$ $cm^3 \cdot mol^{-1}$
		α-Alanine			
334.65	19.977	1.18	422.42	10.036	2.07
383.20	19.939	1.51	477.24	10.058	3.40
423.47	19.976	2.00	523.36	10.063	5.90
478.67	19.967	3.22	288.15	0.10	1.12
523.39	19.934	5.27	298.15	0.10	1.12
333.21	10.047	1.20	313.15	0.10	1.15
381.70	10.057	1.55	328.15	0.10	1.21
		β-Alanine			
423.63	20.533	2.00	291.15	0.10	1.12
334.59	10.315	1.21	298.15	0.10	1.12
383.34	10.355	1.57	313.15	0.10	1.15
423.60	10.290	2.09	328.15	0.10	1.21
		Proline			
334.93	20.199	1.18	423.71	10.173	2.09
383.66	20.157	1.52	479.04	10.115	3.46
423.90	20.205	2.01	524.07	10.094	5.96
479.15	20.194	3.23	288.15	0.10	1.12
523.98	20.240	5.30	298.15	0.10	1.12
334.56	10.157	1.21	313.15	0.10	1.15
383.39	10.168	1.57	328.15	0.10	1.21

4.6.3 Standard Partial Molar Volume of Polarization of a Dissolved Neutral Dipolar Species.

The standard partial molar volume of polarization of a dissolved neutral dipolar species $\Delta_{solv}V^{o}_{dipole}$ was evaluated using equation (1.3.2.21).

$$\Delta_{solv}V^{o}_{dipole} = \frac{\mu^2 N_A}{4\pi\varepsilon_o r_e^3}\left(\frac{-3}{(2\varepsilon_r+1)^2}\right)\left(\frac{\partial\varepsilon_r}{\partial p}\right)_T \qquad (1.3.2.21)$$

The "effective" radius r_e of each dissolved amino acid was set to the value of r listed in Table 4.6.2.1 for that aqueous amino acid.

A review of the relevant literature revealed a number of temperature dependent values of the molar dielectric increment δ and the dipole moment μ for α-alanine, β-alanine, and proline. These values are summarized in Table 1.6.3.3. For the purpose of these calculations, the values of μ obtained for α-alanine by Aaron and Grant (1967), β-alanine by Aaron and Grant (1967), and proline by Shepherd and Grant (1968) were extrapolated to elevated temperatures by fitting each set of temperature dependent data to the following empirical expression:

$$\mu = \mu_o\,[A\,(T_c/T)^j + 1]^{0.5} \qquad (4.6.3.1)$$

where μ_o is the gas phase dipole moment and T_c = 647.14 K is the critical temperature of water. The terms A and j are fitting parameters. Equation (4.6.3.1) is similar in form to an expression used by Fernandez *et al.* (1997) to fit dielectric constant data for liquid water at steam saturation.

The gas phase dipole moments for α-alanine, β-alanine, and proline were estimated

from the following expression:

$$\mu_o = qd \qquad (4.6.3.2)$$

where q is the magnitude of the separated charges and d is the distance between the charges. The X-ray crystallographic data contained in the compilation of Bowen *et al.* (1958) were used to calculate d for α-alanine and proline. The X-ray crystallographic data obtained by Averbuch-Pouchot *et al.* (1988) were used to calculate d for β-alanine. The positive charge was assumed to reside on the nitrogen atom. A realistic view of the amino acids would have the negative charge shared by both oxygen atoms. However, the calculation of d is greatly simplified by assuming that the negative charge can be assigned to a single oxygen atom. Since the shorter oxygen-carbon bond is likely to have more double bond character, the negative charge was assumed to reside on the oxygen atom with the longer carbon-oxygen bond. It was assumed that α-alanine and β-alanine adopt a rotational conformation with the closest possible approach between the ammonium and carboxylate groups. The charge separation in proline is fixed by its ring structure.

The values of d, μ_o, A, and j determined for α-alanine, β-alanine, and proline are summarized in Table 4.6.3.1. The variation of μ with temperature is illustrated in Figures 4.6.3.1, 4.6.3.2, and 4.6.3.3 for α-alanine, β-alanine, and proline, respectively. Table 4.6.3.2 tabulates the values of $\Delta_{solv}V^{o}_{dipole}$ for α-alanine, β-alanine, and proline calculated using equation (1.3.2.21) at the temperatures and pressures associated with the experimental values of $V°$.

Table 4.6.3.1 Values of d, μ_o, A, and j for α-alanine, β-alanine, and proline.

Amino Acid	d m	μ_o Debye	A	j
α-Alanine	2.67×10^{-10}	12.87	4.153×10^{-2}	3.475
β-Alanine	1.98×10^{-10}	9.50	1.884	0.6194
Proline	3.26×10^{-10}	15.68	3.106×10^{-5}	12.52
Glycine	2.65×10^{-10}	12.79	—	—

Table 4.6.3.2 Standard partial molar volumes of polarization for aqueous solutions of α-alanine, β-alanine, and proline at selected temperatures and pressures.

T K	p MPa	$\mu \cdot 10^{29}$ C·m	$\Delta_{solv}V^{o}_{dipole}$ $cm^3 \cdot mol^{-1}$	T K	p MPa	$\mu \cdot 10^{29}$ C·m	$\Delta_{solv}V^{o}_{dipole}$ $cm^3 \cdot mol^{-1}$
			α-Alanine				
334.65	19.977	5.10	-5.89	422.42	10.036	4.67	-12.28
383.20	19.939	4.81	-8.21	477.24	10.058	4.54	-22.94
423.47	19.976	4.67	-11.74	523.36	10.063	4.48	-45.36
478.67	19.967	4.54	-21.45	288.15	0.10	5.58	-5.25
523.39	19.934	4.48	-39.62	298.15	0.10	5.45	-5.33
333.21	10.047	5.11	-6.01	313.15	0.10	5.29	-5.60
381.70	10.057	4.82	-8.46	328.15	0.10	5.15	-6.39
			β-Alanine				
423.63	20.533	5.88	-10.43	291.15	0.10	6.41	-3.94
334.59	10.315	6.20	-5.02	298.15	0.10	6.37	-4.07
383.34	10.355	6.02	-7.49	313.15	0.10	6.30	-4.45
423.60	10.290	5.88	-11.05	328.15	0.10	6.23	-4.94
			Proline				
334.93	20.199	5.53	-2.97	423.71	10.173	5.25	-6.73
383.66	20.157	5.29	-4.26	479.04	10.115	5.23	-13.36
423.90	20.205	5.25	-6.38	524.07	10.094	5.23	-26.85
479.15	20.194	5.23	-12.25	288.15	0.10	6.97	-3.51
523.98	20.240	5.23	-23.31	298.15	0.10	6.42	-3.17
334.56	10.157	5.53	-3.06	313.15	0.10	5.90	-2.99
383.39	10.168	5.29	-4.43	328.15	0.10	5.62	-3.07

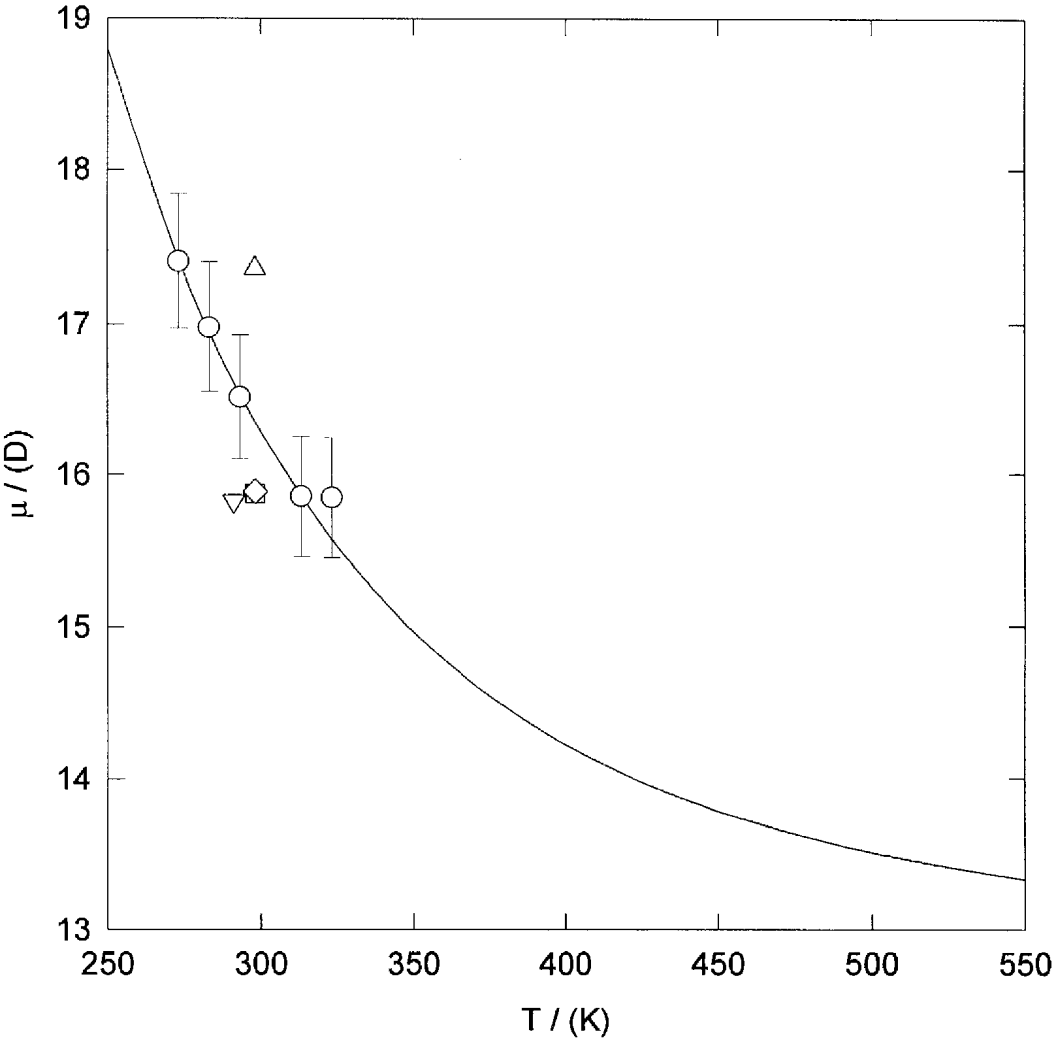

Figure 4.6.3.1 The aqueous dipole moment μ of α-alanine plotted against temperature. Symbols are the experimental values of: □, Wyman and McMeekin (1933); ○, Aaron and Grant (1967); Δ, Devoto (1930); ▽, Hederstrand (1928); ◇, Osborn (1945). The solid line represents the least squares fit obtained using equation (4.6.3.1) and the data of Aaron and Grant (1967).

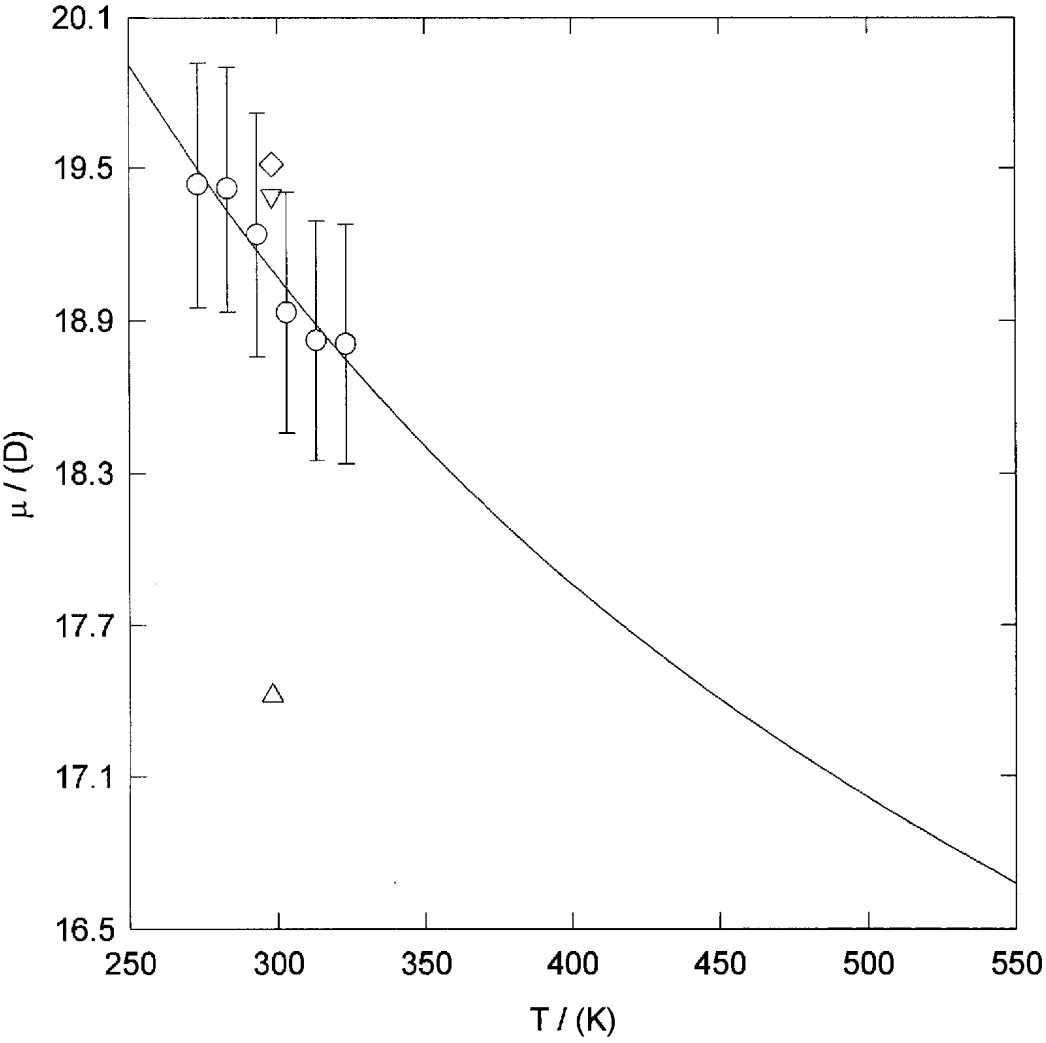

Figure 4.6.3.2 The aqueous dipole moment μ of β-alanine plotted against temperature. Symbols are the experimental values of: □, Hederstrand (1928); ○, Aaron and Grant (1967); ▽, Wyman and McMeekin (1933); ◇, Devoto (1933); Δ, Edward *et al.* (1974). The solid line represents the least squares fit obtained using equation (4.6.3.1) and the Data of Aaron and Grant (1967).

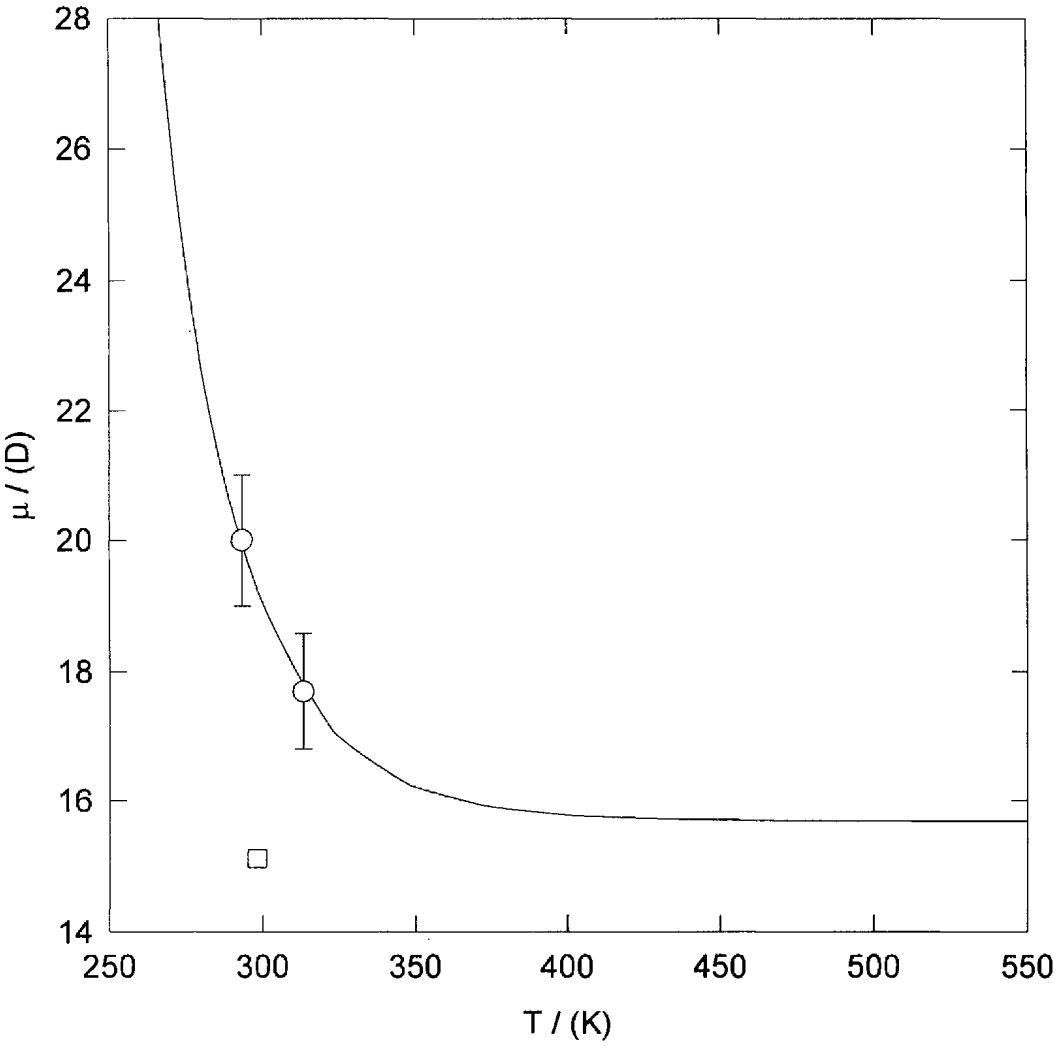

Figure 4.6.3.3 The aqueous dipole moment μ of proline plotted against temperature. Symbols are the experimental values of: □, Devoto (1931); ○, Shepherd and Grant (1968). The solid line represents the least squares fit obtained using equation (4.3.3.1) and the data of Shepherd and Grant (1968).

4.6.4 Hydration Effects.

The magnitude of the molar volume of hydration $\Delta_{solv}V^{o}_{hydr}$ was estimated from equation (4.6.1.1) using the values of V^{o}_{intr}, $\Delta_{solv}V^{o}_{ss}$, and $\Delta_{solv}V^{o}_{dipole}$ obtained in Sections 4.6.2 and 4.6.3. Table 4.6.4.1 summarizes the values of $\Delta_{solv}V^{o}_{hydr}$ calculated for α-alanine, β-alanine, and proline at the temperatures and pressures associated with the experimental values of V°.

Figures 4.6.4.1, 4.6.4.2, and 4.6.4.3 illustrate the relative contributions of V^{o}_{intr}, $\Delta_{solv}V^{o}_{ss}$, $\Delta_{solv}V^{o}_{dipole}$, and $\Delta_{solv}V^{o}_{hydr}$ as a function of temperature for α-alanine at 19.96 MPa, β-alanine at 10.30 MPa, and proline at 20.20 MPa, respectively.

Table 4.6.4.1 Standard partial molar volumes of hydration for aqueous solutions of α-alanine, β-alanine, and proline at selected temperatures and pressures.

T K	p MPa	$\Delta_{solv}V^{o}_{hydr}$ $cm^3 \cdot mol^{-1}$	T K	p MPa	$\Delta_{solv}V^{o}_{hydr}$ $cm^3 \cdot mol^{-1}$
		α-Alanine			
334.65	19.977	33.13	422.42	10.036	37.63
383.20	19.939	35.08	477.24	10.058	43.98
423.47	19.976	37.38	523.36	10.063	57.66
478.67	19.967	43.05	288.15	0.10	30.33
523.39	19.934	53.68	298.15	0.10	31.20
333.21	10.047	32.99	313.15	0.10	32.12
381.70	10.057	35.15	328.15	0.10	33.24
		β-Alanine			
423.63	20.533	7.88	291.15	0.10	0.60
334.59	10.315	3.72	298.15	0.10	1.43
383.34	10.355	5.68	313.15	0.10	2.58
423.60	10.290	7.74	328.15	0.10	3.11
		Proline			
334.93	20.199	8.55	423.71	10.173	13.47
383.66	20.157	11.15	479.04	10.115	18.12
423.90	20.205	13.22	524.07	10.094	25.84
479.15	20.194	17.48	288.15	0.10	5.93
523.98	20.240	24.06	298.15	0.10	6.48
334.56	10.157	8.52	313.15	0.10	7.31
383.39	10.168	11.24	328.15	0.10	8.12

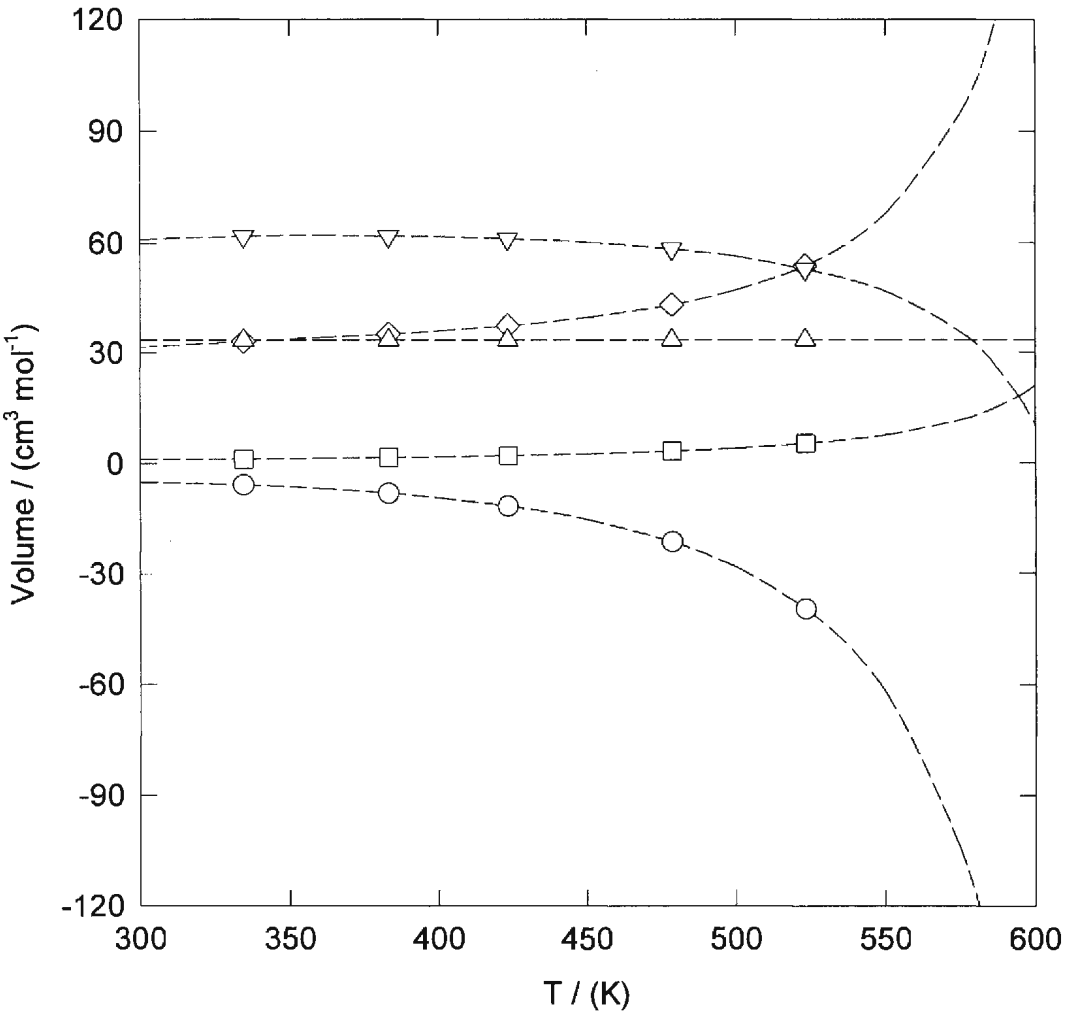

Figure 4.6.4.1 Relative contributions of V°_{intr}, $\Delta_{solv}V^{o}_{ss}$, $\Delta_{solv}V^{o}_{dipole}$, and $\Delta_{solv}V^{o}_{hydr}$ for α-alanine at 19.96 MPa. Symbols are the values calculated at the temperatures and pressures associated with the experimental values of V°: Δ, V°_{intr}; ○, $\Delta_{solv}V^{o}_{dipole}$; □, $\Delta_{solv}V^{o}_{ss}$; ◇, $\Delta_{solv}V^{o}_{hydr}$; ▽, V°.

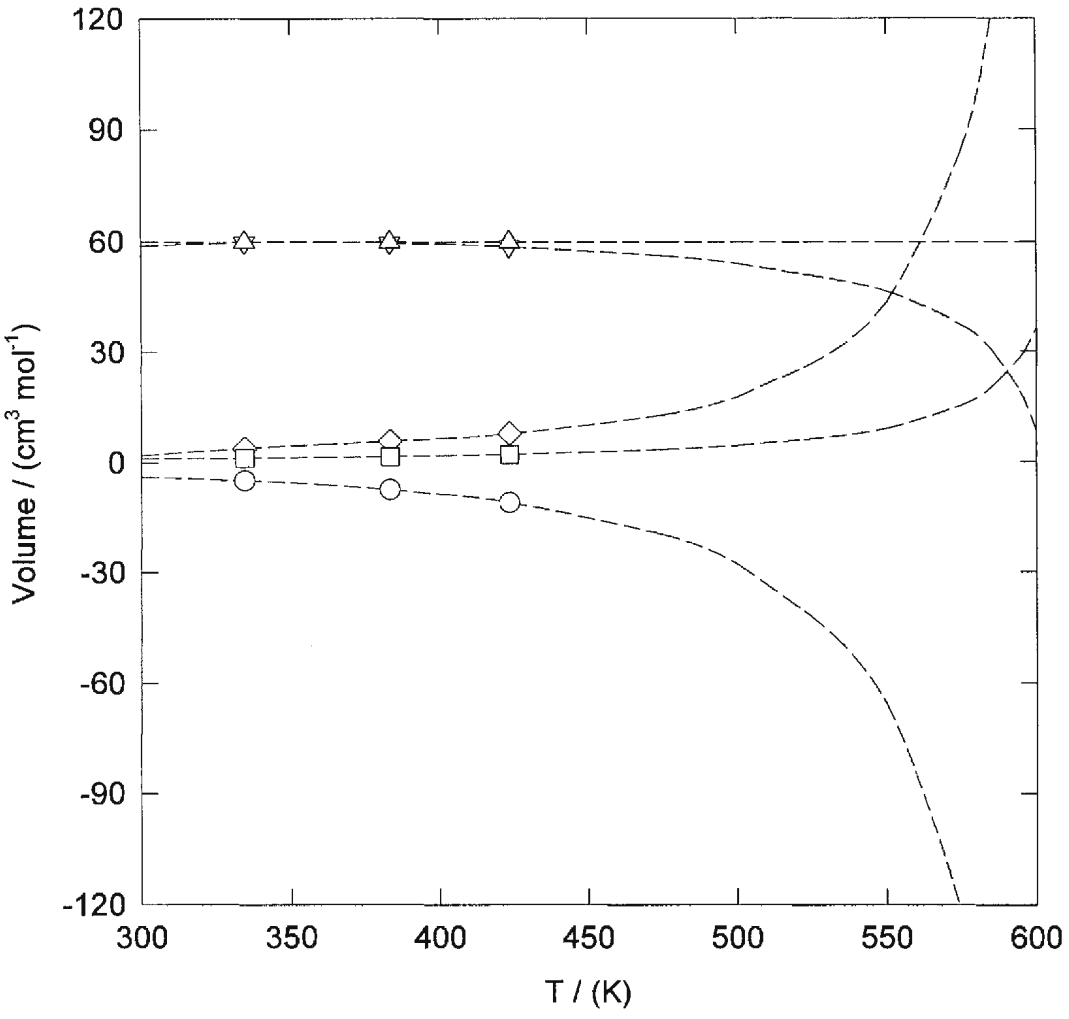

Figure 4.6.4.2 Relative contributions of V°_{intr}, $\Delta_{solv}V^{o}_{ss}$, $\Delta_{solv}V^{o}_{dipole}$, and $\Delta_{solv}V^{o}_{hydr}$ for β-alanine at 10.30 MPa. Symbols are the values calculated at the temperatures and pressures associated with the experimental values of V°: Δ, V°_{intr}; ○, $\Delta_{solv}V^{o}_{dipole}$; □, $\Delta_{solv}V^{o}_{ss}$; ◇, $\Delta_{solv}V^{o}_{hydr}$; ▽, V°.

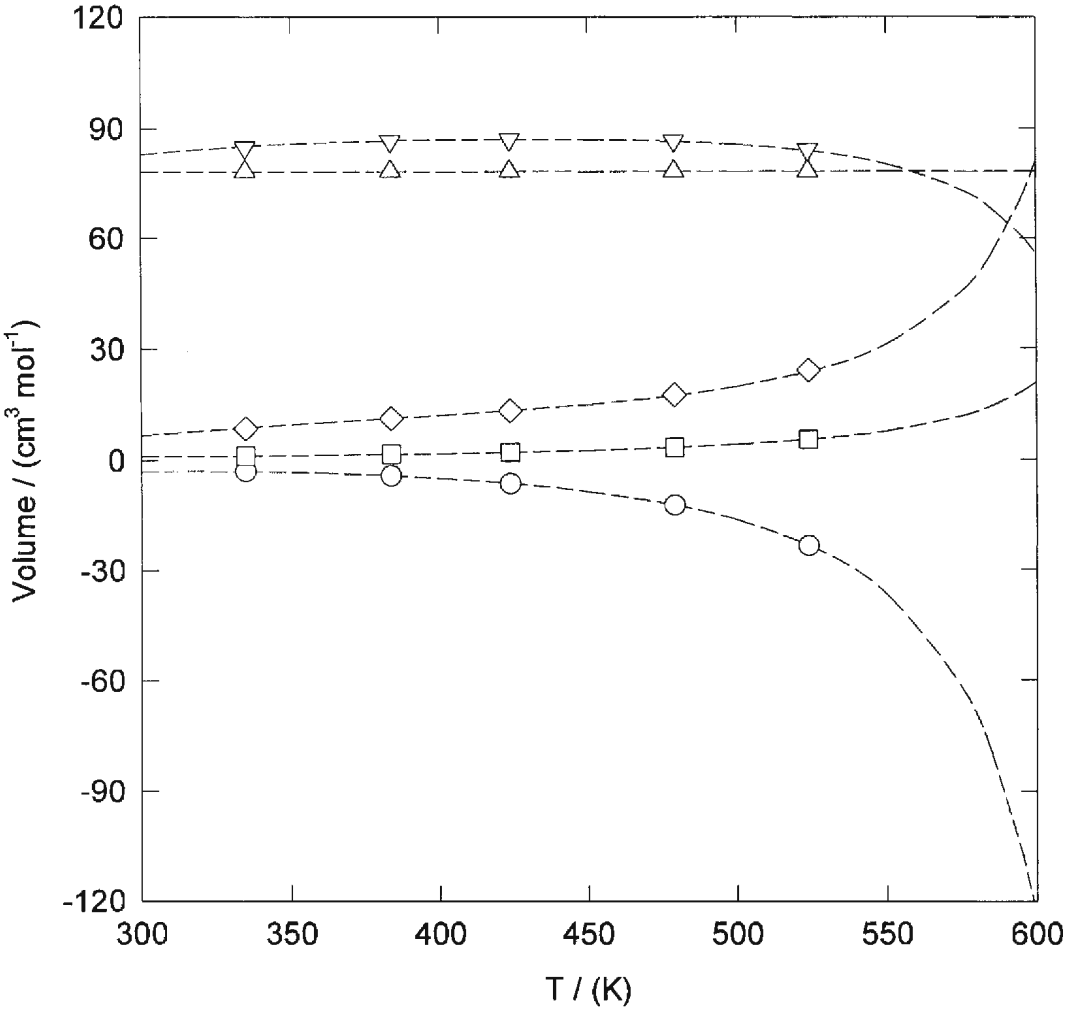

Figure 4.6.4.3 Relative contributions of V°_{intr}, $\Delta_{solv}V^{o}_{ss}$, $\Delta_{solv}V^{o}_{dipole}$, and $\Delta_{solv}V^{o}_{hydr}$ for proline at 20.20 MPa. Symbols are the values calculated at the temperatures and pressures associated with the experimental values of V°: Δ, V°_{intr}; ○, $\Delta_{solv}V^{o}_{dipole}$; □, $\Delta_{solv}V^{o}_{ss}$; ◇, $\Delta_{solv}V^{o}_{hydr}$; ▽, V°.

4.6.5 Comparison of the Contribution due to $\Delta_{solv}V^{o}_{dipole}$ with those due to $\Delta_{solv}V^{o}_{hydr}$.

As illustrated in Figures 4.6.4.1, 4.6.4.2, and 4.6.4.3 that the values of $\Delta_{solv}V^{o}_{dipole}$ deviate toward negative values at $T \geq 398$ K. As the temperature increases, the dipole polarization term over-predicts the observed decrease in the experimentally determined values of $V°$. As a result, the residual term $\Delta_{solv}V^{o}_{hydr}$ displays an increasingly large positive deviation that cancels some of the contribution from the dipole polarization term. Although this behaviour of $\Delta_{solv}V^{o}_{hydr}$ is consistent with the behaviour of $\Delta_{solv}V^{o}_{hydr}$ for many non-electrolytes, its magnitude is larger than that for other molecules of similar size; Shock and Helgeson (1990), Criss and Wood (1996), Shvedov and Tremaine (1997).

It is well known that the use of crystallographic radii in the Born equation over-predicts the contribution of electrostriction to the partial molar volumes of aqueous ions. This over-prediction is due to severely restricted dipolar-reorientation of the water molecules in the primary solvation sphere. Helgeson and Kirkham (1976) noted that an effective Born cavity radius $r_e = r + 0.94Z$ yields approximate agreement with the behaviour of C_p^{o} and $V°$ for cations of the type M^{z+} at elevated temperatures and pressures. Although it is generally assumed that the magnitude of $\Delta_{solv}V^{o}_{dipole}$ is small relative to $\Delta_{solv}V^{o}_{Born}$, a comparison of equations (1.3.2.10) and (1.3.2.21) indicates that this is not the case when the charge separation in the zwitterion is of similar magnitude to the cavity radius. Therefore, it is likely that the dipolar water in the primary solvation sphere of the zwitterion are immobilized and the use of an effective cavity radius $r_e > r$ is appropriate. The use of $r_e = r + 0.94$Å in

equation (1.3.2.21) yielded values of $\Delta_{solv}V^{o}_{dipole}$ for aqueous α-alanine and β-alanine that are in good agreement with the high temperature values of $V°$. The resulting values of $\Delta_{solv}V^{o}_{hydr}$ were relatively independent of temperature over the entire temperature range of the experimental data. Figures 4.6.5.1 and 4.6.5.2 illustrate the relative contributions of V^{o}_{intr}, $\Delta_{solv}V^{o}_{ss}$, $\Delta_{solv}V^{o}_{dipole}$, and $\Delta_{solv}V^{o}_{hydr}$ as a function of temperature for α-alanine at 19.96 MPa and β-alanine at 10.30 MPa when $r_e = r + 0.94$Å. The use of $r_e = r + 0.94$Å yielded values of $\Delta_{solv}V^{o}_{hydr}$ for aqueous proline that retained a significant temperature dependence. This is likely due to the dipole being off-centre in the proline solvation cavity. Figure 4.6.5.3 illustrates the relative contributions of V^{o}_{intr}, $\Delta_{solv}V^{o}_{ss}$, $\Delta_{solv}V^{o}_{dipole}$, and $\Delta_{solv}V^{o}_{hydr}$ as a function of temperature for aqueous proline at 20.20 MPa when $r_e = r + 0.94$Å.

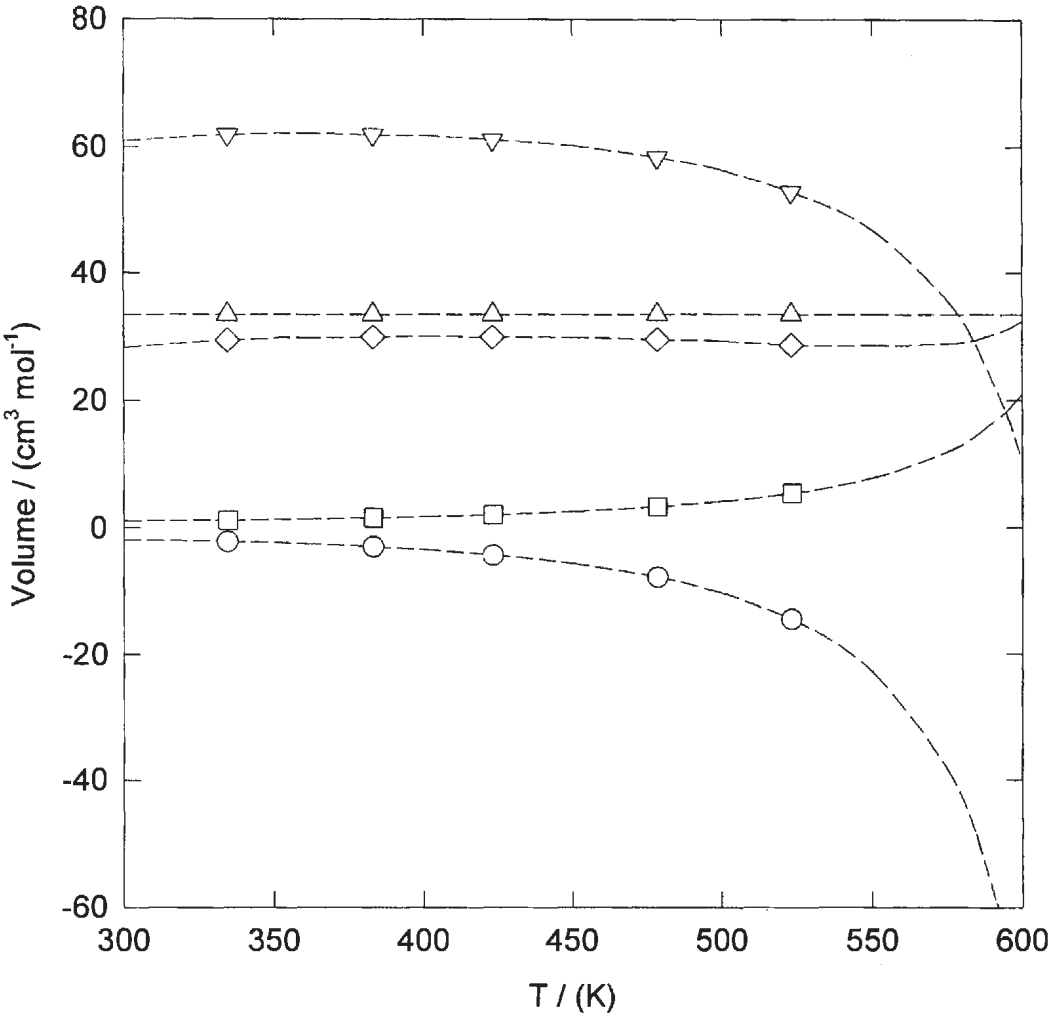

Figure 4.6.5.1 Relative contributions of V^{o}_{intr}, $\Delta_{solv}V^{o}_{ss}$, $\Delta_{solv}V^{o}_{dipole}$, and $\Delta_{solv}V^{o}_{hydr}$ for α-alanine at 19.96 MPa with $r_e = r + 0.94$Å. Symbols are the values calculated at the temperatures and pressures associated with the experimental values of V^{o}: Δ, V^{o}_{intr}; ○, $\Delta_{solv}V^{o}_{dipole}$; □, $\Delta_{solv}V^{o}_{ss}$; ◇, $\Delta_{solv}V^{o}_{hydr}$; ▽, V^{o}.

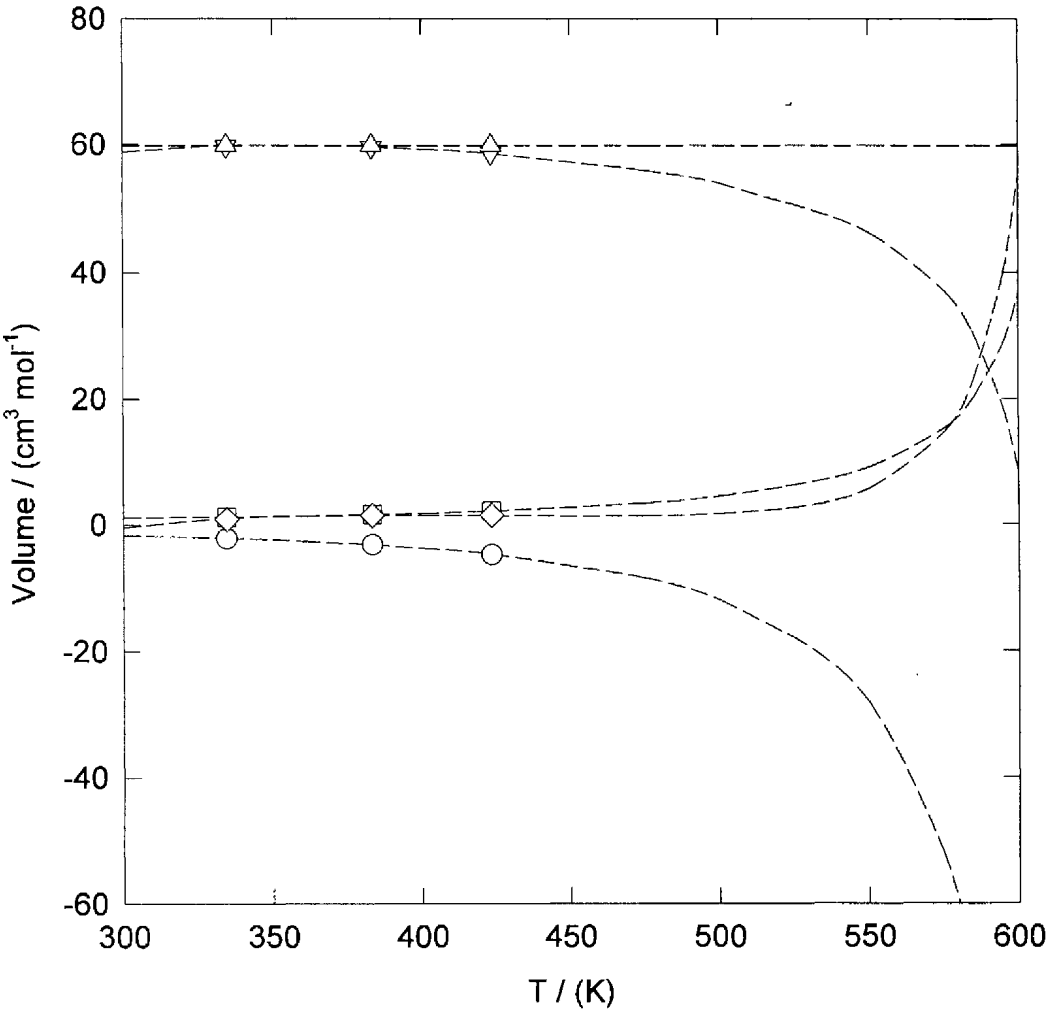

Figure 4.6.5.2 Relative contributions of V°_{intr}, $\Delta_{solv}V^{o}_{ss}$, $\Delta_{solv}V^{o}_{dipole}$, and $\Delta_{solv}V^{o}_{hydr}$ for β-alanine at 10.30 MPa with $r_e = r + 0.94$Å. Symbols are the values calculated at the temperatures and pressures associated with the experimental values of V°: Δ, V°_{intr}; ○, $\Delta_{solv}V^{o}_{dipole}$; □, $\Delta_{solv}V^{o}_{ss}$; ◇, $\Delta_{solv}V^{o}_{hydr}$; ▽, V°.

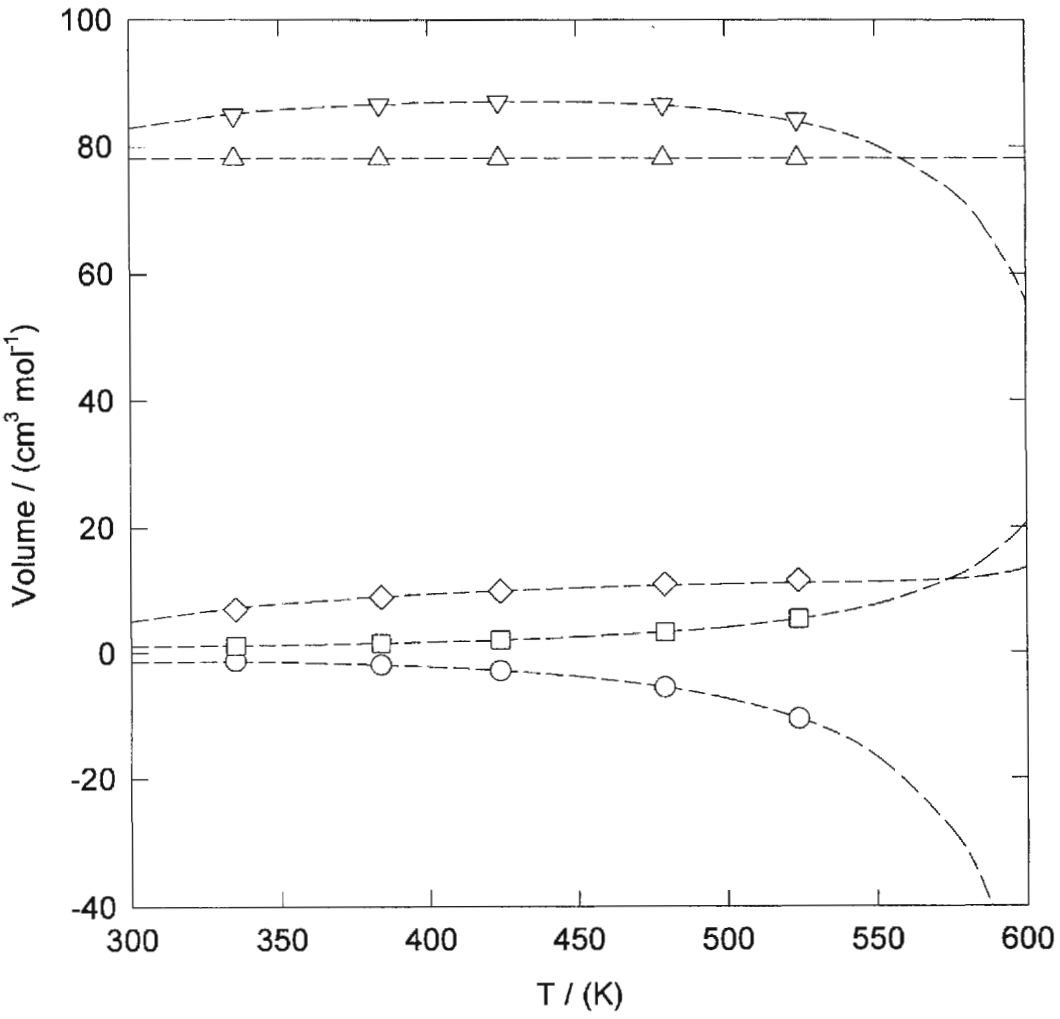

Figure 4.6.5.3 Relative contributions of V°_{intr}, $\Delta_{solv}V^{o}_{ss}$, $\Delta_{solv}V^{o}_{dipole}$, and $\Delta_{solv}V^{o}_{hydr}$ for proline at 20.20 MPa with $r_e = r + 0.94$Å. Symbols are the values calculated at the temperatures and pressures associated with the experimental values of V°: Δ, V°_{intr}; ○, $\Delta_{solv}V^{o}_{dipole}$; □, $\Delta_{solv}V^{o}_{ss}$; ◇, $\Delta_{solv}V^{o}_{hydr}$; ▽, V°.

4.7 Contribution of Solvation Effects to C_p^o.

The standard partial molar heat capacity C_p^o of an aqueous species is expressed as:

$$C_p^o = C_{p,intr}^o + \Delta_{solv}C_{p,ss}^o + \Delta_{solv}C_{p,pol}^o + \Delta_{solv}C_{p,hydr}^o \qquad (1.3.1.9)$$

The terms $C_{p,intr}^o$, $\Delta_{solv}C_{p,ss}^o$, $\Delta_{solv}C_{p,pol}^o$, and $\Delta_{solv}C_{p,hydr}^o$ have the same meaning as the analogous terms for $V°$ described in Section 4.6.1. Again using the assumption that $\Delta_{solv}C_{p,pol}^o$ is approximately equal to $\Delta_{solv}C_{p,dipole}^o$ and equation (1.3.1.9) becomes:

$$C_p^o = C_{p,intr}^o + \Delta_{solv}C_{p,ss}^o + \Delta_{solv}C_{p,dipole}^o + \Delta_{solv}C_{p,hydr}^o \qquad (4.7.1)$$

An expression for $\Delta_{solv}C_{p,ss}^o$ was obtained from equation (1.3.1.2):

$$\Delta_{solv}C_{p,ss}^o = -R + 2RT\alpha_w + RT^2\left(\frac{\partial\alpha_w}{\partial T}\right)_p \qquad (4.7.2)$$

As illustrated in Figures 4.6.3.1, 4.6.3.2, and 4.6.3.3 there are a limited number of experimentally determined values of μ for aqueous amino acids in the literature. Since the temperature dependance of the mean dipole moment of the amino acids is not well known, we have chosen to use a simpler calculation in which the dipole moment μ was taken to be independent of temperature and equal to the gas phase value μ_o, as listed in Table 4.6.3.1. Therefore equation (1.3.2.19) becomes:

$$\Delta_{solv}C_{p,dipole}^o = \frac{N_A}{4\pi\varepsilon_o r_e^3}\left[\left(\frac{3T\mu^2}{(2\varepsilon_r+1)^2}\right)\left(\frac{\partial^2\varepsilon_r}{\partial T^2}\right)_p - \left(\frac{12T\mu^2}{(2\varepsilon_r+1)^3}\right)\left(\frac{\partial\varepsilon_r}{\partial T}\right)_p^2\right] \qquad (4.7.3)$$

The effective radius r_e was taken to be equal to the crystallographic radius as listed in Table 4.6.2.1. The intrinsic and hydration contributions to solvation were represented by an

adjustable constant $\Delta_{solv}C^{o}_{p,non\text{-}dipole} = C^{o}_{p,intr} + \Delta_{solv}C^{o}_{p,hydr}$. The value of $\Delta_{solv}C^{o}_{p,non\text{-}dipole}$ was chosen for each amino acid such that the calculated value of C_p^o fitted the experimental value at 373 K and the highest pressure studied. Therefore, the standard partial molar heat capacity of the solute was expressed as:

$$C_p^{\,o} = \Delta_{solv}C^{\,o}_{p,non-dipole} + \Delta_{solv}C^{\,o}_{p,dipole} + \Delta_{solv}C^{\,o}_{p,ss} \qquad (4.7.4)$$

The standard partial molar heat capacities obtained for aqueous glycine and α-alanine using $r_e = r$ in equation (4.7.4) are illustrated in Figures 4.7.1 and 4.7.2. The behaviour of C_p^o at elevated temperatures is consistent with the effects of dipole polarization. However, the agreement with the experimental results is only qualitative. Glycine is the simplest amino acid, with the most centrosymmetric dipole. Yet, the values for $\Delta_{solv}C^{o}_{p,dipole}$ show a much stronger temperature dependence and a slightly stronger pressure dependence than the experimental results. Comparison of Figures 4.7.1 and 4.7.2 reveals that the error in the predicted temperature dependence is much greater for α-alanine than it is for glycine. This is likely due to the presence of a hydrophobic methyl group and an off-entered dipole in α-alanine. While the dipole contribution is larger than the hydration- and standard-state terms, these terms are not negligible. The hydration term becomes larger for larger molecules necessitating a more realistic modelling approach in which the presence of hydrophobic groups and the location of the dipole are specifically considered.

In their treatments of aqueous ions, Helgeson and Kirkham (1976) have successfully approximated the primary-sphere hydration effects for M^{Z+} cations by using an effective

radius, $r_e \approx r + (0.9 \cdot Z)$ Å, in the Born equation. Our attempts to develop a similar treatment for C_p^o and V° for these dipolar zwitterions, based on equation (4.7.3) with a self-consistent formula for estimating the effective radius, have not been successful. Clearly a more detailed and rigorous treatment is needed.

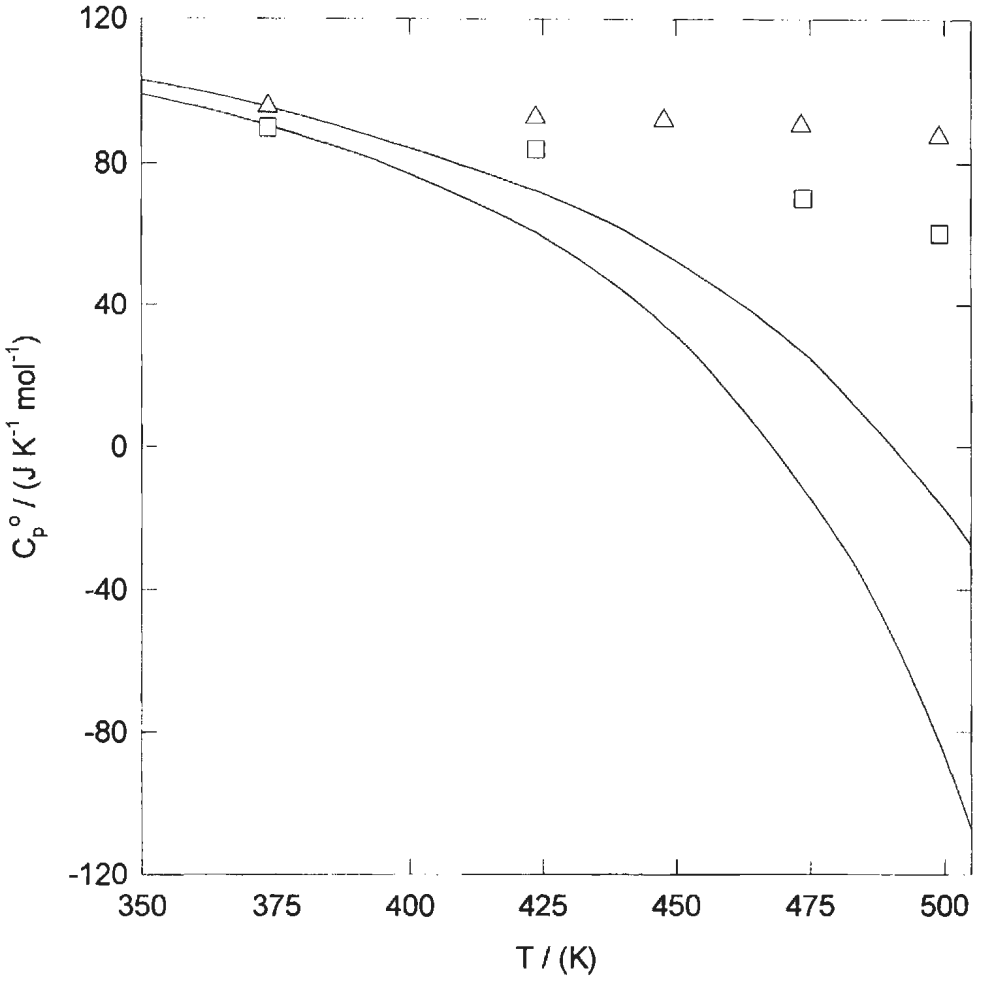

Figure 4.7.1 Temperature and pressure dependence of C_p° for glycine as predicted by equation (4.7.4). Symbols are the fitted isotherms obtained in Section 3.3: □, steam saturation pressure; Δ, 30 MPa. Lines are the fitted values.

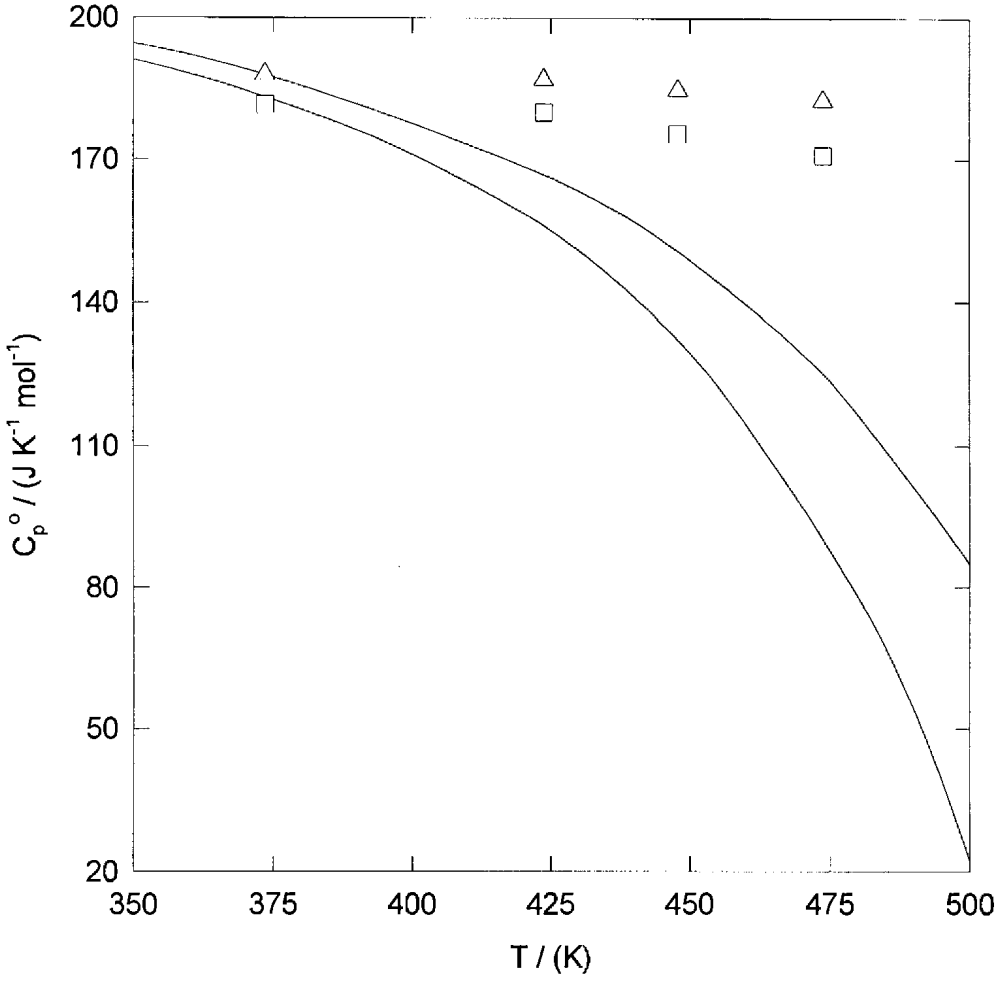

Figure 4.7.2 Temperature and pressure dependence of C_p° for α-alanine as predicted by equation (4.7.4). Symbols are the fitted isotherms obtained in Section 3.3: □, steam saturation pressure; Δ, 30 MPa. Lines are the fitted values.

CHAPTER 5.0 CONCLUSIONS

In this work the first experimentally determined apparent molar volumes V_ϕ for aqueous α-alanine, β-alanine, and proline were obtained between the temperatures of 343 K and 523 K and at pressures in excess of steam saturation. The first experimentally determined apparent molar heat capacities $C_{p,\phi}$ for aqueous α-alanine, β-alanine, glycine, and proline were also obtained between the temperatures of 328 K and 498 K and at pressures in excess of steam saturation. These are the first experimental values of $C_{p,\phi}$ for aqueous amino acids above 328 K. The measurements made at the lowest temperatures compare extremely well with the available literature. The standard partial molar volumes $V°$ and the standard partial molar heat capacities C_p° were calculated from the isothermal experimental values of V_ϕ and $C_{p,\phi}$, respectively. The values of $V°$ increase slowly with temperature until they reach their maximum value at $T = 398$ K and then deviate toward negative values at $T \geq 398$ K. The values of C_p° increase sharply until they reach their maximum value and then slowly decline in the range 423 - 523 K.

Two models were used to fit the molality, temperature, and pressure dependencies of the V_ϕ data for each of the aqueous amino acids. The revised HKF model uses both a non-solvation term and a modified Born function to represent the temperature and pressure dependence of the thermodynamic properties of aqueous species. The density model uses the compressibility of water to represent the thermodynamic properties of aqueous species as a

function of temperature and pressure. A comparison of the overall weighted standard deviations and the behaviour of systematic errors for the fit of each model, indicated that the density model reproduces the experimental results better than the revised HKF model for all of the aqueous amino acids studied. To fit the temperature and pressure dependencies of both the V° and C_p° data, the density model was extended by including a number of additional temperature- and/or pressure-dependent terms.

Amend and Helgeson (1997) have used the revised HKF model as applied to organic species to predict the standard partial molar volumes V° and standard partial molar heat capacities C_p° of aqueous α-alanine, glycine, and proline as a function of temperature. Unlike the experimental values of V° which deviate toward negative values at temperatures above 423 K and the experimental values of C_p° which deviate toward negative values at temperatures above 373 K to 423 K, the predicted values of both V° and C_p° continue to become more positive as the critical temperature of water is approached. This reflects the neglect of the zwitterionic nature of the aqueous amino acids by Amend and Helgeson (1997). Our work has shown that the effect of solvent polarization can not be ignored and is in fact strong enough to reverse the direction of the temperature and pressure dependencies of V° and C_p°.

The very recent functional-group additivity model of Yezdimer *et al.* (2000) was used to predict V° and C_p° for aqueous α-alanine and glycine. Although the predicted values do deviate toward negative values as the critical temperature of water is approached in a manner

similar to the experimental results, the agreement is not quantitative. An attempt to recalculate the parameters for the amino acid functional group using the V° and C_p° data obtained in this work and the V° data obtained by Hakin *et al.* (1998) did not significantly improve the accuracy of the model. This behaviour suggests that there is insufficient flexibility in the equations of state developed by Sedlbauer *et al.* (2000) upon which Yezdimer *et al.* (2000) have developed their model.

The hydrothermal colorimetric pH indicators identified by Ryan *et al.* (1997) and Xiang and Johnston (1997) were successfully used to obtain the first experimentally determined acid/base dissociation constants for aqueous α-alanine between the temperatures of 423 K and 523 K and between the pressures of 5.3 MPa and 5.6 MPa. These showed that the dissociation constants that were estimated with the functional-group additivity model of Yezdimer *et al.* (2000) and those obtained from the isocoulombic extrapolation of room temperature data are an upper limit. The colorimetric method is a convenient method of measuring solution pH under hydrothermal conditions. The colorimetric indicators are stable in aqueous solution up to and above the critical temperature of water. Since both forms of the colorimetric indicators are colored, the absorbance spectrum measured for a solution is the linear combination of the absorbance spectra due to the protonated and deprotonated forms of the indicator. Thus providing a relatively simple means of measuring the molality of H^+ in solution. The flow cell described in this work minimizes the amount of time that a sample solution remains at the temperature of interest. This allows measurements to be made

at temperatures at which the solute has limited hydrothermal stability.

Using the values of $V°$, C_p^o, K_1, K_2, and K_3 predicted by the functional-group additivity model of Yezdimer *et al.* (2000) it was found that the contribution of the ionic and neutral forms of the aqueous amino acids to the experimental values of $V°$ and C_p^o were negligible at all but the highest temperatures. Even when significantly different from zero these contributions remained small (less than ± 0.15 $cm^3 \cdot mol^{-1}$ and ± 2.4 $J \cdot K^{-1} \cdot mol^{-1}$).

The contributions to the V^o values for each of the aqueous amino acids can be identified as an intrinsic molar gas phase volume, a partial molar volume of polarization, a molar volume due to standard state correction, and a molar volume of hydration. The partial molar volume of polarization considers the electrostatic interaction between the dipole associated with the zwitterionic aqueous amino acid and the bulk solvent. While there is qualitative agreement between the partial molar volume of polarization and the $V°$ values, the partial molar volume of polarization becomes negative faster than the $V°$ values as the critical temperature of water is approached. Therefore a molar volume of hydration is obtained which is of similar magnitude to the partial molar volume of polarization but tends toward positive values as the critical temperature of water is approached. By increasing the effective radius used in the estimation of the partial molar volume of polarization the temperature dependence of the molar volume of hydration can be virtually removed in the case of α-alanine and β-alanine.

There are a number of projects that naturally extend the work described in this thesis.

The batch experiments were only used to confirm that α-alanine and proline were stable on the time scale required for our measurements at the temperatures, pressures, and molalities required for this work. The identities of the major thermal products were predicted from literature reports to be amino acid condensation and decarboxylation. Our amino acid analysis indicated that these were indeed the primary routes for amino acid loss. However, there are a number of minor products that are either produced directly from the amino acids or from other thermal products. A complete study of the thermal reactions involving the aqueous amino acids would involve identifying all species in solution after heating and determining the kinetics of their production. The kinetics of the thermal reactions producing colored products could easily be studied using the UV-visible spectrophotometer and high temperature flow cell. By stopping the flow when the amino acid solution is in the flow cell, the change in the concentration of a colored product can be monitored by measuring the change in absorbance as a function of time. The kinetics of thermal reactions involving the loss or production of protons could be studied using UV-visible spectroscopy and the hydrothermally stable colorimetric indicators.

The standard partial molar volumes V° and heat capacities C_p° were determined for aqueous α-alanine, β-alanine, glycine, and proline as a function of temperature and pressure. The experimental results were found to be equal to the zwitterionic contribution within ± 0.15 $cm^3 \cdot mol^{-1}$ and ± 2.4 $J \cdot K^{-1} \cdot mol^{-1}$. A more complete study would involve measuring the apparent molar volumes V_{ϕ} and heat capacities $C_{p,\phi}$ of the protonated and deprotonated

forms of the aqueous amino acids as a function of temperature. The experimental values of V° and C_p° for the three significant forms of aqueous amino acids would provide a solid experimental foundation for the development of a model capable of predicting the thermodynamic properties of amino acids as a function of temperature, pressure, and pH.

The measurement of high temperature acid/base dissociation constants for α-alanine using UV-visible spectroscopy with hydrothermally stable colorimetric indicators was sufficient to prove that speciation effects could be safely ignored when interpreting the V° and C_p° results. I believe that this area of my work offers great potential for further study. The α-alanine buffer solutions were prepared such that the buffer ratio was 1 : 1. By varying the buffer ratio, the pH of the buffer solutions could be adjusted to lie within the indicator range of the appropriate colorimetric indicator over a larger range of temperatures. The high temperature acid/base dissociation constants for glycine and proline could also be measured using UV-visible spectroscopy with hydrothermally stable colorimetric indicators.

Aqueous amino acids are known to form complexes with a wide variety of metal ions (Martell and Smith, 1974). For those complexes that are colored, the formation constants can be measured as a function of temperature using UV-visible spectroscopy. It is also suspected that aqueous amino acids form complexes with nitrate and other anions (Pradhan *et al.*, 1997; Pradhan and Vera, 1997). The structure and stability of these amino acid complexes could be investigated using raman spectroscopy.

CHAPTER 6.0 BIBLIOGRAPHY

Aaron M.W. and Grant E.H. (1967) Comparison Between the Dielectric Properties of α- and β-Alanine Solutions. *Trans. Faraday Soc.* **9**, 2177-2180.

Abelson P.H. (1957) Organic Constituents of Fossils. Treatise on Marine Ecology and Palaeoecology. *Mem. Geological Society of America.* **2**, 67, 87-92.

Ahluwalia J.C., Ostiguy C., Perron G., and Desnoyers J.E. (1977) Volumes and Heat Capacities of Some Amino Acids in Water at 25°C. *Can. J. Chem.* **55**, 3364-3367.

Albert H.J. and Wood R.H. (1984) High-Precision Flow Densimeter for Fluids at Temperatures to 700 K and Pressures to 40 MPa. *Rev. Sci. Instrum.* **55**, 589-593.

Amend J.P. and Helgeson H.C. (1997) Calculation of the Standard Molal Thermodynamic Properties of Aqueous Biomolecules at Elevated Temperatures and Pressures: Part 1. L-α-Amino Acids. *J. Chem. Soc., Faraday Trans.* **93**, 1927-1941.

Anderson G.M., Castet S., Schott J., and Mesmer R.E. (1991) The Density Model for Estimation of Thermodynamic Parameters of Reactions at High Temperatures and Pressures. *Geochim. Cosmochim. Acta.* **55**, 1769-1779.

Archer D.G. (1992) Thermodynamic Properties of the NaCl + H_2O System II. Thermodynamic Properties of NaCl(aq), NaCl·$2H_2O$(cr), and Phase Equilibria. *J. Phys. Chem. Ref. Data* **21**, 793-823.

Atkins P.W. (1990) *Physical Chemistry*. Fourth Edition; W.H. Freeman and Company: New York.

Averbuch-Pouchot M.T., Durif A., and Guitel J.C. (1988) Structures of β-Alanine, DL-Alanine and Sarcosine Monophosphates. *Acta Cryst.* **C44**, 1968-1972.

Bada J.L. and Miller S.L. (1970) The Kinetics and Mechanism of the Reversible Nonenzymatic Deamination of Aspartic Acid. *J. Am. Chem. Soc.* **92**, 2774-2782.

Bada J.L., Miller S.L., and Zhao M.X. (1995) The Stability of Amino Acids at Submarine Hydrothermal Vent Temperatures. *Origins of Life and Evolution of the Biosphere* **25**, 111-118.

Balakrishnan P.V. (1988) Liquid-Vapour Distribution of Amines and Acid Ionization Constants of Their Ammonium Salts in Aqueous Systems at High Temperature. *J. Sol. Chem.* **17**, 825-840.

Baross J.A. and Deming J.W. (1983) Growth of 'Black Smoker' Bacteria at Temperatures of at Least 250°C. *Nature* **303**, 423-426.

Belibagli K.B. and Ayranci E. (1990) Viscosities and Apparent Molar Volumes of Some Amino Acids in Water and in 6*M* Guanidine Hydrochloride at 25°C. *J. Solution Chem.* **19**, 867-882.

Ben-Naim A. (1987) *Solution Thermodynamics.* Plenum Press: New York.

Bennett G.E. and Johnston K.P. (1994) UV-Visible Absorbance Spectroscopy of Organic Probes in Supercritical Water. *J. Phys. Chem.* **98**, 441-447.

Beveridge D.L. and Schnuelle G.W. (1975) Free Energy of a Charge Distribution in Concentric Dielectric Continua. *J. Phys. Chem.* **79**, 2562-2566.

Biggerstaff D.R. and Wood R.H. (1988) Apparent Molar Heat Capacities of Aqueous Argon, Ethylene, and Xenon at Temperatures up to 720 K and Pressures to 33 MPa. *J. Phys. Chem.* **92**, 1994-2000.

Böttcher C.J.F. (1973) *Theory of Electric Polarization.* Second Edition, Volume 1; Elsevier Scientific Publishing Company: Amsterdam.

Bowen H.J.M. (1958) *Tables of Interatomic Distances and Configuration in Molecules and Ions.* Special Publication No. 11; The Chemical Society: London.

Born M. (1920) Volumen und Hydratationswärme der Ionen. *Zeitschr. Physik* **1**, 45-48.

Cabani S., Conti G., and Matteoli E. (1977) Apparent Molal Heat Capacities in Aqueous Solution of Molecules Containing the Peptide Linkage: Cyclic and Open Chain Dipeptides. *Biopolymers.* **16**, 465-467.

Cabani S., Gianni P, Mollica V., and Lepori L. (1981) Group Contributions to the Thermodynamic Properties of Non-ionic Organic Solutes in Dilute Aqueous Solution. *J. Solution Chem.* **10**, 563-595.

Chalikian T.V., Sarvazyan A.P., Funck T., Cain A., and Breslauer K.J. (1994) Partial Molar Characteristics of Glycine and Alanine in Aqueous Solutions at High Pressures Calculated from Ultrasonic Velocity Data. *J. Phys. Chem.* **98**, 321-328.

Chalikian T.V., Sarvazyan A.P., and Breslauer K.J. (1993) Partial Molar Volumes, Expansibilities, and Compressibilities of α,ω-Aminocarboxylic Acids in Aqueous Solutions Between 18 and 55 °C. *J. Phys. Chem.* **97**, 13017-13026.

Chlistunoff J., Ziegler K.J., Lasdon L., and Johnston K.P. (1999) Nitric/Nitrous Acid Equilibria in Supercritical Water. *J. Phys. Chem.* **103**, 1678-1688.

Cobble J.W. and Murray R.C. Jr. (1977) Unusual Ion Solvation Energies in High Temperature Water. *Faraday Disc. Chem. Soc.* **64**, 144-149.

Corti H.R., Prini R.F., and Svarc F. (1990) Densities and Partial Molar Volumes of Aqueous Solutions of Lithium, Sodium, and Potassium Hydroxides up to 250°C. *J. Solution Chem.* **19**, 793-809.

Crabtree R.H. (1997) Where Smokers Rule. *Science.* **276**, 222.

Criss C.M. and Wood R.H. (1996) Apparent Molar Volumes of Aqueous Solutions of some Organic Solutes at the Pressure 28 MPa and Temperatures to 598 K. *J. Chem. Thermodynamics* **28**, 723-741

Desnoyers J.E., Verrall R.E., and Conway B.E. (1965) Electrostriction in Aqueous Solutions of Electrolytes. *J. Chem. Phys.* **43**, 243-250.

Desnoyers J.E., Visser C. de, Perron G., and Picker P. (1976) Reexamination of the Heat Capacities Obtained by Flow Microcalorimetry. Recommendation for the use of a Chemical Standard. *J. Solution Chem.* **5**, 605-616.

Devine W. and Lowe B.M. (1971) Viscosity B-Coefficients at 15 and 25°C for Glycine, β-Alanine, 4-Amino-n-butyric Acid, and 6-Amino-n-hexanoic Acid in Aqueous Solution. *J. Chem. Soc. A.* 2113-2116.

Devoto P. (1930) Ricerche Sulla Constante Dielettrica dei Liquidi. - Nota III. Soluzioni Acquose di Alcuni Composti Organici. *Gazz. Chim. Ital.* **60**, 520-530.

Devoto P. (1931) Ricerche Sulla Constante Dielettrica dei Liquidi. - Nota V. Soluzioni Acquose di Sostanze Organiche. *Gazz. Chim. Ital.* **61**, 897-909.

Devoto P. (1933) Ricerche Sulla Constante Dielettrica dei Liquidi. - Nota VIII. *Gazz. Chim. Ital.* **63**, 50-58.

Dipaola G. and Belleau B. (1978) Apparent Molal Heat Capacities and Volumes of Amino Acids in Aqueous Polyol Solutions. *Can. J. Chem.* **56**, 1827-1831.

Edsall J.T. and Wymann J. (1958) *Biophysical Chemistry.* Volume 1; Academic Press: New York.

Edward J.T., Farrell P.G., and Job J.L. (1974) The Dielectric Increments of Amino Acids. *J. Am. Chem. Soc.* **96**, 902-906.

Ellerton H.D., Reinfelds G., Mulcahy D.E., and Dunlop P.J. (1964) Activity, Density, and Relative Viscosity Data for Several Amino Acids, Lactamide, and Raffinose in Aqueous Solution at 25°. *J. Phys. Chem.* **68**, 398-402.

Fabes L. And Swaddle T.W. (1975) Reagents for High Temperature Aqueous Chemistry: Trifluoromethanesulfonic Acid and its Salts. *Can. J. Chem.* **53**, 3053-3059.

Fernandez D.P., Goodwin A.R.H., Lemmon E.W., Levelt Sengers J.M.H., and Williams R.C. (1997) A Formulation for the Static Permittivity of Water and Steam at Temperatures from 238 K to 873 K at Pressures up to 1200 MPa, Including Derivatives and Debye-Huckel Coefficients. *J. Phys. Chem. Ref. Data* **26**, 1125-1166.

Flegmann A.W. and Tattersall R. (1979) Energetics of Peptide Bond Formation at Elevated Temperatures. *J. Mol. Evol.* **12**, 349-355.

Fox S.W. and Dose K. (1977) *Molecular Evolution and the Origin of Life.* Marcel Dekker Inc.: New York.

Franck E.U. (1956) Hochverdichteter Wasserdampf II. Ionendissociation von KCl in H_2O bis 750°C. *Z. Phys. Chem.* **8**, 107-126.

Franck E.U. (1961) Überkritisches Wasser als electrolytisches Lösungsmittel. *Angew. Chem.* **73**, 309-322.

Gopal R., Agarwal D.K., and Kumar R. (1973) Variation of Limiting Apparent Molal Volume with Temperature in Some Amino Acids in Aqueous Solutions. *Indian J. Chem.* **11**, 1061-1062.

Greenstein J.P. and Winitz M. (1961) *Chemistry of the Amino Acids.* Volume 1; John Wiley and Sons: New York.

Gucker F.T. and Allen T.W. (1942) The Densities and Specific Heats of Aqueous Solutions of *dl*-α-Alanine, β-Alanine and Lactamide. *J. Am. Chem. Soc.* **64**, 191-199.

Gucker F.T., Lamb F.W., Marsh G.A., and Haag R.M. (1950) The Adiabatic Compressibility of Aqueous Solutions of Some Simple Amino Acids and their Uncharged Isomers at 25°. *J. Am. Chem. Soc.* **72**, 310-317.

Hakin A.W., Duke M.M., Klassen S.A., McKay R.M., and Preuss K.E. (1994) Apparent Molar Heat Capacities and Volumes of Some Aqueous Solutions of Aliphatic Amino Acids at 288.15, 298.15, 313.15, and 328.15 K. *Can. J. Chem.* **72**, 362-368.

Hakin A.W., Copeland A.K., Liu J.L., Marriott R.A., and Preuss K.E. (1997) Densities, Apparent Molar Volumes, and Apparent Molar Heat Capacities of *l*-Arginine, *l*-Proline and *d,l*-Methionine in Water at 288.15, 298.15, 313.15, and 328.15 K. *J. Chem. Eng. Data* **42**, 84-89.

Hakin A.W., Daisley D.C., Delgado L., Liu J.L., Marriott R.A., Marty J.L., Tompkins G. (1998) Volumetric Properties of Glycine in Water at Elevated Temperatures and Pressures Measured with a New Optically Driven Vibrating-Tube Densimeter. *J. Chem. Thermodynamics* **30**, 583-606.

Hederstrand G. (1928) Über die Dielektrizitätskonatanten Wässeriger Lösungen Einiger Aminosäuren. *Z. Physik. Chem.* **135**, 36-48.

Helgeson H.C. and Kirkham D.H. (1976) Theoretical prediction of the Thermodynamic Behaviour of Aqueous Electrolytes at High-temperatures and Pressures: III. Equation of State for Aqueous Species at Infinite Dilution. *Amer. J. Sci.* **276**, 97-240.

Helgeson H.C., Kirkham D.H., and Flowers G.C. (1981) Theoretical Predictions of the Thermodynamic Behaviour of Aqueous Electrolytes at High Pressures and Temperatures. IV. Calculation of Activity Coefficients, Osmotic Coefficients, and Apparent Molar and Standard and Relative Partial Molar Properties to 600°C and 5 kb. *Amer. J. Sci.* **281**, 1249-1516.

Hill P.G. (1990) A Unified Fundamental Equation for the Thermodynamic Properties of H_2O. *J. Phys. Chem. Ref. Data* **19**, 1233-1274.

Hnedkovsky L., Hynek V., Majer V., and Wood R. (1999) Heat Capacities of Aqueous Solutions at Superambient Conditions by Differential Flow Calorimetry. *Proc. 13th Int. Conf. Prop. Water and Steam.* Paper TTP3.4.

Hoiland H. (1986) *Thermodynamic Data for Biochemistry and Biotechnology*. Springer-Verlag: Berlin.

Impey R.W., Madden P.A., and McDonald I.R. (1983) Hydration and Mobility of Ions in Solution. *J. Phys. Chem.* **87**, 5071-5083.

Inglese A., Sedlbauer J., Yezdimer E.M., and Wood R.H. (1997) Apparent Molar Heat Capacities of Aqueous Solutions of Propylamine, 1,4-Butanediamine, 1,6-Hexanediamine, Propylamine Hydrochloride, Propionamide, Pyridine, and Sodium Benzenesulfonate at Temperatures form 300 K to 528 K and a Pressure of 28 MPa. *J. Chem. Thermodynamics* **29**, 517-531.

Johnston K.P. and Chlistunoff J.B. (1998) Neutralization of Acids and Bases in Subcritical and Supercritical Water: Acetic Acid and HCl. *J. Supercrit. Fluids.* **12**, 155-164.

Jolicoeur C. and Boileau J. (1978) Apparent Molal Volumes and Heat Capacities of Low Molecular Weight Peptides in Water at 25°C. *Can. J. Chem.* **56**, 2707-2713.

Jolicoeur C., Riedl B., Desrochers D., Lemelin L.L., Zamojska R., and Enea O. (1986) Solvation of Amino Acid Residues in Water and Urea-Water Mixtures: Volumes and Heat Capacities of 20 Amino Acids in Water and in 8 Molar Urea at 25°C. *J. Solution Chem.* **15**, 109-128.

Kharakoz D.P. (1989) Volumetric Properties of Proteins and Their Analogues in Diluted Water Solutions. 1. Partial Volumes of Amino Acids at 15-55°C. *Biophys. Chem.* **34**, 115-125.

Kharakoz D.P. (1991) Volumetric Properties of Proteins and Their Analogues in Diluted Water Solutions. 2. Partial Adiabatic Compressibilities of Amino Acids at 15-70°C. *J. Phys. Chem.* **95**, 5634-5642.

Kikuchi M., Sakurai M., and Katsutoshi N. (1995) Partial Molar Volumes and Adiabatic Compressibilities of Amino Acids in Dilute Aqueous Solutions at 5, 15, 25, 35, and 45°C. *J. Chem. Eng. Data* **40**, 935-942.

Kirkwood J.G. (1934) Theory of Solutions of Molecules Containing Widely Separated Charges with Special Applications to Zwitterions. *J. Chem. Phys.* **2**, 351-361.

Kirshnerova J., Farrell P.G., and Edward J.T. (1976) Dielectric Increments and the Conformations of Amino Acids and Betaines in Water. *J. Phys. Chem.* **80**, 1974-1980.

Kratky O., Leopold H., and Stabinger H. (1969) Dichtemessungen an Flüssigkeiten und Gasen auf 10^{-6} g / cm^3 bei 0.6 cm^3 Präparatvolumen. *Angew. Phys.* **27**, 273-277.

Lide D.R. (1990) *CRC Handbook of Chemistry and Physics, 71st Edition.* CRC Press: Boston.

MacDonald D.D., Hettiarachchi S., Song H., Makela K., Emerson R., and Ben-Haim M. (1992) Measurement of pH in Subcritical and Supercritical Aqueous Systems. *J. Solution Chem.* **21**, 849-879.

Majer V., Crovetto R., and Wood R.H. (1991) A New Version of the Vibrating-Tube Flow Densitometer for Measurements at Temperatures up to 730 K. *J. Chem. Thermodyn.* **23**, 333-344.

Marshall, W.L. and Franck, E.U. (1981) Ion Product of Water Substance, 0-1000°C, 1-10,000 bars. New International Formulation and its Background. *J. Phys. Chem. Ref. Data* **10**, 295.

Martell A.E. and Smith R.M. (1974) *Critical Stability Constants. Volume 1: Amino Acids.* Plenum Press: New York.

Mesmer R.E., Marshall W.L., Palmer D.A., Simonson J.M., and Holmes H.F. (1988) Thermodynamics of Aqueous Association and Ionization Reactions at High Temperatures and Pressures. *J. Solution Chem.* **17**, 699.

Mesmer R.E., Patterson C.S., Busey R.H., and Holmes H.F. (1989) Ionization of Acetic Acid in NaCl(aq) Media: A Potentiometric Study to 573 K and 130 bar. *J. Phys.Chem.* **93**, 7483-7490.

Mesmer R.E. and Baes C.F. (1974) Phosphoric Acid Dissociation Equilibria in Aqueous Solutions to 300°C. *J. Solution Chem.* **3**, 307-322.

Miller S.L. and Bada J.L. (1988) Submarine Hot Springs and the Origin of Life. *Nature* **334**, 609-611.

Millero F.J., Surdo A.L., and Shin C. (1978) The Apparent Molal Volumes and Adiabatic Compressibilities of Aqueous Amino Acids at 25°C. *J. Phys. Chem.* **82**, 784-792.

Mishra A.K. and Ahluwalia J.C. (1984) Apparent Molar Volumes of Amino Acids, N-Acetylamino Acids, and Peptides in Aqueous Solutions. *J. Phys. Chem.* **88**, 86-92.

Ogawa T., Yasuda M., and Mizutani K. (1984) Volume and Adiabatic Compressibility of Amino Acids in Urea - Water Mixtures. *Bull. Chem. Soc. Jpn.* **57**, 662-666.

Osborn J.A. (1945) Demagnetizing Factors of the General Ellipsoid. *Phys. Review* **67**, 351-357.

Padmanabhan S., Suresh S., and Vijayan M. (1995) DL-Proline Monohydrate. *Acta Cryst.* **C51**, 2098-2100.

Pepela C.N. and Dunlop P.J. (1972) Diffusion and Density Data for One Composition of System H_2O-*n*-Pr_4NBr-β-Alanine at 25 °C. *J. Chem. Eng. Data.* **17**, 207-208.

Perrin D.D. and Armarego W.L.F. (1988) *Purification of Laboratory Chemicals.* 3rd Edition; Pergamon Press: New York.

Picker P., Ludec P.A., and Desnoyers J.E. (1971) Heat Capacity of Solutions by Flow Microcalorimetry. *J. Chem Thermodyn.* **3**, 631-642.

Picker P., Tremblay E., and Jolicoeur C. (1974) A High-Precision Digital Readout Flow Densimeter for Liquids. *J. Solution Chem.* **3**, 377-384.

Povoledo D. and Vallentyne J.R. (1964) Thermal Reaction Kinetics of the Glutamic Acid - Pyroglutamic Acid System in Water. *Geochim. Cosmochim. Acta.* **28**, 731-734.

Pradhan A.A., Spicer J., and Vera J.H. (1997) Effect of pH on the Solubility of Salts and Amino Acids at 298 K. *Proc. 47th Can. Chem. Eng. Conf.* Paper 472.

Pradhan A.A. and Vera J.H. (1997) Study of the Effect of Anions on the Solubility of Zwitterionic Amino Acids. *Proc. 47th Can. Chem. Eng. Conf.* Paper 656.

Prasad K.P. and Ahluwalia J.C. (1976) Heat Capacity Changes and Partial Molal Heat Capacities of Several Amino Acids in Water. *J. Solution Chem.* **5**, 491-507.

Ranganayaki S., Srivastava B., and Bahadur K. (1977) Synthesis of Amino Acids and Peptides in Sterilised Aqueous Mixtures Under Different Conditions. *Proc. Nat. Acad. Sci. India* **47(A)**, 1II, 182-188.

Ried R.C., Prausnitz J.M., and Poling B.E. (1987) *The Properties of Gases and Liquids.* McGraw- Hill: New York.

Ryan E.T., Xiang T., Johnston K.P., Fox M.A. (1997) Absorption and Fluorescence Studies of Acridine in Subcritical and Supercritical Water. *J. Phys. Chem.* **101**, 1827-1835.

Sedlbauer J., O'Connell J.P., and Wood R.H. (2000) A New Equation of State for Correlation and Prediction of Standard Molal Thermodynamic Properties of Aqueous Species at High Temperatures and Pressures. *Chemical Geology.* **163**, 43-63.

Shahidi F. and Farrell P.G. (1978) Partial Molar Volumes of Organic Compounds in Water. Part 4. - Aminocarboxylic Acids. *J. Chem. Soc. Faraday Trans.* **1**, 858-868.

Shepherd J.C.W. and Grant E.H. (1968) Dielectric Properties of Amino Acid Solutions II. Dielectric Dispersion in Aqueous Proline and Hydroxyproline Solutions. *Proc. Roy. Soc. A.* **307**, 345-357.

Shock E.L. and Helgeson H.C. (1988) Calculation of the Thermodynamic and Transport Properties of Aqueous Species at High Pressures and Temperatures: Correlation Algorithms for Ionic Species and Equation of State Predictions to 5 kb and 1000°C. *Geochim. Cosmochim. Acta.* **52**, 2009-2036.

Shock E.L. (1990) Do Amino Acids Equilibrate in Hydrothermal Fluids? *Geochim. Cosmochim. Acta.* **54**, 1185-1189.

Shock E.L. and Helgeson H.C. (1990) Calculation of the Thermodynamic and Transport Properties of Aqueous Species at High Pressures and Temperatures: Standard Partial Molar Properties of Organic Species. *Geochim. Cosmochim. Acta.* **54**, 915-945.

Shock E.L. (1992) Stability of Peptides in High Temperature Aqueous Solutions. *Geochim. Cosmochim. Acta.* **56**, 3481-3491.

Shock E.L., Oelkers E.H., Johnson J.W., Sverjensky D.A., and Helgeson H.C. (1992) Calculation of the Thermodynamic Properties of Aqueous Species at High Pressures and Temperatures. *J. Chem. Soc. Faraday Trans.* **88**, 803-826.

Shock E.L. (1995) Organic Acids in Hydrothermal Solutions: Standard Molal Thermodynamic Properties of Carboxylic Acids and Estimates of Dissociation Constants at High Temperatures and Pressures. *Am. J. Sci.* **295**, 496-580.

Shvedov D. and Tremaine P. R. (1997) Thermodynamic Properties of Aqueous Dimethylamine and Dimethylammonium Chloride at Temperatures from 283 K to 523 K-Apparent Molar Volumes, Heat-Capacities, and Temperature-Dependence of Ionization. *J. Solution Chem.* **26**, 1113 - 1143.

Smith R.M. and Martell A.E. (1982) *Critical Stability Constants. Volume 5: First Supplement.* Plenum Press: New York.

Smith-Magowan D. and Wood R.H. (1981) Heat Capacities of Aqueous Sodium Chloride from 320 to 600 K Measured with a new Flow Calorimeter. *J. Chem. Thermodyn.* **13**, 1047-1073.

Spies F.N., MacDonald K.C., Atwater T., Ballard R., Carranza A., Cordoba D., Cox C., DiazGarcia V.M., Francheteau J., Guerrero J., Hawkins J., Haymon R., Hessler R., Juteau T., Kastner M., Larson R., Luyendyk B., MacDougall J.D., Miller S., Normark W., Orcutt J., Rangin C. (1980) East Pacific Rise: Hot Springs and Geophysical Experiments. *Science* **207**, 1421-1433.

Spink C.H. and Wadsö I. (1975) Thermochemistry of Solutions of Biochemical Model Compounds. 4. The Partial Molar Heat Capacities of Some Amino Acids in Aqueous Solution. *J. Chem. Thermodynamics* **7**, 561-572.

Tanger J.C. and Helgeson H.C. (1988) Calculation of the Thermodynamic and Transport Properties of Aqueous Species at High Pressures and Temperatures: Revised Equations of State for the Standard Partial Molal Properties of Ions and Electrolytes. *Am. J. Sci.* **288**, 19-98.

Trent J.D., Chastain R.A., and Yayanos A.A. (1984) Possible Artefactual Basis for Apparent Bacterial Growth at 250°C. *Nature* **307**, 737-740.

Trevani L.N., Roberts J.C., and Tremaine P.R. (*in prep.*) Copper(II)-Ammonia Complexation Equilibria in Aqueous Solutions at Temperatures from 30 to 250°C by Visible Spectroscopy.

Tyrrell H.J.V. and Kennerley M. (1968) Viscosity β-Coefficients between 5° and 20° for Glycolamide, Glycine, and N-Methylated Glycines in Aqueous Solution. *J. Chem. Soc.* (A), 2724-2728.

Vallentyne J.R. (1964) Biogeochemistry of Organic Matter - II. Thermal Reaction Kinetics and Transformation Products of Amino Compounds. *Geochim. Cosmochim. Acta.* **28**, 157-188.

Vallentyne J.R. (1968) Pyrolysis of Proline, Leucine, Arginine and Lysine in Aqueous Solution. *Geochim. Cosmochim. Acta.* **32**, 1353-1356.

Vliegen J., Yperman J., Mullens J., François J.P., and Van Poucke L.C. (1984) Excess Volumes of Aqueous Mixtures of the Zwitterion and the Acid Chloride Salt of L-Amino Acids. *J. Solution Chem.* **13**, 245-256.

Wadi R.S. and Goyal R.K. (1992) Temperature Dependence of Apparent Molar Volumes and Viscosity B-Coefficients of Amino Acids in Aqueous Potassium Thiocyanate Solutions from 15 to 35°C. *J. Solution Chem.* **21**, 163-170.

Wang P., Oscarson J.L., Gillespie S.E., Izatt R.M., and Cao H. (1996) Thermodynamics of Protonation of Amino Acid Carboxylate Groups from 50 to 125 °C. *J. Sol. Chem.* **25**, 243-265.

White D.E., Gates J.A., and Wood R.H. (1987) Heat Capacities of Aqueous NaBr from 306 to 603 K at 17.5 MPa. *J. Chem. Thermodyn.* **19**, 493-503.

White R.H. (1984) Hydrolytic Stability of Biomolecules at High Temperatures and its Implication for Life at 250°C. *Nature* **310**, 430-432.

White D.E. and Wood R.H. (1982) Absolute Calibration of Flow Calorimeters used for Measuring Differences in Heat Capacities. A Chemical Standard for Temperatures Between 325 and 600 K. *J. Solution Chem.* **11**, 223-236.

Wilson H. and Cannan R.K. (1937) The Glutamic Acid-Pyrrolidonecarboxylic Acid System. *J. Biol. Chem.* **119**, 309-331.

Wood R.H., Buzzard C.W., Majer V., and Inglese A. (1989) A Phase-Locked Loop for Driving Vibrating Tube Densimeters. *Rev. Sci. Instrum.* **60**, 493-494.

Wood R.H., Quint J.R., and Grolier J-P.E. (1981) Thermodynamics of a Charged Hard Sphere in a Compressible Dielectric Fluid. A Modification of the Born Equation to Include the Compressibility of the Solvent. *J. Phys. Chem.* **85**, 3944-3949.

Wyckoff R.W.G. (1966) *Crystal Structures.* Second Edition; John Wiley & Sons: New York.

Wyman J. and McMeekin T.L. (1933) The Dielectric Constant of Solutions of Amino Acids and Peptides. *J. Am. Chem. Soc.* **55**, 908-922.

Xiang T. and Johnston K.P. (1994) Acid-Base Behavior of Organic Compounds in Supercritical Water. *J. Phys. Chem.* **98**, 7915-7922.

Xiang T. and Johnston K.P. (1997) Acid-Base Behavior in Supercritical Water: β-Naphthoic Acid - Ammonia Equilibrium. *J. Solution Chem.* **26**, 13-30.

Xiang T. (1996) *Spectroscopic Studies of Acid-Base Behavior in Supercritical Water*. Ph.D. Thesis; University of Texas at Austin.

Xiao C. and Tremaine P.R. (1996) Apparent Molar Volumes of $La(CF_3SO_3)_3$(aq) and $Gd(CF_3SO_3)_3$(aq) at 278 K, 298 K, and 318 K at Pressures to 30.0 MPa. *J. Chem. Eng. Data* **41**, 1075-1078.

Xiao C., Bianchi H., and Tremaine P.R. (1997) Excess Molar Volumes and Densities of (Methanol + Water) at Temperatures Between 323 K and 573 K and Pressures of 7.0 MPa and 13.5 MPa. *J. Chem. Thermodynamics* **29**, 261-286.

Xiao C. and Tremaine P. R. (1997) Apparent Molar Volumes of Aqueous Sodium Trifluoromethanesulfonate and Trifluoromethanesulfonic Acid from 283 K to 600 K and Pressures up to 20 MPa. *J. Solution Chem.* **26**, 277-294.

Yanagawa H. and Kojima K. (1985) Thermophilic Microspheres of Peptide-Like Polymers and Silicates Formed at 250°C. *J. Biochem.* **97**, 1521-1524.

Yayanos A.A. (1993) Partial Molal Isothermal Compressibility of Glycine, DL-α-Alanine, Glycylglycine, Glycolamide, and Lactamide. *J. Phys. Chem.* **97**, 13027-13028.

Yezdimer E.M., Sedlbauer J., and Wood R.H. (2000) Predictions of Thermodynamic Properties at Infinite Dilution of Aqueous Organic Species at High Temperatures via Functional Group Additivity. *Chemical Geology*. **164**, 259-280.

Zittle C.A. and Schmidt C.L.A. (1935) Heats of Solution, Heats of Dilution, and Specific Heats of Aqueous Solutions of Certain Amino Acids. *J. Biol. Chem.* **108**, 161-185

APPENDIX ANCILLARY CALCULATIONS

7.1 Calculation of Standard Partial Molar Isothermal Compressibilities κ_T° from Standard Partial Molar Adiabatic Compressibilities κ_S°.

The standard partial molar isothermal compressibility κ_T° is related to the standard partial molar adiabatic compressibility κ_S° through the following expression:

$$\kappa_T^o = \kappa_S^o + \left(\frac{T\alpha_1^2}{\rho_1 c_{p,1}}\right)\left[\left(\frac{2E}{\alpha_1}\right) - \left(\frac{C_p^o}{\rho_1 c_{p,1}}\right)\right] \tag{7.1.1}$$

where T is the temperature, ρ_1 is the density of the solvent, $c_{p,1}$ is the specific heat capacity of the solvent, C_p° is the standard partial molar heat capacity of the solution, α_1 is the expansitivity coefficient of the solvent, and E is the standard partial molar expansibility of the solution. κ_T° and κ_S° have units of $cm^3 \cdot MPa^{-1} \cdot mol^{-1}$.

The expansitivity coefficient of water α_w can be expressed in terms of the molar volume of water V_w or the density of water ρ_w.

$$\alpha_w = \frac{1}{V_w}\left(\frac{\partial V_w}{\partial T}\right)_p = \frac{-1}{\rho_w}\left(\frac{\partial \rho_w}{\partial T}\right)_p \tag{7.1.2}$$

E is defined in terms of the standard partial molar volume of the solute V^o.

$$E = \left(\frac{\partial V^o}{\partial T}\right)_p \tag{7.1.3}$$

The values of κ_S° listed in Table 1.6.3.2 have been measured at temperatures ranging

from 278.15 K to 328.15 K. The values of V° obtained by Hakin *et al.* (1994) for α-alanine, Chalikian *et al.* (1993) for β-alanine, Hakin *et al.* (1994) for glycine, and Hakin *et al.* (1997) for proline have a sufficiently wide temperature range to allow for the calculation of E at each temperature of interest. For each aqueous amino acid the values of V° were fitted to the following expression:

$$V^{o} = a_1 + \left[\frac{a_2}{(T - 228\text{K})}\right] + a_5 R T \beta_w \tag{7.1.4}$$

The terms a_1, a_2, and a_5 are temperature and pressure independent constants, R is the universal gas constant, and β_w is the compressibility coefficient of water as obtained from the equations of state reported by Hill (1990). The values of a_1, a_2, and a_5 obtained for each of the aqueous amino acids are summarized in Table 7.1.1. By substituting equation (7.1.4) into equation (7.1.3) the following expression for E was obtained:

$$E = \left[\frac{-a_2}{(T - 228\text{K})^2}\right] + a_5 R \left[\beta_w + T\left(\frac{\partial \beta_w}{\partial T}\right)_p\right] \tag{7.1.5}$$

The values of C_p^{o} obtained by Hakin *et al.* (1994) for α-alanine, Gucker and Allen (1942) for β-alanine, Hakin *et al.* (1994) for glycine, and Hakin *et al.* (1997) for proline were fitted to the following expression:

$$C_p^{o} = c_1 + \left[\frac{c_2}{(T - 228\text{K})^2}\right] + c_3 R \left[-1 + 2T\alpha_w + T^2\left(\frac{\partial \alpha_w}{\partial T}\right)_p\right] \tag{7.1.6}$$

The terms c_1, c_2, and c_3 are temperature and pressure independent constants, R is the universal gas constant, and α_w is the expansitivity coefficient of water as obtained from the equations of state reported by Hill (1990). The values of c_1, c_2, and c_3 obtained for each of the aqueous amino acids are summarized in Table 7.1.2. Table 1.6.3.2 summarizes the values of κ_T° that were calculated from the values of κ_S° found in Table 1.6.3.2.

Table 7.1.1 Fitting parameters for equation (7.1.4).

	a_1 / ($cm^3 \cdot mol^{-1}$)	a_2 / ($K \cdot cm^3 \cdot mol^{-1}$)	a_5
α-Alanine	69.31 ± 1.29	-328.21 ± 14.06	-3.73 ± 0.98
β-Alanine	79.32 ± 0.14	-471.48 ± 1.63	-12.74 ± 0.10
Glycine	49.50 ± 0.63	-324.19 ± 6.90	-1.45 ± 0.50
Proline	84.91 ± 0.01	-377.15 ± 0.12	2.74 ± 0.01

Table 7.1.2 Fitting parameters for equation (7.1.6).

	c_1 / ($J \cdot K^{-1} \cdot mol^{-1}$)	$c_2 \cdot 10^{-4}$ / ($J \cdot K \cdot mol^{-1}$)	c_3
α-Alanine	188.56 ± 2.47	-24.02 ± 1.57	7.58 ± 4.09
β-Alanine	144.25 ± 6.30	-33.79 ± 3.59	3.95 ± 4.60
Glycine	110.37 ± 2.51	-36.63 ± 1.60	10.82 ± 4.17
Proline	262.54 ± 4.46	-43.49 ± 2.83	33.12 ± 7.40

7.2 Calculation of Dipole Moments μ from Molar Dielectric Increments δ.

The molar dielectric increment δ is defined as:

$$\delta = \left(\frac{d\varepsilon}{dC} \right) \tag{7.2.1}$$

ε is the dielectric constant associated with the dissolved species and C is the concentration of the dissolved species in $mol \cdot L^{-1}$.

In the Kirkwood theory of dielectrics, described by Edsall and Wymann (1958), $\boldsymbol{\mu}_k$ is defined as the permanent dipole moment of molecule k in solution. Since molecule k has a dipole moment, it may interact with its nearest neighbours through electrostatic repulsion or attraction. It may also interfere with their rotation by steric hindrance. Therefore, at any given instant, the orientation of the nearest neighbours of molecule k will not be random with respect to the orientation of molecule k. The vector sum of the moment of molecule k and the moments due to all of the neighbouring molecules is denoted as $\bar{\boldsymbol{\mu}}_k$. In general $\bar{\boldsymbol{\mu}}_k$ is different in magnitude and direction from $\boldsymbol{\mu}_k$. Molecules that are farther than two or three molecular diameters away from molecule k do not contribute to $\bar{\boldsymbol{\mu}}_k$ since they are too far from molecule k to interact with it. Therefore, these molecules have essentially random orientations with respect to molecule k.

Now consider the equation that arises from the Kirkwood theory of dielectrics as applied to systems with several components:

$$\frac{(2\varepsilon+1)(\varepsilon-1)}{9\varepsilon} = \frac{1}{4\pi\varepsilon_o}\sum_k \frac{4\pi n_k}{3}\left(\alpha_{0k} + \frac{\boldsymbol{\mu}_k \bar{\boldsymbol{\mu}}_k}{3kT}\right) \tag{7.2.2}$$

where ε_o is the permittivity of free space, n_k is the number of molecules of species k per unit volume, and α_{0k} is a constant that depends only on k. In the case of highly polar systems, equation (7.2.2) takes on its limiting form as expressed as.

$$\frac{2\varepsilon}{9} = \frac{1}{4\pi\varepsilon_o}\sum_k \frac{4\pi n_k}{3}\left(\alpha_{0k} + \frac{\boldsymbol{\mu}_k \bar{\boldsymbol{\mu}}_k}{3kT}\right) \tag{7.2.3}$$

In the Kirkwood theory the molar polarizability P is defined as:

$$P = \frac{4\pi N_A}{3}\left(\alpha_0 + \frac{\boldsymbol{\mu}\bar{\boldsymbol{\mu}}}{3kT}\right) \tag{7.2.4}$$

where N_A is Avogadro's number. Substitution of equation (7.2.4) into equation (7.2.3) gives:

$$\frac{2\varepsilon}{9} = \frac{1}{4\pi\varepsilon_o}\sum_k C_k P_k \tag{7.2.5}$$

The term $C_k = (n_k / N_A)$ is the concentration of species k in mol·mL^{-1}. If a two component solution is considered, then equation (7.2.5) becomes:

$$\frac{2\varepsilon}{9} = \frac{C_1 P_1 + C_2 P_2}{4\pi\varepsilon_o} \tag{7.2.6}$$

Similarly, for a one component system:

$$\frac{2\varepsilon_r}{9} = \frac{C_1 P_1}{4\pi\varepsilon_o} \tag{7.2.7}$$

Here ε_r is the dielectric constant of the solvent. In a two component solution C_1 and C_2 are related through their respective standard partial molar volumes V_1° and V_2° as follows:

$$C_1 V_1^o + C_2 V_2^o = 1 \tag{7.2.8}$$

Combination of equation (7.2.6) and equation (7.2.8) gives:

$$\frac{2\varepsilon}{9} = \frac{1}{4\pi\varepsilon_o}\left(C_2 P_2 + \frac{(1 - C_2 V_2^o) P_1}{V_1^o} \right) \tag{7.2.9}$$

Substitution of equation (7.2.7) into equation (7.2.9) yields:

$$\frac{2\varepsilon}{9} = \left(\frac{C_2 P_2}{4\pi\varepsilon_o} \right) + \left(\frac{2\varepsilon_r (1 - C_2 V_2^o)}{9} \right) \tag{7.2.10}$$

If the subscript 2 is allowed to represent the solute while the subscript 1 represents the solvent, then the derivative of equation (7.2.10) with respect to C_2 is equal to the molar dielectric increment. A minor correction factor is required to account for differences in units.

$$\frac{2000}{9}\delta = \left(\frac{P_2}{4\pi\varepsilon_o} \right) - \left(\frac{2\varepsilon_r V_2^o}{9} \right) \tag{7.2.11}$$

Only highly polar substances are being considered for which 1000δ is much greater than $\varepsilon_r V_2^\circ$ and for which α_{02} can be neglected. Therefore, equation (7.2.11) can be rearranged to give

an expression for P_2:

$$P_2 = \frac{8000\,\delta\,\pi\,\varepsilon_o}{9} \tag{7.2.12}$$

Comparison of equations (7.2.4) and (7.2.12) yield an expression for $\boldsymbol{\mu}_2\bar{\boldsymbol{\mu}}_2$. Substitution of values for the constants in the expression yields:

$$(\boldsymbol{\mu}_2\bar{\boldsymbol{\mu}}_2)^{0.5} = 0.1910\sqrt{T\delta} \tag{7.2.13}$$

where $(\boldsymbol{\mu}_2\bar{\boldsymbol{\mu}}_2)^{0.5}$ is expressed in Debye and δ is expressed in $m^3 \cdot mol^{-1}$. The dipole moment μ is defined as $(\boldsymbol{\mu}_2\bar{\boldsymbol{\mu}}_2)^{0.5}$ and therefore:

$$\mu = 0.1910\sqrt{T\delta} \tag{7.2.14}$$

The standard deviation associated with the dipole moment σ_μ can be calculated from the standard deviation associated with the molar dielectric increment σ_δ as follows:

$$\sigma_\mu = \frac{0.09551\,\sigma_\delta\,T^{0.5}}{\delta^{0.5}} \tag{7.2.15}$$